Novel approaches to target infectious diseases: the utility of Auger electrons and scFvs for imaging and control

C. C. Rathje

September 2013

A thesis submitted to the University of Kent for the degree of PhD in Biochemistry in the Faculty of Science, Technology and Medical Studies.

The School of Biosciences

No part of this thesis has been submitted in support of an application for any degree or qualification of the University of Kent or any other University or institute of learning

Claudia Cattoni Rathje

September 2013

Acknowledgements

I would first and foremost like to thank my supervisor Dan Lloyd, who gave me the opportunity to study for a PhD and for support and guidance throughout the course of my project.

Secondly I would like to thank my semi second supervisor Peter Nicholls for trusting me to carry out the anti-LAM scFv design and for helpful guidance.

I would furthermore like to thank Ian Blomfield for support and constructive discussion and for providing the *E. coli* K-12 strain for my studies.

For technical support I would like to give a special thanks to Kevin Howland for performing the HPLC-MS on my peptides. Furthermore, I would like to thank the following people for providing the model strains used in my toxicology studies: Gary Robinson (*S. aureus* NCIMB 8625), Claudia Solschied (*S. cerevisiae* BY4741) and Kara Turner (*C. albicans* sc5314). Furthermore, I would like to give a big thanks to Jeff Joynson from Mologic for immense help with scFv expression.

I would like to give a special thanks to Ben Skinner for proof-reading my thesis and giving helpful feed-back. An additional thanks goes to Sheran Attanapola for helping with the final stages of the writing process. Furthermore I would like to give thanks to Ingeborg and Matias Grynderup for providing help with statistical analysis. Additionally, I would like to thank my partner Bill Morris for providing support and encouragement during the entirety of my project.

Finally, I would like to thank my family for being understanding in all my life choices and especially my mum for trying to understand the lack of phone calls during my thesis writing.

I Contents

Contents

II List of Figures

III List of Tables

IV Abbreviations

α-MF	= α mating factor
Aa	= Amino acid
ACN	= Acetonitrile
ADE2	= phosphoribosylaminoimidazole carboxylase gene
AG	= arabinogalactan
AOX1	= Alcohol oxidase 1
BCG	= Bacillus Calmette–Guérin
BMGY	= Buffered Glycerol Complex Medium
BMMY	= Buffered Methanol Complex Medium
BY4741	= strain of S. cerevisiae
C. albicans	= *Candida albicans*
CDR 1-3	= Complementary determining regions 1-3
CFP-10	= Culture Filtrate Protein 10
CFP-21	= Culture Filtrate Protein 21
CFU	= Colony forming unit
C_H2 domain	= Heavy chain conserved region 2
CT	= Computerised tomography scan
CV	= Column volumes
D segment	= Diversity segment in antibody gene assembly
Da	= Daltons
DSB	= Double stranded breaks
EC	= Electron capture
ECL	= Enhanced Chemiluminescense
E. coli	= *Escherichia coli*
ESAT-6	= Early Secreted Antigenic Target 6
Fab	= Antigen binding fragment of antibody
Fc	= Conserved fragment of antibody
FT	= Flow through
GOI	= Gene of interest

HPLC = High Pressure Liquid Chromatography
HPV = Human Papilloma Virus
HRP = Horseradish peroxidase
IC = Internal conversion
IFN-γ = Interferon γ
ITLC = Instant thin layer chromatography
J segment = Junction segment in antibody gene assembly
LAM = Lipoarabinomannan
LB = Lysogeny Broth
LET = Linear energy transfer
LM = Lipomannan
LPS = Lipopolysaccharide
M. tuberculosis = *Mycobacterium tuberculosis*
mAGP = Mycolyl arabinogalactan-peptidoglycan
MDR-TB = Multi-drug resistant tuberculosis
MHC = Major histocompatibility complex
MRI = Magnetic resonance imaging
MS = Mass spectrometry
ORF = Open reading frame
P. pink = *Pichia pink*
PAD = Pichia Adenine Dropout
PBS = Phosphate buffered saline
PCR = Polymerase chain reaction
PG = Peptidoglycan
PIM = Phosphatidylinositol mannosides
PPB = Potassium phosphate buffer
pPinkα-HC = Pichia pink vector incl. α-mating sequence, High copy
rAb = Recombinant antibody
RD1 = Region of difference 1
RIT = Radio immunotherapy
RNS = Reactive nitrogen species

ROS	= Reactive oxygen species
RPM	= Revolutions per minute
S. aureus	= *Staphylococcus aureus*
scFv	= Single-chain variable fragment
SDS-PAGE	= Sodium dodecyl sulphate polyacrylamide gel electrophoresis
SN	= Supernatant
SPR	= Surface Plasmon Resonance
TB	= Tuberculosis
TDR-TB	= Total drug resistant tuberculosis
TFA	= Trifluoroacetic acid
TNF-α	= Tumour necrosis factor α
T/NT	= Target over non-target ratio
UBI	= Ubiquicidine
UBI 29-41	= Ubiquicidine fragment composed of residues 29-41
V segment	= Variable segment of antibody gene assembly
V_H	= Heavy chain variable domain
V_L	= Light chain variable domain
W	= Wash
WHO	= World Health Organisation
XDR-TB	= Extensively drug resistant tuberculosis
YNBM	= Yeast nitrogen base with methanol
YPD	= Yeast Extract Peptone Dextrose

V Abstract

With an increasing number of infectious agents resistant to one or more existing antibiotics, there is a global requirement for new therapeutics. One possible method for treatment of infectious diseases proposed in this study is the adaptation of a technique developed for cancer treatment, targeted radionuclide therapy, with particular interest in Auger electron radiation. Auger electrons are short range and low energy particles emitted from a range of radioactive isotopes.

As a targeting agent, the antimicrobial peptide fragment UBI 29-41 was used. Antimicrobial peptides have a broad range of target microorganisms, ideal for toxicological studies of Auger electrons. Here, the baseline toxicity of UBI 29-41 was established in a range of model organisms. This enabled the analysis of the toxic effect of Auger electron emitting radio-nuclides using the isotope ^{125}I. Although no direct toxic effect was observed with this particular isotope, the labelling allows easy replacement with more potent isotopes.

To further develop the targeting agent a lipoarabinomannan (LAM) specific single-chain variable fragment (scFv) was developed. LAM is a glycolipid and virulence factor associated with *M. tuberculosis,* the primary cause of tuberculosis in humans. By isolating the variable domains of a LAM specific monoclonal antibody, linked via a poly-glycine linker, the scFv was assembled *in silico*. The nucleotide sequence was optimised for and transfected into a *Pichia pink* expression system. Expression was successful with a ~27kDa product being secreted.

The novel anti-LAM scFv generated in this study combined with the potential toxic effects of Auger electrons could provide a new avenue for the treatment and diagnosis of tuberculosis.

1 Introduction

1.1 Infectious diseases

Despite the massive efforts that have been put into the fight against infectious disease, it is estimated that they still are accountable for approximately 25% of all deaths worldwide with increasing globalisation and mass gatherings posing further challenges (Abubakar *et al*., 2012; Fauci and Morens, 2012).

Infectious diseases have several characteristics that distinguish them from other non-communicable human diseases (Fauci and Morens, 2012):

- They have the potential for unpredictable global impact
- Following infection the host commonly acquires stable and potent immunity against re-infection
- They are transmissible
- They only require a single agent to cause disease
- They can be preventable
- They have the potential to be eradicated
- They are highly adaptive and have an edge on human evolution due to replicative and mutational capacities
- They have a close dependence on nature and are highly reliant on human behaviour
- They are frequently derived from or coevolved in other animals

The human body has several defence mechanisms to prevent infection. These include the primary barriers such as skin, and commensal bacteria on the skin and in the gut. If the microorganisms overcome these barriers they are initially met by a complex innate immune defence system comprising the complement system, phagocytic cells and antimicrobial peptides. If the infection persists an adaptive immune response is mounted in extension of the innate defence system. Most infections are prevented from being established by either of these barriers. However, in some cases where the individual is immuno-compromised, the immune system is overwhelmed, or the barriers for other reasons are incapable of preventing the continual infection of the body, alternate means are required for the elimination of the infection (Janeway, 2005).

1.1.1 Current diagnosis and treatment

For most cases, infectious diseases are fairly easily diagnosed as they generally display unique alterations in the human physiology. However, this is not always the case. Some microorganisms are capable of being internalised into human cells and lie dormant for years and in some cases stay completely unnoticed by the human immune defence systems. The most common diagnostic methods are currently primarily culture isolation and identification, microscopic evaluation, immunoassays and PCR analysis, which are all fairly time-consuming (Madigan *et al*., 2003).

Antibiotics today primarily comprise chemical components that either interfere with the integrity of the microorganisms or inhibit the intracellular machinery (Table 1) (Madigan *et al*., 2003).

Target	Class of antibiotic	Use
Cell wall synthesis	β-lactams	Broad range antibiotic, newly developed β-lactams have proven effective against both gram negative and gram positive bacteria
	Carbapenems	Broad range antibiotic which is more resistant to β-lactamases than penicillins.
	Cephalosporins	Broad range antibiotic which is more resistant to β-lactamases than penicillins.
	Glycopeptides	Used primarily for gram positive cocci bacteria and where β-lactam resistance has been observed
	Penicillins	Used primarily against gram positive bacteria, however a large number of bacteria now exhibit resistance
Protein synthesis by binding to the 30S ribosomal subunit	Aminoglycosides	Broad spectrum antibiotic, but primarily used for aerobic gram negative bacteria
	Tetracyclines	Broad range antibiotic, primarily used for urinary tract and intestinal infections as well as severe cases of acne and rosacea
Protein synthesis by binding to the 50S ribosomal subunit	Chloramphenicol	Broad range antibiotic that is also effective against most anaerobic bacteria, however many cases of resistance
	Fusidic acid	Primarily effective against gram positive bacteria
	Lincosamides	Primarily used against gram positive bacterial infections
	Macrolides	Primarily used against gram positive bacterial infections and some gram negative bacterial infections in the respiratory tract and soft tissues

DNA replication and transcription	Quinolones	Second line broad spectrum antibiotic primarily used in severe infections resistant to first-line antibiotics
RNA synthesis	Rifampicin	Commonly used against Mycobacterial infections
Folate synthesis	Sulfonamides	Primarily used to treat acne and urinary tract infections but is also used in cases where other antibiotics have proven unsuccessful

Table 1 Overview of the most common antibiotic chemicals (Krause, 1998; Madigan *et al*., 2003).

As can be seen in table 1 all the chemicals commonly used to combat infectious diseases require not only internalisation into the microorganisms in order to execute their function, but are also commonly quite specific in their mode of function. This opens up a myriad of possibilities for the microorganisms to adapt to the new chemicals. There are several mechanisms that microorganisms have developed to counter the antibiotics including reduced cell uptake, active efflux and modifications of the target to reduce binding efficiency to name a few (Krause, 1998).

The great ability of microorganisms to adapt to chemicals has led to an increasing number of them today being resistant to either one or numerous antibiotic compounds, increasing the difficulty of treatment (Fox, 2011).

There are several reasons that are hypothesised to be the primary ones for the emergence of resistant strains (Pechère, 2001; Fox, 2011):

1) The increased low-dose routine use of antibiotics in livestock fodder
2) The indiscriminate prescription of antibiotics by doctors often pressured by patients

3) The failure of patients to complete an entire course of antibiotic treatment

As microorganisms are capable of horizontal gene transfer via conjugation, transduction and transformation this allows the spread of resistance genes rapidly especially in environments with high density of varied bacterial strains such as hospitals. For this reason, more research than ever is focusing on novel ways not only to fight the problematic multi resistant strains, but also to produce new ways to combat infections efficiently and with minimised possibility of generating resistance. One infectious disease that currently is being thoroughly researched for new ways of both diagnosis and treatment is *M. tuberculosis*.

1.2 Tuberculosis

Tuberculosis (TB) remains a major cause of death and loss of life quality in the world today. It is estimated that it infects approximately one third of the world's population and is the second leading cause of death in the world caused by an infectious disease. Approximately 1.2 million lives are lost to the disease each year and it is estimated that there are 9 million new cases each year, most of which are reactivated dormant infections (Gegenbacher and Kaufmann, 2012; WHO Global Tuberculosis Report 2012). Even with the great efforts currently being put into tuberculosis control, the emergence of a growing number of increasingly resistant strains and the further complications added by the HIV pandemic raises the need for research into new ways of managing the disease.

1.2.1 Physiology

The primary causative agent of tuberculosis in humans, *Mycobacterium tuberculosis*, is an aerobic rod shaped bacterium. Furthermore, it is a very slowly dividing bacterium, that even under optimal conditions, only divides every 18-24 hours making it harder to not only diagnosis but to eradicate as well (Gegenbacher and Kaufmann, 2012).

1.2.2 Genomic structure

The genome size of the various strains of *Mycobacteria* fluctuates considerably as illustrated by the size difference between strains of *Mycobacterium leprea* and *M. tuberculosis*. Where *M. leprea* has a genome size of 3.27 Mb and ~1600 open reading frames (ORF) *M. tuberculosis* is much larger with 4.41 Mb genome and approximately 4000 ORFs (Cole *et al*., 2001; Cosma *et al*., 2003; Gegenbacher and Kaufmann, 2012). The genome size is also associated with virulence. Three regions in particular have been identified that are all present in both *M. tuberculosis* and *M. bovis* but absent in Bacillus Calmette–Guérin **(**BCG) referred to as “Regions of Difference” (RD) 1-3. Especially RD1 has been shown to have great impact on mycobacterial virulence and is the only region present in all tested virulent strains of the mycobacterial complex (Figure 1) (Mahairas *et al*., 1996; Berthet *et al*., 1998; Pym *et al*., 2002; Lewis *et al*., 2003; Guinn *et al*., 2004; Kurenuma *et al*., 2009; Ernst, 2012).

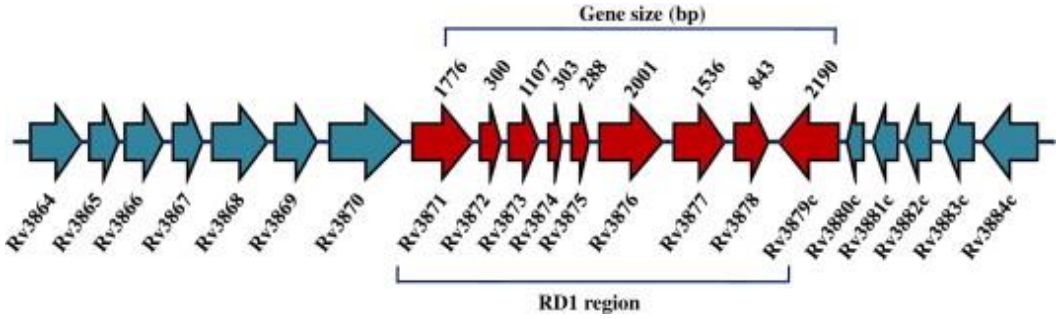

Figure 1 Overview of the Region of difference 1 (RD1)

RD1 from *M. tuberculosis* including flanking regions. Arrows indicate transcriptional direction (Rai *et al*., 2012)

RD1 is a 9.5 kb gene segment comprising 9 genes including ESAT-6 (Early Secreted Antigenic Target 6), CFP-10 (Culture Filtrate Protein 10) and CFP-21 (Culture Filtrate Protein 21). These are important T-cell antigens and have been hypothesised to be the reason for the poor induction of an immune response and thereby generation of protective immunity by the BCG vaccine (Mahairas *et al*., 1996; Rai *et al*., 2012). A combination of secretory proteins of the RD1 region, ESX-1, has been indicated to be important in the transport of the abovementioned antigens and therefore in the functionality.

1.2.3 *M. tuberculosis* cell wall

Although it lacks an outer lipid bilayer, *M. tuberculosis* is not considered a typical gram positive bacterium due to its heavily glycosylated and waxy surface, which makes traditional gram staining very difficult. For this reason, the general visualisation of the bacteria is done using Ziehl-Neelsen acid-fast staining (Gegenbacher and Kaufmann, 2012).

The cell wall of *M. tuberculosis* is one of the most striking features of the bacteria and is associated not only with its unique survival pattern, but also with the virulence of the bacteria (Figure 2). The complexity of the cell wall has also been indicated to have a function as a protective barrier against the acidic environment of the phagosomes in which they primarily reside, as will be elaborated below (Gegenbacher and Kaufmann, 2012).

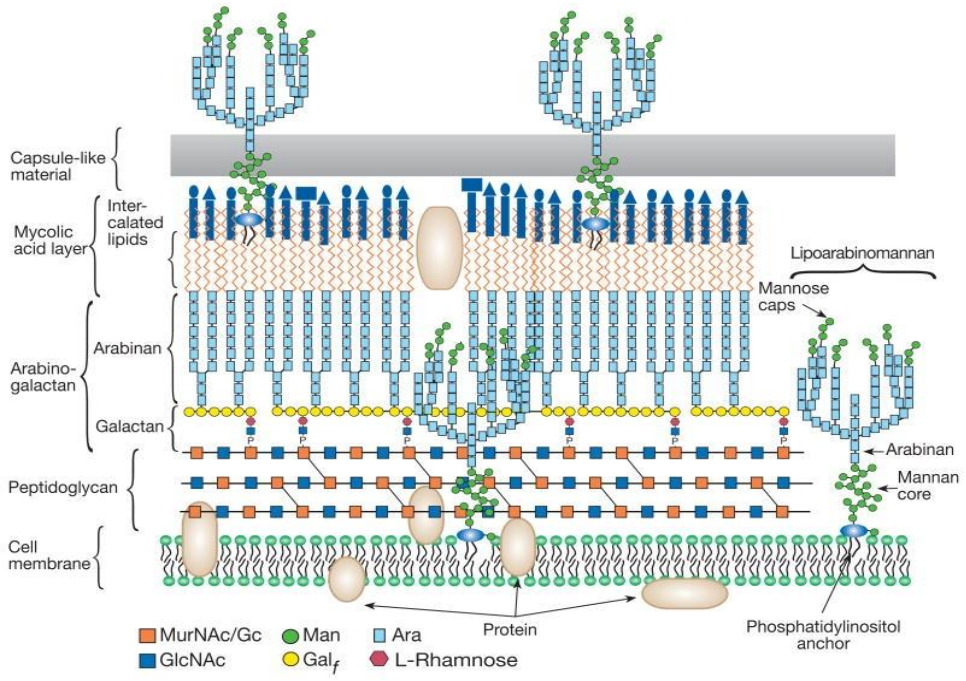

Figure 2 Schematic representation of *M. tuberculosis* cell wall

The core comprises peptidoglycan covalently attached to arabinogalactan which is further bound to mycolic acids. The upper layer is composed of cell wall proteins, phosphatidylinositol mannosides, phticerol containing lipids as well as lipomannan and lipoarabinomannan. It is only the upper layer that gets solubilised upon disruption (web 1; Brennan, 2003).

The structure of the mycobacterial cell wall is generally divided into two segments: the upper and the lower segment, with the lower also defined as the cell wall core, or the mycolyl arabinogalactan-peptidoglycan (mAGP) complex (Chatterjee and Khoo, 1998; Brennan, 2003).

The core is situated just above the cell membrane and is a complex matrix composed of peptidoglycan (PG), which is covalently attached to arabinogalactan (AG) and hereafter further attached in the ends to mycolic acids in an esterified fashion. The mycolic acids comprise long meromycolate and short α-chains.

The upper layer is also interspersed with cell wall proteins, as well as phosphatidylinositol mannosides (PIMs), phthicerol containing lipids, lipomannan (LM) and lipoarabinomannan (LAM).

If the cell wall is disrupted somehow it is only the upper layer that is solubilised. This indicates that the upper layer is primarily composed of signalling and effector molecules, whereas the lower layer is primarily associated with viability of the bacteria (Brennan, 2003). Of special interest is lipoarabinomannan (LAM), which has also been shown to be not only associated with *M. tuberculosis* survival, but also virulence of the pathogen and is the target of the scFv designed in this project.

1.2.3.1 Lipoarabinomannan (LAM)

LAM is an important heterogeneous glycolipid of the Mycobacterial cell wall. The size was found to differ greatly in size and branching pattern as well as acylation and phosphorylation on both the arabinan and mannose portions of the molecule. In the native state however, LAM of *M. tuberculosis* has an average size of 17.3 kDa (Chatterjee and Khoo, 1998).

It is both important for survival as well as a virulence factor of *M. tuberculosis* (Knutson *et al*., 1998; Rademacher *et al*., 2007; Minion *et al*., 2011). The importance is indirectly reflected in the abundance of the molecule which can account for up to

1.5% of the total bacterial weight (Hunter *et al*., 1986; Chan *et al*., 1991; Minion *et al*., 2011).

LAM from *M. tuberculosis* is capped by short mannose-containing caps, which enable it to bind to mannose receptors on the surface of macrophages allowing phagocytosis (Chatterjee and Khoo, 1998). Although this structural motif is absent from *Mycobacterium smegmatis* LAM it is present on virtually all other strains of mycobacteria, including attenuated strains, indicating that the cap is not a virulence factor as first hypothesised (Chatterjee and Khoo, 1998; Brennan, 2003). Furthermore, LAM is capable of binding to Toll receptors as well as physically introducing itself into the host membranes.

LAM is primarily involved in the survival of *M. tuberculosis* via causing the deactivation of macrophages; it causes this by impairing Ca^{2+} concentration rise in infected macrophages and hence inhibits phagosome maturation (Chan *et al*., 1991; Chatterjee and Khoo, 1998; Poirier and Av-Gay, 2012). This has a myriad of downstream effects:

1) Impaired antigen presentation
2) Restricted activation of IFN-γ inducible genes
3) Decreased production of cytokines
4) Inhibition of protein kinase C
5) Lower levels of oxidative and nitrogen free radicals
6) Inhibition of host cell apoptosis

Studies have further indicated that LAM may have an indirect ability to reduce T-cell proliferation by inhibiting the transcriptional activation of MHC-II molecules. This significantly reduces the presentation of antigens on the surface of macrophages which thereby results in less T-cell activation and proliferation (Chan *et al*., 1991). Furthermore, LAM appears to have an impact on the maturation, MHC expression and antigen presentation of dendritic cells by binding to the DC-SIGN receptor, hence having a great impact on the establishment of the adaptive immune response (Doherty, 2012).

Interestingly, it has been found that LAM is released from metabolically active, as well as degrading bacterial cells which has enabled the potential diagnostic approach of urine analysis for the presence of LAM, which also eases the diagnosis of children, where sputum tests are harder to perform (Minion *et al*., 2011).

1.2.4 Pathology

There are several ways in which *M. tuberculosis* can cause disease in humans; the most common of which in adults is pulmonary tuberculosis. However, other extra pulmonary forms of TB exist, which are found more often in immuno suppressed individuals and young children. These include tuberculous meningitis (central nervous system), tuberculous pleurisy (pleura), scrofula (lymphatic system), urogenital tuberculosis (genitourinary system) and Pott's disease (bones and joints) (Krause, 1998). Finally, there is the more serious version referred to as miliary tuberculosis where *M. tuberculosis* spread systemically to other organs via either the

blood or lymphatic system. Due to the septic nature of miliary TB it is considered much more serious than pulmonary TB.

1.2.4.1 Primary infection

The route of infection of *M. tuberculosis* is primarily via the pulmonary system by inhalation of droplets containing tuberculosis bacteria. The likelihood of infection transmission is dependent on a variety of variables including exposure duration, exposure intensity, virulence characteristics of the tuberculosis strain among others (Dheda *et al*., 2010). As the bacteria are inhaled into the lower levels of the lungs, they are taken up by alveolar macrophages, where they start replicating and form the initial lesions (Davis and Ramakrishnan, 2009). Some infected phagocytic cells travel to the hilar lymph nodes and together with the initial lesions in the lungs, referred to as the Ghon focus, comprise the primary complex.

Normally, as microorganisms are phagocytised, the resulting phagosome contains hydrolytic enzymes, reactive oxygen and nitrogen species (ROS and RNS, respectively) and antimicrobial peptides, all involved in the breakdown of the ingested microorganisms (Figure 3) (Gegenbacher and Kaufmann, 2012).

M. tuberculosis, however, is capable of inhibiting this (Poirier and Av-Gay, 2012). Apart from aiding in immediate survival, this inhibits antigen presentation and the establishment of an adaptive immune response. However, eventually some of the bacteria will be broken down by the phagolysosome pathway and bacterial antigens will be mounted into major histocompatibility complex II (MHCII) allowing recruitment of CD4+ T_H1 cells (Doherty, 2012).

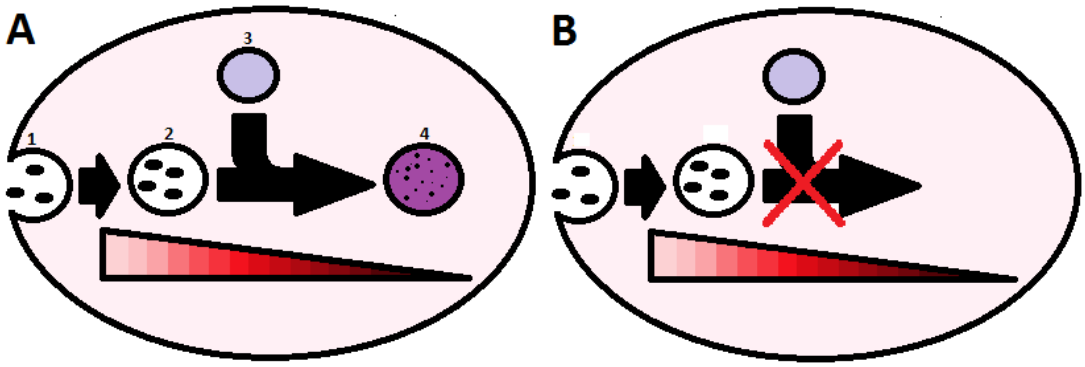

Figure 3 Schematic overview of mycobacterial inhibition of phagolysosome formation
A simplified overview of the inhibitory effect of macrophages on the generation of the phagolysosome. **A)** Shows the normal progression of phagolysosomal generation. Following entry, the pH of the phagosome decreases followed by the fusion with a lysosome. The lysosome contains enzymes that are activated by the low pH thereby accelerating the degradation of the phagocytised material **B)** Shows the inhibited step in phagosome and lysosome fusion. The gradient bar indicates the decreasing pH as the phagosome is increasingly internalised and finally fused with the lysosome 1) Early phagosome 2) Phagosome 3) Lysosome 4) Phagolysosome.

Following the establishment of the primary complex, an immune response by the host is triggered, recruiting the first line of defence including more immature macrophages, neutrophils, monocytes and dendritic cells to the site of infection. However, as these cells are also the primary host cells, this only recruits more cells for *M. tuberculosis* to spread to. As the macrophages cannot eradicate the infection the number of cells only continues to increase and this results in the formation of solid granulomas, the initial evidence of infection (Dheda *et al*., 2010; Ernst, 2012; Gegenbacher and Kaufmann, 2012).

The primary route for the establishment of protective immunity against *M. tuberculosis* is primarily mediated by CD4+ T_H1 cells and CD8+ T cells.

Although it has not been completely established how the phagocytic cells are capable of mounting a CD8+ T cell response, some indications have been made

that *M. Tuberculosis,* after a couple of days of phagosome compartmentalisation, is capable of escaping the phagosome into the cytosol of the host cell (Van der Wel, 2007). In the cytosol, the bacteria will be able to be degraded by host cell enzymes, internalised into the endoplasmic reticulum (ER) and mounted into an MHC class I for cell surface presentation and CD8+ T-cell recruitment (Janeway *et al*., 2005; Van der Wel, 2007). Interestingly, there seems to be a clear connection between the virulence of the bacteria and the capacity to enter the cytosol, which may have great implications for the development of vaccines.

CD4+ T_H1 cells, upon activation, generate large amounts of cytokines such as interferon gamma (IFN-γ) and tumour necrosis factor alpha (TNF-α), both of which result in the activation of the macrophages, further inducing bactericidal activity, phagosome-lysosome fusion and result in the recruitment of more phagocytic cells (Pearl *et al*., 2001).

As the CD4+ T_H1 cells normally function by activating the macrophages and facilitate the fusion of phagosomes with endosomes, the recruitment is to a large extent redundant and only increases the size of the granulomas. So where normal pathogens are inhibited or even eradicated by the recruited T_H1 cells, macrophages and dendritic cells, *M. Tuberculosis* has found a way of turning it into an advantage as it now has more cells to infect. Furthermore, in many granulomas it has been found that the macrophages have fused with one another forming massive multi nucleated giant cells. This further enables *M. tuberculosis* to infect new cells without being exposed to the extracellular space.

To help promote its pathogenesis, *M. tuberculosis* has developed multiple means to inhibit host cell apoptosis and favour necrosis. This not only gives the bacteria prolonged survival, but also ensures a longer timeframe for multiplication before the rupture of the cells, thus enabling the bacteria to infect more cells upon release, not only by the increased number of bacteria released, but also thereby allowing more phagocytic cells to be recruited to the site of infection (Davis and Ramakrishnan, 2009; Ernst, 2012). Necrosis is normally something that is found at the centre of the secondary state of granulomas and as time progresses the necrotic centre will cause the granuloma to become perforated forming the third state of granulomas, caseous granulomas. This allows the escape of *M. tuberculosis* to the surrounding tissue and airways and it is at this stage that TB becomes infectious (Gegenbacher and Kaufmann, 2012).

With the maturation of the granulomas there is an increased deposition of both fibrin and calcium around the site of infection. Due to this, the tissue damage caused by tuberculosis infection is irreversible making it even more important to be diagnosed at an early stage (Cosma *et al*., 2003).

Even if *M. tuberculosis* seems like an invincible organism, in most cases, i.e. , individuals with a fully functioning immune system, the primary disease will be contained and enter into a latent stage that is only ever activated in 5-10% of all infected individuals (Doherty, 2012).

1.2.4.2 Latent infection

Following the initial *M. tuberculosis* infection and immune system activation, *M. tuberculosis* can revert to a dormant state, often held in place by the complex mounted immune response. In 90-95% of cases the immune system is capable of retaining the mycobacterial infection in a compartmentalised fashion with a constant replacement of CD4+ T cells with expression of IFN-γ and TFN-α production and nitric oxide formation (Lazarevic *et al*., 2005). This state is characterised by low metabolic activity and more importantly increased drug resistance (Gegenbacher and Kaufmann, 2012).

At the onset of the adaptive immune response most individuals initially show temporary signs of infection such as fever and skin rashes. However, as soon as the infection enters the latent stage, the disease becomes asymptomatic. The onset of the adaptive immune response also disrupts the exponential bacterial growth and the bacterial load in mouse models seem to level out at approximately 10^6 bacteria. The bacterial load in human latent TB infection has not yet been established (Ernst, 2012).

Although the adaptive immune response towards *M. tuberculosis* is able to stop the progressive growth it seems incapable of eradicating the infection altogether. The primary reasons for their limitation is the decreased MHC class II-mediated antigen presentation and antigen processing mediated by a 19 kDa lipoprotein. This induces the production of the anti-inflammatory protein lipoxin, inflammatory restriction by regulatory T-cells, down regulation of mycobacterial antigen expression leading to a failure in inducing CD4+ T cell response and finally an inhibition of the macrophage-

activating effects of IFN-γ (Noss *et al*., 2001; Scott-Browne *et al*., 2007; Divangahi *et al*., 2010; Bold *et al*., 2011; Ernst, 2012).

Interestingly, some evidence has indicated that there might not necessarily be a complete distinction between latent and active phase of tuberculosis infection, but more a gradient so that in the latent phase there exists a small population of active *M. tuberculosis* bacilli and vice versa. This has great implications for treatment of tuberculosis (Lewis, 2010; Gegenbacher and Kaufmann, 2012).

1.2.5 Tuberculosis control

Both diagnostic tools and modes of treatment of TB is associated with many uncertainties although several are present.

1.2.5.1 Diagnosis

Diagnosis of TB today comprises most commonly a sputum test of patients with active TB, chest X-ray imaging and the Mantoux tuberculin skin test (Jassal and Bishai, 2009).

The sputum test is only an effective diagnostic tool in the case of active TB as it requires the presence of bacilli in great enough numbers to be detectable under a microscope

A major issue with *M. tuberculosis* culture growth is the long generation time. Even under optimal growth conditions it takes up to 6 weeks to get analysable colonies. Furthermore, it is quite often necessary to repeat the diagnosis making this a very time-consuming endeavour. However, culture growth allows the establishment of

chemotherapeutic susceptibility of the tested organism, thereby more accurately set up the correct course of antibiotics for the individual (Jassal and Bishai, 2009).

The problem associated with chest X-ray imaging is that it is practically impossible to detect the infection at the early stages as tissue alterations, due to granuloma formation, are required for recognition. This means that the disease will already be at an evolved stage making it harder to treat and more importantly the patient will at this point already have suffered irreversible damage to the lungs.

In the case of latent infections of TB the gold standard is still the Mantoux tuberculin skin test. However false-positives do occur in individuals that have received the Bacillus Calmette-Guerin (BCG) vaccine. The skin test is also associated with false-negatives, in particular in immune-compromised individuals (Ducati *et al*., 2006; Jassal and Bishai, 2009).

A new alternative to the Mantoux skin test has been developed and relies on the detection of IFN-γ release in blood samples exposed to an array of *M. tuberculosis* specific antigens. As the antigens are specific to *M. tuberculosis,* previous vaccination with the BCG vaccine does not interfere with the result (Jassal and Bishai, 2009; Dheda *et al*., 2010). Furthermore, there are DNA based diagnostic tools that allow rapid amplification of tuberculosis specific genes. However, staff training and laboratory facilities in many regions worldwide which have limited resources, has limited the application of these diagnostic tools (Jassal and Bishai, 2009).

1.2.5.2 Treatment

Although TB in most cases in the developed parts of the world is to a large extent curable, for the chemotherapy susceptible strains, it still takes administration of 3-4 antibiotics over the course of >6 months. These antibiotics normally comprise isoniazid and rifampicin for 6 months with an addition of pyrazinamide and ethambutol for the first 2 months (Table 2) (Ducati *et al*., 2006; WHO Global Tuberculosis Report 2012).

First line drugs	Second line drugs
Isoniazid	Aminoglycosides
Rifampicin	Polypeptides
Ethambutol	Fluoroquinolones
Pyrazinamide	Thioamides
Streptomycin	Cycloserine
	Aminosalicylic acid

Table 2 First- and second line drugs used in tuberculosis treatment.

Although treatment with first-line antibiotics is inexpensive, the length of the treatment results in many patients failing to complete the course of antibiotics. This has resulted in the emergence of an increasing number of increasingly resistant strains, which will be addressed below. Treatment of resistant strains is not only more costly but also commonly takes longer and more importantly, has a lower success rate (Doherty, 2012).

As both diagnosis and treatment primarily performed after symptoms of infection have been established, the infected individual already is at an infectious state meaning that treatment is primarily a type of disease control that has little effect on the actual spreading of the disease (Doherty, 2012). To counter this diagnosis, treatment has to either be done on all individuals regardless of symptoms or a proper vaccine has to be developed.

1.2.5.3 BCG and vaccine development

Currently only one vaccine exists for commercial use. The BCG vaccine is an attenuated strain of *M. bovis* and it is most commonly distributed to children as it has proven most effective in preventing tuberculous meningitis and miliary TB. However, the vaccine has a very varied efficiency in preventing pulmonary TB, which is the most prevalent form of TB in adults (Leung *et al*., 2001; Rodrigues *et al*., 2005, Ducati *et al*., 2006; Doherty, 2012).

A lot of research is being put into the development of new vaccines. One avenue that has been investigated is increasing the efficiency of the existing BCG vaccine by introduction of specific parts of the RD1 domain (Pym *et al*., 2003; Skeiky and Sadoff, 2006). Another approach is the generation of a new attenuated tuberculosis strain by deleting specific virulence genes to render the bacteria non-pathogenic, but still capable of mounting a potent immune response (Skeiky and Sadoff, 2006). Finally, some groups have worked on the incorporation of specific *M. tuberculosis* antigen sequences into viral vectors, which are then introduced to mount a controlled immune response towards the produced antigen.

However, the creation of a new vaccine is a lengthy process and as time passes the number and complexity of resistant tuberculosis strains increases.

1.2.5.4 Resistant strains and incidence

It is estimated that today approximately 50 million individuals are infected with multidrug-resistant TB (MDR-TB) and of these around half a million develop active TB each year (Gegenbacher and Kaufmann, 2012; WHO Global Tuberculosis Report 2012).

MDR-TB is defined as a strain resistant to more than one antibiotic. Especially troublesome is the increased number of extensively drug-resistant (XDR-TB) strains, resistant to rifampicin, isoniazid, fluoroquinolone and to any of the injectable antibiotics capreomycin, kanamycin and amikacin (Jassal and Bishai, 2008). Of particular concern is the emergence of totally drug-resistant (TDR-TB) strains which have recently been described that are also resistant to all second-line drugs (Velayati *et al*., 2009; Udwadia *et al*., 2012).

Compared to the normal >6 month treatment regimen, the WHO has recommended that patients with MDR-TB receive intensive treatment for 8 months and then continue treatment for a total duration of 20 months (WHO Global Tuberculosis Report 2012). Furthermore, resistant strains require a more individualised treatment than susceptible individuals' further complicating infections with resistant strains, especially in resource limited regions (Jassal and Bishai, 2009).

The requirement for new efficient and low-cost diagnostic tools and chemotherapeutics is desperately needed if the WHO goals of eliminating TB as a

global health issue by 2050 are going to be fully realised (WHO Global Tuberculosis Report 2012).

As most anti-tuberculosis treatments require the internalisation of the drug in order to be functional, a new approach to anti-tuberculosis treatment could be the implementation of non-internalising sterilisation techniques, for example targeted radionuclide therapy, which has already proven efficient in cancer treatment. Apart from helping in sterilising already resistant strains it could potentially also aid in the prevention of the establishment of new ones, while also having potential for diagnosis.

1.3 Targeted radio nuclide therapy and imaging

1.3.1 Types of radiation and applications

There are three types of radioactive emissions important for radio nuclide therapy, α-, β^- and Auger electron radiation, and two central for imaging: γ- and β^+ radiation (Dearling and Pedley, 2007).

α-radiation is the result of nuclear decay, which results in the release of a double positively charged helium nucleus consisting of two neutrons and two protons. Due to the relatively large mass compared to other types of radiation and its charge, it has a very low tissue penetration rate and thereby short range. As a consequence of this the linear energy transfer (LET) is generally very large, in the range of 80 keV/μm making it a suitable candidate for therapy (Kassis and Adelstein, 2005; Sadeghi *et al*., 2010). LET is a term associated with particular emissions. The unit for LET is most commonly keV/μm or MeV/cm and as a consequence a denotation of the amount of energy on average deposited along a pathlength by an emitted particle. It is in some cases referred to as the “stopping power” (ICRU report 16, 1970). LET is dependent on 3 factors: velocity, charge and mass of the emitted particle. Although the value of LET technically varies along the trajectory it is for most intents and purposes considered as an average distribution. However, an important general feature of LET is the shorter the pathlength of the emitted particle, the higher the LET. Upon emission the particles will have a certain intrinsic energy and as they interact along a path with other atoms this energy will be deposited in fractions until the energy is so low that an interaction will make the particle come to a halt or be absorbed. As photons do not have mass they interact differently with their

surroundings. LET is therefore generally not associated with γ-radiation (ICRU report 16, 1970). γ photons have 3 ways of losing energy, largely depending of the initial energy of the photon: 1) all energy can be absorbed by an orbital electron via the photoelectric effect, causing the ejection of the recipient electron; 2) Compton scattering in which part of the energy of the photon is transferred to an orbital electron thereby decreasing the energy of the photon and increasing the wavelength; and 3) the photon result in pair production in which the photon is converted to mass and kinetic energy of an electron-positron pair. This is generally for high energy photons as this requires nuclear interactions (ICRU report 16, 1970). To designate LET to γ-radiation is therefore practically meaningless.

Another term important with relation to radiation is the inverse square law. Although the inverse square law is applicable to many domains in physics from gravity to magnetic fields etc., it also relates to the distribution of radiation of ionising radiation from a source. In essence it states that intensity, or dose, is inversely correlated to the square of the distance:

$$Intensity \propto \frac{1}{r^2}$$

This is not only important in health and safety considerations when working with radiation, but has implications for the use of ionising radiation, particularly in therapeutic settings. It should not be confused with LET although they seem very similar. The inverse square law is particularly important for both α particles and Auger electrons as they have very short path lengths meaning that they deposit a very large dose in a very confined area.

β^- radiation consists of emitted electrons, the result of the internal conversion (IC) of a neutron into a proton resulting in the release of a small charged particle and an anti-neutrino. Due to the smaller mass and less charge of the β-particle it has a longer range and a generally lower LET compared to α-particles. The benefits of using this β-radiation over α-radiation would be the lower degree of tissue damage, however as the range is larger this damage would be spread over a larger area. Furthermore, due to the lower energy, generally larger doses are needed in the targeted tissue in order to elicit a response (Sadeghi *et al*., 2010). Despite the disadvantages, β^- emitters are the main isotopes utilised for radiation therapies in cancer (Kassis and Adelstein, 2005; Buchegger *et al*., 2006; Sadeghi *et al*., 2010).

β^+ particles are created by the internal conversion of a proton into a neutron. These particles are primarily used for imaging purposes and will not be elaborated further.

γ-radiation is, as mentioned previously, an emitted photon and thereby has no mass. It can be generated via several pathways including nuclear fission, nuclear fusion, in concert with either α- or β- emissions or simply when an atom returns from an excited state. As γ-radiation is composed of photons it has a very high tissue penetration rate compared to α- and β- radiation (Table 3).Consequently γ-radiation is a poor candidate for therapeutic purposes but is optimal for imaging, for which it is primarily used. However, many isotopes that emit γ-radiation also release so-called Auger electrons, which shows potential in therapeutic settings and will be addressed later.

Type of radiation	Range in tissue	$E_{(min)}$-$E_{(max)}$	Linear Energy Transfer (LET)	Application
γ-photon	-	~ 100 keV		Imaging
α-particle	40-100μm	5-9,000 keV	80 keV/μm	Therapy
β-particle	0.05-12 mm	50-2,300 keV	0.2 keV/μm	Therapy
Auger electron	2-500 nm	eV- keV	4-26 keV/μm	Therapy

Table 3 An overview of the various types of radiations, their range, average LET, examples of isotopes with that emission and typical applications (Kassis and Adelstein, 2005; Buchegger *et al*., 2006).

1.3.2 Radioactive isotopes

The different properties of the various existing types of nuclear radiation means that each type of radiation has very specialised use in medical settings, which opts for careful consideration when choosing the isotopes to be used in each particular situation (Table 4).

Several factors need to be evaluated: the physical and chemical properties of the candidate isotope including half-life and the LET of the isotope (Table 4), the methodology of the labelling and the behaviour in biological settings, with particular interest in the potential dissociation of radionuclide from the targeting agent, or effects on the bio distribution of the targeting agent (Sadeghi *et al*., 2010).

Radio nuclide	Type of radiation	Energy	Range	T1/2	Application
^{99m}Tc	γ + Auger electrons	140 keV + 0.9 keV	-* + several nm†	6 hrs	Imaging/(therapy)
^{111}In	γ + Auger electrons	173, 247 keV + 0.9 MeV	-* + several nm†	2.8 d	Imaging/(therapy)
^{125}I	γ + Auger electrons	35 keV + 0.179 MeV	-* + several nm†	60.1 d	Imaging/(therapy)
^{123}I	γ + Auger electrons	159 keV + 1.2 MeV	-* + several nm†	13.2 hrs	Imaging/(therapy)
^{213}Bi	α	8.3 MeV	60-85 µm	0.8 hrs	Therapy
^{211}At	α	6.8 MeV	61 µm	7.2 hrs	Therapy
^{225}Ac	α	6.8 MeV	50-80 µm	10.0 d	Therapy
^{188}Re	β^-	2.1 MeV	10.4 mm	0.7 d	Therapy
^{90}Y	β^-	2.3 MeV	11.3 mm	2.7 d	Therapy
^{131}I	β^-	0.6 MeV	2.3 mm	8.0 d	Therapy
^{67}Cu	β^-	0.6 MeV	2.1 mm	2.6 d	Therapy
^{177}Lu	β^-	0.5 MeV	1.8 mm	6.7 d	Therapy

Table 4 Overview of some commonly used radio nuclides in radio pharmacy

*= γ-photons have virtually unlimited range †= Auger electrons have shown to have very short range in biological material and the range varies with the energy of the emitted electrons (O'Donoghue and Wheldon, 1996) (Becker and Meller, 2001; Häfeli *et al*, 2001; Anderson *et al*., 2003; Milenic *et al*, 2004; Martinez *et al*, 2006; Dearling and Pedley, 2007; Bryan *et al*, 2008; Sadeghi *et al*., 2010; Sharkey and Goldenberg, 2011; Jurcic, 2013)

Interestingly, it has been shown that the various radio nuclides demonstrate considerable differences in bio-distribution. It was shown that an anti-glucouronoxylomannan murine antibody labelled with either ^{188}Re or ^{111}In revealed that although their uptake in lung tissue was comparable, their blood clearance rate varied, where the ^{188}Re labelled fragment was cleared approximately 5 times faster. Furthermore, their uptake in liver was also significantly varied with a much higher degree of accumulation in the liver of the ^{111}In-labeled fragment (Dadachova *et al.,* 2007). This particular case could be explained by the accumulation of ^{111}In mAb catabolites in the liver, whereas the ^{188}Re nuclide is attached to the mAb via SH groups. Upon mAb catabolism this is converted into a perrhenate anion (ReO_4^-), which is rapidly cleared through the kidneys (Dadachova et al., 2007). Thus, it is not only the targeting moiety that is important in the design of the pharmaceutical; the radio labelling may affect the distribution as well as the kinetics of the targeting moiety and potential catabolites (Blok *et al*, 1999; Staud *et al*, 1999).

Furthermore, the stability of the labelling technique itself is an important factor to consider. A study showing antibodies chelate-labelled with various radio nuclides, as well as using various chelating agents displayed varied degrees of stability in serum and biodistribution (Cole *et al*., 1987; Arano *et al*., 1995). This may have an effect on the applicability of the construct in both imaging and therapeutic scenarios.

1.3.2.1 Imaging isotopes

Isotopes chosen for imaging have generally short half-lives and are generally γ and β^+emitters.

The most commonly used radionuclide for pharmaceutical imaging purposes is ^{99m}Tc, a metastable decay product of molybdenum-99 (Table 1) (Urch and Welch, 2006). Several advantages are associated with ^{99m}Tc, including low cost and a relatively short half-life. In addition, the energy emitted by ^{99m}Tc photons is optimal for scintigraphic detection with a gamma detector thus resulting in high quality data (Brouwer *et al*., 2008). Additionally, ^{99m}Tc has been shown to also emit Auger electrons, which may have therapeutic value at increased dose rates and will be explored later (Donoghue and Wheldon, 1996). However, this does mean that potential damaging effects on the targeted tissue has to be taken into consideration. Recently however, there has been a decreased production of ^{99m}Mo production, the precursor to ^{99m}Tc due to the shutdown of old nuclear reactors. This has researchers and medical staff either try other isotopes, decrease the dose of ^{99m}Tc and/or increase the sensitivity of the imaging equipment (Thomas and Maddahi, 2010).

Another γ-emitter is ^{111}In, which also emits Auger electrons, and is also primarily utilized for imaging (Khaw *et al*., 1980).

1.3.3 Radio imaging

Due to the tissue penetration ability of in particular γ-radiation and the fairly easily detectable nature, radio imaging is a very attractive means to detect the localisation of not only cancers but recently it is also being used to visualise the location of infections, specifically targeting bacteria and furthermore being able to distinguish between infections and sterile inflammation as well as between bacterial and fungal

infections (Welling, 2002; Meléndez-Alafort *et al*., 2004; Lupetti *et al*., 2003; Dadachova and Casadevall, 2009).

This is of particular interest in immuno-compromised individuals as localisation of infections can be more problematic as an immune response is not mounted thereby potentially masking infections. Furthermore, it could be particularly useful to not only localise but also visualise the spread of an infectious agent and help determine the efficiency of the utilised antimicrobial treatment.

As opposed to the available techniques such as ultrasonography, CT and MRI, radio imaging offers a more specific detection of infection (Walker *et al.*, 2007). Whereas CT and MRI rely on alterations in the tissue, radio imaging is potentially able to visualize infection at a much smaller scale, and allows whole body imaging at once as opposed to CT and MRI where the focus primarily is on parts of the body. This can help in elucidating localisation of infections in patients with fevers of otherwise unknown source (Becker and Meller, 2001; Akhtar *et al*., 2005; Walker *et al*., 2007; Brouwer *et al*., 2008).

One of the most important aspects for *in vivo* imaging is contrast, or signal-to-noise-ratio. Greater contrast can be achieved by lowering the circulation time of the imaging agent, thereby increasing target to non-target ratios, and by enhancing the binding specificity (Blok et al, 1999; Weisser and Hall, 2009). For this reason a lot of research has been put into developing targeting agents that have low circulation time. This not only increases the contrast of the imaging, as imaging will to a larger extent be based on binding affinity to the target and not blurred by retention of imaging agent in circulation, but also decreases the timeframe the patients are

subjected to radiation (Müller and Schibli, 2013). Other important aspects include excellent tissue penetration, high affinity to the target, high specific uptake and retention in the target tissue, stability *in vivo*, easy preparation and safe in human settings (Müller and Schibli, 2013). Some promising agents include single chain variable fragment (scFvs), which will be discussed later. However, a low circulation time could prevent the imaging agent from reaching detectable levels at the site of interest.

Another aspect that has garnered attention in the field of imaging is the pre-targeting of unlabelled targeting agents. This has proven very efficient in reducing non-target organ localisation. This increases localisation of labelled targeting agents in target tissues due to the reduced non-specific binding (Schoffelen *et al*., 2010; Sharkey and Goldenberg, 2011).

In 2003 the existing radiopharmaceuticals included ^{67}Ga, ^{111}In, or ^{99m}Tc-labeled polyclonal antibodies as well as ^{111}In-oxine or ^{99m}Tc-hexamethylenepropyleneamine labelled white blood cells. These were, however, unable to distinguish between infection and sterile inflammation (Becker and Meller, 2001; Welling *et al*., 2001; Lupetti *et al*., 2003; Akhtar *et al*., 2005; Walker *et al*., 2007; Goldsmith and Vallabhajosula, 2009). Furthermore, there were several drawbacks associated with the use of leukocytes including difficult protocols and time-consuming procedures with the risk of transferring blood-borne infections such as Hepatitis C and HIV (Akhtar *et al*., 2005; Walker *et al*., 2007; Goldsmith and Vallabhajosula, 2009). Even considering these drawbacks, radio-labelled leukocytes remain the most utilized agent for infection imaging (Goldsmith and Vallabhajosula, 2009).

In one clinical trial researchers were able to distinguish between infection and sterile inflammation by using a truncated mouse antimicrobial agent, UBI 29-41, labelled with ^{99m}Tc (Akhtar *et al*., 2005). Sterile inflammation was induced by injection of bacterial lipopolysaccharides. ^{99m}Tc-labelled ubiquicidine 29-41 was shown to be able to detect both bacterial as well as fungal infections and more importantly able to distinguish between infection and sterile inflammation (Welling *et al*., 2002). A study by Akhtar *et al*. (2005) showed that optimum in imaging was obtained only 30 minutes following injection (Akhtar *et al*., 2005; Walker *et al*., 2007). Although the prospects are good, more investigation is needed within the field of radio imaging.

By exchanging the radionuclide upon the targeting agent with one emitting a different type of radiation, it may be that a targeting agent utilized for imaging could be used in radiotherapy.

1.3.4 Radio nuclide therapy

The structural integrity of DNA is of vital importance to all organisms. For this reason a considerable amount of research has been put into the controlled utilisation of radio nuclides for the destruction of, most commonly, unwanted cancerous cells. Recently, research has been put into expanding the repertoire of radiation therapy to infectious diseases as well, which will be detailed below.

The most basic type of radiotherapy is the irradiation of a specific area of the body with external photonic radiation sources. By utilising several sources a focal point is created where the absorbed dose is much higher than the surrounding tissue. This method is very often utilised in concert with chemotherapy (Web 2).

Although in theory it is only the focal point that experiences high enough doses for cell death, many patients experience damage to the surrounding tissue making wound healing, among others, a major issue (Haubner *et al*., 2012). Furthermore, a big problem with cancer therapy is the common establishment of secondary cancers (Trott, 2009; Tubiana, 2009). Generally, the side-effects of radiation therapy are grouped into early and late side effects. The early side effects of radiation therapy include erythema, dry desquamation, hyperpigmentation and hair loss where the late side effects comprise skin atrophy, telangiectasia, dyschormia, dyspigmentation, fibrosis and ulcers (Haubner *et al*., 2012). For this reason, much research has been put into targeted radio therapy (Adelstein *et al*., 2003; Dadachova *et al*., 2004; Buchegger *et al*., 2006; Dadachova *et al*., 2007; Dearling and Pedley, 2007; Sharkey and Goldenberg, 2011; Jurcic, 2013). By targeting the radiation source to where it is needed it is not only possible to increase the absorbed dose of the cells of interest, but also decrease the adverse effects to the healthy surrounding tissue. Furthermore, problematic metastases can potentially be more easily targeted.

Most research into the field of radiotherapy has been performed with cancer in mind, however the disadvantage of cancerous cell lines is their often indistinguishable antigenic properties compared to healthy cells. As the surface antigens of infectious agents are comparably considerably different to human cells, research has been put into investigating whether targeted radiotherapy can be used for infectious diseases as well.

1.3.4.1 Radiotherapy of infectious diseases

Most research of radiotherapy has been in the field of cancer therapy. However, recently there has been a lot of interest in targeting infectious diseases as well due to not only the emergence of multi resistant strains but also due to the increased number of immuno-compromised individuals. Finally, there is an increased use of incorporated medical devices such as catheters, pacemakers and prosthetic joints, which often is complicated by the development of bio films towards which radiotherapy has proven effective. (Martinez *et al*., 2006; Dadachova and Casadevall, 2009). Martinez *et al.* (2006) found that monoclonal antibody 18B7, specific for capsular polysaccharides on the surface of *Cryptococcus neoformans*, labelled with the α-emitting isotope ^{213}Bi was able to penetrate a biofilm composed of *C. neoformans*. In contrast unlabelled, nonspecific ^{213}Bi labelled antibodies as well as β- and γ- radiation had no effect.

It seems that the general effect of radio therapy upon microorganisms is primarily “direct-hit”, in which cells are killed by radiation from a source directly attached to the cell, however, the “crossfire” effect, where cells are killed by radiation from a source attached to neighbour or distant cells, also appear to be important (Dadachova *et al*., 2004; Dadachova and Casadevall, 2009). The type of radiation used has an impact on whether the primary mode of function is down to “direct-hit” or “cross-fire”. Not surprisingly, α-radiation is primarily responsible to “direct-hit” induced cell death, whereas β-radiation primarily worked through “cross-fire” effects (Nosanchuk and Dadachova, 2012).

Several studies showed that targeted radio-immunotherapy towards two fungal infections with either α- or β-emitters were 100-1000 fold more efficient than gamma radiation in sterilising the infections (Dadachova and Casadevall, 2009). Interestingly, it appears that the various types of radiation induce different types of cell death in fungi. Experiments made on *C. neoformans* showed that gamma radiation primarily induced cell death by membrane disruption, whereas α-radiation significantly reduced the metabolic activity (Bryan *et al*., 2008; Nosanchuk and Dadachova, 2012).

There are several advantages to the use of ionising radiation to combat infectious diseases. One of the advantages of targeting infectious disease over cancerous cell lines is the obvious difference in surface antigens, which minimises the chance of cross-reactivity. However, it has to be stressed that some microorganisms may release certain antigens. This could lead to a more systemic distribution of the radio therapeutic agent. Although it has been hypothesised that in the case of analysed capsular polysaccharide released by *C. neoformans*, the antibodies are thought to have greater affinity to the bound than soluble form. However, it is an issue that has to be considered for each targeted antigen (Dadachova *et al*., 2003; Nosanchuk and Dadachova, 2012).

Another advantage of the use of radiation therapy to combat infectious diseases, over the traditional chemical approach, is that microorganisms are less likely to generate resistance towards ionising radiation compared to the traditional chemical antibiotics as it does not interfere with specific pathways within the cell (Nosanchuk and Dadachova, 2012). However, microorganisms have shown great adaptability

and have been shown to survive very high doses of radiation, such as *Deinococcus radiodurans* surviving doses of 5.000 Gy of γ radiation without effect on viability due to a very efficient DNA repair system (Battista, 1997). So the same considerations for chemotherapeutic agents apply to radio nuclear therapy that treatments must ensure eradication of all infectious agents. Another advantage is that radiotherapy is very unlikely to interfere with any other potential drugs administered. With many complicated infections a cocktail of drugs is administered each of which may have adverse effects when co-administered with other pharmaceutical compounds.

One of the problematic aspects considered from radiotherapy are the potential adverse effects on the host physiology. This was addressed by analysing both platelet counts as well as the generation of fibrous connective tissue in the lungs of treated model mice. Fibrosis, an abnormal generation of fibrous connective tissue at site of injury, had previously been observed in patients irradiated with external radiation sources. Several doses were analysed and no notable difference in platelet count was observed, and as opposed to external beam radiation therapy of the lungs, no fibrous connective tissue was encountered indicating that targeting of radio therapeutic isotopes is much less destructive than the traditional radio therapeutic methods. Most of this can be attributed to the targeting of the radiation (Dadachova *et al*., 2004; Dadachova and Casadevall, 2009).

Interestingly, some groups have shown that radio therapy can not only be used to combat bacterial and fungal diseases but also some viral diseases as well. Considerable success has been found when eradicating mammalian cells infected with Human Immunodeficiency Virus (HIV) and Human Papilloma Virus (HPV) and

it has been hypothesised that radio immunotherapy in combination with traditional antiviral drug therapy may be the key to eradicate a HIV infection (Casadevall *et al*., 2007; Wang et al., 2007; Phaeton et al., 2010; Nosanchuk and Dadachova, 2012). However, as mentioned above a key aspect in radio nuclide therapy is choosing the most suitable isotope.

1.3.4.2 Therapeutic isotopes

When dealing with therapeutic isotopes, here meaning radioactive isotopes that have significant DNA damaging abilities, different aspects of the bio-distribution have to be considered. The most important feature for imaging is the contrast and for this reason the clearance rate of the radio imaging conjugate is of great importance. The same is not necessarily optimal for a therapeutic isotope. If clearance is too fast the therapeutic isotope may not have time enough to inflict the necessary damage to cause cell death. It was found that a conjugate consisting of a therapeutic isotope, ^{131}I, labelled to an anti-CD20 antibody was very quickly cleared. By pre-dosing with unlabelled anti-CD20 antibody to saturate the antibody conjugate “sink”. In this particular case the sink was the spleen and by saturating non-specific antigenic sites a more favourable bio distribution was achieved due to the competition between labelled and unlabelled antibodies. This was evidenced by multiple tumour sites became detectable following the pre-dose of anti-CD20 indicating a better access of the radio labelled antibody to the site of interest. (Kaminski *et al*., 1993; Sharkey and Goldenberg, 2011). Another problem with targeted therapeutic isotopes is that if the targeting agent used is less than 50 kDa, the primary route of clearance is through

the kidneys increasing the possibility of renal toxicity (Sharkey and Goldenberg, 2011)

When choosing the radionuclide for a specific situation it is of interest what the retention time of the targeting agent is. Utilising an isotope with a much longer half-life than the retention time of the targeting agent is not beneficial and neither is using an isotope with a much shorter half-life than the circulation time of the targeting agent.

Radiation sources frequently used in therapeutic settings include ^{213}Bi, which emits a high LET α-particle and ^{188}Re, an energy-rich β-emitter (Dadachova *et al*., 2004; Milenic *et al*., 2004; Bryan, 2008). Both isotopes have very short half-lives, 0.8 hours and 0.7 days, respectively.

As mentioned previously, one of the advantages of an α-emitter over a β-emitter is that the former has a much shorter path-length as opposed to β-emitter making α-emitters much more focused thus reducing the chances of toxicity in adjacent tissue (Milenic *et al*., 2004). However, cross-fire effects can be beneficial when larger areas need to be affected. Furthermore, logistics also has to be considered. As ^{213}Bi has a half-life of only 0.8 hours, this makes it problematic to not only to manufacture but also administer within a very short time-frame. Hence this makes ^{188}Re a potential more realistic therapeutic isotope, despite its disadvantages (Sharkey and Goldenberg, 2011). However a study by Rivera *et al.* showed that ^{213}Bi was had a greater bactericidal effect than ^{188}Re against *Bacillus anthracis* (Rivera *et al.*, 2009)

Other isotopes with value in therapeutic settings include the α-emitting isotopes ^{211}At and ^{225}Ac and the β-emitting ^{131}I, ^{90}Y, ^{177}Lu and ^{67}Cu (Sharkey and Goldenberg,

2011).However, γ-emitting isotopes as ^{123}I, ^{125}I, ^{99m}Tc and ^{111}In have recently garnered increased attention as therapeutic isotopes as they emit another type of radiation in therapeutic settings, Auger electrons.

1.3.5 Auger electrons

In 1925 Pierre Victor Auger discovered that by irradiating a cloud chamber with low energy X-rays multiple electron tracts were generated. These were later dubbed Auger electrons (Kassis, 2004; Kassis, 2011).

Auger electrons are generated by the excitation loss of an inner shell electron. This can happen by several routes: either by the excitation of an inner shell electron, causing it to be emitted (IC), by the uptake of an inner shell electron by a proton (EC) or by photoelectric interactions with outer shell electrons (Adelstein, 2003; Balagurumoorthy *et al*., 2012). In both cases this leaves an unfilled space, most commonly in the innermost electron shell, the K-shell, which is then filled by an electron from one of the outer shells (Kassis and Adelstein, 2005). This transfer releases energy, which can be emitted either as X-ray photons or transferred to another outer shell electron. Upon the reception of this additional energy the electron is emitted as an Auger electron (Kassis, 2004). Depending on the location of the electrons in relation to each other and the shells in which they reside, the emitted electrons are referred to as Auger, Coster-Kronig or super Coster-Kronig monoenergistic electrons (Figure 4). They are all however, collectively termed Auger electrons, which will also be the term used henceforth (Kassis and Adelstein, 2005).

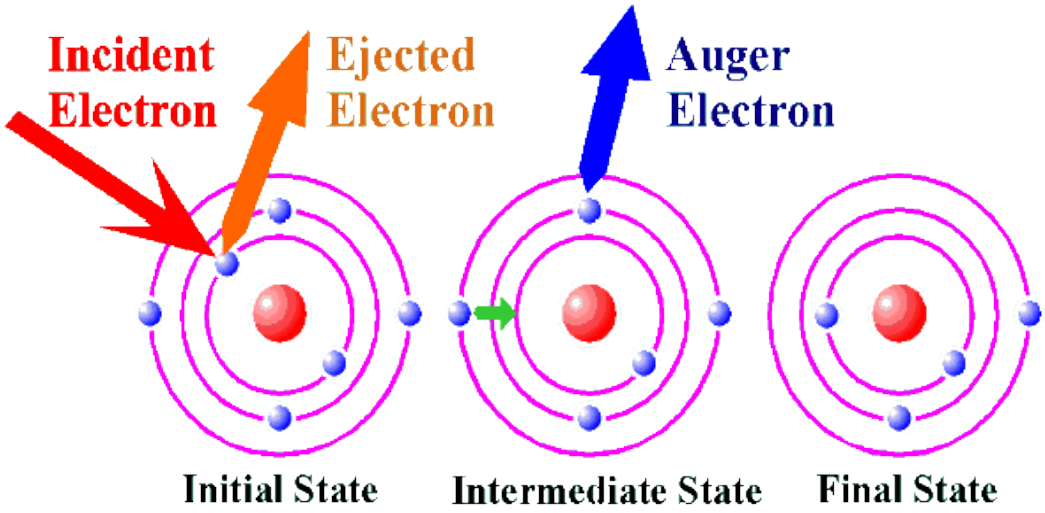

Figure 4 Simplified overview of the process of generating Auger electrons.
In the Initial state, an inner shell is excited by either an incident electron or a photon causing it to be ejected as a photoelectron. This process leaves the atom in an intermediate excited state with an inner shell lacking an electron. Due to the unfavourable conditions of this state an outer shell electron will jump in to fill the place and upon doing so will release energy. This energy can be emitted as either photons or be transferred to another outer shell electron, which upon the reception will become excited and be emitted as an Auger electron. This leaves the atom in the most favourable energetic state (web 3)

In general, there are generated anywhere between 5-50 Auger electrons per decay, depending on the isotope (Kassis and Adelstein, 2005; Kassis, 2011). As this is an average number of electrons generated by decay, this effectively means that in some cases the atom is left in a 50^{+} state. This would result in an immediate filling of the orbitals by stealing electrons from the immediate environment, causing this event to be devastating to everything in close proximity to the decay site.

The energy of the individual Auger electrons, however, is very small when compared to the classical radiation types. Furthermore, the range of Auger electrons is equally very short, varying from a few nanometres up to ~0.5 µm (Figure 5). Due the inverse square law, mentioned previously, this eventually results in a relatively high LET comparable to that of both α-particles and β-particles (Kassis *et al*., 1982; Buchegger *et al*., 2006; Reilly and Kassis, 2010). Furthermore, as Auger electrons have a very small focal point compared to both α- and β- particles this means that it is more likely that the target cell, with an equal dose, is overwhelmed by the DNA damage (Kassis and Adelstein, 2005). It has been estimated that the majority of electrons are deposited within a sphere of a few nm of the decaying atom and in general deposit in the range of 10^6-10^9 rad/decay within this field (Figure 6) (Kassis and Adelstein, 2005).

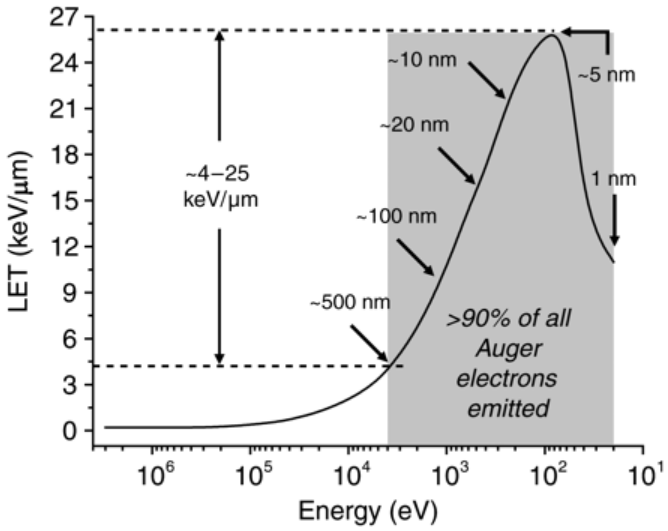

Figure 5 An overview of the LET of Auger electrons in relation to the emitted energy

As indicated the range of the electrons is for the majority inversely related to the LET (Kassis, 2011).

The energy of the Auger electrons ranges from a few eV up to approximately 1 keV and the higher the energy the longer the range (Kassis and Adelstein, 2005). However, as mentioned previously, the range of Auger electrons is very limited and they are therefore very reliant on the inverse square law. Interestingly this means that the lower the energy of the electrons, the higher the LET. But again, due to the short range, there is a point where the range of the electrons is so short that any target is out of reach. This is a particular disadvantage of the Auger electrons as they generally require very close proximity to their target to induce damage. This dependence on close proximity to the target was further investigated by Balagurumoorthy *et al*. (2012). By labelling minor groove binding components of varying length with ^{125}I it was found that the smallest molecules resulted in direct DSB whereas in molecules where the ^{125}I was positioned >12 Å from the DNA helix resulted in DSB caused by indirect mechanisms.

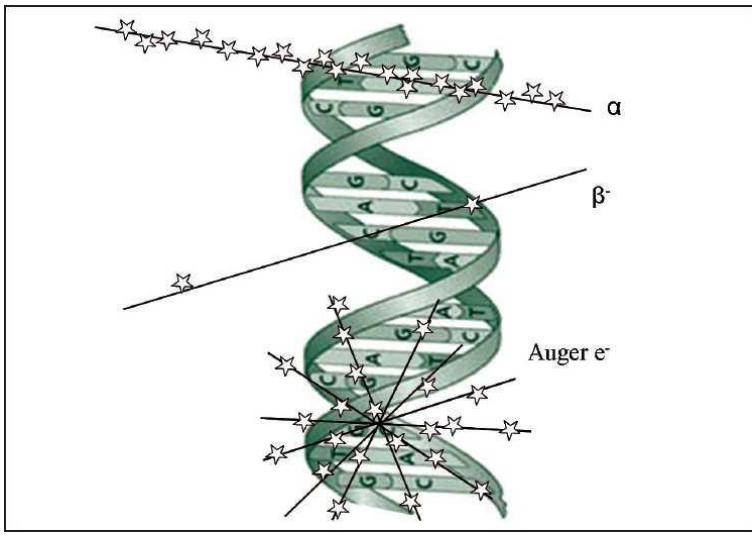

Figure 6 Overview of the difference in therapeutic effects on DNA of α-, β- and Auger radiation

Due to the close proximity of the Auger emitting isotope a large dose is transferred in the immediate vicinity of the decay site as opposed to both α- and β- emissions (Sadeghi *et al*., 2010).

Auger emitters have been for a while considered a candidate for cancer therapy, and several groups have shown indications that Auger electrons indeed can be used for the destruction of cancerous cell lines despite the size of mammalian cells (Buchegger *et al*., 2006). To circumvent this problem many groups have enabled internalisation of the Auger emitters and localisation of the emitters to the nucleus of the cell, by targeting the conjugate to high turn-over receptors which thereby allows rapid internalisation and increased proximity to the target DNA (Narra *et al*., 1992; Michel *et al*., 2003; Sharkey and Goldenberg, 2011; Balagurumoorthy *et al*., 2012). Because of their short range they are particular interesting in treating cancers, particularly in radiosensitive organs such as the bone marrow (Sharkey and Goldenberg, 2011). However, the positive effects of the highly targeted nature of Auger induced toxicity is also one of the drawbacks. Whereas α- and β- radiation has a range of μm-mm in tissue, they can rely on cross-fire effects meaning that not all target cells require targeting to be affected. With Auger electrons, the little cross-fire effects results in a high dependence on efficient targeting (Adelstein *et al*., 2003). The effects of Auger electrons have been analysed in both mammalian and bacterial systems, however the effects analysed were based on incorporation of ^{125}I- labelled deoxyuridine into the genome (Krisch and Ley, 1974; Feinendegen, 1975; Adelstein *et al*., 2003; Balagurumoorthy *et al*., 2012). However, this is not a particularly practical approach to a therapeutic agent. Furthermore as the effects do not appear to require direct incorporation into target DNA to induce DSB, but still close proximity, it was interesting to analyse whether the toxic effect could be accomplished by

simple attachment of the radionuclide to the surface of microbial cells due to the small size compared to mammalian cells (Balagurumoorthy *et al*., 2012).

1.4 Targeting Agents

In the previous section radioactive isotopes were evaluated as damaging agents for fighting infectious diseases. However, due to the destructive and non-specific nature, targeting is very desirable to prevent substantial damage to non-target host tissue.

There are several ways of introducing targeting to a damaging component including selecting an agent, which has a natural bio-distribution in the desired target tissue. An example is radioactive iodine that naturally accumulates in the thyroid gland and for this reason is a well suited agent for treating various thyroid maladies such as thyroid cancer (Keating *et al*., 1949; Beierwaltes, 1978). However, most agents do have an undesirable bio-distribution and accumulate in tissues with high blood flow as the spleen, kidneys, bone marrow and liver. Especially problematic is the bone marrow that is very radiosensitive (Benua *et al*., 1962).

Many types of targeting agents have been evaluated, but the most commonly analysed are antibodies and antibody derivatives such as single chain variable fragments (scFvs), which will be evaluated later.

Most recently, antimicrobial peptides have garnered considerable attention for their non-specific microbial targeting capacity.

1.4.1 Antimicrobial peptides

Several hundreds of both non-ribosomally and ribosomally synthesised antimicrobial peptides have been identified (Hancock and Chapples, 1999). The former are primarily synthesised by bacteria and form the basis for many antibiotics, whereas

the latter are generated by everything from viruses to mammals and will be the focus in this section (Hancock and Chappels, 1999).

1.4.1.1 Synthesis and structure

Although there are few cases of homology there are some shared general characteristics. They are generally between 50-60 amino acids (aa), they have a generally positive net charge (cationic), facilitated by arginine and lysine, and they are generally amphipathic and membrane active (Blok *et al*., 1999; Hancock and Chappels, 1999; Lupetti *et al*., 2003; Brouwer *et al*., 2008). Furthermore, the majority consists of approximately 50% hydrophobic amino acids and generally have a low proportion of both negatively charged and neutral polar amino acids (Hancock and Chappels, 1999).

Despite their limited size they do generally form some secondary structures. Generally, the antimicrobial peptides fall into 4 categories based on their secondary structures (Brouwer *et al*., 2008): Peptides that contain

1. Amphipathic α-helices
2. Two or more disulphide bridges
3. Intermolecular disulphide bridges and also contain a loop/hairpin like structures and
4. Linear peptides lacking cysteine but rich in amino acids such as tryptophan (Indolicidin) or proline and arginine (PR39)

The structure seems to be more important for antimicrobial peptides than size. Many form α-helices and have disulphide bonds, however due to the low degree of

conservation and sequence homology they can adopt most secondary structural motifs. One feature many antimicrobial peptides have in common is the lack of secondary structures in water, when no disulphide bridges are present, and only form the structures when in a membranous or hydrophobic environment or if they self-aggregate (Bello *et al*., 1982; Falla *et al*., 1996; Hancock and Chappels, 1999). Although there is little sequence homology to be found between the various antimicrobial peptides, even within closely related species, there have been some indications of homology in the preproregion of the precursor molecules indicating that there is some limitation to the variation of the sequence involved in translation, secretion or intracellular trafficking (Simmaco *et al*., 1998; Zanetti *et al*., 2000; Zasloff, 2002).

Due to the low degree of sequence homology between antimicrobial peptides and the considerable pharmaceutical potential, some research has also been put into the design of new synthetic peptides, however presently they are primarily alterations made to already existing antimicrobial peptides to modify characteristics such as specificity, stability and toxicity (Hancock and Chappels, 1999).

Antimicrobial peptides are primarily produced by epithelial, endothelial and phagocytic cells during inflammation and they play an important role in both the innate as well as the adaptive immune responses and possibly in linking the two (Figure 7A) (Hancock and Chappels, 1999; Lupetti *et al*., 2003). However, antimicrobial peptides have been found to also come from the degradation product of cationic proteins as for example lactorferricin from lactoferrin and buforin II from histone 2A (Hancock and Chappels, 1999; Zasloff, 2002).

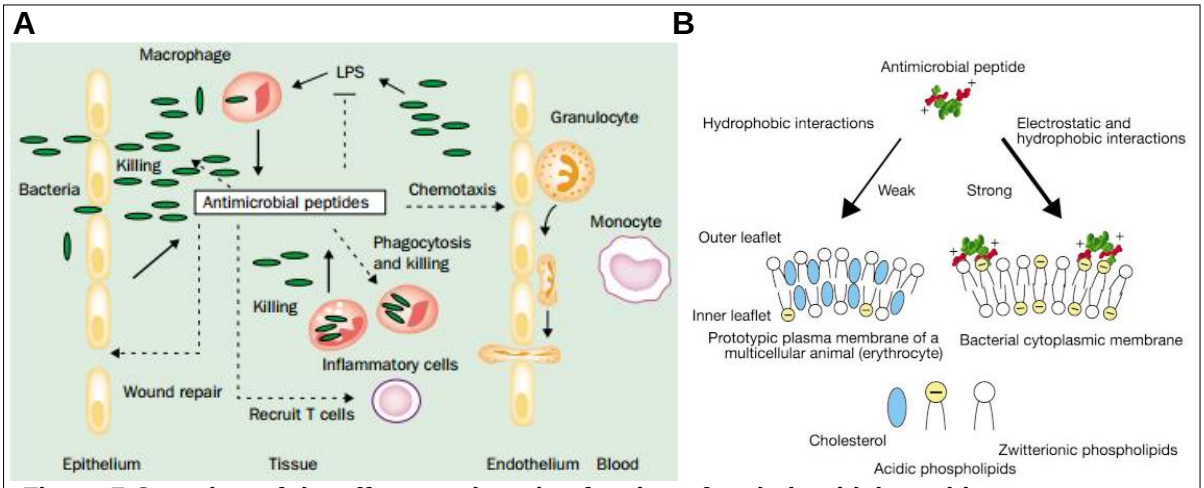

Figure 7 Overview of the effects and mode of action of antimicrobial peptides

A) shows a schematic representation of the complex network of the innate immune defence system where antimicrobial peptides are produced and exert their multi-facetted mode of function. LPS= Lipopolysaccharide (Lupetti *et al.*, 2003). **B)** Shows the electrostatic and hydrophobic interactions with a microbial membrane. This is shown in contrast to a mammalian plasma membrane upon which antimicrobial peptides have no effect. The negatively charged acidic phospholipids are situated in both inner and outer leaflet in bacteria as opposed to only the inner leaflet in mammalian cells. This enables the antimicrobial peptides to distinguish between the membranes (Zasloff, 2002).

The initiation of production of antimicrobial peptides is thought to be induced by contact of antimicrobial peptide producing cell lines with microorganisms, microbial products such as lipopolysaccharide (LPS) or pro-inflammatory cytokines (Brouwer *et al*., 2008).

All antimicrobial peptides are derived from larger precursors, which also include a signal sequence. These undergo proteolytic cleavage and in some cases post-translational modifications which include glycosylation, carboxy-terminal amidation and amino acid isomerisation as well as halogenation (Zasloff, 2002).

Due to their relatively small size and very versatile structures the mode of function of antimicrobial peptides is very simple but efficient.

1.4.1.2 Antimicrobial effects

Antimicrobial peptides have been found to affect the survival of many desirable targets, including gram positive and -negative bacteria, fungi, parasites, enveloped viruses and tumour cells (Brouwer *et al*., 2008). Their mode of function ranges from toxin neutralization to membrane destabilization, perforation, inhibition of metabolic processes and bacteriolysis (Brouwer *et al*., 2008).

Apart from having antimicrobial activities, antimicrobial peptides are thought to have anti-tumour activity, aid in bone repair and play a role in angiogenesis (Figure 7A) (Cornish *et al*., 2004; Otvos, 2005; Steinstraesser *et al*., 2006; Brouwer *et al.*, 2008). It is thought that the Shai-Matsuzaki-Huang (SMH) model primarily explains their general mode of function. The model proposes that the antimicrobial peptides form initial contact with the target microorganisms by electrostatic interactions. Where microorganisms are generally negatively charged on the surface, both due to the cell wall but also due to the existence of negatively charged lipids in the outer membrane leaflet, mammalian and plant cells only contain negatively charged lipids in the cytoplasmic leaflet and do not have a cell wall (Figure 7B) (Yang *et al*., 2000; Zasloff, 2002). Thereby, due to their cationic nature antimicrobial peptides are attracted to the negatively charged surface of microorganisms (Brouwer *et al*., 2008).

Following binding they exert a number of actions including displacement of lipids, alteration of the membrane structure and integrity and in some cases the antimicrobial peptides are internalised into the microorganism enabling interactions and neutralisation of important effector molecules within the cell (Yang *et al*., 2000; Zasloff, 2002). So the lethal effects on the membrane are thought to be caused by

depolarisation of the microbial membrane, perforation of the membrane leading to cellular contents leaking out, membrane potential being disrupted as well as normal membrane functions being affected and induction of hydrolases that degrade the cell wall (Bierbaum and Sahl, 1985; Zasloff, 2002).

Due to their primary action on the membrane of target cells it has been found that the presence of cholesterol in the membrane reduces antimicrobial peptide activity due to the stabilising nature of cholesterol on the lipid bilayer (Zasloff, 2002). Furthermore, increasing the ionic strength of the environment decreases the activity of antimicrobial peptides by reducing the electrostatic interactions on which they rely for binding.

Interestingly, many antimicrobial peptides link the innate and the adaptive immune defence systems. A large group of antimicrobial peptides referred to as defensins are able to recruit peripheral CD4+ T-cells as well as attract immature dendritic cells to the site of infection via chemotaxis, both of which can help fight the impending infection (Zasloff, 2002).

For these reasons antimicrobial peptides are being increasingly evaluated for potential therapeutic and diagnostic purposes.

1.4.1.3 Therapeutic and diagnostic value

Several advantages are associated with the use of antimicrobial peptides as targeting agents. They are small and thus they are able to penetrate the extra vascular tissue and thereby be transported to the site of infection. They also show rapid clearance from circulation and fast excretion (Blok *et al*., 1999; Lupetti *et al*.,

2002). Their ability to better bind to pathogens over host cells (Figure 7B), leukocytes and other cells may be the reason for their excellence in distinguishing between infection and sterile inflammation. Additionally, they distribute more uniformly than monoclonal antibodies (Blok *et al*, 1999; Welling *et al.*, 2002).

As the antimicrobial peptides were among the first lines of defence before the development of the adapted immune responses, this indicates that the structure and function of the antimicrobial peptides are excellent candidates for utilization in imaging as well as therapy (Brouwer *et al*., 2008). That they have existed for so long and still function efficiently, indicates difficulty in developing resistance for microorganisms, which is an important property of new antibiotics as well as imaging agents (Zasloff, 2002; Lupetti *et al*., 2003; Walker *et al*., 2007). Finally, they can be produced *in vitro* relatively easy and at low cost as opposed to larger proteins (Blok *et al*., 1999).

A disadvantage may be the very low plasma half-life of the peptides due to proteolytic cleavage. This can, however, be circumvented by substituting L-amino acids, with their D equivalent (Maloy, 1995; Blok *et al*., 1999; Zasloff, 2002).

Many antimicrobial peptides have been evaluated for the targeting abilities and as new potential carriers of therapeutic or imaging components to sites of infection. One of the most successful and analysed to date is the ubiquicidine peptide fragment 29-41.

1.4.1.4 Ubiquicidine

Ubiquicidine (UBI) is a 6.6kDa, 59 residue, human antimicrobial peptide found in low concentration inside and primarily synthesised by activated macrophages and human airway epithelial cells. It is also found in the human colon mucosa (Brouwer *et al*., 2006). It is, opposed to the majority of antimicrobial peptides, primarily found intracellularly and only released into the extracellular space upon damage due to acute infection (Brouwer *et al*., 2006).

The structural motifs of ubiquicidine has been analysed multiple times and the main observations of its secondary structure indicate the existence of multiple α-helices and a single β-sheet. Analysis showed that fragments encompassing segments of an α-helical domain displayed much greater antibacterial activity than fragments comprising β-sheet (Brouwer *et al*., 2006).

The structure appears to be primarily lipophilic with a single lipophobic domain (Browuer *et al*., 2006). Interestingly, it was found that where the number of lipophilic and cationic amino acids had no observed effect, the order of residues was very important (Welling, 2002; Brouwer *et al*., 2006).

The mode of function is primarily through electrostatic interactions with negatively charged groups on the surface of bacterial cell wall and for this reason UBI has been shown to have a broad targeting potential across many microorganisms (Walker *et al*., 2007).

It is the most utilised peptide in radiopharmaceuticals for treating infectious agents, however, it is primarily fragments of the peptide rather than the native full length peptide that are used (Lupetti *et al*., 2003; Walker *et al*., 2007; Brouwer *et al*., 2008).

A very commonly used derivative of the ubiquicidine peptide is the fragment UBI 29-41, however other variants such as UBI 18-35 and UBI 31-38 also exist (Welling *et al*., 2001; Welling *et al*., 2002; Brouwer *et al*., 2006; Walker *et al*., 2007). The motive for the success of UBI 29-41 is attributed to that over the other peptides generated from ubiquicidine, UBI 29-41 had a high Target-to-Non Target (T/NT) ratio, which in targeting is pivotal (Welling *et al*., 2000).

The half-life in circulation has been estimated to be approximately 16 minutes and it is excreted from the system primarily through renal clearance with little accumulation in liver, spleen and other tissues (Welling *et al*., 2002). No accumulation was observed in thyroid glands or stomach which have previously been showed to be accumulation sites for free ^{99m}Tc, indicating a stable conjugate, which is of utmost importance (Welling *et al*., 2002; Meléndez-Alafort, 2004). Finally, it is not believed to be immunogenic in humans, which has been validated in several studies, and more importantly it has been shown to localise to sites of infection (Akhtar *et al*., 2005; Melendez-Alafort *et al*., 2005; Brouwer *et al*., 2006; Brouwer *et al*., 2008).

Apart from the above mentioned advantages of using ubiquicidine as a targeting agent it has one further benefit that made it particularly suited for this project; it contains a single tyrosine residue allowing the peptide to be single-site labelled with ^{125}I and will therefore ease the monitoring of the labelling process.

1.4.2 Iodine radio nuclides

^{125}I was the radionuclide chosen as Auger emitting radionuclide, despite the low energy, for several reasons.

Initially it was chosen not only due to it being an Auger emitter, which was the type of radiation that was the focus of the radiation study, but it also has a long half-life (60 days) which is well suited for the optimisation of the experimental setup. It would also allow careful optimisation of the labelling process without compromising the potency of the nuclide significantly.

Furthermore, ^{125}I is very well characterised as a radionuclide and has previously shown to induce a greater decrease in survivability in a rodent cell line even compared to two β-emitting isotopes. This shows that despite its low energy compared to for example ^{123}I, it is still capable of inducing toxic effects in the target cells (Bradley *et al*., 1975; Narra *et al*., 1992; Adelstein *et al*., 2003). However, toxic effects of extracellular ^{125}I on a mammalian system appeared to be very low, even when the nuclide was internalised into the cytoplasm but not incorporated into the genome (Bradley *et al*., 1975, Adelstein *et al*., 2003). It was interesting to investigate whether the reduced size of microorganisms compared to mammalian cells would overcome this.

Finally, the labelling chemistry of ^{125}I allows easy replacement with an isotope such as ^{123}I, which emits Auger electrons of higher eV, thereby having a longer range, for therapeutic purposes or ^{131}I for imaging purposes (Adelstein *et al*., 2003). The labelling method chosen for conjugation was the Iodogen labelling method.

1.4.2.1 Radio labelling

Iodination using the Iodogen labelling method uses the chemical 1,3,4,6-tetrachloro-3α, 6α- diphenylglycouril to iodinate the ortho positions of tyrosine residues (Figure 8). This is considered a less invasive iodination process compared to the previously utilised method of chloramines-T (N-chloro-4-methylbenzenesulfonamide) as well as more efficient (Fraker and Speck, 1978). Being solid-phase shows indications of being less invasive on the structural integrity, and thus the functionality as well as the binding affinity, of the labelled proteins (Fraker and Speck, 1978).

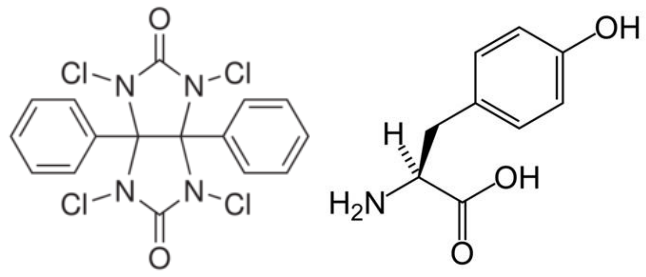

Figure 8 A) Structure of 1,3,4,6-tetrachloro-3α, 6α-diphenylgly-couril (web 3), B) Structure of tyrosine.

The Iodogen labelling is interesting in that it creates positively charged free iodine by oxidisation of the negatively charged iodine. This allows the free iodine to undergo an electrophilic attack on the ortho position(s) on the tyrosine residues in a neutral pH range. Evidence has shown that at more alkaline levels (pH>9), the imidazole ring of histidine residues has shown to be labelled as well (Pierce® Pre-Coated Iodination Tubes protocol).

The mildness of the Iodogen labelling method compared to the previously utilised chloramine-T even allows labelling of live cells and the survivability of the cells labelled with Iodogen was only very slightly affected (Fraker and Speck, 1978).

The Iodogen labelling methods was particularly useful with UBI 29-41 due to the existence of a single tyrosine residue.

One disadvantage of using antimicrobial peptides and UBI 29-41for targeting is the very unspecific nature of the binding. If more specificity is required one of the most analysed and versatile targeting agents are antibodies.

1.4.3 Antibodies

1.4.3.1 Structure and function

In monomeric form antibodies are large proteins composed of two heavy chains and two light-chains (Janeway *et al*., 2005).

There are 5 isotypes of antibodies in vertebrates designated IgA, IgD, IgE, IgG and IgM. The size of the immunoglobulin varies between the subtypes with IgG being the smallest of approximately 150 kDa and the largest being IgM which forms both penta and hexamers of 950 kDa and 1150 kDa in total, respectively (Weisser and Hall, 2009).The size of the antibodies is closely related to the primary function of each subtype. IgGs are by far the most common antibody comprising approximately 85% of antibodies in the blood and are the primary antibody generated when fighting infections (Weisser and Hall, 2009). IgGs can further be divided into 4 distinct isotypes: IgG1, IgG2, IgG3 and IgG4, where IgG1 and IgG3 has the most profound effector functions with IgG1 being the most efficient (Janeway *et al*., 2005; Weisser and Hall, 2009). IgMs, which are the largest are primarily involved in complement system activation. They are the first antibodies to be secreted during an infection and have, compared to the other subtypes, a relatively low affinity but compensates

by forming pentamers (Janeway *et al*., 2005). IgE is slightly larger than IgG at 190 kDa and is primarily involved in mast cell activation and release of histamine making this the primary effector against parasitic infection (Janeway *et al*., 2005). Finally, IgA is primarily secreted to epithelial surfaces and are for that reason primarily involved in antigen neutralisation as neither complement system or phagocytic cells are present in this environment (Janeway *et al*., 2005). The function of IgD, the final isotype of antibodies, is largely unknown. IgGs are however by far the most utilised antibody for therapeutic purposes as they are the primary antibody able to diffuse into the extravascular spaces and are potent in not only the neutralisation and opsonisation of antigens but also in sensitising the target for NK (Natural Killer cell) killing and complement system activation (Janeway *et al*., 2005).

The antibody structure can be divided into two sub-domains: the Fc and the Fab domain (Figure 9). The Fab domain is important in antigen recognition and binding while the Fc region is important in transmitting the antigen binding to other cells in the immune system e.g. via binding to Fc receptors present on the surface of phagocytic cells (Janeway *et al.*, 2005; Weisser and Hall, 2009).

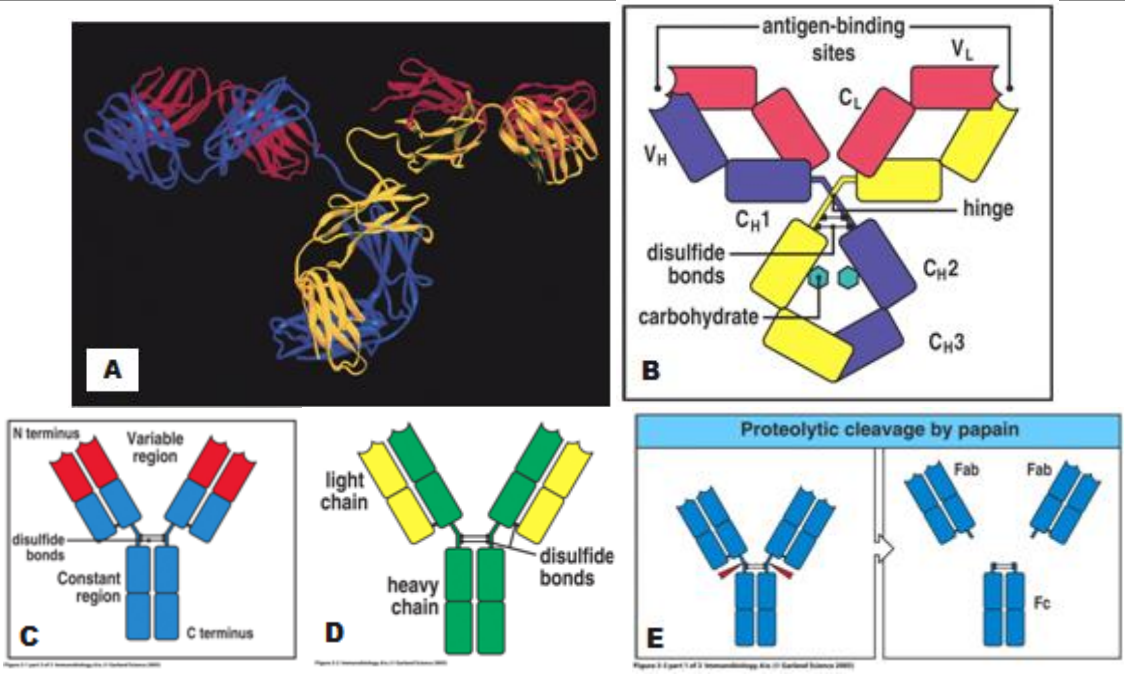

Figure 9 Structural overview of antibody structure and components

(A) Ribbon diagram of an IgG antibody solved by x-ray crystallography. **(B)** Shows a schematic representation of the ribbon diagram in **(A)** displaying the various immunoglobular regions of the antibody as well as the positioning of carbohydrates in the IgG molecule, the position of hinge region as well as the disulphide bridges. **(C)** Shows a stylized overview of the antibody and the positioning of the variable antigen binding region (red) and the conserved region (blue). **(D)**Depicts the positioning of the light chain (yellow) and heavy chain (green). **(E)**Shows a schematic representation of a single cleavage of the antibody by the protease papain (red arrow), which releases the fragments Fab and Fc. All images modified from Janeway *et al*., 2005.

The antigen recognition site is created by a combination of the heavy- and light chain variable regions. The variable region in the heavy chain is composed by a recombination of variable (V), diversity (D) and junctional (J) gene segments. The light chain variable region is created by recombination of V and J gene segments (Janeway *et al*., 2005; Weisser and Hall, 2009). These variable domains come together to form a unique 3-dimensional pattern that is complementary to the antigen they recognise. For this reason the hyper variable regions are also referred to as the complementary determining region (CDR) of the antibody.

The general mode of antigen recognition is based on the complementarity in structure found on the surface of antigens. The binding itself is based on non-covalent interactions such as electrostatic interactions, hydrogen bonds, Van der Waals forces and hydrophobic forces. So although these interactions are rather weak on their own, the better the complementary structure found on the antibody and the better the fit, the more interactions take place thereby increasing the overall binding affinity.

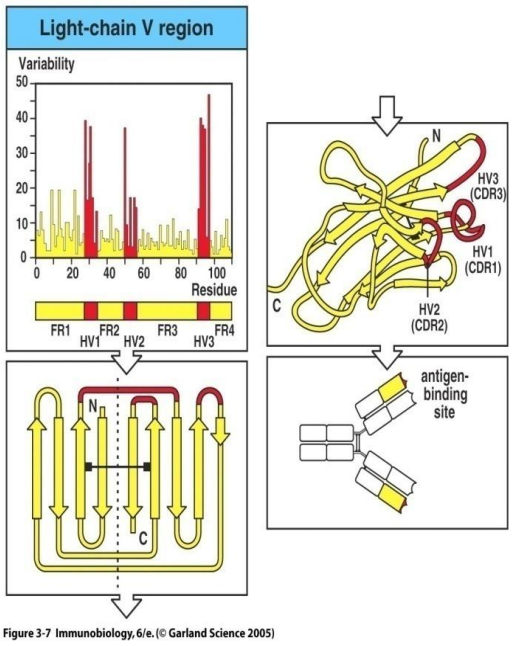

Figure 10 Schematic representation of the CDR- and FR regions

The CDR regions of the variable domains are interspersed in between the framework regions. The framework regions ensure correct folding, enabling and ensuring the assembly of the CDR regions into an antigen recognising region (Janeway *et al*., 2005)

Although the variable domains of heavy and light chains are the most versatile parts of an antibody, the diversity varies greatly as can be seen in Figure 10.

The hyper variable domains are primarily responsible for the antigen recognition whereas the more conserved regions, referred to as framework regions (FR), are important in the stabilisation and correct folding of the antigen-recognising region of the antibody. This allows the hyper variable domains to be exposed on the surface of the protein for easier interaction with the antigen. For this reason the binding affinity of antibodies is often affected when scFvs are created.

Of the three hyper variable domains, CDR3 (Complementary Determining Region 3) is the most variable and of the heavy and light chain domains it is only in CDR3 of the heavy chain in which hyper mutations take place.

There are 3 CDRs per variable domain giving a total of 6 CDRs. Interestingly each CDR contribute differently to the overall antigen specificity accordingly: CDR3H (29%) > CDR2H (23%) > CDR3L (21%) > CDR1H (10%) > CDR1L (9%) > CDR2L (4%). Finally, the framework contributes approximately 4% to the binding affinity (Wilson and Stanfield, 1994; Weisser and Hall, 2009).

Although there are a limited number of gene segments of each type, the recombination in itself also introduces variability. In addition, the antibodies undergo somatic hyper mutation, which introduces point-mutations, thus increasing the variability. This consequently results in virtually unlimited possibilities with regard to antibody design (Janeway *et al*., 2005).

So due to the amazing versatility of the antibodies and the ease with they can be manipulated and designed to be targeted to virtually any target makes them very useful in both therapeutic and diagnostic settings.

1.4.3.2 Therapeutic and diagnostic value

Although monoclonal antibodies appear to be the ideal targeting agents there are several factors that may pose problems for the generation of new pharmaceuticals. These factors include immunogenicity, cross-reactivity with non-target-associated antigens, loss of antigen-binding following conjugation and limited ability of the antibody to access the inflamed area (Blok *et al.*, 1999). Finally, they have a slow

blood clearance rate (Goldsmith and Vallabhajosula, 2009). All these factors are especially important with regard to radio imaging and radio therapy. The long retention time reduces the imaging contrast and with regards to therapy, they have a tendency to have a non-uniform bio distribution and more importantly the long retention time could cause unwanted side-effects by extending non-target tissue exposure (Weisser and Hall, 2009). However, further engineering upon antibodies has generated new antigen recognition moieties, which have shown potential for both imaging and therapeutic application.

1.4.3.3 Single chain variable fragments (scFv)

Due to the large retention time of conventional antibodies, much research has been put into the separation of the antigen recognising part of the antibody to free the antibody of the Fc region.

Many recombinant antibody fragments (rAb) have been generated including scFvs, dia-, tria- and tetrabodies, minibodies and bi- and multispecific scFvs (Weisser and Hall, 2009). ScFvs are however, the most researched and evaluated antibody fragment and is one the most advancing classes of therapeutic molecules (Weisser and Hall, 2009).

ScFvs are antibody fragments composed of the V_H and V_L chains connected by a hydrophilic flexible linker consisting of 10-25 residues. Most commonly they have a high content of glycine, which due its flexibility allows the proper folding of the scFv and therefore is less likely to impact the binding affinity, which is often is seen (Desplancq *et al*., 1994; Weisser and Hall, 2009). However, the fragments can also

be connected non-covalently (Fv), by a disulphide bond (dsFv) or both disulphide bond and linker (sc-dsFv), however when neither linker or disulphide bond are present the scFv shows very low stability and has a large tendency to dissociate at low concentrations (Glockshuber *et al*., 1990; Wörn and Plückthun, 2001; Weisser and Hall, 2009).

The length of the linker has an impact on the aggregation of the molecules, whereas shorter linkers of 0-12 aa have a greater tendency to form dimers and trimers (Todorovska *et al*., 2001; Weisser and Hall, 2009). Linkers of these lengths prevent the scFv from folding properly, which promotes association with a second scFv to form dimers and even smaller linkers force the formation of trimers or even tetramers (Holliger *et al*., 1993; Illiades *et al*., 1997; Dolezal *et al*., 2003; Weisser and Hall, 2009). This and other examples of recombinant antibodies can be seen in Figure 11.

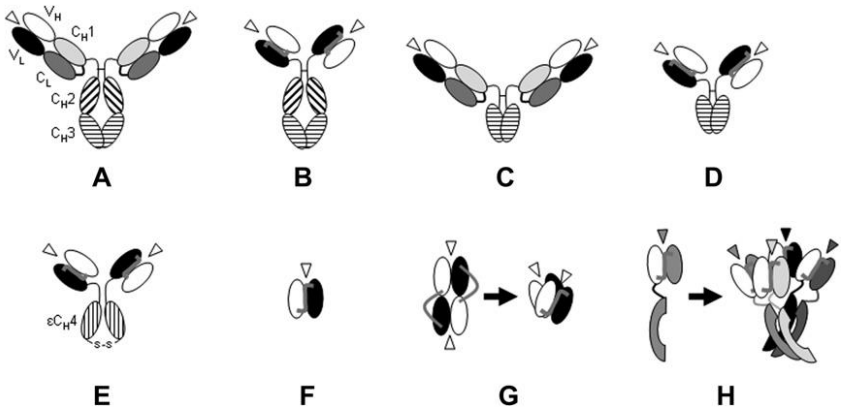

Figure 11 Examples of recombinant antibodies (rAb).

(A) Conventional antibody. White arrow depicts antigen recognition site. Designations and colour-codes are the same through the various representations **(B)** scFv-Fc, **(C)** conventional antibody with deleted CH2-domain **(D)** Minibody, scFv-CH3 **(E)** small immunoprotein (SIP). **(F)** ScFv (VH-linker-VL), linker behind **(G)** diabody **(H)** streptavidin-based tetrameric molecule, scFv linked to streptavidin molecule which allows aggregation into multimeric complexes. (Dearling and Pedley, 2007)

.A big problem when designing scFvs from existing hybridoma fusion cell lines, expressing antibodies towards a desirable target, is the existence of aberrant kappa light chains that may be transcribed (Carroll *et al*., 1988). Aberrant kappa light chains are thought to be a remnant from the parental MOPC-21 tumour which is used for all standard fusion hybridoma cell lines (Carroll *et al*., 1998). The transcript does not result in a functional light chain for which reason it is vital to sequence and analyse the purified mRNA for transcriptional products that fulfil the structural motifs required that will result in functional light chains. The aberrant light chains can be particularly problematic by interfering with sequencing; however cloning into separate vectors will enable them to be distinguishable. Only one product from each hybridoma will result in a functional light chain (Carroll *et al*., 1988).

When designing scFvs two conformations exist: V_H-linker-V_L and V_L-linker-V_H, with the former being more common. Expression efficiency, stability and antigen recognition all vary between the two constructs with the latter having greater binding activity (Desplancq *et al*., 1994; Weisser and Hall, 2009).

The most common template for scFv is the isotype IgG1 due to it being the antibody with greatest effector functions. Furthermore, it has shown great reliability and has desirable physical properties for further engineering (Desjarlais, 2007; Weisser and Hall, 2009).

As scFvs are much smaller than the conventional antibodies, they have a shorter half-life as they are below the 65 kDa cut-off size for filtration in the kidneys (Weisser and Hall, 2009). The average circulation half-life is therefore around 3.6 hours compared to 18-36 hours for a full size antibody (Khazaeli *et al*., 1991; Powers *et*

al., 2001; Weisser and Hall, 2009). As they furthermore do not comprise the Fc region, Fc mediated recycling is not possible (Weisser and Hall, 2009). Thus, scFvs have a much shorter plasma half-life than the original antibody, which increases their applicability, especially with regard to imaging (Milenic *et al*., 2004). However, a short circulation half-life is not always beneficial as for example in many therapeutic settings. If a prolonged circulation half-life is required, the scFvs could be modified by either PEGylation, by including heavy-chain Fc fragments, by associating the Ab fragments with long-circulating serum proteins such as albumin or by including the Fc region both with and without the C_H2 domain, that is primarily involved in the Fc receptor binding (Milenic *et al*., 2004; Weisser and Hall, 2009). Incorporation of cysteines has been shown to improve stability (Desplancq *et al*., 1994).

As scFvs on their own have little therapeutic value they are often evaluated for conjugation purposes for either imaging or therapeutic settings.

1.4.3.3.1 ScFv conjugates

Due to their much higher clearance rate and great adaptability, much research has been put into the development of scFvs conjugated with either radioactive isotopes or toxins for targeted delivery of imaging or therapeutic agents to the sites of infection or tumours. ScFvs have particularly garnered considerable attention in the development of anti-tumour drugs as they not only have a greater tissue penetration rate than traditional antibodies and therefore distribute more uniformly in tumours, but due to the targeting they are also more capable of binding to metastatic tumour sites. This also means both visualisation of the extent of the disease and monitoring

of the progress of the therapy can be performed but also it more fundamentally aids in the eradication of the problematic metastases.

ScFvs are particularly useful in combating infectious diseases. Whereas tumours express antigens that are often indistinguishable from non-tumour cells, infectious agents are antigenically very different from mammalian cells easing the design of novel targeting agents. Furthermore, scFvs can be modified to include segments of the Fc region, which has shown to re-introduce some of the immunogenic properties of the native antibody, such as promotion of opsonisation and complement system activation, further aiding in the eradication of the infectious agent alongside the effects of the conjugated toxic agent (Weisser and Hall, 2009).

However, one issue when utilising recombinant antibodies for therapeutic or imaging purposes is immunogenicity. Most scFvs are expressed in non-mammalian expression systems and this can have an effect on the antigenicity profile of the recombinant targeting agent (Weisser and Hall, 2009). For this reason it is of vital importance to carefully choose the correct expression system as this can affect the down-stream applications. This will be reviewed in the next section.

1.5 Protein expression systems

Once the targeting agent has been chosen and engineered it is often of vital importance to express the protein in the right expression system.

There are several factors that are important to consider when choosing expression systems:

1. Expression rate
2. Expression stability
3. Protein yield
4. Post-translational modifications
5. Toxicity of the product to the factory cells
6. Ease of system
7. Cost of large-scale manufacturing

All of these factors need to also be included in the design of the vector containing the product, as different expression systems potentially require, for example, optimisations of promoter regions or codon optimisation (Casali, 2003).

There are essentially 4 types of expression systems: bacterial, yeast, mammalian and plant expression systems, which will all be evaluated briefly below (Table 5).

1.5.1 Bacterial expression systems

Bacterial expression systems has many advantages including fast expression rate, high yields and has non-complex promoter regions associated with protein expression (Weisser and Hall, 2009). For this reason it is also one of the most commonly used methods for scFv production (Casali, 2003; Leong and Chen, 2008).

System	Protein yield	Post-translational modifications	Ease of system	Cost of production
Bacterial	Up to g/L	No	Easy	Low
Yeast	μg/L- g/L	Yes- but may differ from mammalian profile	Easy	Low
Mammalian	mg/L	Yes	Complex	Expensive
Plant	>1% of total soluble protein	Yes	Easy	Expensive set-up- then low cost

Table 5 Overview of various recombinant protein expression systems.

There are, however, also many disadvantages depending on the protein that needs to be expressed. One of the biggest problems with bacterial expression systems is the lack of post-translational modifications. These are particularly important when expressing antibodies and some antibody derivatives such as glycosylations and proper folding are of vital importance for not only the function of the molecule but also for the immunogenicity of the product (Jefferis, 2005). This may affect the use of the product *in vivo*, which is the eventual end-product. Most glycosylations are found in the Fc region of antibodies, however, 15-20% of antibodies have been found to have N-linked glycosylations in the Fab region (Youings *et al.*, 1996; Jefferis,

2005). Therefore, a glycosylation profile has to be established prior to expression in order to evaluate the potential consequences of choosing a bacterial expression system.

Expression of recombinant proteins in bacterial expression systems can happen via three routes that can all have effects on the structural integrity of the manufactured protein.

The three routes are:

1. Cytoplasmic secretion
2. Periplasmic secretion
3. Inclusion body formation in the cytoplasm

The big problem with cytoplasmic expression of proteins is the very reducing environment often causing misfolding or the generation of insoluble inclusion bodies (Leong and Chen, 2008). However, it has been shown that by slight manipulation of the amino acid sequence, correct folding can be induced and even result in very high yields with as much as 3.1 g/L having been monitored (Martineau *et al*., 1998; Leong and Chen, 2008). Generally, secretion into the periplasmic space allows for better probability of correct protein folding and disulphide bond formation due to the more oxidising environment compared to the cytoplasm (Kipriyanov *et al*., 1997; Chen *et al*., 2004; Leong and Chen, 2008). Although inclusion bodies seem to be an undesirable result, it can be beneficial for the protein production if the generated engineered proteins are either toxic to the bacterial cells or proteolytically unstable

(Leong and Chen, 2008). However, the inclusion bodies would require further *in vitro* refolding in order to result in functional products (Tai *et al*., 1990; Cao, *et al*., 2005; Leong and Chen, 2008). As a consequence the ability of the protein to be *in vitro* refolded has a direct impact on the final yield and for this reason the refolding step has to be carefully optimised for each product (Leong and Chen, 2008).

One of the most common bacterial expression systems is *E. coli*, which has the advantage that it is very easy to manipulate and generally has potential to generate high yields, up to as much as several grams per litre culture (Martineau *et al*., 1998; Chen *et al*., 2004; Weisser and Hall, 2009). Furthermore, as it one of the most characterised microorganisms with a well-established knowledge of basic cellular processes; this allows easy genetic manipulation to attempt improvement of quality and yield of the engineered protein (Casali, 2003; Leong and Chen, 2008).

Furthermore, bacterial expression systems due to their simple culturing processes and inexpensive fermentation costs are able to generate abundant and cheap products (Leong and Chen, 2008). They are however, not capable of post-translational modifications, so if the desired product has a complex glycosylation profile or structure requiring disulphide bridges, eukaryote systems are required.

1.5.2 Mammalian expression systems

Mammalian expression systems have one advantage over bacterial expression systems, which is the ability to implement the correct post-translational modifications. This makes the end product more employable *in vivo*.

However, one of the major drawbacks of mammalian systems is the complexity of use and the lower yields compared to bacterial systems. Nonetheless, concentrations comparable to yields attained in the yeast system *P. pastoris* have been achieved, between 1 and 10 mg/L (Braren *et al*., 2007; Leong and Chen, 2008). Mammalian system do however have more disadvantages compared to yeast systems including high large-scale running cost and complexity of the system, both of which increase the end price of the product, which can easily be avoided using other systems (Streatfield, 2007; Leong and Chen, 2008).

A further disadvantage of mammalian systems over for example bacterial expression systems is the complexity of the cellular pathways. Where bacteria are fairly easy to manipulate to increase yields, mammalian cells are inherently more complex (Leong and Chen, 2008).

Mammalian expression systems are generally considered more appropriate when dealing with complex proteins as they normally require a more complex folding and post-translational modifications as glycosylations, however as scFvs rarely contain glycosylations and are fairly non-complex proteins with regards to folding. Hence, mammalian systems are rarely considered a viable expression system over bacterial or yeast systems (Leong and Chen, 2008).

However, if a complex eukaryotic system is required for protein expression, using the relatively new plant expression system can to some extent, circumvent the cost.

1.5.3 Plant cell expression systems

Plants as expression systems are relatively undeveloped; however, there are implications for future replacement of mammalian expression systems for large-scale protein production.

As plant cells are eukaryotic cells, they are, as mammalian cells, capable of complex post-translational protein modifications and are capable of complex protein folding. There have already been reports of successful scFv production in plants (Streatfield, 2007; Leong and Chen, 2008). However, the yields are still considered sub-optimal for large-scale productions with only as little as 1% of the total soluble protein extracted.

With regards to running costs, plant systems are only considered expensive in the start-up period. As it takes a while for the plants to grow and attain maturity, for the initial period the protein production is very low, however when the plant has fully grown, it is the very easy maintenance, which is a feature inherent to plants systems. Furthermore, one of the advantages is that all the harvesting techniques are already well researched. So when established, plant recombinant protein expression running costs are very low making this one of the primary advantages.

Furthermore, protein pharmaceuticals expressed in plant systems are considered much safer than using native or recombinant animal cell lines (Streatfield, 2007). Plants are particularly considered interesting for the development of edible vaccines, particularly because protein purification is not required, further reducing the costs (Streatfield and Howard, 2003; Streatfield, 2007).

However, there are still many hurdles such as batch-to-batch variability and unoptimised product extraction that needs to be overcome before plant systems can be considered a real competitor to mammalian systems (Streatfield, 2007; Leong and Chen, 2008). For this reason plant systems are for now not viable for large-scale production, but have great implications for the future in replacing mammalian systems for complex protein expression. For now the most utilised eukaryotic system is yeast.

1.5.4 Yeast expression systems

Yeast expression systems can to some extent be considered halfway between mammalian and bacterial expression systems. They are able to perform most post-translational modifications as a lower eukaryote but are still able to give fairly high yields (approximately 5 times higher) when compared to mammalian expression systems, and are reasonably low cost in large-scale manufacturing when compared to mammalian cells (Gasser and Mattanovich, 2007; Leong and Chen, 2008).

As mentioned, the advantages of using a yeast strain over a bacterial strain are important when considering molecules that are dependent on post-translational modifications. As yeast are eukaryotic they have a higher degree of similarity to mammalian cells than bacteria and are able to perform post-translational modifications, as for example glycosylations, disulphide bond formation and proteolytic processing, which are executed by mammalian cell lines (Cereghino *et al*., 2002). However, although yeast is capable of glycosylation, they are not always capable of replicating the glycosylation profile generated by mammalian cells. *S.*

cerevisiae for example has a higher glycosylation rate than *P. pastoris*, sometimes resulting in hyperglycosylation, which may render the product useless due to generated antigenicity (Cereghino *et al*., 2002; Porro and Mattanovich, 2004; Braren *et al*., 2007; Streatfield, 2007; Leong and Chen, 2008).

Yeast expression systems are easily adaptable on a genetic level, and are capable of high levels of expression of proteins both intracellularly as well as extracellularly (Cereghino *et al*., 2002).

Additionally, the purity of yeast product appears to be greater than that of both bacterial and mammalian systems, where toxic pyrogens can be found in *E. coli* product and potential oncogenic and viral nucleic acids from mammalian products (Cregg *et al*., 1993; Porro and Mattanovich, 2004; Leong and Chen, 2008).

One of the problems with yeast expression systems is the great variance in product yields, however more research is needed to understand the intracellular processes that inhibit expression or secretion that may be present, which eventually can affect protein production (Huang and Shusta, 2005; Leong and Chen, 2008).

The most common yeast expression systems for scFv production are *Saccharomyces cerevisiae* and *Pichia pastoris*, the latter of which is the expression system utilised in this project.

1.5.4.1 Pichia expression system

Pichia pastoris is a methylotrophic yeast, capable of metabolising methanol in small doses, surviving on methanol as the carbon source (Bora, 2012).

Foreign gene expression is driven by the alcohol oxidase I gene (AOX1) promoter, which is considered one of the strongest promoters in the yeast species (Cereghino *et al*., 2002; Porro and Mattanovich, 2004; Bora, 2012). Technically there exist two genes encoding alcohol oxidase, AOX1 and AOX2, however AOX1 is vastly overrepresented and can be expressed to levels of more than 30% of total soluble protein in methanol fed cultures (Higgins and Cregg, 1998).

When only glucose is present as carbon source, the promoter is repressed and there is hardly any gene expression, however, when the glucose is replaced by methanol, promoter activity is increased 1000 fold, thereby initiating foreign gene expression (Higgins and Cregg, 1998; Cereghino *et al*., 2002). For this reason it is important to rid the cells of any traces of glycerol when starting protein expression, otherwise the glycerol will greatly inhibit the expression rate. However, in some cases a gradual methanol feeding may be implemented if cell viability is vital, as methanol introduction greatly decreases the growth rate of the organism and concentrations that exceed 5g/L are generally considered toxic (Cereghino *et al*., 2002; Bora, 2012).

The initial step of methanol oxidation by alcohol oxidase (AOX) results in the formation of formaldehyde and hydrogen peroxide. Due to the toxicity of hydrogen peroxide, the initial step in methanol metabolism is performed in the so-called peroxisome where the hydrogen peroxide is kept away from the rest of the cell (Higgins and Cregg, 1998).

It is possible to get a secreted production of protein in *P. pastoris*. This is done by including the α-mating factor (MF-α) prepro signal immediately prior to the gene of interest (GOI) in the plasmid (Higgins and Cregg, 1998). This allows the protein to

be transported out of the cells following post-translational modifications. The MF-α is translated as a N-terminal extension which acts as a secretion signal peptide allowing the peptide to be introduced to the secretory pathway and which, following signal sequence removal, cleaved by Kex2 proteinase as well as 2 Glu-Ala dipeptides by the Ste13 dipeptidase in the Golgi-apparatus from the final secreted protein (Higgins and Cregg, 1998; Cereghino *et al*., 2002, Porro and Mattanovich, 2004). The dipeptidase does not appear to be entirely restricted to that sequence, however, which has previously resulted in a non-homogenous protein mixture, which could have implication for downstream pharmaceutical applications (Porro and Mattanovich, 2004).

Although the signal sequence is inserted immediately prior to the GOI the efficiency of export of the final protein varies greatly (Cereghino *et al*., 2002). It has been found that the exchange of the signal sequence from other yeast strains has proven to be better suited for some proteins. The reason for this is mostly unclear; however there are indications that *cis*-acting elements in the signal sequence and the GOI might play a role as well as the structural nature of the protein. However, being that the exact reason for this difference in secretion efficiency is unknown it is mostly down to trial and error to find the right signal sequence. The *S. cerevisiae* α-mating factor prepro signal sequence, however, remains to be the most widely used sequence and is the one utilised in the plasmid that is used for the expression of the generated anti-LAM scFv (Porro and Mattanovich, 2004).

Expression levels of *P. pastoris* has several times shown to be able to compete with bacterial systems in protein yields with up to as much as 12 g/L produced and

routinely gives protein yields of between 5-40% of total protein in the cells (Bora, 2012).

Furthermore, *P. pastoris* is a fairly tolerant species that can grow under very variable conditions as pH range of 3-7, temperature range of 15-32ºC and Dissolved Oxygen (DO) level range of 5-40%, which allows much room for optimisation of growth conditions (Bora, 2012).

The fact that *P. pastoris* preferably grows under respiratory conditions makes it more useful for large-scale manufacturing compared to organisms that preferably grow under fermenting conditions, as higher cell densities can be achieved and hence higher protein concentrations (Higgins and Cregg, 1998). In fact, oxygen is an important factor in methanol metabolism and oxygen is for this reason a rate-limiting step for recombinant protein expression. For this reason, growing *P. pastoris* cultures in a fermenter generally generates higher protein concentrations, as it is much easier to observe and manipulate the oxygen levels to the optimal levels (Higgins and Cregg, 1998).

Furthermore, as *P. pastoris* preferably grows under respiratory conditions rather than fermenting conditions, there are fewer problems with the accumulation of toxic end products as ethanol and acetic acid with high cell density, as seen in organisms that preferably grow and express foreign proteins under fermenting conditions (Cereghino *et al*., 2002).

Although *P. pastoris* is capable of glycosylations, this does not mean that it is completely identical to the mammalian product. There are two types of glycosylations, *O*- and *N*- linked. Although *P. pastoris* is capable of both it differs

from the mammalian counterpart. In mammalian systems *O*-linked glycosylations comprise a variety of carbohydrates, including N-acetylgalactosamine, galactose and sialic acid. *O*-linked glycosylations in yeast is composed solely of mannose residues. Furthermore, it has been found that although the human counterpart of the human IGF-1 protein there existed no *O*-linked glycosylations, approximately 15% was found glycosylated when expressed in *P. pastoris* (Higgins and Cregg, 1998). Furthermore, the *N*-linked glycosylations differ as well. The oligosaccharide unit in mammalian cells is trimmed to a length of 5-6 mannose components whereas lower eukaryotes generally have longer chains containing 8-11 mannose sugars (Higgins and Cregg, 1998). The length is hypothesised to not only increase antigenicity of the end-product but also potentially interfere with the proper folding and/or function of the protein (Higgins and Cregg, 1998). This clearly demonstrates that although *P. pastoris* is capable of the same post-translational modifications as mammalian cells, it does not mean that the end-product necessarily is identical to the original protein.

Another substantial problem with *P. pastoris* expression is the proteolytic degradation, especially by vacuolar proteases, due to stress responses, irregular growth rates, imbalances in the media and insufficient feeding (Zhang *et al*., 2007; Bora, 2012). Several modifications can be made in an attempt to reduce proteolytic degradation. By supplementing the media with amino-acid rich supplements such as peptone or casamino acid it is to some extent possible to reduce degradation, as the supplements act as decoys for the proteases allowing less proteases to degrade the expressed product. Furthermore, by changing the pH it is possible to reduce the proteolytic activity of the enzymes without affecting the growth of the organism.

Finally, strains with protease mutations have been developed, in an attempt to increase protein yields and enhance stability of the product (Gleeson *et al*., 1998; Higgins and Cregg, 1998). This includes *Pichia pink (P. pink)*, which is the organism utilised for scFv expression in this project.

1.5.4.1.1 Pichia pink

P. pink differs from the original *P. pastoris* cell line in several ways. First and foremost, several mutations have been introduced to the *P. pink* strain compared to the *P. pastoris*. The first mutation is the knock-out mutation of the *ade2* gene, which encodes phosphoribosylaminoimidazolecarboxylase, which is involved in the 6th step of purine biosynthesis. This gene is included in the pPinkα-HC vector utilised as the expression vector of the anti-LAM scFv. This allows the use of adenine-free media as the base for selection.

The lack of *ade2* is also the reason for the pink colour of the colonies of *P. pink*. This is caused by the accumulation of purine precursors. This is also why a colour shift from pink to white is seen in transformed *P. pink*, white being transformed, thus not accumulating the purine precursor. There are furthermore 4 subtypes of *P. pink* as can be seen in Table 6.

***Pichia pink* strain**	**Protease *prb1* knock-out**	**Protease *pep4* knock-out**
1	No	No
2	No	Yes
3	Yes	No
4	Yes	Yes

Table 6 Overview of knock-outs mutant variants of *Pichia pink* strains.

As protease activity on the protein of interest can have a major impact on the expression levels, 4 variants of protease knock outs are available. *Prb1* encodes the vacuolar proteinase B and *pep4* encodes the proteinase A, an aspartyl protease, which among other things is involved in the activation of other vacuolar proteases such as proteinase B and carboxypeptidase Y (Gleeson *et al*., 1998).

One of the side-effects of the protease knock out is the growth rate of the organism. The more knock out mutations the slower the growth rate. Furthermore, the knock-out-mutants are generally weaker than the *wt* (wildtype) strain and require extra care in both storage and growth (Gleeson *et al*., 1998). For this reason the knock out mutations are only generally utilised if protein degradation is a major issue in the production.

1.6 Rationale for this thesis

In the light of the increasing emergence of microbial strains resistant to both first line and second line antibiotics it is becoming increasingly important to find new ways of sterilising these agents. Radioactive isotopes labelled to antimicrobial peptides have already been evaluated for their imaging potential and Auger electrons have been tested for their ability to destroy cancerous cell lines with limited success. It was interesting to combine these methods by conjugating Auger electrons to antimicrobial peptides to evaluate if this might be more advantageous compared to cancerous cell lines due to the reduced size of microorganisms. The use of antimicrobial peptides would enable the analysis to be executed on a range of model organisms due to the relatively non-specific binding.

To alter the strategy a new specific targeting agent was designed. As a target *M. tuberculosis* was chosen which, being an intracellular bacterium is not only complicated to treat but also to diagnose. Therefore, there is a great need for new diagnostic tools and/or therapeutic agents. As scFvs are the isolated variable domains of monoclonal antibodies they are a good candidate as novel targeting agent. Due to the expressed nature and being abundant in *M. tuberculosis* cell wall, LAM seemed a good candidate as antigen to the scFv.

Since therapeutic use would require large concentrations, *P. pink* was deemed a good choice for expression system as this would also allow any potential post-translational modifications mimicking mammalian expression.

1.6.1 Specific Aims

Given the above, this thesis has the following specific aims:

Chapter 3 - To optimise labelling of an anti-microbial peptide with radioactive iodine

Chapter 4 - To evaluate the toxic effects of this radio labelled antimicrobial peptide on a range of model organisms

Chapter 5 - To design *in silico* a targeted construct – i.e. an scFv – against LAM

Chapter 6 - To express and purify the product from chapter 5 for further analysis

2 Materials and methods

2.1 Materials

Unless otherwise stated, all bulk chemicals were analytical grade and purchased from Fischer Scientific Ltd, Loughborough, Leicestershire, UK and all fine chemicals were purchased from Sigma-Aldrich, Poole, Dorset, UK

Ubiquicidine 29-41 stock

Material	Provider/recipe
Ubiquicidine 29-41	Alta Bioscience, Birmingham, UK
Storing buffer	5% acetic acid, pH 4

Iodine labelling

Material/solution	Supplier/recipe
5 mCi $Na^{125}I$ in 10^{-5} M NaOH pH 8-11	Perkin Elmer, Waltham, MA, USA
Tris Iodination Buffer pH 7.5	25 mM Tris HCl. 0.4 M NaCl
Pierce Pre-Coated Iodination Tubes	Thermo Fisher Scientific Inc., Waltham, MA, USA

Instant Thin Layer Chromatography (ITLC) analysis

Material	Recipe
ITLC Running Buffer	85 % Methanol, trace of Coomassie stain solution
ITLC Paper	Pall Life Sciences, Portsmouth, UK

Model organisms

Organism	Supplier
E. coli K-12	From School of Biosciences, University of Kent
S. aureus NCIMB 8625	
C. albicans sc5314	
S. cerevisiae BY4741	

Bacterial and yeast maintenance

Material	Supplier
Bacto™ Peptone	BD Biosciences, Cowley, Oxfordshire, UK
Difco™ Yeast Nitrogen Base w/o Amino Acids	BD Biosciences, Cowley, Oxfordshire, UK
Yeast extract	Oxoid, Basingstoke, Hampshire, UK

Media	Concentration
Lysogeny Broth	1% Bacto Peptone 0.5% Yeast Extract 1% NaCl
YPD	2% Bacto Peptone 1% Yeast extract 2% Glucose
LB/YPD Agar	Media as above with 2% Agar Petridishes (Normal)

Hybridoma CS-35 Maintenance

Material	Concentration
Foetal Calf Serum media	10% Foetal Calf Serum DMEM
CS-35 anti-LAM IgG3 hybridoma cell line	BEI resources, Manassas, VA, USA

Antibody expression analysis

SDS-PAGE

Material	Recipe/supplier
NuPAGE LDS 4x sample buffer	Invitrogen, Paisley, Scotland, UK
Kaleidoscope pre-stained molecular weight standards	Bio-Rad Laboratories, Hercules, CA, USA
20x MES SDS Running Buffer pH 7.7	50 mM MES, 50 mM Tris Base. 0.1 % SDS, 1 mM EDTA
Rabbit anti-Mouse IgG Secondary Antibody, HRP conjugate	Thermo Fisher Scientific Inc., Waltham, MA, USA

Protein Immunoblotting

Material	Concentration
Bjerrum and Schafer-Nielsen	48 mM Tris Base, 39 mM Glycine, 20 % Methanol, $3.75x10^{-4}$% SDS
Bio-Rad trans-blot transfer medium, 0.45 µm	Bio-Rad Laboratories, Hercules, CA, USA
Blocking Buffer	1x PBS 5% Marvel Original Dried Skimmed Milk
6x His MAb/HRP conjugate	TAKARA BIO/Clontech, St. Germaine-en-Laye, France
Washing buffer	1xPBS 0.2% Tween
Super Signal West Pico Chemiluminescent Substrate	Thermo Fisher Scientific Inc., Waltham, MA, USA
Amersham Hyperfilm ECL	GE Healthcare, Buckinghamshire, UK

Gel Staining and drying

Material	Recipe
Coomassie Blue Staining solution	0.25% Coomassie Brilliant Blue R250, 50 % Methanol, 10 % Acetic acid
Destain solution	7.5 % Acetic acid, 5 % Methanol
SilverXpress Silver Staining Kit	Invitrogen, Paisley, Scotland, UK
Gel Drying solution	40 % Methanol, 7.5 % Acetic Acid, 10 % Glycerol
Gel Drying Film	Promega, Madison, WI, USA

V_H and V_L segment isolation

Materials	Provider
Straight A's mRNA Isolation System	Novagen, Darmstadt, Germany
First Strand cDNA Synthesis	Novagen, Darmstadt, Germany
Ig Primer Set kit	Novagen, Darmstadt, Germany
pGEM-T Easy Vector System I	Novagen, Darmstadt, Germany

Transformation of pPinkα-HC anti-LAM into XL-1 Blue Competent cells

Material	Recipe/provider
XL1-Blue Competent Cells	Agilent Technologies Inc., Santa Clara, CA, USA
SOB	2 % tryptone, 0.5 % Yeast extract, 0.05 % NaCl, 1% 1M $MgCl_2$(filter sterilised and added after autoclaving)
SOC	1 % filter sterilised 2 M glucose SOB medium
LB-Ampicillin Agar	LB-Agar 1 % 10 mg/mL Ampicillin stock added where required

Miniprep and Maxiprep of anti-LAM scFv pPinkα-HC vector

Material	Provider
QIAprep Spin Miniprep Kit	QIAGEN Ltd, Manchester, UK
QIAGEN Plasmid Plus Maxi Kit	QIAGEN Ltd, Manchester, UK

Linearisation of anti-LAM scFv pPinkα-HC

Material	Provider
EcoNI	New England Biolabs, Ipswich, MA, USA
NEBuffer4	New England Biolabs, Ipswich, MA, USA

Pichia pink transformation

Media	Components
PAD Agar	1.34% Yeast Nitrogen Base with Ammonium Sulfate without Amino Acids (YNB-aa) 0.125% (-) Adenine Amino Acid Mix (CSM-ADE) 2% Agar

Protein expression induction

All media and components were either filter sterilised or autoclaved prior to use.

Media	Recipe/provider
PPB (Potassium Phosphate Buffer)	132 mL 1M K_2HPO_4 (dibasic) 868 mL 1M KH_2PO_4 (monobasic)
BMGY (Buffered Glycerol Medium)	1% Yeast extract 2% Bacto peptone 100 mM Potassium phosphate buffer (PPB) pH 6 1.34% Yeast Nitrogen Base with Ammonium Sulfate without Amino Acids (YNB-aa) $4x10^{-5}$% Biotin 1% Glycerol
BMMY (Buffered Methanol Medium)	Same as BMGY but with 1% Glycerol replaced with 0.5% Methanol
1M SPB (Sodium Phosphate Buffer) pH 6	1 M NaH_2PO_4
YNBM	2.68% YNB, 0.5% methanol, $4x10^{-5}$ % biotin, 100 mM SPB
Casein	20% Casein stock
cOmplete, EDTA-Free Protease Inhibitor Cocktail tablets (EASYpack)	Roche Diagnostics Ltd, Burgess Hill, UK

Protein purification using HisTrap

All recipes for HisTrap column use were made with MilliQ water.

Solution	Recipe
Sodium phosphate buffer (SPB) pH 7.4	20 mM NaH_2PO_4, 500 mM NaCl
HisTrap column imidazole wash buffer/equilibration buffer	25 mM imidazole in SPB
HisTrap column imidazole wash/equilibration buffer	100 mM imidazole in SPB
HisTrap column imidazole elution buffer	100-500 mM imidazole in SPB
HisTrap column cleaning solution	20% EtOH
HisTrap column "stripping" buffer	2 M imidazole in SPB
HisTrap column recharging solution	0.1M $NiSO_4$

2.2 Methods

2.2.1 Ubiquicidine 29-41 (UBI 29-41) stock

UBI 29-41 was chosen as the antimicrobial candidate as it has a wide host range and has already been evaluated by other groups (Welling *et al*., 2002; Brouwer *et al*., 2006; Walker *et al*., 2007). The UBI 29-41 peptide (AltaBioscience) was resuspended in 0.01 M Acetic acid pH 4 to a stock concentration of 0.5 mM and stored at -80°C as per (Welling *et al*., 2002).

2.2.2 Labelling of UBI 29-41 with NaI

Pierce Iodination Tubes were utilised for the activation of the iodine. The labelling process followed the first 6 steps of the manufacturers' protocol.

A Pierce Pre-coated Iodination Tube was wetted with 1 mL Tris Iodination Buffer and the buffer was hereafter discarded. 100 µL of Tris Iodination Buffer was then added to the tube at the bottom. 10 µL NaI (5 mM) was added to the buffer and mixed. The mixture was incubated at RT for 6 mins to allow the iodine to be activated. The tube was flicked every 30 secs to ensure homogenous activation. The activated iodine mix was added to 1 nmol of protein and incubated for 9 mins again with flicking of the tube every 30 secs to ensure even labelling.

Several concentrations of "cold" NaI, the initial source of Iodine, were tested- 1 mM, 2 mM, 3 mM, 4 mM and 5 mM.

2.2.3 Analysis of labelling using HPLC-MS

100 µL of labelled and unlabelled UBI 29-41 was analysed using HPLC-MS for labelling optimisation. This was done by Kevin Howland at the Department of Biosciences, University of Kent.

Electrospray mass spectra were recorded on a Bruker micrOTOF-Q II mass spectrometer. Samples were separated on-line by reverse-phase HPLC on a Restek Viva Column (C18, 3 µm, 300Å, 2.1 mm x 150 mm) running on an Agilent 1100 HPLC system at a flow rate of 0.2 ml/min using a water, acetonitrile, 0.05% trifluoroacetic acid gradient. The eluant was monitored at 214 nm and then directed into the electrospray source, operating in positive ion mode and mass spectra recorded from 50-3000 m/z. Data was analysed with Bruker's Compass Data Analysis software.

2.2.4 Labelling of UBI 29-41 with ^{125}I

Labelling of UBI 29-41 with ^{125}I was conducted identically to non-radioactive iodine labelling (section 2.2.2); however, this was conducted in a flow chamber behind lead fortified glass shield for protection. 1.0 mCi (37 MBq) Na^{125}I was furthermore added instead of 5 mM NaI.

2.2.5 Labelling analysis by Instant Thin Layer Chromatography (ITLC)

ITLC was performed on 10x1 cm strips of ITLC paper (Pall Life Sciences, Portsmouth, UK). 2 µL radio conjugated UBI 29-41 or activated Na^{125}I was loaded at the centre of the paper 2 cm from the bottom and allowed to dry for 1 hour. The

bottom of the strip was placed in 85% methanol containing a trace of Coomassie staining solution for visualisation of the soaking process. This was done until the solvent reached the top of the paper and the strip was removed and allowed to air dry from 1 hour. The paper was then analysed using Bioscan Miniscan radio TLC strip scanner (Bioscan Europe, Ltd., Paris, France) at 0.5 mm/sec and ITLC LAURA imaging software (LabLogic Systems Limited, Sheffield, UK) for analysis.

2.2.6 HPLC analysis of ^{125}I labelled UBI 29-41

The HPLC analysing the hot labelled UBI 29-41 was conducted at the Rayne Institute, St. Thomas Hospital, London. It was performed on an Agilent HPLC using an Ascentis Express C18 reverse phase column (10 cm x 4.6 mm, 2.7 µm) using an Acetonitrile (ACN) + 0.05% Trifluoroacetic acid (TFA) gradient for elution of the labelled product. The gradient was as follows:

0-10 mins = 5% ACN + 0.05% TFA

10-15 mins = 20% ACN + 0.05% TFA

15-18 mins = 80% ACN + 0.05% TFA

18-21 mins = 5% ACN + 0.05% TFA

The flow rate was set at 2 mL/min and the eluate was collected in fractions of 1 min for the first 9 minutes, 30 seconds from 9-14 minutes and 1 minute fractions from 14-21 minutes. The fractions were then analysed on a Wallack LKB 1282 Gamma Counter Compugamma.

2.2.7 Strain growth and model organism maintenance

2.2.7.1 Organisms

Four organisms were included in the toxicology experiments: the *Saccharomyces cerevisiae* strain BY4741, the *Candida albicans* strain sc5314, the *Escherichia coli* strain K-12 and the *Staphylococcus aureus* strain NCIMB 8625 (. It was decided to include a wide variety of organisms as representatives of various microbial strains. The *S. cerevisiae* strains were chosen to represent non-pathogenic yeast strains, where *C. albicans* represented the pathogenic strains. *E. coli* represented gram negative bacterial strains and *S. aureus* the gram positive bacterium.

Table 7 Overview of model organisms utilised

Strain	Genotype	References
S. cerevisiae **BY4741**	MATα his3Δ1 leu2Δ0 met15Δ0 ura3Δ0	Cohen and Engelberg, 2007
C. albicans **sc5314**	Wt	Diez-Orejas *et al*., 1997
S. aureus **NCIMB 8625 (FDA 209-P)**	Wt	Cowan and Shaw, 1954; Trakulsomboon *et al*., 2001
E. coli **K-12 MG1655**	Wt	Jensen, 1993 McVicker *et al*., 2011

2.2.7.2 Growth curves

All yeast strains were grown in YPD medium consisting of 2% Glucose, 1% Yeast extract and 2% Bacto Peptone. *C. albicans* was grown at 37°C and the *S. cerevisiae* strains were grown at 30°C. All bacterial strains were grown on LB medium made up of 1% NaCl, 0.5% Yeast extract and 1% Bacto peptone and grown at 37°C.

To establish growth curves, 5 mL media was inoculated with one strain and incubated for 1 hr prior to distribution into 24 well plates and loading into the plate reader (SpectroMax multimode plate reader; Molecular Devices, Sunnyvale, CA, USA). The reader was set to grow the organisms at the appropriate temperature and shaking speed, and make measurements of the cultures every 30 min for 24 h for the bacterial strains and 48 h for the yeast strains.

OD_{600} comparisons were made by making several dilutions of the finished cultures and measured on an Eppendorf BioPhotometer Plus spectro-photometer (Eppendorf AG, Hamburg, Germany) as the data from the two machines was incomparable otherwise.

2.2.7.3 OD_{600} versus cell number

10 mL appropriate media was inoculated with overnight culture to an OD_{600} of 0.1 and OD_{600} measurements were made each hour, as well as dilutions were made and the cell numbers were counted using a standard haemocytometer. The linearity between the two data sets was compared allowing conversion of OD_{600} to cell concentration.

2.2.8 Hydrogen peroxide toxicity assay

Overnight cultures of the model organisms were diluted 1:1000 and grown at the optimal growth temperature until they reached the beginning of the log phase, established by OD_{600} readings. They were hereafter diluted appropriately to cell number which would ultimately result in approximately 100 colonies per petri-dish.

Diluted cell cultures were added hydrogen peroxide for a variety of final concentrations (0.5 mM to 70 mM) and media was added to a final volume of 100 µL.

The cultures were incubated at room temperature for 1 hour and hereafter spread onto plates. Yeast strains were grown in 5cm petri dishes; bacterial strains were grown in large 9cm petri dishes for improved spreading and reproducibility of results. Following incubation 50 µL was diluted in 450 µL media. For the yeast strains 20 µL was spread to the small petridishes in triplicates and grown at the optimal temperature for 1 day (*C. albicans*) and 2 days (*S. cerevisiae* BY4741). For the bacterial strains 100 µL was spread to the large petri dishes in triplicates and grown at 37°C for 1 day.

2.2.9 UBI 29-41 toxicity assays

Model organisms were diluted from overnight cultures and grown to the beginning of the log phases. The cells were added to Eppendorf tubes with media and UBI 29-41 to a concentration of 0 µM, 50 µM and 100 µM and a final volume of 100 µL. The procedure was otherwise conducted as in section 2.2.8.

2.2.10 Cold iodine toxicity experiments

The cold iodine toxicity experiments were conducted as elaborated in section 2.2.8. The cells were subjected to two levels of iodine: 0.5 mM and 1 mM. A control group not subjected to iodine was included. All plates were done in triplicate.

2.2.11 Toxicity analysis of ^{125}I-UBI 29-41

The experiment was conducted as per the protocol for innate toxicity assays (section 2.2.9). The dose added to the cells was based on the theoretical MBq values. Two doses were tested: 1 MBq and 5 MBq. The actual values following addition to the cells was measured using a dose calibrator set on ^{125}I setting (Dose Calibrator Model VDC-404, Veenstra Instruments, Joure, Holland). Following incubation, the cells were washed with their respective medium to minimise the amount of free iodine transferred to the plates. This was done by spinning at 13,000 rpm in a Eppendorf table-top centrifuge, removal of the media with care not to remove the pellet and resuspending pellet in the appropriate media for the organism,. This was done 3 times to remove any excess ^{125}I, whether labelled or not. The cells were hereafter plates and incubated as previously elaborated (section 2.2.8). All experimental procedure was performed in flow chamber behind lead glass shielding.

2.2.12 Binding experiments

The experiment was conducted as elaborated in section 2.2.11. Radioactivity associated with *S. cerevisiae* and *E. coli* was measured using dose calibrator before

and after washing as explained above. This was done for the doses of 1 MBq and 5 MBq and the actual doses were established using a dose calibrator.

2.2.13 Hybridoma cell line maintenance

For the purification of mRNA of the anti-LAM monoclonal antibody the murine cell line CS-35 was utilised. This was obtained from BEI resources (Bei Resources, Manassas, VA, USA). The cells were revived by gently thawing the cells and adding the cells to their appropriate media in a T25 flask. The cells were the day after spun down and transferred to fresh media.

Cells were grown on RPMI media containing 10% Foetal Calf Serum at 37°C, 5% CO_2.

2.2.14 SDS-PAGE analysis

Precast NuPAGE Novex 4-12% Bis-Tris Gel, 1.0 mm, 10 well were loaded onto an Xcell SureLock gel running tank. 500 mL 1x MES running buffer was added to the tank. The samples to be analysed were added to 5 µL NU-PAGE LDS sample buffer (4x) (Invitrogen, Paisley, Scotland, UK) and heated to 70°C where after they were carefully loaded to the gel alongside 6 µL Kaleidoscope pre-stained molecular weight marker (Bio-Rad Laboratories, Hercules, CA, USA) The gels were run at 200 V for 35 mins.

2.2.15 Transfer of proteins to nitrocellulose membrane

NuPAGE gels were soaked in Bjerrum and Schafer-Nielsen buffer at room temperature for 30 mins at room temperature. Nitrocellulose membrane (Transblot

transfer medium 0.45 µm; Bio-Rad Laboratories, Hercules, CA, USA) and 4x extra-think blotting paper (Bio-Rad) were soaked in Bjerrum and Schafer-Nielsen buffer for 10 mins. Both blotting paper and Nitrocellulose membrane was cut to the size of the gel.

The papers were assembled accordingly (from top to bottom): 2x buffer soaked blotting paper, SDS-PAGE gel, nitrocellulose membrane, 2x blotting paper.

The sandwich was loaded to a Trans-blot semi-dry electrophoretic transfer cell (Bio-Rad Laboratories, Hercules, CA, USA) and 10V was passed through the gels for 30 mins.

2.2.16 Western blot analysis of anti-LAM IgG3 expression

30 mL blocking buffer (1x PBS, 5% Marvel, 0.2% Tween) was added to the nitrocellulose membrane with transferred protein and was shaken at room temperature for 1 hour. The blocking buffer was hereafter discarded and replaced by 1:1000 rabbit anti-mouse polyclonal IgG HRP conjugate (Catalogue#: PA1-28761; Thermo Fisher Scientific Inc., Waltham, MA, USA) in blocking buffer at room temperature for 1 hour with shaking. The nitrocellulose membrane then underwent three 10 mins washes in 2% Tween in PBS with shaking. The nitrocellulose membrane was then exposed to Super Signal West Pico Chemiluminescent Substrate (Thermo Fisher Scientific Inc., Waltham, MA, USA) for 5 mins according to manufacturer's protocol. The membrane was hereafter transferred to a film cassette and exposed to Amersham Hyperfilm ECL (GE Healthcare,

Buckinghamshire, UK) in a darkroom. The film was developed using a Compact X4 developer (Xograph Healthcare Ltd., Gloucestershire, UK)

2.2.17 mRNA purification and agarose gel analysis

For mRNA purification the Straight A's™ mRNA Isolation System (Novagen, Darmstadt, Germany) was used. $2x10^7$ cells were harvested for the purification of mRNA. Cells were counted using a haemocytometer.

Cells were washed with PBS and quickly after transferred to an RNase free Eppendorf tube where after 5 mL lysis buffer was added. Immediately 50 µL DTT was added to a final concentration of 10 mM. The cells were homogenised for 1-2 minutes by pipetting up and down until the mixture appeared homogenous in colour and texture, then centrifuged for 15 min at 9000xg at RT to remove insoluble material.

2.2.17.1 Preparation of magnetic beads

Magnetic beads were prepared in the meantime: 400 µL (4 mg) magnetic bead solution was transferred to an RNase free 1.5 mL Eppendorf tube and put onto a magnetic column. The beads were captured and the storage solution decanted. The beads were washed with 400 µL wash buffer and vortexed gently until beads were resuspended. The beads were again captured on the magnetic column and the supernatant decanted. 400 µL wash buffer was added again and the magnetic beads once again resuspended and ready for use.

2.2.17.2 mRNA purification

Following centrifugation, the supernatant was gently added to a clean RNase free 15 mL falcon tube. The washed beads (from section 2.2.17.1) were hereafter added and the cell mixture was allowed to incubate at room temperature (RT) for 5 mins.

The particles were hereafter captured on the magnetic column as described previously and supernatant was decanted. 6x400 µL (2.4 mL) wash buffer was added, the solution mixed, beads captured and supernatant decanted. This was repeated with the only alteration that the tube was removed slowly to ensure all beads were at the bottom of the tube. Following the decanting of the supernatant 400 µL wash buffer was added, the solution mixed and the beads were transferred to an RNase free 1.5 mL Eppendorf tube. The beads were once again captured and as much supernatant as possible was removed. 0.5 mL nuclease free water was added and mixed briefly where after the mixture was incubated at 60°C for 10 mins to elute mRNA.

The beads were again captured, but the supernatant was now added to a new RNase free 1.5 mL Eppendorf tube and 2 µL 10 mg/mL glycogen and 50 µL 3M Sodium acetate was added. Hereafter 331 µL (0.6 volumes) isopropanol was added to precipitate the mRNA and the mixture was mixed by vortexing followed by centrifugation at 14.000xg for 10 mins.

The supernatant was removed with care not to touch the pellet. The pellet was washed with 0.5 mL 70% EtOH made with RNase free water and spun at 14.000xg for 5 mins. The supernatant was again removed, as much as possible, with care not

to touch the pellet. The pellet was resuspended in 25-50 µL RNase free water and the absorbance at 260 nm was measured.

The product was analysed on a 1 % agarose gel visualised by incubating in EtBr.

2.2.18 cDNA construction

The purified mRNA was immediately converted to cDNA using the First Strand cDNA Synthesis Kit (Novagen, Darmstadt, Germany) using oligo(dT) primers. 1 µL mRNA mix was mixed with 0.5 µL oligo(dT) primers and 11 µL nuclease free water and heated at 70°C for 10 mins where after 4 µL First Strand buffer, 2 µL 100 mM DTT, 1 µL dNTP mix and 0.5 µL MMLV reverse transcriptase was added and incubated at 37°C for 1 hour. The solution was stored at 4°C.

2.2.19 PCR amplification and analysis of anti-LAM hybridoma VH and VL gene fragments and agarose gel analysis

The light and heavy chain fragments were amplified using the Mouse Ig- primer set from Novagen (Novagen, Darmstadt, Germany), specific for the amplification of a variety of mouse heavy and light chain fragments. The cDNA previously generated was used as template and the primer combinations were assembled as directed by the manufacturer's protocol.

The following program was used for the amplifications:

94°C for 1 min

94°C for 1 min
50°C for 1 min
72°C for 2 mins
} 30x cycles

72°C for 6 mins

4°C hold

The PCR products were analysed on a 1% agarose gel and visualised with ethidium bromide. Positive PCR products were gel purified according to manufacturers' protocol using the QIAquick Gel Extraction Kit (QIAGEN Ltd, Manchester, UK).

2.2.20 Ligation of amplified gene segment into pGEM-T Easy vector and transformed into XL1-Blue competent cells

Following the manufacturers' protocols, the positive gel purified PCR products were ligated into the pGEM-T Easy vector (Novagen, Darmstadt, Germany) using T4 ligase as instructed in the manufacturers notes (Figure 12).

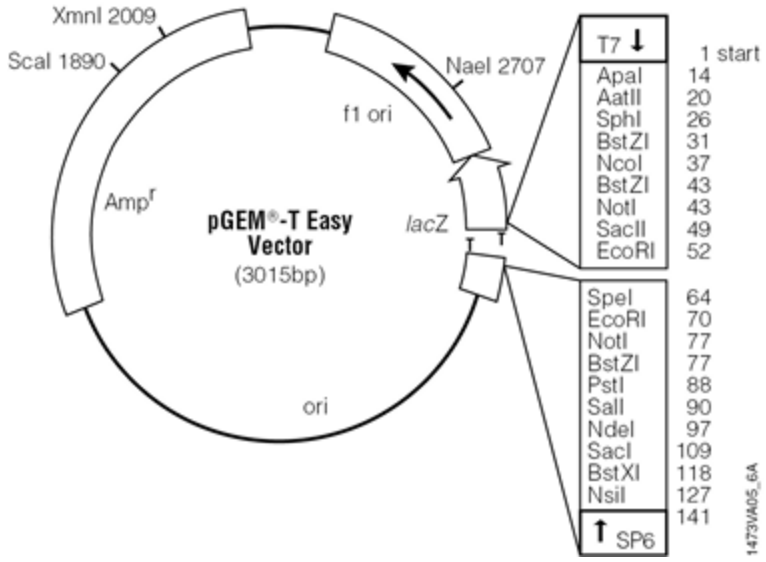

Figure 12 Schematic representation of the pGEM-T Easy vector.

The pGEM-T Easy vector has already been linearised prior to ligation and contain a single 3'-T overhang at the insertion site. This combined with the 5' overhangs generated by the Taq-polymerase utilised for the amplification of the variable domains made ligation straightforward (From Novagen, Darmstadt, Germany).

Each ligation was analysed by digestion with BstZI for insert and the vectors containing insert were transformed into XL1-Blue competent cells (Stratagene) for amplification according to the manufacturers' instructions. Successful clones were analysed for vectors containing insert. DNA was extracted using a QIAprep Spin Miniprep Kit (QIAgen) and the purified products were digested with BstZI for insert verification by analysis on a 1 % agarose gel. Vectors with confirmed inserts were sent to Beckman Coulter Genomics (Beckman Coulter (UK) Ltd., High Wycombe, UK) for sequencing with M13 forward and reverse primers.

2.2.21 Sequencing analysis and editing

All sequences were initially analysed using Chromas Lite for quality control. Questionable regions were deleted in BioEdit which was also used for annealing sequences and removal of vector sequence

2.2.22 *In silico* assembly and optimisation of variable domains

Using expasy.org the result from the removal of vector sequence allowed the translation of the inserts in all reading frames. This allowed the identification of the most promising inserts which were then compared to published variable domain sequences in "Sequences of proteins of immunological interest" (Kabat *et al*., 1991).

2.2.23 Vector construction

StuI was chosen as the 5’ restriction site and KpnI at the 3’ end for vector linearisation in order to ensure correct orientation of the insert. The insert was designed with a MlyI restriction site in the 5’ end and a KpnI restriction site in the 3’ end. The insert was furthermore modified with a His-tag in the 3' end and two stop codons were introduced as well to ensure termination of translation. The *in silico* designed insert was sent to GeneArt along with pPinkα-HC vector (Figure 13) for manufacture.

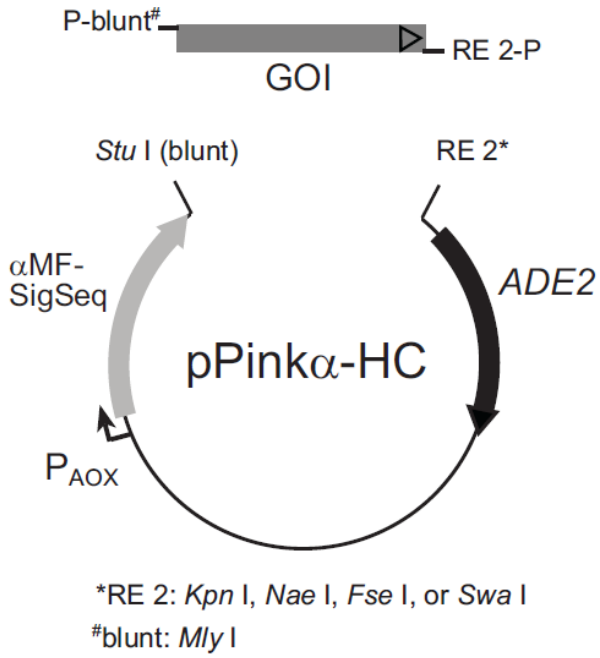

Figure 13 pPinkα-HC vector including important restriction sites.

Schematic overview of the pPinkα-HC vector and the location of the two important features: the α mating factor signal sequence (αMF-SigSeq), which allows the secretion of the gene of interest (GOI), which is inserted immediately after this. Furthermore, the vector contains the ADE2 gene which allows only the transformed cells to grow on the nutrient selective adenine deficient PAD plates. Furthermore, the restriction sites recommended by Invitrogen are included to allow optimal insertion of GOI at the site of interest. In this project, KpnI was chosen as 3' end restriction enzyme (RE 2). StuI and MlyI was kept as restriction enzymes for the 5' end preparation (From Invitrogen, Paisley, Scotland, UK).

2.2.24 Growth of *P. pink*

5mL BMGY in a sterile falcon tube was inoculated with *P. pink* strain I and grown overnight at 30°C shaking at 180 rpm.

2.2.25 Transformation of Pichia pink strains 1 with pPinkα-HC containing anti-LAM scFv

Prior to transformation into Pichia pink, the vector containing the anti-LAM scFv was linearised using EcoNI (New England Biolabs, Ipswich, MA, USA). This was one of

the restriction enzymes recommended by Invitrogen as this enables cleavage at an inconsequential site. The gene of interest was analysed prior to purchase for the presence of EcoNI cleavage sites and found to contain no such sites. Further gel analysis confirmed a single cleavage site. The plasmid was digested using the recommended NEBuffer 4 at 37°C for 1 hour and de-activated at 65°C for 10 min. Following digest with EcoNI the plasmid DNA was purified using the QIAGEN QIAquick Gel Extraction Kit (Cat No. 28704).

100 mL of YPD media was inoculated with Pichia pink and left to grow for 2 days. 35 mL of the culture was hereafter harvested by centrifugation at 3000 rpm for 3 min at room temperature using Beckman Avanti J-25 JA rotor 25.50 (Beckman Coulter (UK) Ltd., High Wycombe, UK). The pellet was resuspended in 45 mL sterile distilled water and again spun at 3000 rpm for 3 min at room temperature using the Beckman Avanti J-25 JA rotor 25.50.

The pellet was resuspended in 1 mL ice-cold sterile 1M sorbitol and transferred to a sterile Eppendorf tube. The pellet was washed 6 times by pulse centrifuging the Eppendorf tube at 10,000 rpm, removing the supernatant and resuspending the pellet in new 1 M ice-cold sterile sorbitol. Following the final wash, the pellet was resuspended in an equal volume of 1 M ice-cold sterile sorbitol. 80 µL of each culture was added to a new sterile Eppendorf tube and added 5 µL linearised plasmid. The tubes were incubated on ice for 30 min. Negative controls without plasmid DNA was prepared in parallel. The contents of the Eppendorf tubes were transferred to chilled 2mmElectroporation cuvettes (Molecular Bio Products, cat# 5520), making sure the cells were at the bottom of the cuvette. The cuvettes were wiped completely dry prior

to electroporation. The cells were electroporated at 2.0 kV, 200 Ω, 25 mF using the Bio-Rad Pulse Controller (Model#: 1652098; Bio-Rad Laboratories, Hercules, CA, USA) and the Bio-Rad Gene Pulser (Model#: 1652078; Bio-Rad Laboratories, Hercules, CA, USA). 1 mL YPD media containing 1/10 20% Dextrose was added to the cells immediately after electroporation and incubated at 30°C for 1 hour.

100 µL of the cell mixture was plated onto 4 PAD plates containing 20% Dextrose and 1 plate YPD plate containing 20% Dextrose. Of the negative controls only 1 PAD and 1 YPD plate was prepared. The plates were incubated for 3-5days at 30°C in loosely tied bags until colonies appeared.

2.2.26 Protein expression screening

White colonies from the PAD plates from the transformed P. pink strains were isolated on new PAD plates as well as transferred to BMGY and grown for 48 hours. 1 mL of the culture was taken out as T=-1 protein expression prior to the exchange of the BMGY media to freshly made BMMY media to induce protein expression. The exchange of the media was done by centrifuging the cells at 5000 rpm for 5 mins at room temperature using the Eppendorf 5810R Centrifuge (Eppendorf AG, Hamburg, Germany). The pellet was resuspended in 5 mL BMMY and another sample was taken as T=0 for later analysis. The cells were incubated at 30°C shaking at 200 rpm and 1 mL samples were taken every 24 hours. Methanol was added to each sample to a final concentration of 0.05%. The last sample was taken after 96 hours giving a total of 6 time points.

The samples taken from the cell cultures were centrifuged in a table-top Eppendorf centrifuge at 13,000 rpm for 1 min and the supernatant was transferred to a new tube for further analysis and both supernatant and pellet was stored at -20°C.

2.2.27 Dot blot analysis of anti-LAM scFv screening

Nitrocellulose membrane (Transblot transfer medium 0.45 µm, Bio-Rad Laboratories, Hercules, CA, USA) was wet with 1xPBS prior to insertion into the dot-blot cassette (Bio-Rad Laboratories, Hercules, CA, USA). Once mounted, 200 µL of each time point sample was loaded as well as a positive control in the anti-CD33 (Emberson *et al*., 2002). Using a vacuum pump, the samples were loaded onto the membrane which hereafter briefly was air dried. The dots were hereafter visualised using immunoprobing techniques described in section 2.2.16.

2.2.28 Large-scale production of anti-LAM scFv

The anti-LAM scFv expressing *Pichia pink* was initially grown in BMGY media until it reached an OD_{600} of ~60. The culture was pelleted using Eppendorf 5810R Centrifuge (Eppendorf AG, Hamburg, Germany) and was then resuspended in 1/3 the volume of BMMY media to reach an OD_{600} of ~160-180. The final volume for large-scale production was aimed at 100 mL BMMY.

2.2.29 ScFv purification

For purification of the His-tagged scFv a 1 mL HisTrap™ nickel affinity column (GE Healthcare, Buckinghamshire, UK) was used.

Supernatant from transformed Pichia pink strains was collected 24 hours following exchange of BMGY media to BMMY and filter sterilised to remove any residual cell debris that might obstruct the HisTrap™ column. A sample was taken to illustrate protein concentration prior to purification.

The tubing in the peristaltic pump was washed with 20% EtOH in MilliQ water for 2 CV (Column Volumes) at a flow rate of 1 mL/min. The tubing was hereafter washed with MilliQ water for 2 CV.

The HisTrap™ column was connected to the tubing taking care not to introduce bubbles that might block the flow in the column. The column was washed with 5 CVs of MilliQ water, and equilibrated with 5 CVs 25 mM imidazole in 1x Sodium Phosphate Buffer, pH 7.4. The supernatant was passed through the column and a sample was collected to later be able to ensure that the protein indeed had bound to the column.

The column was then washed with 5 CVs of equilibration buffer and again a sample was taken to ensure that the protein was not eluted in the washing.

The scFv was now eluted from the column using 100 mM imidazole and 500 mM imidazole, both in 1x Sodium Phosphate Buffer, pH 7.4. 10 samples of 1 mL each was taken for each elution buffer.

The column was finally washed with 20% EtOH in MilliQ water and stored at 4°C.

2.2.30 Optimisation of imidazole concentration

The initial wash buffer has an imidazole concentration of 100 mM and elution buffers with imidazole concentrations of 150 mM, 200 mM, 250 mM, 300 mM and 500 mM

were analysed. Due to premature elution the wash buffer imidazole concentration was lowered to 25 mM with 100 mM included as an elution buffer

2.2.31 Recharging of HisTrapTM columns

Prior to recharging the HisTrap^{TM} column it was stripped using a “stripping buffer” consisting of 2M imidazole in Sodium Phosphate Buffer, pH 7.4. 5 CV of stripping buffer was passed through the column at a speed of 1 mL/min, which was unchanged for all procedures. Hereafter, the column was recharged with a reload buffer consisting of 0.1M $NiSO_4$ in MilliQ water. 2 CV of reload buffer was passed through the column. Finally the column was washed using 20% EtOH in MilliQ water, disconnected from the peristaltic pump and stored at 4°C.

2.2.32 Western blot analysis of scFv purification

The western blot was performed as previously directed (section 2.2.16) with anti-His HRP conjugated antibody as visualising agent. The antibody was used at a 1:2000 dilution in blocking buffer.

2.2.33 Coomassie stain analysis of elutions for degradation analysis

The gels, run as in section 2.2.14, were removed from the cassette and suspended in Coomassie staining solution (0.25 % Coomassie Brilliant Blue R250, 10 % acetic acid, 50% methanol) for 1 hour. The gels were hereafter destained using destaining solution (5% methanol, 7.5% acetic acid) for 1+ hours until bands were clear.

2.2.34 Silver stain analysis of scFv purification

Gels were run as in section 2.2.14 and silver staining was executed with the use of SilverXpress Silver Staining kit (Invitrogen, Paisley, Scotland, UK) and was carried out according to manufacturer's protocol.

2.2.35 Gel drying

Gels were dried using Gel Drying Film (Promega, Madison, WI, USA) according to manufacturer's protocol.

2.2.36 Minimal media vs. complex media with and without casein

The cells were grown to and OD_{600} of 60 in regular BMGY media as described in section 2.2.28. The cells were hereafter divided into 2 flasks and added BMMY and YNBM to an OD_{600} of 160-180. Each flask was further divided into two separate flasks, ending up with 4 flasks in total. In one flask of BMGY and one in YNBM 1% casein was added. The cultures were hereafter grown and analysed as described previously.

2.2.37 Temperature and protease inhibitor analysis

Culture setup was performed as described (section 2.2.28). As the cultures had been transferred to BMMY to an OD_{600} of 160-180 the culture was divided into 4x50 mL aliquots and transferred to 4x 250 mL flasks. Two flasks were hereafter added a protease inhibitor tablet (Roche Diagnostics Ltd, Burgess Hill, UK). One flask without

protease inhibitor and another flask with was grown for 24 hrs at 20°C and the same at 25°C. The cultures were hereafter grown and analysed as previously directed.

3 Labelling optimisation of UBI 29-41

3.1 Introduction

When designing an experimental strategy for the evaluation of the toxicity of a labelled compound, an important first step prior to performing toxicity studies was to optimise the labelling of the targeting agent. This not only eases later evaluation of the toxic effects by knowing the exact level of labelling, but would be beneficial if the amount of radioactive iodine used could be minimised to not only reduce solid waste accumulation but also make the stock last longer.

The targeting agent used in the toxicity studies was fragment 29-41 (TGRAKRRMQYNRR) of the antimicrobial peptide Ubiquicidine (UBI 29-41). An antimicrobial peptide was chosen for the initial toxicity studies, based on the broad targeting range of the peptide due to it binding via electrostatic interactions (see section 1.4.1.2). This would allow the testing of the effects of Auger electrons on a range of model organisms, which will be evaluated later.

^{125}I had several advantages as the initial isotope for radiotoxic evaluation of Auger electrons. It has a long half-life (60 days), it has an uncomplicated labelling technique, the labelling chemistry for iodine would likely allow easy replacement with isotopes such as ^{123}I emitting higher energy Auger electrons, which albeit having a lower LET has a longer range, and finally it may have uses as an imaging agent as it also emits γ-radiation.

The use of UBI 29-41 had further advantages as the labelling method utilised was Iodogen labelling. As mentioned previously (section 1.4.2.1), this labels the ortho positions of the hydroxyl group on tyrosine, of which only one exist in UBI 29-41.

In the initial optimisation steps of the labelling process, “cold” iodine was to be utilised as this would enable analysis of the labelled product using HPLC-MS, which would enable the analysis of the homogeneity and labelling efficiency of the Iodogen labelling method for this peptide. UBI 29-41 has a single tyrosine residue and thereby two labelling positions as iodine is conjugated in the orthopositions of the hydroxyl group of which there are two.

Prior to labelling UBI 29-41 with “hot” iodine, the labelling process was investigated and before directly assessing the effect of the radiation on the model organisms.

Since HPLC-MS equipment in the department is not suited for the handling of radioactive materials, the initial evaluations of the labelling was done using non-radioactive iodine. It was furthermore of interest to study the stability of the labelling to not only evaluate the possibility of batch creation, but also for analysis of the stability of the conjugate during the experiments.

3.1.1 Specific aims

Given the above, this chapter had the following specific aims:

1) To successfully label UBI-29-41 with 'cold' iodine using the Iodogen labelling techniques
2) To analyse the labelled UBI29-41 by HPLC-MS, thereby confirming the success of the labelling protocol
3) To adjust the labelling parameters based on (2) to optimise labelling reaction for uniformity of labelling and to minimise use of radioactive products

4) To perform labelling with 'hot' iodine based on the optimised protocol established by the above

5) To assess the stability of labelled UBI 29-41 and thereby suggest the maximum time labelled products should be stored before subsequent experiment.

3.2 Optimisation of iodine concentrations for labelling using non-radioactive iodine

In order to be able to ensure reproducibility of experiments and correct interpretation of results the labelling process had to be carefully characterised and optimised. HPLC-MS at the University of Kent is not cleared for use with radioactive material and for this reason the molecular analysis of the labelling process had to be done using “cold” iodine instead of ^{125}I.

The first step was to test UBI 29-41 labelled with a range of “cold” iodine concentrations (see section 2.2.2). UBI 29-41 was labelled with concentrations of cold activated NaI ranging from 1 mM to 3 mM to 2 nmol of UBI 29-41 per labelling in 100 µL Tris iodination buffer. The labelled product was analysed using reverse phase HPLC using a C18 column at a flow rate of 0.2 ml/min using a water, acetonitrile, 0.05% trifluoroacetic acid gradient. The retention times were detected and are visualised in Figure 14.

As can be seen in Figure 14, increasing the concentration of activated iodine to the UBI 29-41 solution changed the running time in the HPLC by changing the chemical composition of the peptide. The retention time on HPLC is affected by the polarity of the peptide. Increased polarity reduces retention time and the addition of two iodides would make the tyrosine less polar, thereby increasing running time in the HPLC. As can be seen three peaks are visible. As there are two ortho-positions to the hydroxyl group in tyrosine means that the tyrosine can be semi-saturated with only one of the ortho positions filled. The intermediate peak is consistent with this. The rightmost peak is consistent with both ortho groups being saturated.

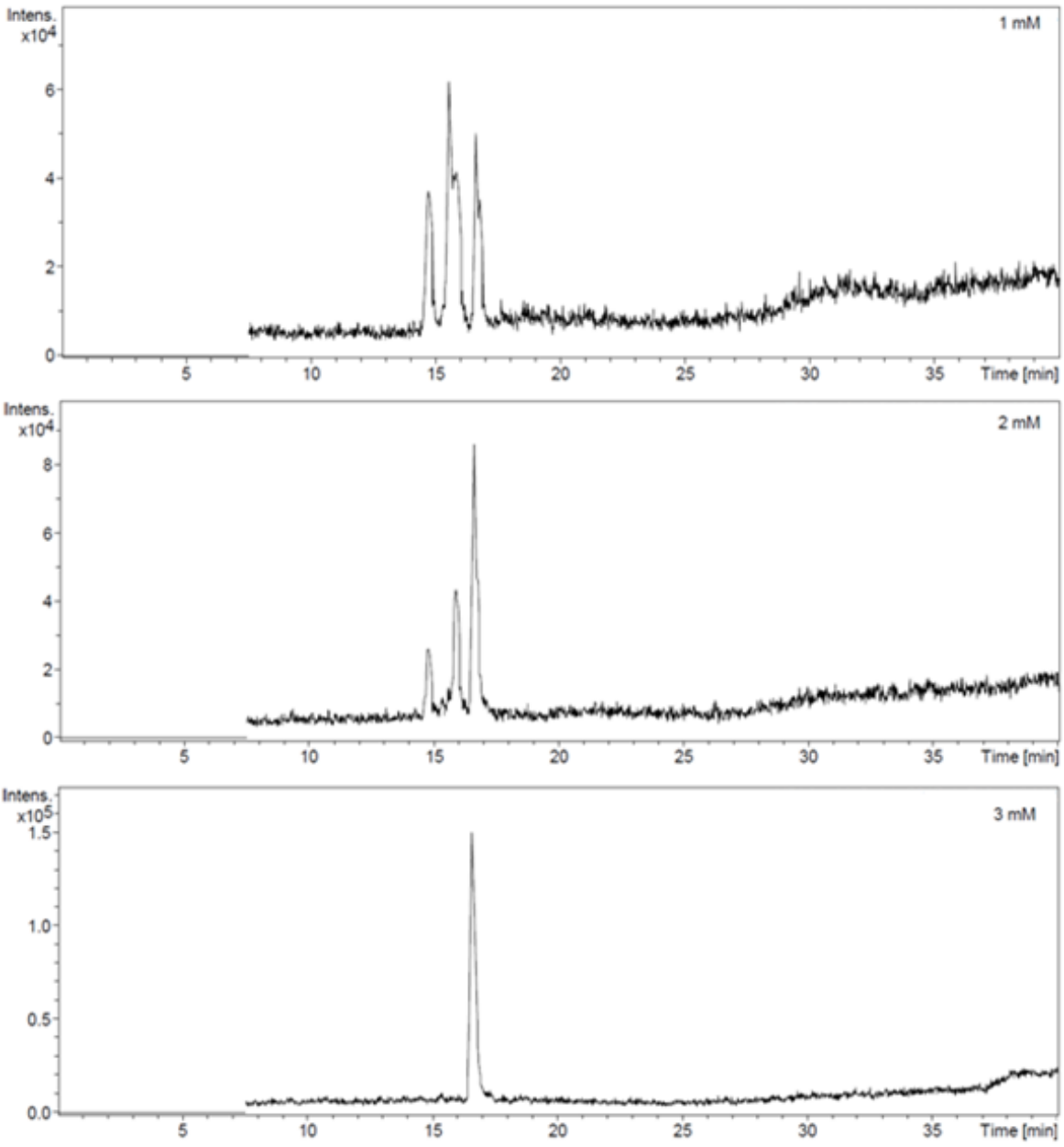

Figure 14 Overview of HPLC analysis of labelling optimisation of UBI 29-41.

HPLC data of UBI 29-41 labelled with 3 concentrations of NaI. The top figure shows retention time in HPLC with 1 mM NaI, the middle figure 2 mM and the bottom figure at 3 mM. Retention time of UBI 29-41 increases as it becomes saturated. The two top figures show three peaks at varying intensity indicating non-saturated labelled UBI 29-41. As the concentration increases so does the proportion of the rightmost peak, representing the fully labelled UBI 29-41.

To further confirm this, the unlabelled and fully labelled UBI 29-41 was analysed by MS.

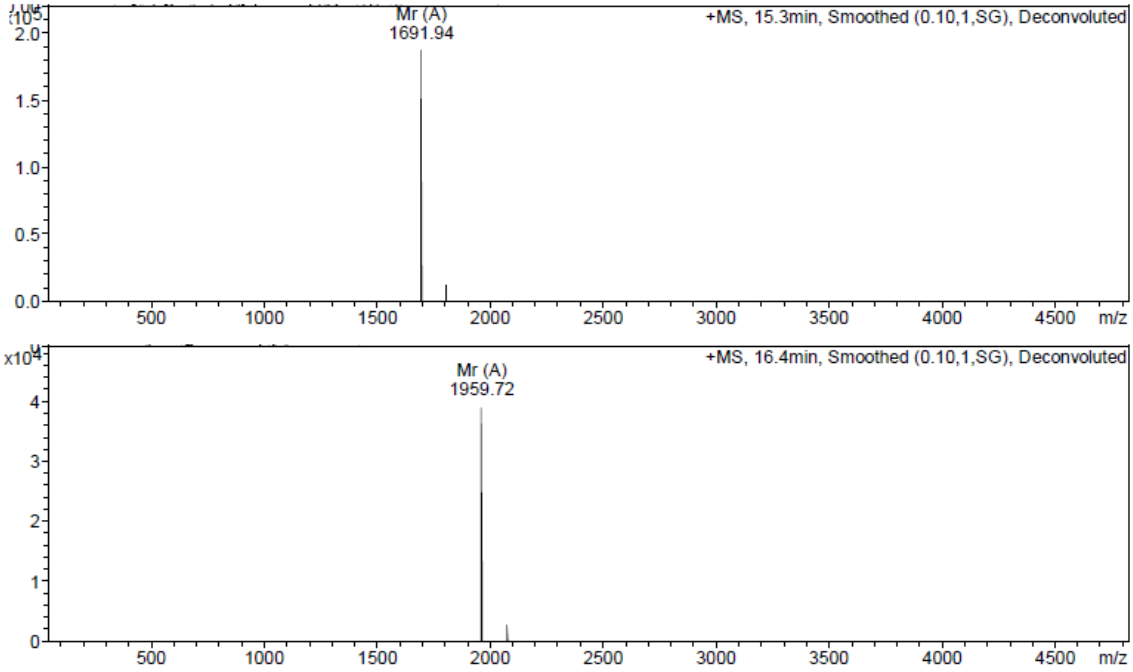

Figure 15 MS analysis of the un-labelled and the fully labelled UBI 29-41.

This figure shows the MS analysis of the molecular weight of unlabelled (top) and labelled (bottom) UBI 29-41. Labelling was performed using a stable isotope of iodine to prevent radioactive contamination of the HPLC-MS equipment. The weight of the unlabelled UBI 29-41 is both consistent with literature (Akhtar *et al*., 2005) and also appears homogeneous. More importantly, the labelled UBI 29-41 population is also homogeneous. The increase in mass is equivalent to two iodides and a single oxygen due to oxidation of UBI 29-41 as a consequence of the labelling process as well as loss of two hydrogen atoms which were replaced by iodine.

As can be seen in Figure 15, there is a right-shifting when comparing the unlabelled UBI 29-41 (top) with fully labelled UBI 29-41 (bottom). The increase in mass corresponds to the addition of two iodine atoms as well as the addition of a single

oxygen and loss of two hydrogen atoms. The calculations are summarised in Table 8 and Table 9:

Table 8 Overview of UBI 29-41 amino acid composition. Upon bond formation water is removed (depicted in red)

Amino acid	Number of amino acids in peptide	Mass	Combined mass
Threonine (T)	1	119 Da	119 Da
Glycine (G)	1	75 Da	75 Da
Arginine (R)	5	174 Da	870 Da
Alanine (A)	1	89 Da	89 Da
Lysine (K)	1	146 Da	146 Da
Methionine (M)	1	149 Da	149 Da
Glutamine (Q)	1	146 Da	146 Da
Tyrosine (Y)	1	181 Da	181 Da
Asparagine (N)	1	132 Da	132 DA
H_2O	12	18 DA	216 Da
Total mass			1691 Da

This mass is identical to the mass of the unlabelled peptide found by MS and found in literature. During labelling it was expected that two hydrogen atoms were replaced with two iodides including the addition of an oxygen atom. This is summarised in Table 9.

Table 9 Overview of the labelling of UBI 29-41 comprising the replacement of two hydrogen atoms (depicted in red) with iodide atoms.

Component	Number	Mass	Combined mass
UBI 29-41	1	1691 Da	1691 Da
Iodine	2	127 Da	254 Da
Hydrogen	2	1 Da	2 Da
Oxygen	1	16 Da	16 Da
Total mass (fully labelled)			1959 Da

This theoretical mass of the fully labelled peptide calculated is the exact molecular weight found by MS.

The amount of peptide used was 2 nmol, whereas the amount of iodine included ranged from $1 \times 10^{-7}\ mol$ (1 mM in 100 µL Tris iodination buffer) to $5 \times 10^{-7}\ mol$ (5 mM in 100 µL Tris iodination buffer), meaning the peptide to iodine ratio ranged between 1:50 and 1:250.These results verified the successful incorporation of iodine using the commercially-obtained Iodogen method, under the conditions described here. They are not, however, directly comparable to labelling with $Na^{125}I$ under the Iodogen tube manufacturers' recommended conditions; these recommend the use of 1 mCi (37 MBq) $Na^{125}I$. This represents a much lower molar concentration of sodium iodide than used in these "cold" experiments, although information obtained from the suppliers prior to the experiments had indicated that the molar concentration of the $Na^{125}I$ used was 5 mM. This means that, while the cold experiments provided useful detailed information about the labelling including MS data the stoichiometry of the Iodogen process would be different between the "hot" and "cold" experiments.

Purification of the labelled peptide on a PD10 column was attempted, however, the cationic nature of the peptide and low concentration made it unfeasible. Anionic exchange column purification was attempted as well, however with the same result (data not shown). As free ^{125}I was later included as an activity control it was decided that a surplus of free ^{125}I would be acceptable

Since HPLC-MS was not a feasible method for the routine analysis of “hot”-labelled peptide due to equipment restrictions in the department, a method was required for the evaluation of the labelling efficiency prior to experiments in order to ensure that UBI 29-41 had been successfully labelled and remained stable. For this ITLC was implemented and is described in section 3.3.

3.3 Optimisation of iodine concentrations for labelling using Na^{125}I

Radio iodination was undertaken according to the protocol published by the manufacturers of the iodination tubes, using 2 nmol peptide and 1mCi (37 MBq) Na^{125}I. In order to assess incorporation of radioiodine, instant thin layer chromatography (ITLC) was used. This was compared with ITLC analysis of activated Na^{125}I; this allowed the determination of the extent of non-incorporation of radioiodine under different experimental conditions, and also to measure stability in later experiments. ITLC profiles are presented in Figure 16, which demonstrates a clear difference in profiles between the free iodine (left) and the labelled UBI 29-41 (right). The free iodine had travelled furthest on the ITLC paper at around 80 mm, where the radio labelled UBI 29-41 was retained at the loading point. These profiles

would later be used to rapidly analyse radio labelled product prior to experiments whether labelling had been successful, which proved a simple, but important tool in verifying radio labelling efficiency. Furthermore, as can be further seen in the radio labelled profile of UBI 29-41, there is a very small peak at the end of the ITLC paper (red circle in figure to the right), correlating with the free iodine peak and indicating that there is a small excess of iodine that has not been conjugated to UBI 29-41.

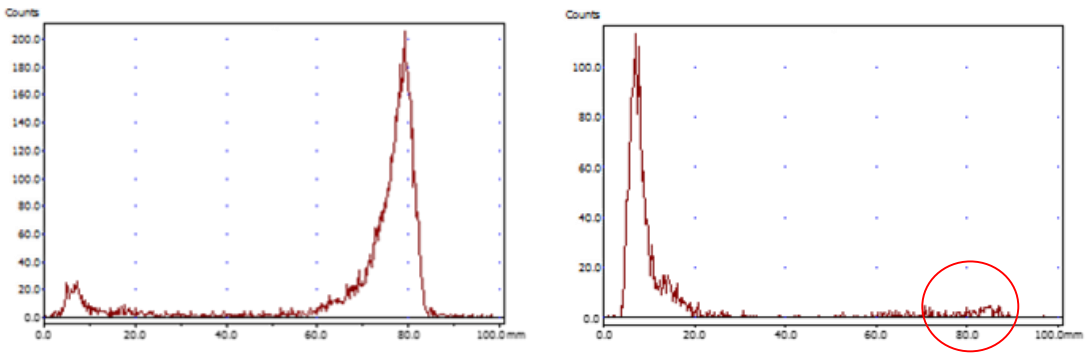

Figure 16 ITLC profiles of radio labelled UBI 29-41 and free iodine.
The left figure shows the profile of free activated iodine. The right figure shows the profile of successfully labelled UBI 29-41 having very little free iodine (red circle). The labelled UBI 29-41 prevented the migration when compared to the free iodine. ITLC analysis of the radio labelled UBI 29-41 was performed prior to all radio toxicity experiments in order to ensure distinction between free iodine and targeted iodine experiments.

Subsequent experiments investigated the impact of a reduction in the activity of $Na^{125}I$ used in the procedure. These experiments again showed a large peak at the origin, corresponding to the labelled peptide, and a small peak around 90 mm from the origin, corresponding to free iodine, under the conditions recommended by the manufacturers (Figure 17A). Reducing $Na^{125}I$ to half (Figure 17B) and one tenth (Figure 17C) of the recommended activity led to absence of the free radioiodine peak. This indicates that the activated ^{125}I has been either labelled to UBI 29-41or bound to the tube in a fashion leaving no iodine free in solution.

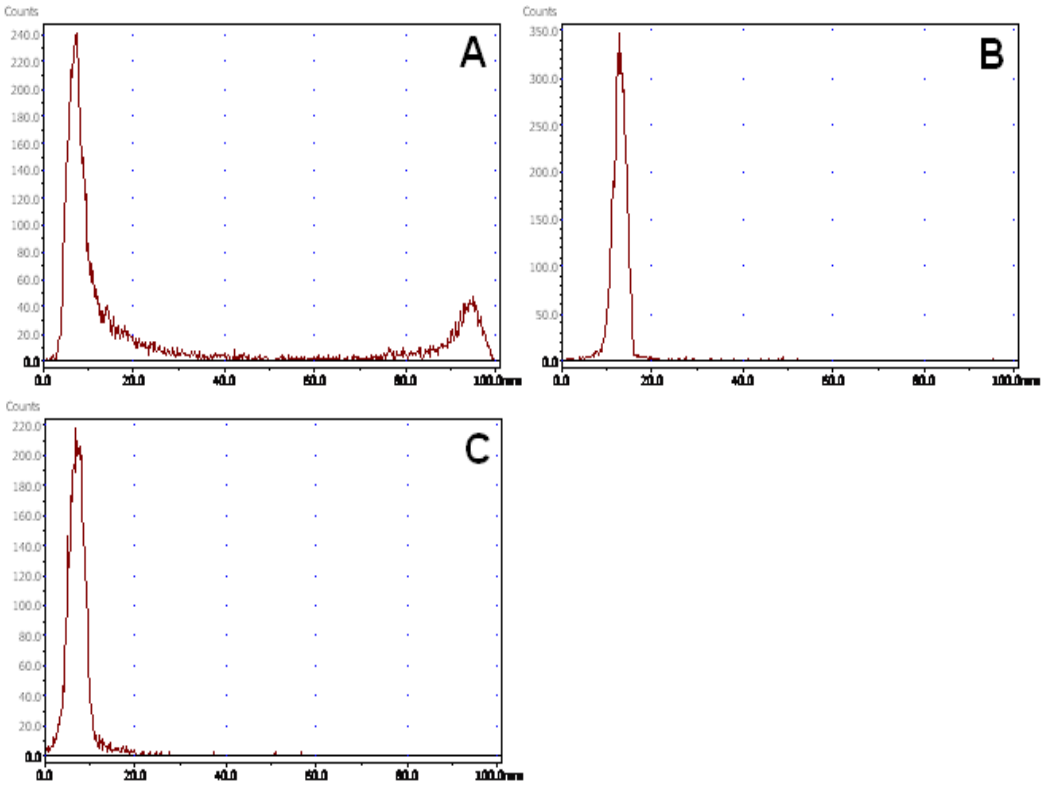

Figure 17 ITLC analysis of radio labelling optimisation.

Using ITLC UBI 29-41 labelled with various concentrations of activated ^{125}I was analysed and compared to establish the optimal labelling conditions for the later toxicity assays. **(A)** UBI 29-41 labelled with the^{125}I activity recommended by Pierce. **(B)** Is UBI 29-41 labelled with half the activity recommended and **(C)** is UBI 29-41 labelled with 1/10 the activity recommended.

3.4 HPLC analysis of ^{125}I labelled UBI 29-41

Due to the significantly lower concentration of Na^{125}I compared to NaI it was desirable to further analyse the nature of the labelling using hot iodine. Although this was undertaken at the Rayne Institute at St. Thomas Hospital, and therefore not feasible for routine analysis, it could potentially provide useful information about the radio labelling process that ITLC could not provide, such as number of ^{125}I conjugated to UBI 29-41.

The analysis was undertaken using a C18 column on a reverse phase HPLC using an acetonitrile (ACN) + 0.05% trifluoroacetic acid (TFA) gradient for elution of the labelled product as well as any free iodine.

Initially, the unlabelled peptide was tested to verify the gradient as well as notify at what point the unlabelled peptide elutes, to have a reference point for later radionuclide analysis. Furthermore, it was important to confirm the stability of the unlabelled peptide following its extended period of storage. 20 µL was injected and the eluate was analysed by standard UV chromatogram at a flow rate of 1 mL/min.

As can be seen in Figure 18 there appears to be a large single peak around 9 minutes. This gives confirmation that the peptide has not degraded and furthermore gives a frame of reference for radio labelling analysis. The reference point allowed the implementation of refined fraction collection around the expected elution time and thereby improved resolution. As there were potentially two peaks, one for single labelled and one for double labelled UBI 29-41, it was desirable to obtain a resolution that would allow the distinction to give an indication of the level of single and double labelled peptides at various $Na^{125}I$ concentrations. Initial experiments with radio-HPLC were unsuccessful due to non-compatibility of the available Bioscan radio probe with ^{125}I detection (data not shown), therefore the eluate from the HPLC was collected in 30 sec-1 min fractions and analysed using a gamma counter.

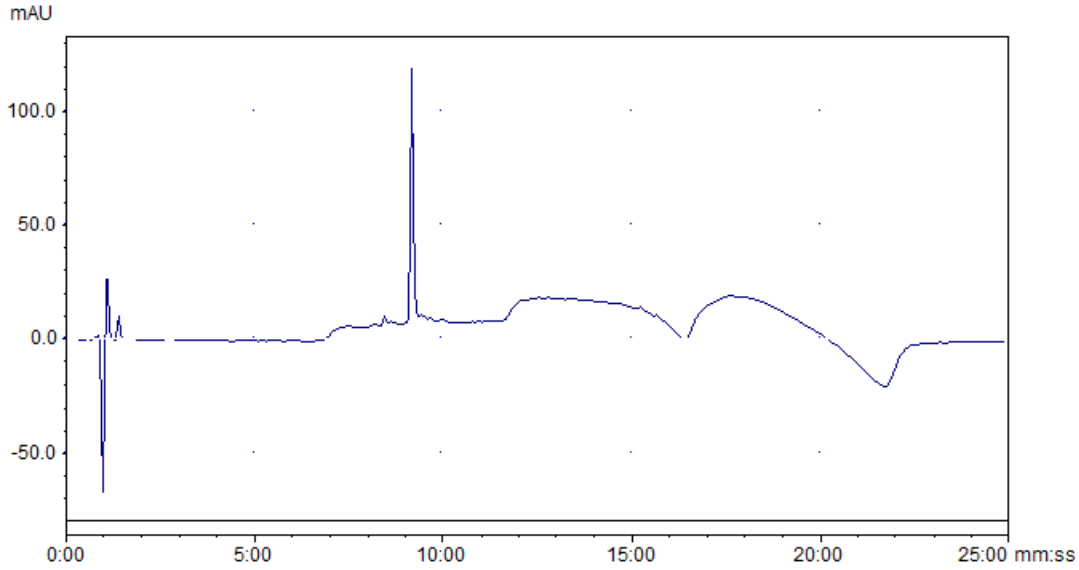

Figure 18 HPLC UV chromatogram of unlabelled UBI 29-41

HPLC UV chromatogram of unlabelled UBI 29-41 to verify that the organic solvent gradient was suitable for peptide elution as well as do initial analysis of the integrity of the peptide. It furthermore provided a reference point for later radio labelled studies as the unlabelled peptide is not visible on the gamma counter. Finally, it gave information about the expected retention time of the radio labelled peptide allowing an increase in the resolution of the collected fractions by reducing the volume of the fractions around the expected elution time.

Following the pre-analysis of the unlabelled peptide, the labelling process was performed as previously described (section 2.2.2). Two activities of $Na^{125}I$ were evaluated; the Pierce recommended activity (1 mCi) and 1/10 (0.1 mCi) the recommended activity, to mirror and verify the ITLC data previously collected.

The radio labelled peptide was initially analysed on a regular UV chromatogram to verify the position of the peptide in relation to the results from the gamma counter. As can be seen in Figure 19, around 9 minutes there is no peak indicating that the peptide concentration was too low to be detectable by UV chromatogram. In order to prevent saturation the gamma counter later, 1 MBq (2.7 µL) of labelled peptide was diluted into 1 mL of water. This gave a peptide concentration of 54 nM, of which

20 µL was injected into the HPLC for analysis. This was sufficient to allow efficient gamma detection, despite not allowing detection of the product by UV. It did, however, prevent the estimation of unlabelled peptide in the batch as this would not show up in subsequent gamma detection analysis.

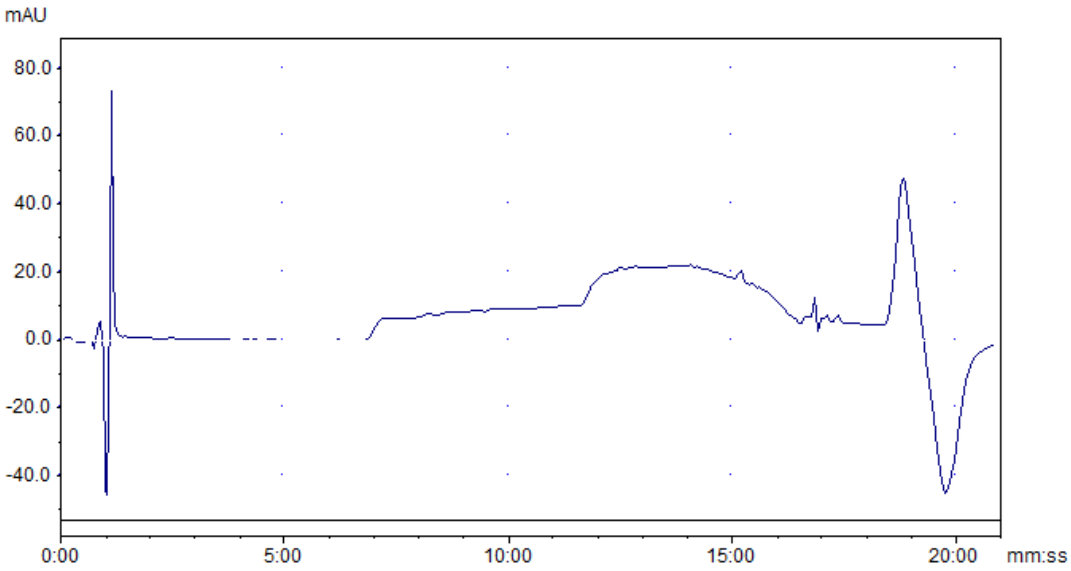

Figure 19 HPLC UV chromatogram of UBI 29-41 labelled with the recommended activity of $Na^{125}I$

HPLC UV chromatogram of the diluted radio labelled UBI 29-41. Due to the dilution no peak is visible around 9 minutes as was expected. The large peak at the beginning is the solvent front and is expected. The white areas is the baseline coloured white.

The eluate from the HPLC was collected in fractions with increased resolution around the expected peptide elution. From 0 to 9 minutes 1 min fractions were collected, from 9 to 14 minutes 30 sec fractions were collected and the remaining eluate was collected at 1 min fractions. The fractions were hereafter analysed on a Wallack LKB 1282 Gamma Counter Compugamma.

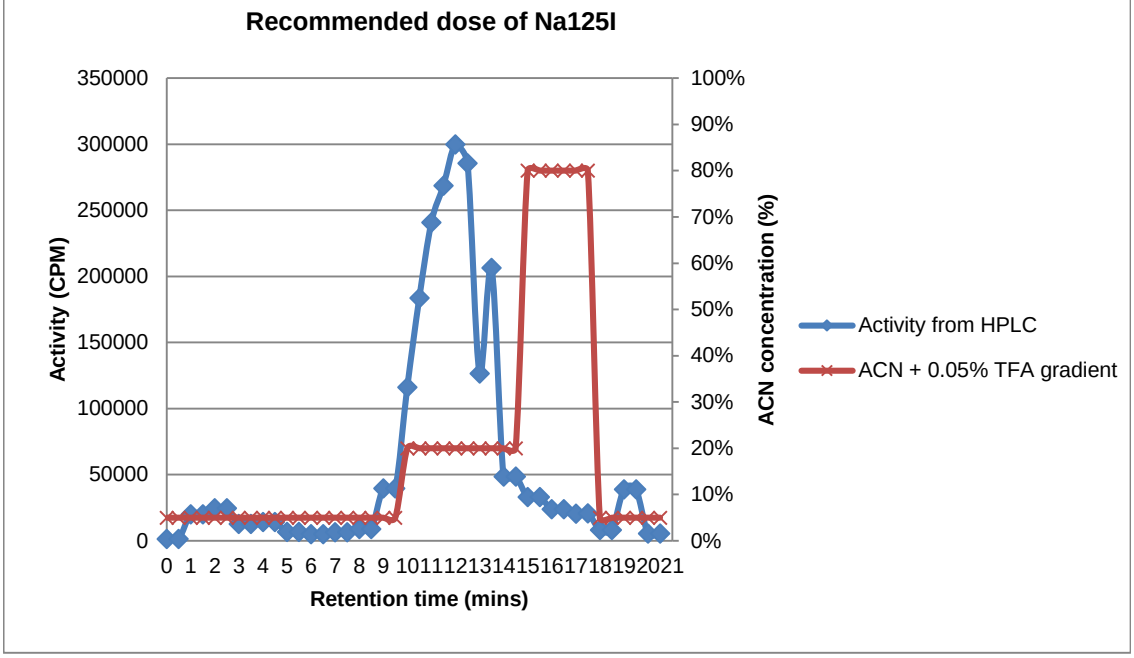

Figure 20 HPLC analysis of UBI 29-41 labelled with the recommended activity of $Na^{125}I$. This graph shows the fractional analysis of the activity eluted from the HPLC at various concentrations of organic solvent. The peak around 1-5 mins represents the free iodine in the sample whereas the peak beginning around 9 minutes ending at 17 minutes represents the labelled peptide. The incorporation of iodine is expected to increase the retention time.

As can be seen in Figure 20 there is a small peak in the first couple of fractions. This presumably represents free iodine in the sample or low level contaminants. The remaining activity elutes between minutes 9 and 17. The primary peak is found between 10 and 14 minutes, with the rest being eluted following increase in organic solvent concentration. There is a second peak around the 13:30 min fraction, however this was probably due to an over collection. In that tube compared to the previous fraction, at the point that fraction collection switched from 30 sec to 1 min in duration.

The resolution provided by the fraction collection was significantly lower when compared to the HPLC of the cold labelled peptides (Figure 14). In order to allow

better separation of the peaks, a longer HPLC run with a more optimised organic solvent gradient would be required; in particular a more suitable radio probe would be required for greater resolution.

Analysis of labelling was then conducted with 1/10 the recommended $Na^{125}I$ activity with fractions collected, as mentioned above, using the same organic solvent gradient. Between the two samples, the column was washed with a high organic solvent concentration to wash any residual ^{125}I out of the system. The fractions collected were inserted into a diagram as above and the results are visualised in Figure 21.

The results are very similar to those in Figure 20. The large peak at the beginning of the fractions is likely to be residual ^{125}I from the previous experiments that had not been eluted in the wash and is not included in the calculations of the labelling yield. Radioiodine is known for its ability to adhere to solid matrices. Interestingly, on the major peak representing radio labelled UBI 29-41 there appears to be a shoulder to the left, which could be indicating a higher percentage single labelled peptide. It has to be taken into consideration that the counts obtained from the single- and double-labelled peptides are not 1:1, as the double-labelled peptide would containing double the number of ^{125}I atoms. This would influence relative peak volume of an equal amount of single- and double-labelled peptides. While the resolution is not sufficient to confirm, the shoulder may correspond to a greater proportion of single-labelled species. If compared to the diagram showing UBI 29-41 labelled with the recommended activity there is less sign of a shoulder to the left of the peak, and if

anything a slight shoulder to the right, possibly the result of a greater proportion of double-labelled species.

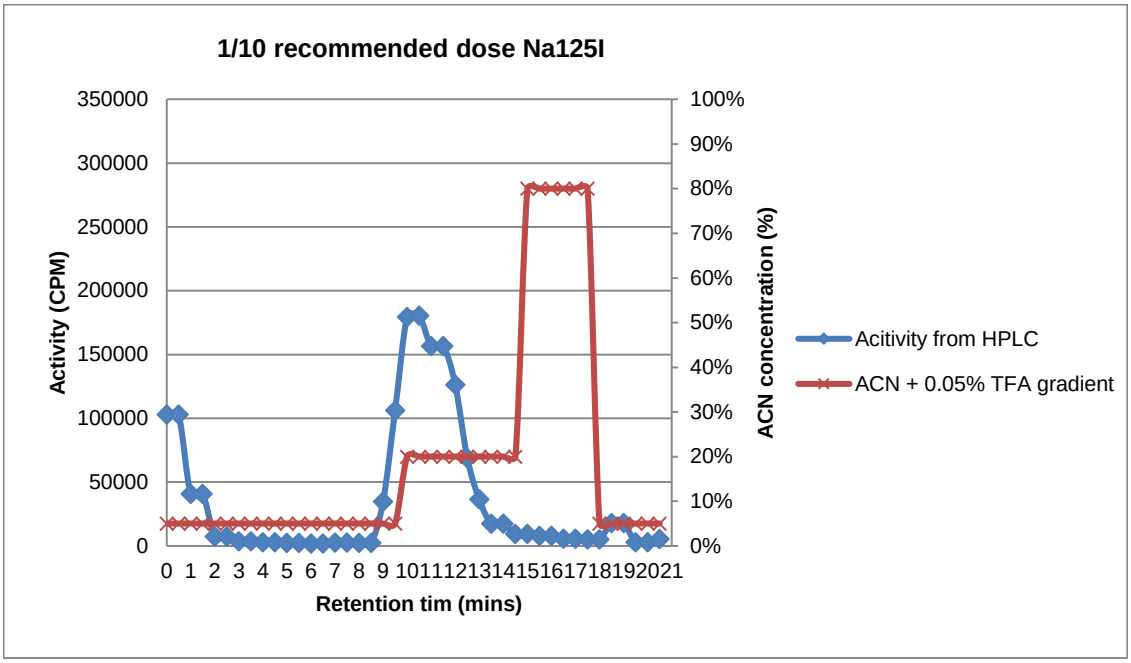

Figure 21 HPLC analysis of UBI 29-41 labelled with 1/10 the recommended activity of $Na^{125}I$
Overview of the fractional analysis of the eluate from HPLC of UBI 29-41 labelled with 1/10 the recommended activity of $Na^{125}I$. The profile resembles that of Figure 20; however there is a slight increase in the shoulder to the left (earlier elution).

When comparing the two peaks of presumably labelled UBI 29-41 from Figure 20 and Figure 21, the level of ^{125}I in the low activity evaluation is not 1/10 the level of the peptide labelled with the recommended activity as would be expected. When comparing the summarised peak counts of the major peak in Figure 20 (recommended) of 1,855,040 CPM (minutes 9-17) and Figure 21 (1/10) of 1,051,809 CPM (minutes 9-16) the 1/10 activity labelled population comprise 57% of the activity of the peptide labelled with the recommended activity. As the same amount of peptide is available, 2 nmol, it is likely that there is more free iodine in the reaction mixture labelled with the recommended activity than the peptide labelled with 1/10

the activity. Although normally a labelling yield can be calculated, the adhesive nature of ^{125}I complicates the correct estimation of free iodine.

In summary, the analysis of labelled products by HPLC and associated fraction collection and gamma counting provided insight into the nature of the labelling which the ITLC could not provide, including a low resolution evaluation of the level of single- and double- labelled peptide in the samples to later be used for toxicity assays. Enhancing resolution using an appropriate radio probe would be a valuable extension to these studies and characterise the proportion of single- and double-labelled peptide species.

3.5 Stability analysis of ^{125}I-labelled UBI 29-41

During the labelling optimisation of UBI 29-41, indications started to occur that over time the labelling profile of UBI 29-41 slowly shifted from a labelled profile to a free iodine ITLC profile indicating issues with labelling stability when stored in Tris iodination buffer at 4°C. Then it became important to monitor stability of the ^{125}I-labelled UBI 29-41 and its implication for subsequent experiments. It was furthermore important to establish how fast this degradation occurred, in order to identify the time-frame in which they could be used in toxicity assays.

A batch of labelled UBI 29-41 was analysed at a range of time points post-labelling using ITLC and compared to the free iodine ITLC profile in order to establish the degree of degradation over time. The peptide was labelled as previously described and, using ITLC, the labelling profile was established immediately after labelling and then after 6, 12, 24, 48, 72 and 144 hours. The labelled peptide was stored in Tris

Iodination buffer at 4°C. As can be seen in Figure 22, the degradation over the course of 144 hours was substantial with loss of peak volume at the origin and increase of the peak at around 80 mm. At the end of the experiment the profile of the labelled UBI 29-41 was identical to the free iodine profile indicating complete degradation of the labelling, and the trend of dissociation over the time series was clear, within the accuracy permitted by ITLC.

In order to analyse whether this could be due to the use of too high a concentration of ^{125}I causing the labelling to destabilise, the experiment was repeated using 1/10 the recommended $Na^{125}I$ (Figure 23).

The profile for 1/10 $Na^{125}I$ was identical to the ITLC profiles from the stability of analysis using the recommended levels. This shows that the levels of radioactive iodine appeared to have no effect on the stability of the labelling within the frames of the experiment. It was not desirable to go lower in concentration as it was felt that this might have too much of an impact on any potential toxicity to be seen in later toxicity experiments. Consequently, it was decided to proceed with the toxicity experiments using the recommended levels of $Na^{125}I$. However, due to the stability assays it was concluded that radio labelling had to be done immediately prior to the radio toxicity experiments in order to attempt minimising the effects of the dissociation of the iodine from UBI 29-41 despite the long half-life of ^{125}I. Furthermore, prior to all experiments, ITLC analysis of the radio labelled UBI 29-41 had to be performed to ensure that labelling had been successful.

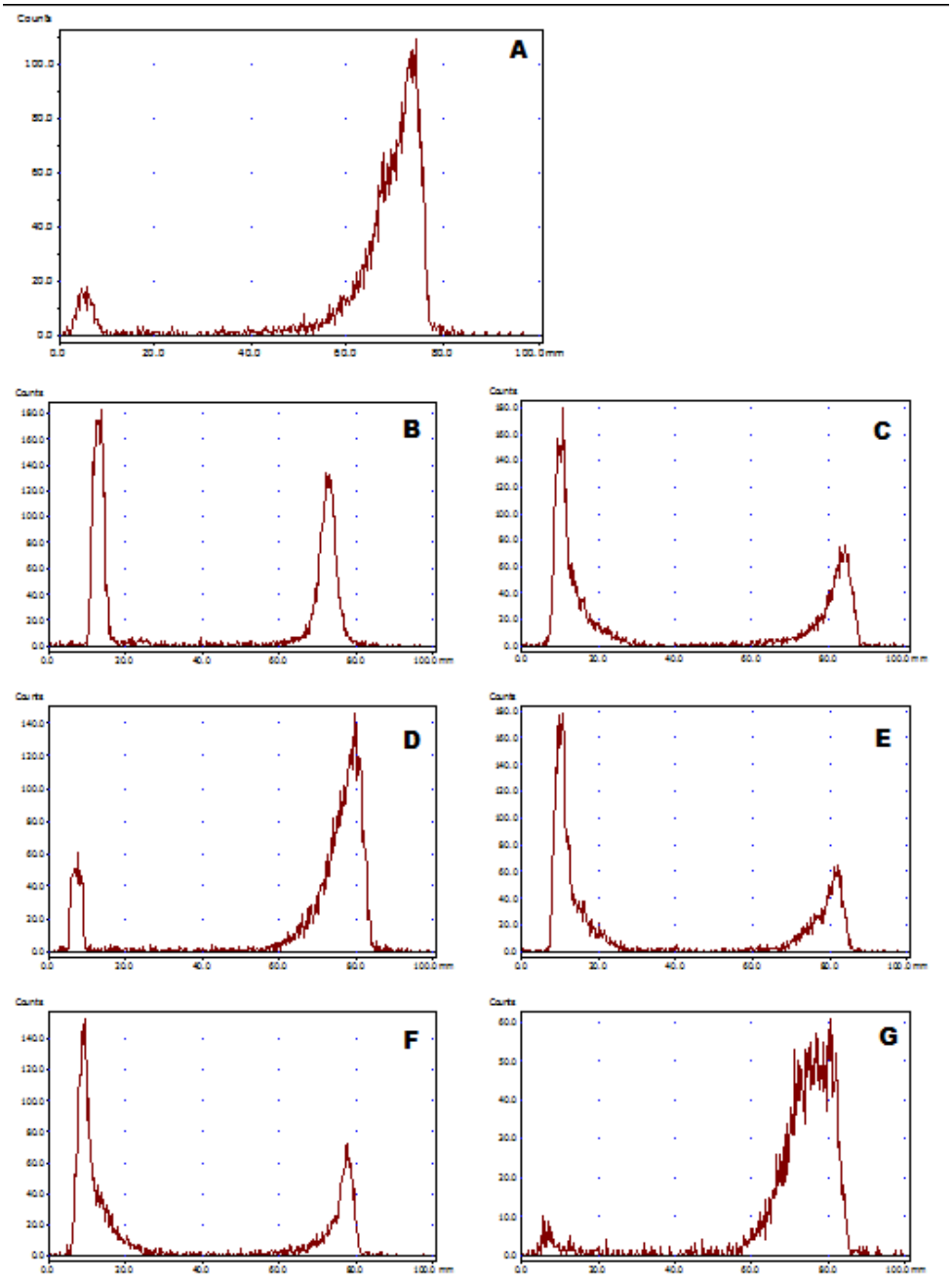

Figure 22 Time course stability analysis of radio labelled UBI 29-41 using recommended concentrations of $Na^{125}I$.

This figure shows an overview of the stability of the labelling of UBI 29-41 over the course of 6 days using the recommended amount of $Na^{125}I$ as recommended. **(A)** Free iodine profile **(B)** T=0 **(C)** T= 6 hrs **(D)** T= 24 hrs **(E)** T= 48 hrs **(F)** T= 72 hrs **(G)** T= 144 hrs.

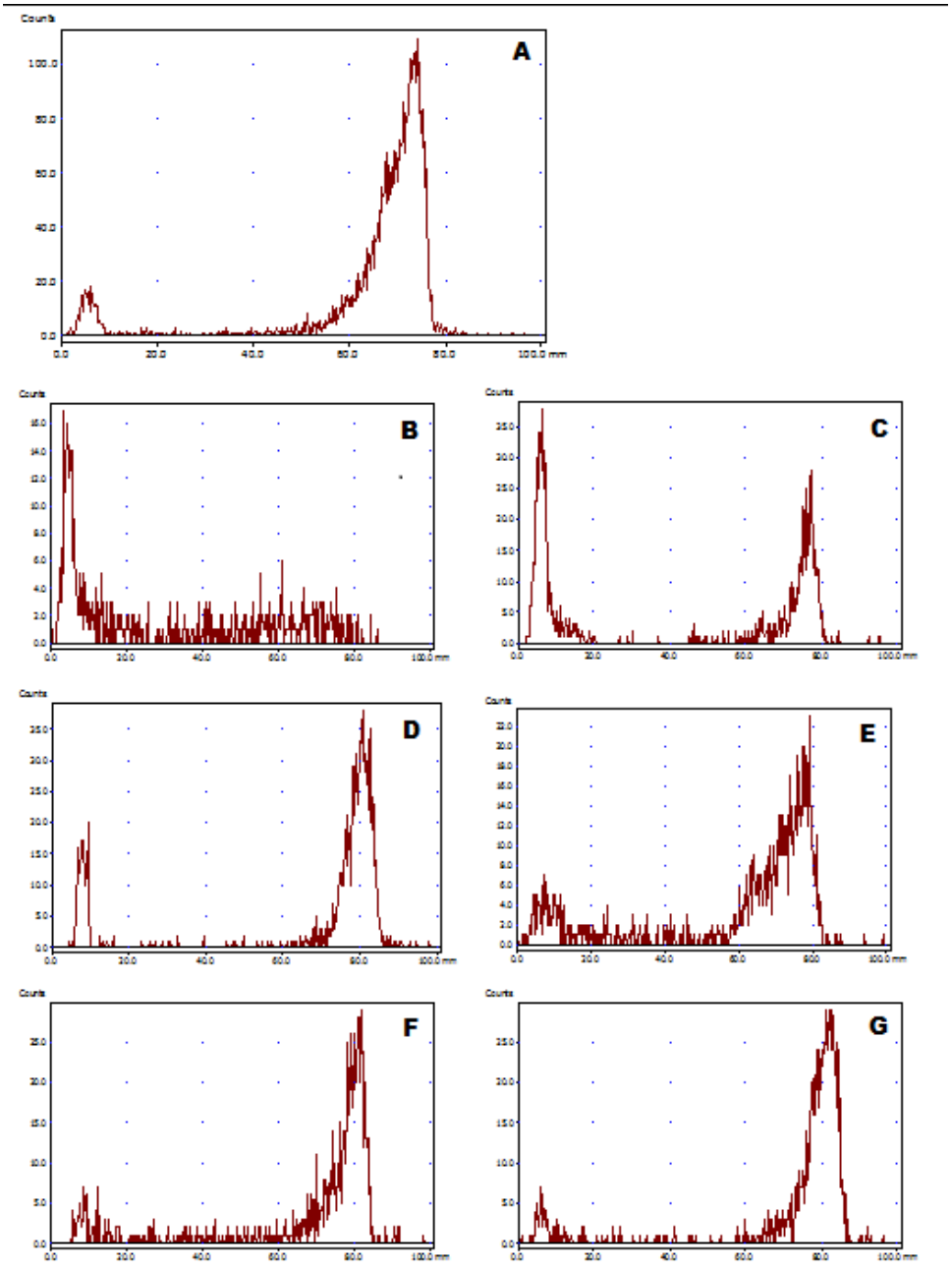

Figure 23 Time course stability analysis of radio labelled UBI 29-41 using 1/10 of the recommended concentrations of $Na^{125}I$.

A complimentary experiments to the previous stabilisation experiment (Figure 18). 1/10 of the amount was used to test if the observed deterioration of labelling was due to the concentration of iodine.**(A)** Free iodine **(B)** T=0 **(C)** T= 6 hrs **(D)** T= 24 hrs **(E)** T= 48 hrs **(F)** T= 72 hrs **(G)** T= 144 hrs.

3.6 Discussion

The aims of this chapter were to analyse the labelling efficiency and optimal labelling conditions of the antimicrobial peptide fragment UBI 29-41 with ^{125}I. This was preliminary work for the later analysis of the radio toxicological effects of Auger electrons.

Two strategies were taken to optimise and analyse radio labelling. Firstly, the Iodogen labelling procedure was assessed using non-radioactive sodium iodide as a replacement for Na^{125}I. The “cold” version of the procedure allowed a refined and detailed characterisation of peptide iodination products using state-of-the-art LCMS technology. This was coupled with ITLC analysis of the standard “hot” procedure, carried out as per manufacturers’ instructions, to verify successful incorporation of radio iodide into UBI 29-41 and monitor stability of the radio peptide over time. While these different analyses were performed on products obtained using different chemical conditions, most notably the concentration of sodium iodide, they did provide insight into the radio labelling process and assisted in establishing the most appropriate chemical conditions.

The cold labelled experiments were useful in analysing the labelling chemistry using the available HPLC-MS. This allowed the verification of the hypothesis that two iodine atoms were able to bind to the peptide. This is consistent with 3 levels of labelling of UBI 29-41 found (Figure 14). The first peak represents un-labelled UBI 29-41, the second peak single labelled UBI 29-41 and the final peak is double labelled UBI 29-41. As the Iodogen labelling method labels the ortho positions of tyrosine residues, and there being two ortho positions on the single tyrosine present

in UBI 29-41, the most likely interpretation of these results is that the first peak is the unlabelled UBI 29-41, the second single labelled and the final top is the double labelled peptide. Comparing the diagrams showing an increasing concentration of iodine further strengthens this argument. This shows that the right-most peak, representing the double labelled peptide increases as the other peaks decrease in size. Furthermore, as the final peak is analysed using MS it shows that the increase in size compared to the unlabelled peptide correlates with the substitution of two hydrogen atoms with two iodine and addition of oxygen by the mechanism elaborated in the introduction (Bennett *et al*., 2000). The MS analysis of the unlabelled UBI 29-41 added further information as it confirmed the size of the antimicrobial fragment and furthermore elucidated that the buffer in which it was kept prevented degradations as only one peak was present following storage for up to a year. MS analysis was performed several times to confirm the stability of UBI 29-41 and no degradation was observed (data not shown).

Unfortunately, due to the constraints of radioisotope-proof equipment the labelling analysis used for cold iodine labelled UBI 29-41 was not available for routine analysis when using ^{125}I due to the long half-life, the volatile nature of ^{125}I and that the HPLC-MS equipment was not cleared for using radioactive isotopes. For this reason ITLC was implemented for rapid analysis of the radio iodinated product. This is commonly used in the analysis of radio labelled proteins (Pedraza-Lopéz *et al*., 2000; Chattopadhyay *et al*., 2010).

A profile for free iodine and labelled UBI 29-41 was established, where after the amount of radioactive iodine added in the labelling process was manipulated to see

if this had effect on the labelling. As anticipated, and in agreement with the HPLC labelling analysis, there indeed appeared to be unsaturated UBI 29-41 at lower concentrations of radioactive iodine, however it has to be appreciated that these concentrations were not comparable. This was visible by the disappearance of the peak at the furthest travelling distance, indicating the free iodine, as seen in the free iodine profile. As this peak completely vanished at half the activity and 1/10 the activity, there was no longer any certainty that all ortho positions of all tyrosine residues had been filled, indicating that at best a heterogeneous population of labelled UBI 29-41 was achieved. As a homogeneous population was desired it was decided that the original and Pierce recommended concentration of $Na^{125}I$would be used.

However the limitations of ITLC included the inability to evaluate the nature of labelling. As the concentration of $Na^{125}I$ was much lower than the concentrations of NaI analysed HPLC was implemented for a single analysis of the radio labelled product at the Rayne Institute, St. Thomas' Hospital. Although the resolution of the fragment collection did not allow for proper distinction of the single and double labelled peptide there were some indications, albeit at a low resolution, of a variance between peptide labelled with the recommended activity and peptide labelled with 1/10 the amount of $Na^{125}I$. The labelling profile of the radio labelled peptide was significantly different compared to the regular HPLC elution profile as radioactivity associated with the peptide was measured rather than concentration of the peptide. As UBI 29-41 contains two ortho positions of the tyrosine residue means that two radio nuclides would be associated with the fully labelled peptide and only a single

^{125}I associated with non-saturated UBI 29-41. Therefore, twice the number of UBI 29-41 labelled with a single radionuclide is required to give the same signal as the fully labelled peptide. Finally, the non-labelled peptide would not be detected, reducing the maximum peak numbers from 3 to 2. When comparing this to the results obtained from the radio labelled HPLC fraction analysis, there is a small shift of a shoulder to the right in the analysis of UBI 29-41 labelled with the recommended activity to a an elution profile with a shoulder slight to the left. This may represent a shift to singly-labelled peptide as Na^{125}I was decreased. Collectively, the ITLC and HPLC data confirmed that to take full advantage of the targeting agent and maximise potential toxicity it appears that the optimal labelling is using the recommended levels of Na^{125}I.

The original intention was to produce batches of labelled UBI 29-41and remove samples as required for subsequent experiments, described in chapter 4.This was considered to be the technically optimal strategy for toxicity analysis to maximise batch for comparability. Furthermore, as the half-life of ^{125}I is 60 days it was hypothesised that the variance in radiation would be minimal within the time frame in which it was intended to be used; this variance would be monitored at each toxicity assays by the establishment of the actual activity using a dose calibrator. However, as it was standard procedure to run an ITLC analysis of the labelled product prior to all experiments, it quickly became apparent that the stability of the labelled product was limited. For this reason it was decided to monitor a batch of labelled UBI 29-41 over the course of several days. Over the course of the 144 hours in which the experiment was run a clear trend was visible. There seemed to be a clear

destabilisation of the labelled product resulting in the profile to shift from a labelled one to one resembling the free iodine profile.

This could be the result of the high energy of the labelled iodine destabilising the covalent bond causing radiolysis as found by Uenak and Uenak (1985). It was found that within a diameter of about 30 Å Auger electrons were radiolytically active, and outside this sphere the absorbed dose was not high enough to cause radiolysis in iodobenzene. This can be compared to the case of iodine labelled tyrosine, as tyrosine comprises a benzene ring to which the iodine is directly labelled. A similar result was found by Kauffman and Johnson that found that the ^{125}I labelling of Staphylococcal enterotoxins at high specific activity lost association with the peptides over the period of 71 days (Kauffman and Johnson, 1975), although this is significantly longer than the 6 days reported here. It has to be noted that these peptides were labelled using chloramine-T and not Iodogen. In order to establish whether it potentially could be due to the high concentration of high energy radioactive isotopes, a 1/10 iodine concentration was analysed similarly to the first stability analysis experiment. Interestingly, this showed the same trend as the previous experiment. This indicates that the level of radiation has no effect on the stability of ^{125}I conjugated UBI 29-41, at least at the levels analysed in these experiments. Previous experiments by Kauffman and Johnson showed that lowering the specific activity labelled to the staphylococcal enterotoxins analysed decreased the level of dissociation of the radionuclide (Kauffman and Johnson, 1975). Again, it has to be noted that the labelling process used was chloramine-T and not Iodogen. Furthermore, the levels of radioactivity analysed ranged from 1.4 MBq/µg protein to

1.8 MBq/µg protein. In order to compare this data with the conditions investigated here an activity to peptide mass relation had to be established. The molecular weight of UBI 29-41 was found and confirmed by literature to be 1691 Da or g/mol. 2 nmol was utilised for the labelling which gives a total of 3.4 µg UBI 29-41 per labelling experiment. As an activity of 37 MBq was added to the labelling experiments this gives an activity of 10.9 MBq/µg UBI 29-41. Thus, taken into consideration, it seems reasonable to expect that the dissociation levels would increase even further when compared to the study by Kauffman and Johnson (1975). They saw a decrease in conjugation from 79% to 55% when they increased the activity from 1.4 MBq/µg to 1.8 MBq/µg and stored at 1°C (Kauffman and Johnson, 1975).

To further analyse whether the degradation was due to radiolysis it would be interesting to also analyse the stability of the labelled product using other radioactive iodine isotopes as ^{123}I. This has a shorter half-life but has higher energy Auger electrons, however this would prevent stability analysis of the conjugation for the same time frame as ^{125}I (144 hours.). If the destabilisation of the labelling was indeed due to radiolysis, by exchanging the isotope for one emitting higher energy Auger electrons, you would potentially see a faster destabilisation of the labelling.

In order to establish whether the degradation of the radio labelled peptide was due to a chemical degradation of the labelling process, it would be informative to run the same experiments over the same time frame with non-radioactive iodine and analyse the stability of the product using HPLC-MS. If destabilisation is due to chemical degradation you would see the same trend as seen in the ITLC analysis of the radio

labelled UBI 29-41 in the format of a reversion of Figure 14 from bottom to top. This, however, would have to be run on HPLC.

In the original Pierce Iodogen labelling protocol, there are steps of purification, which are left out in these settings. Initially it was attempted to purify the labelled peptide using both standard PD10 columns as well as anionic exchange columns, however no peptide was recovered from either column. Furthermore, the purifications steps using columns would later cause additional issues with regards to the accumulation of solid waste of which the storage capacity in the department was limited, both with regards to dose and bulk. This resulted in the final steps of the protocol being cut out and the freshly labelled peptide would be considered ready for use. In the absence of HPLC-MS equipment in the department cleared for radioactive use, analysis of non-radioactive iodinated products was performed. Although not optimal, the cold labelling analysis did provide information about the labelling nature of UBI 29-41 showing that two iodides could be added to each peptide. The ITLC also provided information directly comparable to the toxicity experiments as this showed not only that there appeared to be a successful labelling of the peptide but also provided information about the stability of the product.

The importance of establishing the labelling stability is first and foremost significant to ensure correct analysis of the later radio toxicity experiments. As Auger electrons are very reliant on close proximity to the target DNA it is vital that the damaging agent is not dissociated from the targeting moiety. Furthermore, for more downstream applications, in therapeutic and diagnostic settings it is vital that the radioactive isotope is not dissociated from the targeting agent. This would lead to

increased accumulation in non-target tissues and in diagnostic settings it could lead to misinformation of the disease in question. In a therapeutic setting it would be detrimental in other ways, as there would be no control over the radioactive isotope and damage to non-target tissues, in the case of iodine a common organ is the thyroid gland, would be very likely. As Auger electrons are DNA damaging agents, this could lead to, for example, an increased risk of cancers and therefore further complicate treatment.

Following this series of optimisations of labelling of the initial targeting agent, UBI 29-41, the next step was to analyse the effects of the Auger electrons emitted from the targeted iodine.

4 Analysis of radio-toxicological effects of Auger electrons

4.1 Introduction

The aims of this chapter was to study the effects of the ^{125}I radio labelled UBI 29-41 from chapter 3 and the effects of Auger electrons on the survival rate of a range of model microorganisms. Auger electrons have previously been evaluated for the potential toxic effects on cancerous cell lines (Xu *et al*., 2002; Bodei *et al*., 2003; Kassis, 2003; Brady *et al*., 2013; Paillas *et al*., 2013) and we wanted to evaluate if this effect could be successfully transferred to microorganisms as a new approach to fight complicated and/or resistant strains. The primary mechanism of Auger electron toxicity is via the generation of double strand breaks (DSBs) in the cell DNA (Sharkey and Goldenberg, 2011; Balagurumoorthy *et al*., 2012).

To take variance in size and potential difference in susceptibility into consideration it was decided to include a broad range of organisms. Four model organisms were chosen for the toxicity assays to obtain a broad characterisation of the toxicity of the Auger emitting isotope ^{125}I. *E. coli* was used to represent gram negative bacteria, *S. aureus* to represent gram positive bacteria and *C. albicans* to represent pathogenic yeast. Finally, *S. cerevisiae* BY471 was included as this is a very well established as model organisms in biomedical settings (Cohen and Engelberg, 2007).

In order to characterise the effects of toxic agents on the organisms, growth characteristics were initially established alongside cell number/absorbance density correlation to ease the analysis of the effects of radiation per cell.

As UBI 29-41 is a known antimicrobial peptide, it is toxic to microorganisms in itself. Therefore, the innate toxicity of the initial targeting agent as well as the labelling buffer and iodine alone had to be established in order to rule out effects of the targeting agent on the survival rate of the model organisms.

Finally, non-targeted ^{125}I had to be included as a negative control to evaluate if the targeting had any effect.

4.1.1 Specific aims:

- To evaluate the growth characteristics of the five model organisms
- To analyse the innate toxicity of non-labelled UBI 29-41 in each of the species
- To evaluate the toxic effects of ^{125}I- labelled UBI 29-41 compared to non-targeted ^{125}I
- To assess the usefulness of radio labelled UBI 29-41 as an antimicrobial agent in light of the above results

4.2 Characterisation of model organisms

Prior to toxicity assays the growth curves of the model organisms had to be characterised. The model organisms included in this project were: *Escherichia coli* K-12, *Staphylococcus aureus* NCIMB 8625, *Candida albicans* sc5314 and *Saccharomyces cerevisiae* BY4741. This was required to ensure that the toxicology experiments are conducted in a way in which the fitness of the cells is as comparable as possible. Furthermore, it was desirable to keep the number of cells for the experiments constant in order to better compare the effects of the doses the organisms were subjected to.

The four organisms were grown as described in section 2.2.6.1. Bacterial strains were grown in LB media and Yeast strains were grown in YPD. Growth curves for most organisms were established using a plate reader and converted to spectrophotometer OD units. Simultaneously, using a haemocytometer, the cell numbers were established at varying cell OD_{600} densities to allow conversion between optical densities and cell numbers. This would later enable the potential link between toxicity observed and amount of radiation per cell.

Growth curves were conducted for all the organisms, with measurements made every 30 minutes (Figure 24A-D).

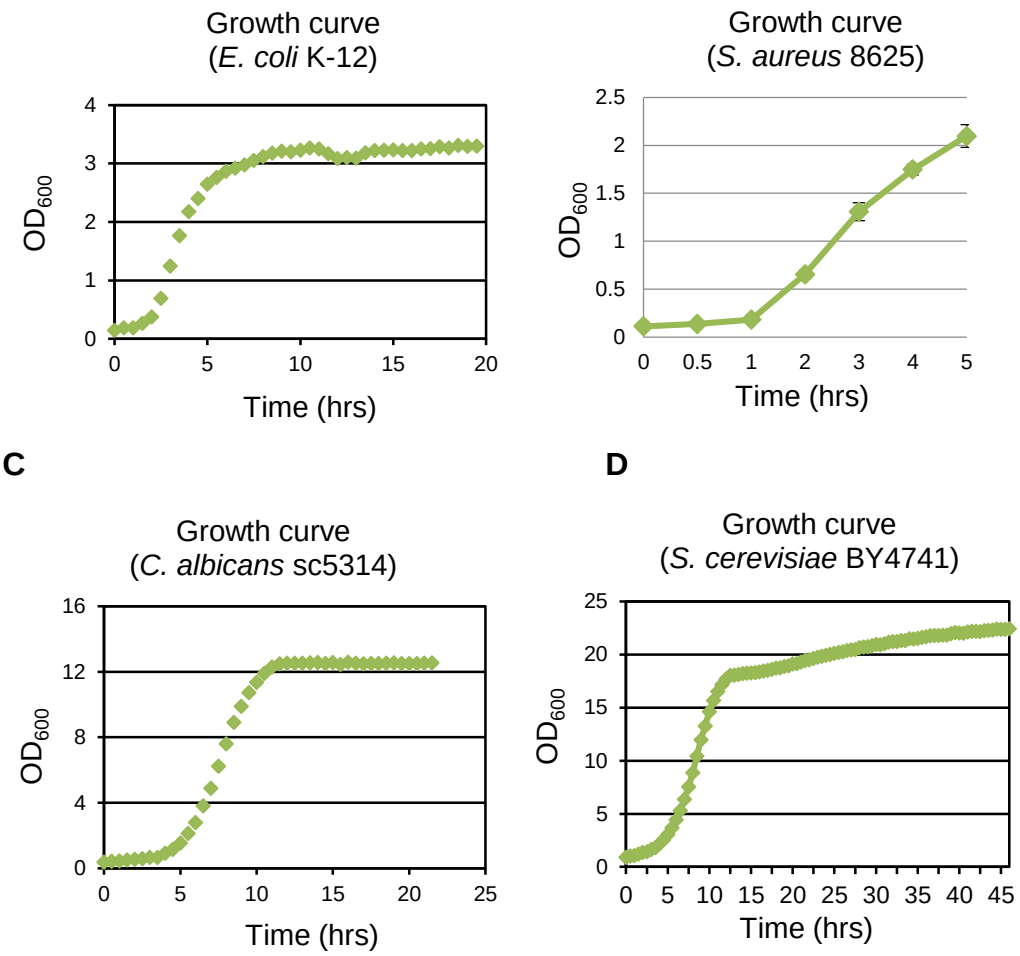

Figure 24 Growth characteristics of model organisms

The basic growth characteristics for all model organisms, save *S. aureus*, were established using a plate reader set to measure the absorption at OD_{600}every 30 minutes. A growth characteristic for S. aureus was found by manual measurements every 30 minutes for the first hour and hereafter every hour for 5 hours. Bacterial strains were grown in LB media whereas yeast strains were grown in YPD. All measurements were done in triplicate.

As can be seen in the above figure, all the growth curves showed a classic lag phase followed by a log phase that plateaus in a stationary phase. The growth curve for *S. aureus* did not reach complete stationary phase as the growth curve was terminated when the log phase was reaching its end. This was based on previous observations

(data not included). Furthermore, the beginning of the log phase had been established, which was the point required for the toxicity experiments.

The growth curves allowed the establishment at what point the cells for the experiments needed to be harvested for the toxicity experiments. To both maximise cell fitness and to ensure optimal colony numbers, the beginning of the log phase was chosen. This meant an OD_{600}=0.1 for *E. coli* and *S. aureus* and an OD_{600}=1 for *C. albicans* and *S. cerevisiae* as established by the results from the growth characteristics obtained.

Following the establishment of the growth characteristics, the cell density had to be correlated to a cell number. This was done by counting cell numbers using a haemocytometer, at various cell densities. Cell numbers were hereafter plotted against the OD_{600} value at which they were collected. This was done for all the organisms and the results can be seen in the Figure 25A-D. The correlation between cell numbers and OD_{600}appeared as expected to be linear. This allowed for a conversion between observed OD readings and the numbers of cells used in subsequent experiments (Table 10).

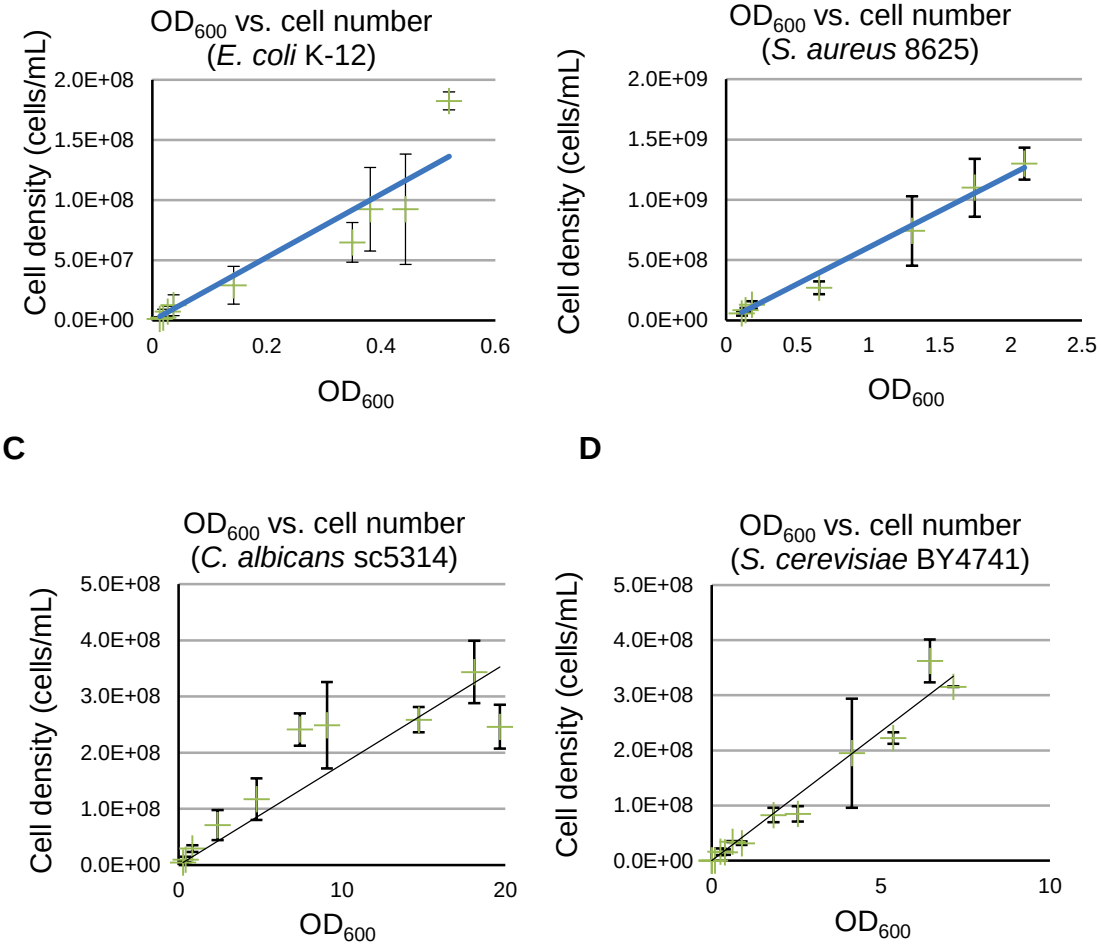

Figure 25 Relationship between OD_{600} and cell number

Cell numbers at various culture densities were established using a haemocytometer. This was done for all model organisms (A-D). All measurements were done in triplicate.

By using the newly acquired conversion factors, and the knowledge that 100 µL of cell culture would be used for the experiments, the number of cells in each experiment could be calculated (Table 10). Prior to experiments the cell culture was diluted 1:1000 to ensure enough even spreading on the plates, leading to well defined colonies easing counting and thereby collection of data.

Organism	Number of cells per OD_{600} unit	OD_{600} unit utilised	Number of cells utilised in experiment
E. coli K-12	$3*10^8$	0.1	$3*10^3$
S. aureus NCIMB 8625	$6*10^8$	0.1	$6*10^3$
C. albicans sc5314	$2*10^7$	1	$2*10^3$
S. cerevisiae BY4741	$5*10^7$	1	$5*10^3$

Table 10 Number of cells utilised in experimental procedures

For each of the model organisms a linear regression was made and the link between OD_{600} and cell numbers was established. In order to attempt to use the same number of cells per experiment regardless of organism and in order to utilise cells in the beginning of their respective growth curves, it was decided to use bacterial strains at OD_{600}=0.1 and yeast strains at OD_{600}=1. This also correlated with a comparable number of cells per experiment. The number obtained in the final column, is based on 100 µL of cells, the volume used in the experiments, taken out at their respective OD_{600} value and diluted 1:1000.

4.3 Optimisation and validation of cytotoxicity assays using hydrogen peroxide as primary toxic agent

Following the establishment of the growth characteristics of the organisms it was important to not only establish the base-line sensitivity of the organisms to DNA damage but also develop the protocol for the toxicity experiments.

Initially, the correct dilutions of the organisms were established. Based on the results found for Table 10, this was done by harvesting the cells at the beginning of their respective log-phases and hereafter performing a round of serial dilutions of each organism. These were then plated in triplicate to find the dilution factor resulting in the highest number of colonies that produced an even and countable spread on the

plates. It was found that a $1x10^{-4}$ dilution of the cells gave the most reliable number (data not included). This dilution factor was the same for all organisms.

The next step was to establish a protocol for the toxicity assays and investigate the baseline toxicity of the model organisms. For this the well-established DNA damaging agent hydrogen peroxide was chosen. Hydrogen peroxide is not only a good model chemical for DNA damage, it has ease of use and finally it also forms reactive oxygen species similar to ionising radiation (Henle and Linn, 1997). For this reason it was an excellent candidate for the development of the experimental setup and would also be useful to establish baseline susceptibility of each organism to DNA damage.

The cells were harvested and diluted in the appropriate media. They were hereafter subjected to a range of concentrations of hydrogen peroxide ranging from 0.5 mM to 70 mM depending on the susceptibility of the organisms. To generate a full toxicity curve and thereby give a complete view of the effects of hydrogen peroxide on the organisms, the dose of hydrogen peroxide was increased until no colonies appeared. This was adapted accordingly over a range of experiments (data not included). All experiments were carried out in triplicate. The final results of the hydrogen peroxide experiments can be seen in Figure 26A-D.

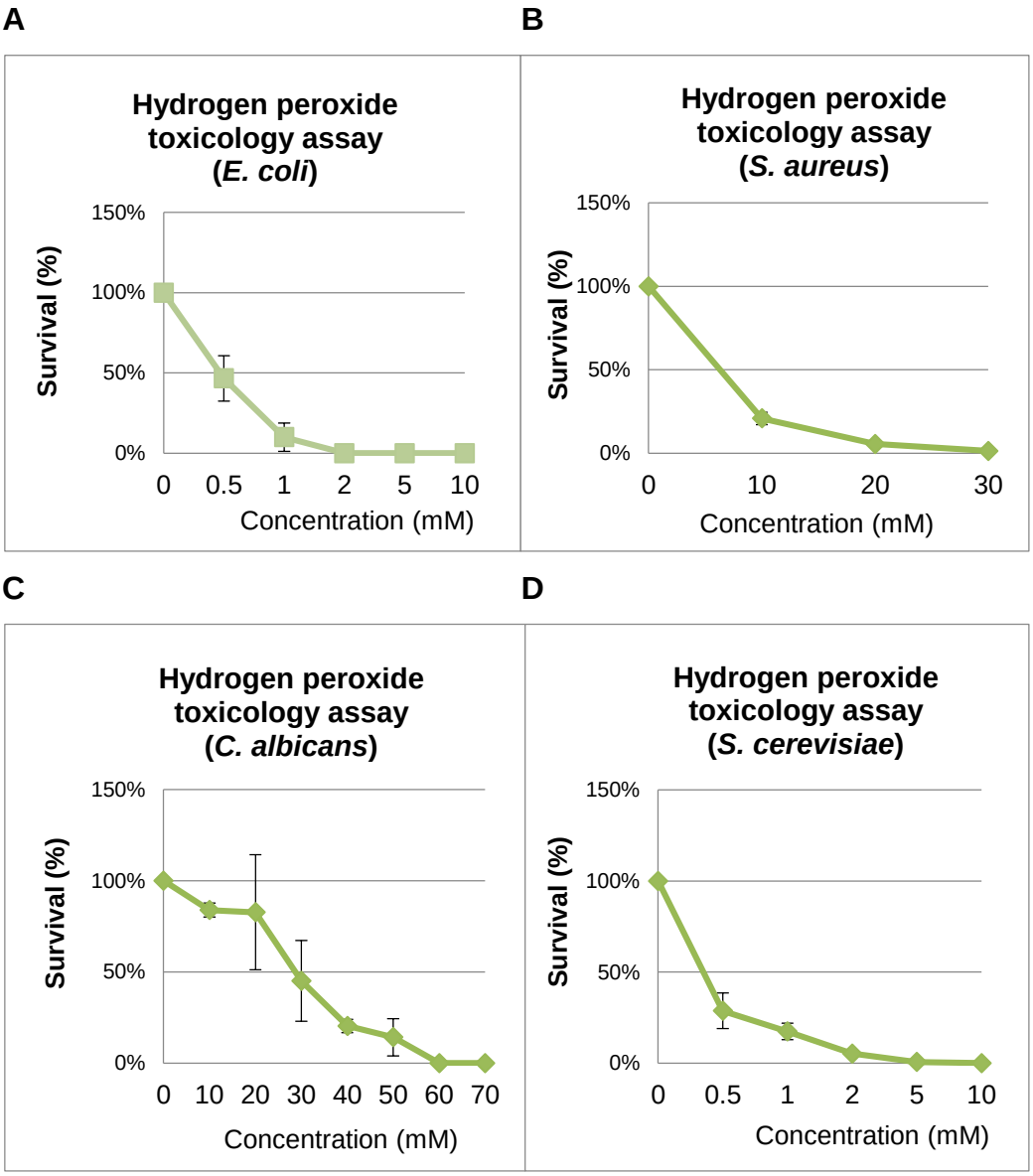

Figure 26 Effects of hydrogen peroxide on survival rate of model organism

Analysis of the effect of 0.5 mM-10 mM hydrogen peroxide on *E. coli* survival. Overall survival rate decreases rapidly showing very high susceptibility. All experiments were performed in triplicate.

The baseline susceptibility of the model organisms to hydrogen peroxide varied between species. Both *E. coli* and *S. cerevisiae* only required exposure to 10 mM hydrogen peroxide for no colonies to appear. Interestingly, the two pathogenic strains, *S. aureus* and *C. albicans* appeared to be more resilient to the effects of

hydrogen peroxide, which may have implications for later interpretation of results. The results were further validated by previous published results showing the same degree of susceptibility to hydrogen peroxide for both *C. albicans* and *S. cerevisiae* (Jamieson, 1996).

All figures show consistent dose-response curves for all organisms. This shows that the establishment of the protocol for toxicity evaluation was successful and could be utilised for later experiments.

The IC_{50} values were calculated from the trend lines for each curve. The results are visible in Table 11.

Organism	**IC_{50}**
E. coli	0.4 mM
S. aureus	1.5 mM
C. albicans	23.1 mM
S. cerevisiae	0.6 mM

Table 11 IC_{50} values of hydrogen peroxide

All organisms showed susceptibility to the damaging effects of hydrogen peroxide, however C. albicans did show a significantly lower susceptibility than the other organisms requiring up to nearly 50 times the concentration to eradicate 50%.

This set of experiments not only developed a successful method for toxicology studies in the model organisms used in this project, it also gave information about the innate susceptibility of the organisms to DNA damaging agents, acquired to aid later interpretation of radio toxicological results. Following the establishment of a

successful protocol for toxicity studies, the next step was to evaluate the toxic effects of the targeting agent UBI 29-41 on the model organisms.

4.4 Innate toxicity of UBI 29-41

After baseline toxicity of the model organisms used had been established, the innate toxicity of the targeting agent had to be assessed using the methods developed from the hydrogen peroxide experiments.

The establishment of the innate toxicity of UBI 29-41 was especially important as antimicrobial peptides, such as Ubiquicidine, have sterilising effects, and the innate toxicity could interfere with later analysis of the results from the radio toxicological assays. Furthermore, observation of innate toxicity would provide a confirmation that the UBI 29-41 was functional and had not deteriorated in any fashion that could compromise binding.

The experiments were conducted as explained in section 2.2.7- 2.2.8 on all of the model organisms described earlier to evaluate if any difference in toxicity would be observed due to variance in susceptibility. Each organism was grown to the desired $OD_{600,}$ where after they were diluted 1:1000 and subsequently subjected to two concentrations of UBI 29-41: 50 µM and 100 µM. These concentrations were selected as being close to the concentration to be evaluated later in a labelled version of the peptide (20 µM). The organisms were subjected to the antimicrobial peptide for 1 hour at room temperature. The organisms were then plated and grown at the appropriate temperature for 1-2 days until colonies appeared and the number of colonies was counted manually. All plates were done in triplicate. The toxicity of

the antimicrobial peptides was established by counting the number of colonies in the control group (which was not subjected to antimicrobial peptides), with the survival rate calculated by counting how many colonies appeared in UBI 29-41 exposed plates and dividing this by the number found in the control group. The toxicological effects of UBI 29-41 are summarised in Figure 27.

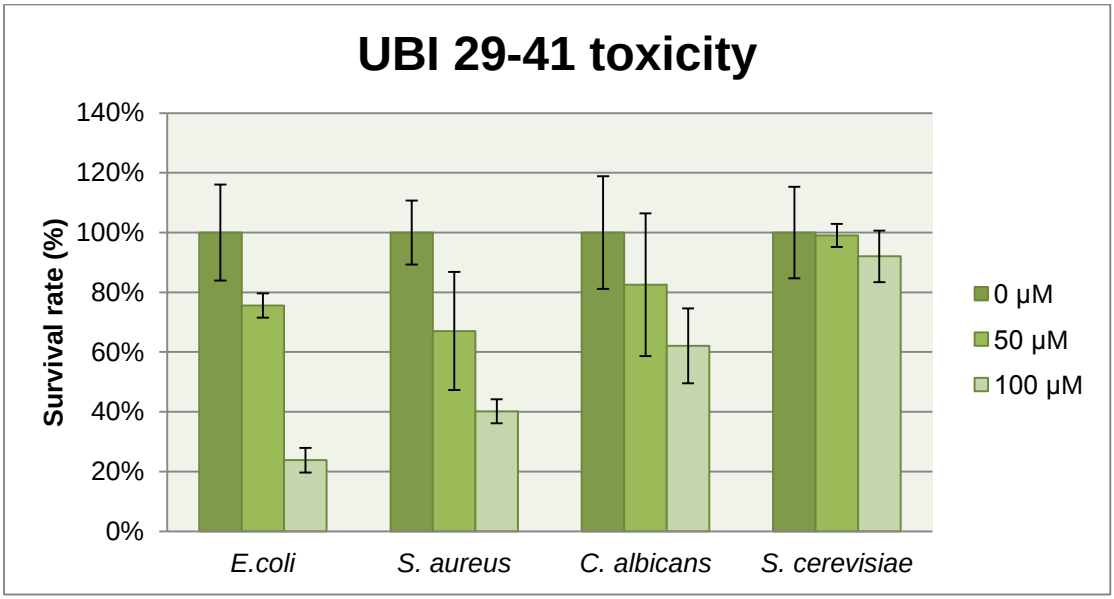

Figure 27 Analysis of the innate toxicity of UBI 29-41

The above figure summarises the experiments analysing the innate toxic effects of UBI 29-41. The most susceptible organisms were the bacterial strains. *C. albicans* had an intermediate susceptibility to the toxic effects of UBI 29-41 and S. cerevisiae showed very little decrease in survival rate compared to the other organisms. All experiments were conducted in triplicate.

The innate toxic effects of UBI 29-41 are quite apparent in the bacterial strains *E. coli* and *S. aureus*, whereas there seems to be a higher degree of resistance in the yeast strains *C. albicans* and *S. cerevisiae*. *C. albicans* displayed an intermediate level of susceptibility whereas *S. cerevisiae* showed very low susceptibility. Taking the mechanism in which antimicrobial peptides work into consideration, including membrane destabilization, perforation and bacteriolysis which are all dependent on

reaching a critical threshold, the smaller size of bacteria compared to yeast could mean that this threshold could be reached at lower concentrations (Brouwer *et al*., 2008).

This experiment, and the observation that UBI 29-41 leads to no more than a 20-30% decrease in survival rate at levels at 50 μM than the concentration to be later evaluated in radiological experiments allowed an analysis of the impact of targeted radio iodine in subsequent experiments.

4.5 Toxicity of non-radioactive non-labelled activated iodine

As iodine itself has been used as a means to sterilise infections, it was necessary to evaluate the toxicity of iodine itself (Block, 2001). Furthermore, the labelling technique required the presence of Tris Iodination buffer which would be incubated with organisms along the labelled peptide. By activating the non-radioactive by the same means as ^{125}I for UBI 29-41 labelling, both factors could be evaluated simultaneously for any effects on microbial survival.

The experiments were conducted as for the hydrogen peroxide (section 2.2.7) with the hydrogen peroxide being replaced by iodine activated by the Iodogen compound in Tris Iodination buffer. Two concentrations were evaluated, 0.5 mM and 1 mM. All experiments were done in triplicate.

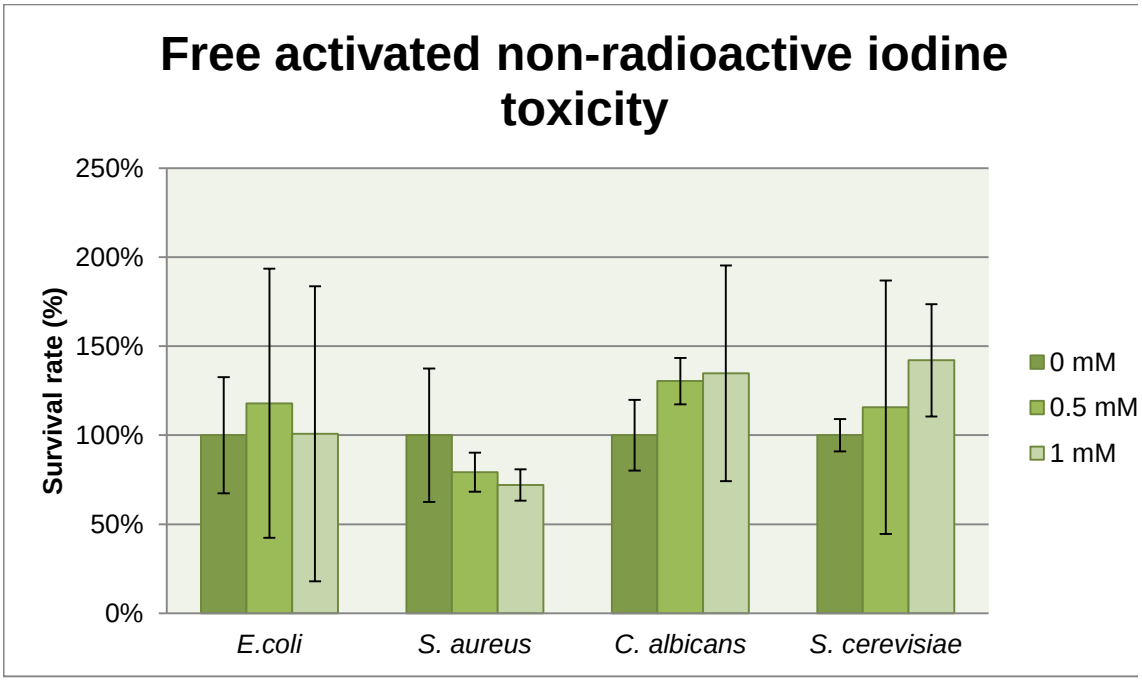

Figure 28 Overview of toxicity of non-radioactive iodine in labelling buffer

This figure summarises the toxicological studies of activated free non-radioactive iodine in Tris Iodination buffer on the four model organisms included in the project: *E. coli*, *S. aureus*, *C. albicans* and *S. cerevisiae*. Two doses were evaluated: 0.5 mM and 1 mM and the survival rates were compared to organisms grown without iodine and Iodination buffer. No difference in survival rate was observed in any of the organisms ruling out the intrinsic antimicrobial effect of iodine and any effect of iodination buffer in later toxicological studies. All experiments were performed in triplicate and error bars display variability in results based on standard deviation.

No significant decrease in survival rate was seen in most of the model organisms, indicating that neither Tris Iodination buffer nor iodine itself had any effect on the survival rate at the levels investigated. (Figure 28).

However, the concentrations of "cold" iodine evaluated are much larger than the concentration of "hot" iodine to be evaluated later. This means that the likelihood of iodine to have an effect on the survival rate in later experiments is low.

4.6 Toxicity of ^{125}I-labelled UBI 29-41 and non-targeted ^{125}I

Following the establishment of the innate toxic effects of UBI 29-41 as well as the effects of buffer and non-radioactive iodine alone, the next step was to label UBI 29-41 with ^{125}I according to the protocols optimised in chapter 3. In order to establish the toxic effects of the targeted Auger electrons it had to be compared to the effects of non-targeted ^{125}I (^{125}I not conjugated to UBI 29-41).

The non-targeted ^{125}I was generated by activating the ^{125}I in the same fashion as when labelling peptide (section 2.2.2), without adding UBI 29-41. This ensured that the only variable was the targeting agent. Two experimental doses per tube were evaluated, 1 MBq and 5 MBq, with actual doses established using a dose calibrator. These values were included as the x-axis values. The error bars were included to show the variability of the data formed by triplicate of organisms plated from the same tube. All model organisms were, following the one hour exposure to either radio-labelled UBI 29-41 or free activated iodine, washed with growth media and plated in triplicate. All work was done in a flow hood behind lead fortified glass. The results can be seen in Figure 29, Figure 30, Figure 31 and Figure 32.

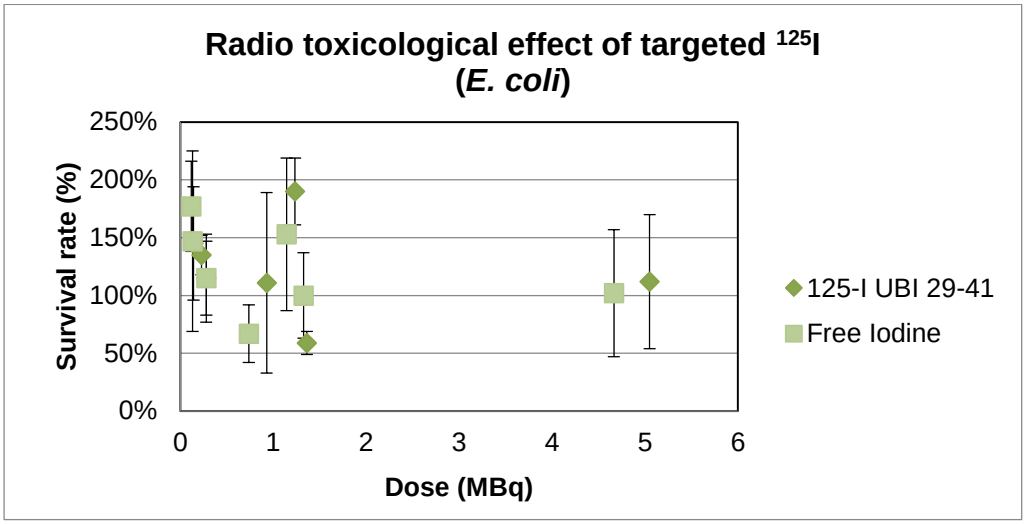

Figure 29 Comparative overview of the radio toxicological effects of ^{125}I labelled UBI 29-41 and free activated ^{125}I in *E. coli*

Overview of the toxic effects of either targeted (^{125}I-UBI 29-41) or non-targeted (free iodine) ^{125}I on *E. coli* survival rate. Several doses were analysed. No significant difference was observed between the two groups. All experiments were done in triplicate.

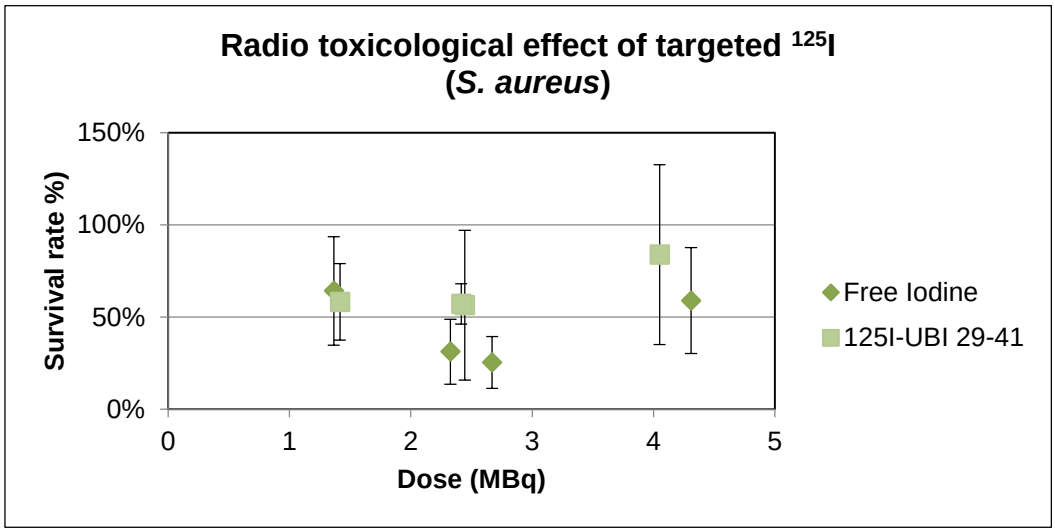

Figure 30 Analysis of the effects of UBI 29-41 targeted Auger electrons compared to non-targeted in *S. aureus*.

S. aureus was exposed to increasing levels of both targeted (^{125}I-UBI 29-41) and non-targeted (free Iodine) Auger emitting isotope ^{125}I No toxic effect of targeting the Auger emitting isotope is observed. All experiments were done in triplicate.

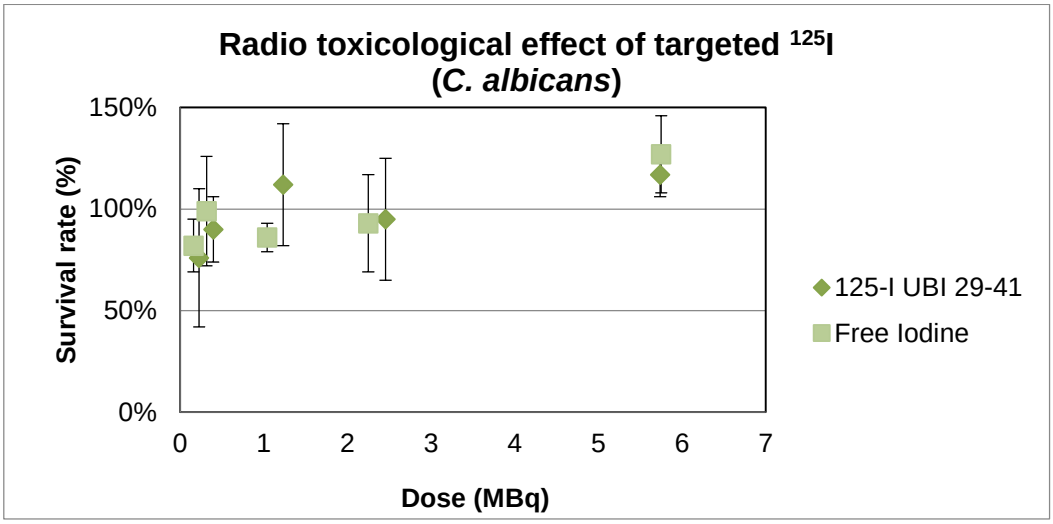

Figure 31 Evaluation of the radio toxicological effects of UBI 29-41 targeted ^{125}I compared to non-targeted activated ^{125}I.

Overview of the radio toxicological effects of UBI 29-41 targeted versus non-targeted ^{125}I on attenuated *Candida albicans***.** No significant difference between the targeted and non-targeted ^{125}I values was seen. All experiments were performed in triplicate.

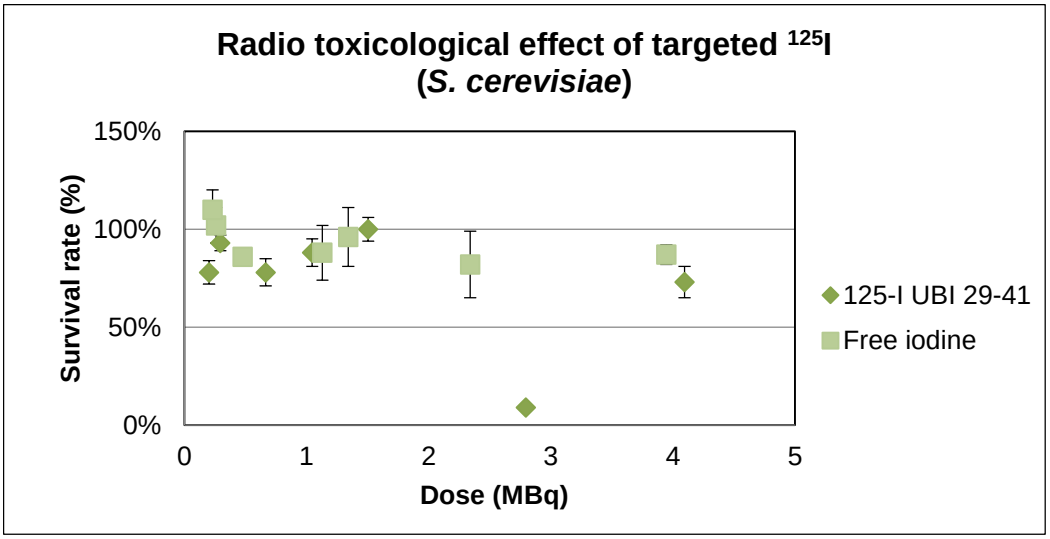

Figure 32 Analysis of the radio toxicological effects of targeted ^{125}I compared to non-targeted ^{125}I on *S. cerevisiae* BY4741

Overview of the toxic effects targeted (^{125}I-UBI 29-41) and non-targeted (free iodine) ^{125}I on *S. cerevisiae* survival rate. No significant difference was observed between the two groups despite on point at ~2.8 MBq. All experiments were done in triplicate.

The results of these analyses provide no evidence of toxic difference between the free ^{125}I and the UBI 29-41 targeted ^{125}I in any of the model organisms. In the *S. cerevisiae* radio toxicity experiments there is one point at around 2.7 MBq that appear to show a high degree of toxicity, however this effect was not observed at higher doses and is therefore considered and outlier. As no such effect was seen in any of the other cell lines and was not replicated in this one, it was concluded that the point was an experimental outlier.

To further validate that no variance between the slopes were statistically significant, the two populations were compared using multiple linear regression analysis. A summary of the results can be seen in Table 12.

Organism	**p-value**
***E. coli* K-12**	0.78
***S. aureus* NCIMB 8625**	0.47
***C. albicans* sc5314**	0.69
***S. cerevisiae* BY4741**	0.54

Table 12 P-values from multiple linear analysis of the two populations of free ^{125}I and targeted ^{125}I

This confirms that there is no statistical significant variance in the slope between ^{125}I-UBI 29-41 and free ^{125}I.

4.7 Binding analysis

To establish whether the observed lack of toxicity was due to inefficient targeting and binding of ^{125}I to the microorganisms, a binding analysis was conducted.

Following incubation of *S. cerevisiae* and *E. coli* with both free activated radioiodine and UBI 29-41 targeted ^{125}I, the exact dose applied to cells was established using a dose calibrator as a frame of reference. The cells were hereafter pelleted by centrifugation and resuspended in 900 µL of appropriate media. The cells were pelleted again, the supernatant was removed and the cells were resuspended in new media. This was conducted 3 times where after the final resuspended pellet was transferred to a new tube to prevent radiation bound to the initial Eppendorf tube from influencing the results. Cells were counted and the level of ^{125}I bound to the pellet was measured by dose calibrator and expressed in Bq/cell.

As can be seen in Figure 33 there appears to be no difference between the free iodine and ^{125}I-UBI 29-41, either before or after the washes, for either organism. A higher degree of radiation associated with cells subjected to ^{125}I-UBI 29-41 could have been expected if targeting was successful.

These results have several possible implications: 1) binding was compromised or so weak in interaction that the washing dissociated the UBI 29-41 from the cells 2) the radiation associated with the cells was so low that it could not be distinguished from background; and finally, 3) the concentration of labelled peptide used in the experiments was too low to allow sufficient binding to cells.

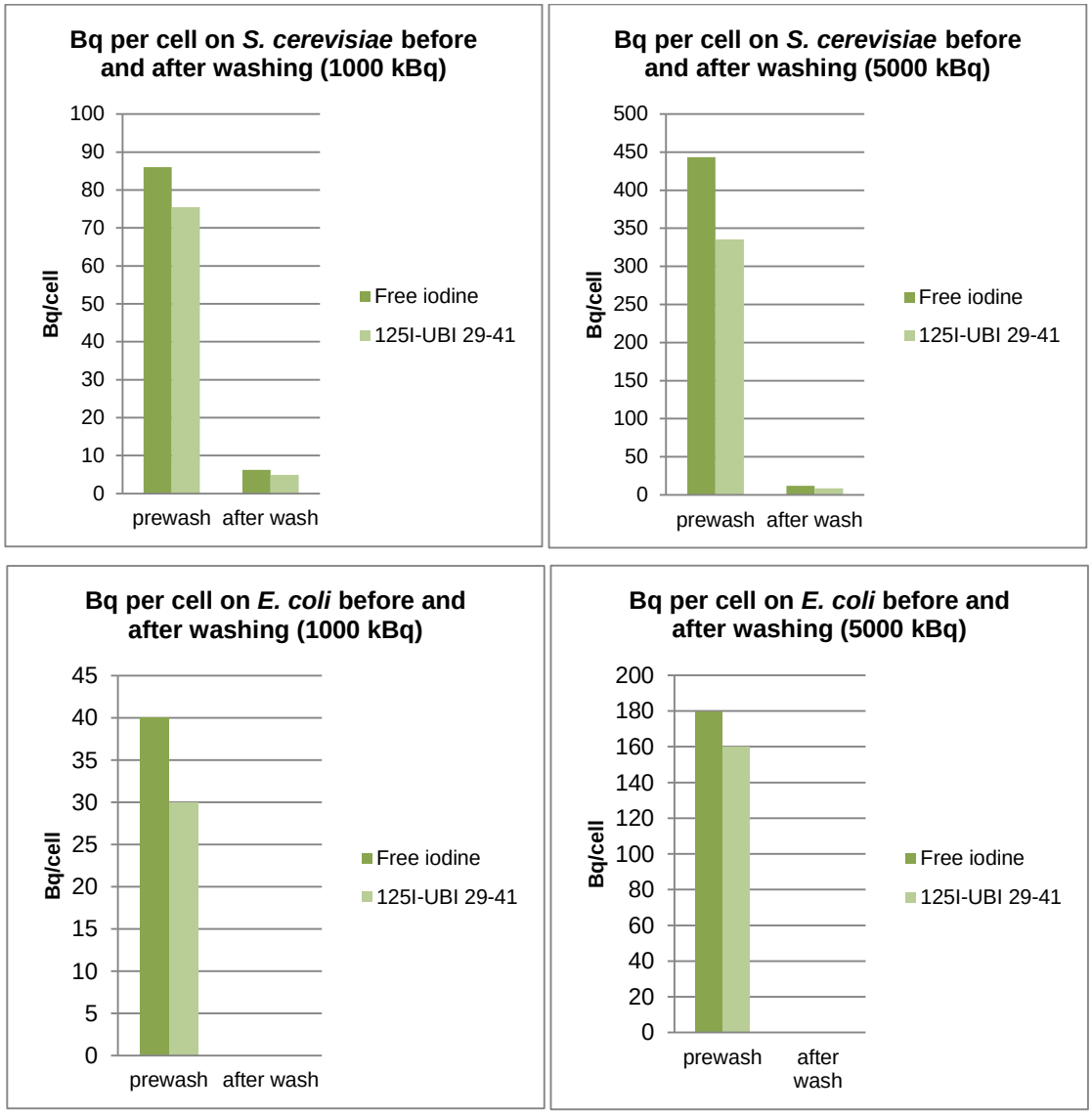

Figure 33 Binding efficiency of ^{125}I-UBI 29-41 compared to free iodine on *S. cerevisiae* and *E. coli* at the two analysed theoretical doses

S. cerevisiae and *E. coli* were subjected to the two doses 1 MBq and 5 MBq radioiodine- either targeted or non-targeted. The actual doses were established using a dose calibrator. Measurements were performed both just prior to washing and after washing. The majority of the radiation appears to have been removed following washing for both free iodine and ^{125}I-UBI 29-41. Furthermore, no difference in radiation associated with the cells was observed in either free iodine or^{125}I-UBI 29-41 indicating that there was either too low concentration of peptide or that binding of UBI 29-41 had been compromised.

Based on these results, there is no conclusive evidence as to whether ^{125}I could be used as a therapeutic agent in the settings tested in this study. The results in this project indicate that under the circumstances tested here, there is no toxicity associated with ^{125}I-UBI 29-41; however as will be outlined below, many parameters could be tested to further investigate the therapeutic potential of Auger electrons.

4.8 Discussion

This chapter aimed to establish a system for evaluating the toxicity of radio labelled UBI 29-41 on four model organisms. The growth curves for these organisms were successfully produced, and the innate levels of toxicity of UBI 29-41 was measured including the innate toxicity of the iodination buffer and experimental conditions as well as iodine itself. No significant additional effects of the radio labelled peptide were observed when compared to free ^{125}I.

Prior to any radio toxicity experiments, the clonogenic assays for the determination of effects of various compounds on survival rate of model organisms, was established. Simultaneously, the baseline susceptibility of the organisms was established using hydrogen peroxide (H_2O_2) as this is a well-known DNA damaging agent. Although hydrogen peroxide is not directly DNA damaging it is harmful indirectly via the Fenton reaction (Henle and Linn, 1997). This made hydrogen peroxide a suitable candidate for the establishment of baseline susceptibility. Interestingly, it was found that the two pathogenic strains, *S. aureus* and *C. albicans* showed higher degree of resistance to the effects of hydrogen peroxide compared to *E. coli* and *S. cerevisiae*. The findings were further backed by previously published

results in *C. albicans* by Jamieson *et al*. when compared to *S. cerevisiae* (1996). Jamieson hypothesised that this resistance could be explained by the fact that *C. albicans* is a pathogenic strain and is therefore more likely to encounter the phagocytic cells of the immune system, which are prone to generate large quantities of ROS as a means to destroy invading microorganisms (Jamieson *et al*., 1996: Janeway *et al*., 2005). It is therefore more likely to have generated an efficient SOS response system to deal with DNA damage compared to the non-pathogenic strain. As *S. aureus* is an opportunistic strain it could be hypothesised to have generated the same resistance. Based on these results it is likely to expect the same tendencies in the later radio toxicity experiments.

The UBI 29-41 innate toxicity assays were included to establish the toxic effects of the targeting agent and to be able to subtract the effects of the targeting agent of any toxic effects seen. The results showed that the bacterial strains were generally much more susceptible than the yeast strains to the toxic effects of UBI 29-41. As one of the modes of function of antimicrobial peptides is the creation of pores in microbial membranes when the concentration reaches a certain threshold, it could be hypothesised that the reason for the increased susceptibility of the bacterial strains is down to size difference. As the bacterial surface area is much smaller than that of the yeast strains, it is reasonable to think that the critical membrane concentration for pore formation is reached faster for bacterial strains (Tyson *et al*., 1979; Grossman *et al*., 1982; Loferer-Krößbacher *et al*., 1998; Brogden, 2005). However, it is possible that other factors could play a role in susceptibility to antimicrobial peptides including the difference in cell wall. Despite the cell wall being

negatively charged in both microbial systems, the chemical components differ greatly, where bacterial cell wall is compose of peptidoglycan and yeast is composed primarily of polysaccharides (Madigan *et al*., 2003). The most likely explanation, however, is the size difference, although other factors may have an impact on the displayed difference in susceptibility.

One of the main aims of the project was to determine the radio toxicological effects of Auger electrons. Auger electrons have previously been evaluated as potential new therapeutic agents for cancer therapy (Xu *et al*., 2002; Bodei *et al*., 2003; Kassis, 2003; Brady *et al*., 2013; Paillas *et al*., 2013). As the surface markers for cancers differs with varying degree from normal human cells, the effects of targeting are limited. This is one of the great challenges with cancer targeting. Secondly, the size of mammalian cells (~2000 μm^3) is much greater when compared to bacterial cells (~1 μm^3), or even yeast (~40 μm^3) (Tyson *et al*., 1979; Grossman *et al*., 1982; Loferer-Krößbacher *et al*., 1998; web 4). As Auger electrons have a very limited range, the requirement for cancer therapy is internalisation in order to get close enough proximity to the target DNA to induce DSBs. This is potentially less of an issue with bacterial cells due to their restricted size.

The overall results obtained showed very little indication of any toxic effects of ^{125}I regardless of the presence of UBI 29-41. Furthermore, as the slopes of the survival rate were zero it is very likely that UBI 29-41 did not show any toxic effects, as this would have given some degree of reduced survivability of the organisms. As mentioned previously there are several potential reasons to why no toxicity was seen when based on the binding studies: 1) binding was compromised or so weak that

washing dissociated UBI 29-41 from the cells. This lack of binding seems unlikely to be due to suboptimal pH. UBI 29-41 binds via electrostatic interactions due to the high number of positively charged amino acids. The sequence is TGRAKRRMQYNRR, which illustrates that nearly 50% of the peptide comprises positively charged amino acids (red letters) (Welling *et al*., 2002; Akhtar *et al*., 2005).UBI 29-41 was stored in an acidic buffer, (5% acetic acid, pH4) whereas the Tris iodination buffer was neutral (pH 7.5) (Welling *et al*., 2002). The addition of acidic buffer containing UBI 29-41 would therefore only slightly acidify the buffer. Furthermore, as the pI of UBI 29-41 is 12.18 (calculated using expasy.org) a pH of 7.5 will not have had any effect on the targeting ability, which therefore can be ruled out as a cause of lost binding.

Another possibility of assessing the targeting effects of UBI 29-41 other than the binding experiment could be to label the peptide with a fluorophore and visualise in a fluorescence microscope or perhaps flow cytometry, however the small size of the microorganisms might be a hindrance. An issue with this might be that the labelling process of UBI 29-41 with a fluorophore might alter the binding of the peptide. Furthermore, the chemical requirements themselves might alter the chemical properties of the peptide itself. All this might make it incomparable to the iodine labelling.

However, iodine might have had an effect on the targeting as well. An easy way to elucidate the effect labelling had on the targeting ability of UBI 29-41 would be the repetition of the innate UBI 29-41 toxicity experiments with "cold" labelled UBI 29-

41. This would have to be done using the same concentrations of UBI 29-41 as in the previous experiments.

Finally, the concentration of labelled peptide was too low to allow sufficient binding, which potentially could have been circumvented by longer incubation time. The organisms were only incubated with the toxic agents for one hour prior to plating to reduce organism growth. Additionally, due to the very small concentration of UBI 29-41 it is plausible that the labelled antimicrobial peptide did not have the time to reach its full potential in binding capacity. Furthermore, the decay rate of ^{125}Ihas to be taken into consideration as only a very small percentage of the isotopes within this timeframe will decay and eject any Auger electrons to cause DSB. Although it was desirable to leave the targeted ^{125}I attached to the cells after plating, this would only still be two additional days out of a half-life of 60 days. However, in order for these studies to make sense the Bq/cell ratio has to be addressed. The preliminary studies included in this chapter showed a very low association of radiation with the cells; ~5 Bq/cell for the 1 MBq experiment and ~10 Bq/cell for the 5 MBq experiment in the case of *S. cerevisiae*, which is very low, practically background, and appears to be insufficient to cause cell death. *E. coli* showed no binding to cells following washing; however this could be due to the low resolution of the dose calibrator. As binding appears to be a significant issue it would be interesting to investigate the radiation associated with a peptide that has a potential better binding affinity than UBI 29-41 to microorganisms. As an antimicrobial peptide was chosen in the first place due to its non-specific binding, the best approach would likely be to analyse a range of antimicrobial peptides for a better binding profile. Using more targeted molecules

such as antibodies, despite binding with better affinity, have greater specificity and would very likely prevent a comparative study of various microorganisms as done here.

Another option could be the exchange ^{125}I for a higher energy emitter such as ^{123}I. Although this would potentially suffer the same fate as ^{125}I if binding was the limiting factor, it would be interesting to see if a higher energy isotope would be able to cause enough damage in the limited time frame. Another advantage of utilising ^{123}I would be the shorter half-life which would allow for better utilisation of the decay rate within the time frame of the experiments. It would also be of interest to analyse the same conditions, isotope and doses, but for a longer period. The problem with a longer incubation time however, could include issues with cell fitness. Two options to address could be the following: 1) either the cells would have to be incubated at the correct temperature to improve the conditions of the cells, however the cells would then be dividing. Considering this, it could potentially be worthwhile to have investigated the growth of the organisms in the presence of free iodine as well as ^{125}I-UBI 29-41 to monitor the effects on the growth of the organisms over a longer period of time. This would also be a better simulation of the physiological conditions under which the potential therapy would be executed *in vivo*. 2) Alternatively the cells could be incubated for longer under the same conditions as the protocols used for the executed radio toxicity experiments, although this could potentially compromise the viability of the cells, potentially masking any effects induced by the radiation, so careful controls would be needed.

Although no effect was seen in the toxicity assays in this project, the effects of the Auger electrons might not have been large enough to cause any detrimental effect in any of the organisms. This does not necessarily mean that no radiological effect took place. There are several ways available for the detection of DSBs in microorganisms. A straightforward method could be the detection of SOS-response genes in the organisms by quantitative reverse transcriptase polymerase chain reaction (qRT-PCR). As the SOS response is activated by a DSB, any up regulation would be an indication of damage to the DNA implying that the range was not too great for Auger electrons to reach. These genes could include RecA for bacteria and either Rad51 or Rad54 for yeast (Clever *et al*., 1997; Cox, 2007). RecA is a highly conserved protein involved in the initial steps in regulation of recombinational DNA repair mechanisms and homologous recombination in prokaryotes. Furthermore, it is found in virtually all bacteria (Roca and Cox 1990; Cox, 2007). Rad51 and Rad54 are both involved in the recombinational DNA repair in yeast, where Rad51 is the RecA homologue and Rad54 is homologue to the Swi2p/Snf2p family of DNA stimulated ATPases (Clever *et al*., 1997). Although they are both highly conserved in eukaryotes, a *rad54*mutation made *S. cerevisiae* particularly susceptible to ionising radiation (Walmsley *et al*., 1997). Furthermore, Rad54 transcription has been found to be up-regulated when *S. cerevisiae* was subjected to DNA damaging agents making this a particularly interesting candidate for DNA damage monitoring. Another example of a method for detecting genotoxicity is the utilisation of strains of microorganisms that have been found or modified to alter their phenotype when subjected to genotoxic compounds. Such organisms include the Salmonella (Ames)

test strain or the SOS Chromotest for bacterial strains and the GreenScreen genotoxicity assay for yeast strains (Quillardet *et al*., 1982; Mortelmans and Zeiger, 2000; Cahill *et al*., 2004). The Salmonella Ames test works by the reversion of Histidine dependent strains back to Histidine independent clones upon subjection to DNA damage. This allows the direct evaluation of the effects of ionising radiation (Mortelmans and Zeiger, 2000). The SOS Chromotest is a colorimetric assay based on the insertion of *lacZ* under the control of *sfiA*, a gene involved in the SOS response allowing the visualisation of induction of an SOS response, indicating genotoxicity (Quillardet *et al*., 1982). Finally, the GreenScreen yeast based system is a colorimetric system based on green fluorescent protein (GFP) under the control of the *RAD54* promoter. This will upon DNA damage induce an expression of Green Fluorescent Protein (GFP) making DNA damage observable (Walmsley *et al*., 1997; Cahill *et al*., 2004).

These simple systems may be able to provide information regarding the efficiency of the radioactive isotopes to induce DNA damage and thereby potentially give an insight into whether the dimensions of the microbial cells are still above the range threshold. Furthermore, they could potentially clarify whether the lack in mortality may be due to an efficient SOS response. These tests would therefore give important information on whether an isotope emitting higher energy Auger electrons would be a beneficial route.

Given that no toxicity was seen under the conditions tested there are some obvious changes that could have been made had time not been an issue, as well as the limitations to the storage of solid waste. The first change would be the exchange of

^{125}I with ^{123}I due to the identical labelling techniques. This would allow testing of higher energy Auger electrons. A second range of experiments could revolve around the issue of proximity. Several studies have shown that in order for Auger electrons to meet their full potential they have to be closely linked to DNA, indicating that range is the main issue when dealing with Auger electrons (Krisch and Ley, 1974; Feinendegen, 1975; Adelstein *et al*., 2003; Buchegger *et al*., 2006). It is for this reason likely due to proximity issues that no toxicity was seen. This could potentially be alleviated by changing the isotope to one of longer range. As Auger electrons are particularly short range perhaps the exchange for an α or β emitter, which have previously been shown to be efficient in for example sterilising biofilms. However, the range is as mentioned also a disadvantage here as this leads to crossfire effects potentially damaging the surrounding tissue.

However, the targeting agent utilised, UBI 29-41, being an antimicrobial peptide has intrinsic porine forming abilities. By increasing the UBI 29-41 concentration, or possibly give a dose of non-labelled UBI 29-41 prior to radio toxicity experiments, this might cause some porine formation allowing the internalisation of the radio labelled peptide and thereby closer proximity to the DNA. There are, however, several complexity factors to be considered in this scenario, the first being the innate toxicity of UBI 29-41. For this reason the baseline toxicity had to initially be established. This would therefore result in four simultaneously conducted experiments to be made: Free iodine alone, free iodine alone with the preliminary dose of UBI 29-41, preliminary dose of UBI 29-41 alone and finally the preliminary dose of UBI 29-41 with targeted ^{125}I-UBI 29-41.

As an alternative targeting agent it could be interesting to see the effects of labelling a known antibiotic (Chattopadhyay *et al*., 2010). As existing antibiotics require internalisation to function this would mean that the radioactive isotope would be internalised as well which would reduce the range to the target DNA.

4.9 Conclusion

The data in this chapter provide a baseline for the further investigation of radio toxicity in a range of model organisms. Despite the results seen in the comparisons of targeted versus non-targeted ^{125}I here, these experiments provide some groundwork for the future experiments as outlined above. Indeed, for most therapeutic settings more targeted molecules are required for the delivery of toxic agents to the site of interest, and therefore this will be the focus of subsequent chapters.

5 Design of anti-LAM scFv

5.1 5.1 Introduction

UBI 29-41has many advantages for testing labelling optimisation and toxicity in a range of species; for example its unspecific nature of binding allowing it to bind to a wide range of microorganisms as previously assessed. However, this unspecific nature also limits its value in most therapeutic settings as previously mentioned. For this reason designing and expressing a second targeting agent that could introduce more specificity to radionuclide delivery was a priority.

Antibodies are renowned for their versatility and generally strong antigen-binding capacity making them good agents for targeted therapeutic and diagnostic agents. The particular part of the antibody of interest is the variable domain, also referred to as the antigen-recognising part, or the complementary determining region, which encompasses the antigen binding part of the antibody. This part needed to be isolated so as to create a targeting agent that would have many advantages in both therapeutic and diagnostic settings over the native antibody (section 1.4.3.3).

The target chosen for the scFv was Lipoarabinomannan (LAM) as it is present on the widely distributed pathogen, *M. tuberculosis*, which is in need of new therapeutic and diagnostic tools. Furthermore, a hybridoma cell line, CS-35, expressing an anti-LAM IgG3 antibody already existed, easing the design process.

The hybridoma would allow extraction of mRNA from the cell line, and amplification of the variable heavy and light chain domains with framework-specific primers. This would allow the sequencing and identification of the correct variable domains which could subsequently be used for the design of the anti-LAM scFv.

5.1.1 Specific aims

1) To test the viability of a hybridoma cell line, CS-35, and confirm that it expressed anti-LAM

2) To extract and purify mRNA from (1) and generate cDNAs

3) To use existing primer sets against variable regions in the IgG, to produce products for cloning

4) To validate products by sub cloning and sequencing

5) To use the sequence obtained to design an anti-LAM scFv expressing coda construct in *silico*

5.2 Hybridoma CS-35 anti-LAM IgG3 expression

The first part of the design process required the verification that the hybridoma cell line, which had been frozen for a prolonged period, was still viable and able to express the desired antibody.

The hybridoma cell line CS-35 was grown in DMEM with foetal calf serum at 37°C and 5% CO_2. In order to verify the expression of anti-LAM IgG3 antibodies from which the anti-LAM scFv would be designed, cell culture supernatant was analysed for IgG3 content.

The hybridoma cell lines were allowed to grow until confluent, where after the medium was harvested and analysed using SDS-PAGE.

In order to analyse whether there was any antibody expression, the gel was analysed on a western blot due to the increased sensitivity using a polyclonal rabbit anti-mouse antibody HRP conjugate for analysis. Western blots uses antibody technology to visualise specific proteins in a protein gel that would otherwise be indiscriminate and show all proteins present. By having the primary or secondary antibody modified with an enzyme, most commonly horse radish peroxidase (HRP), and the addition of a chemiluminescent agent, a luminescent product is produced in the vicinity of the protein of interest in proportion to the concentration of the protein and this can be visualised using photographic film.

As can be seen in Figure 34, there are dark bands at ~150 kDa, which is the expected size for an IgG3 antibody and more importantly, this band is not present in fresh media, confirming antibody expression.

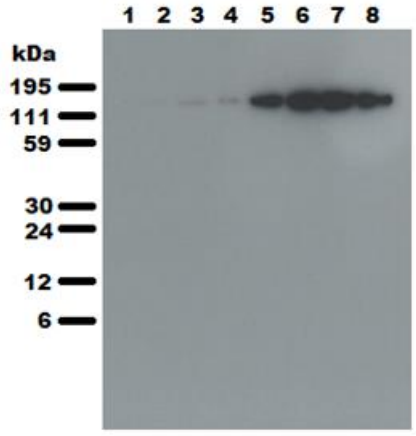

Figure 34 Hybridoma CS-35 anti-LAM IgG3 antibody expression analysis using western blot analysis.

Western blot analysis of the scFv expression in hybridoma supernatant at increasing concentrations. Bands with increasing strength was visible with a size of ~150 kDa consistent with the expected size Lanes: **(1)** 1 µL media **(2)** 10 µL media **(3)** 20 µL media **(4)** 1 µL CS-35 supernatant **(5)** 5 µL CS-35 supernatant **(6)** 10 µL CS-35 supernatant **(7)** 15 µL CS-35 supernatant **(8)** 20 µL CS-35 supernatant

5.3 Purification of mRNA from CS-35 anti-LAM IgG3 hybridoma

Following the successful verification of the antibody expression the next step was to initiate the scFv design process by purifying the mRNA from the hybridoma cell line, which would include the mRNA for the light and heavy chains of the anti-LAM IgG3. From this, the variable domain would be later isolated. As later primers would be used to amplify the variable regions, it was not necessary at this stage to specifically purify the mRNA of the desired transcripts. The mRNA was therefore purified as a bulk by utilising poly-dT coated magnetic agarose beads that would anneal anything with a poly-A tail. By using a magnet the beads would be attached to the tube wall allowing wash of the lysate and thereby a pure mRNA sample.

Due to the very unstable nature of mRNA, the purification was done in an RNase free environment and the purified product was immediately converted to cDNA using the First Strand cDNA synthesis kit (Novagen), when mRNA purification had been verified. This would ease downstream protocol execution.

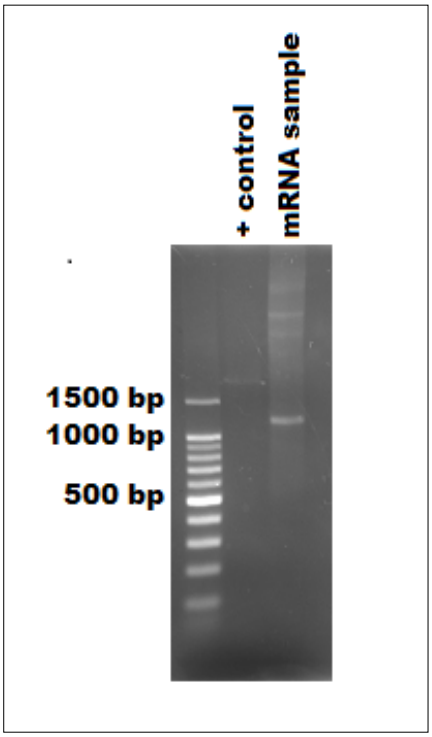

Figure 35 Agarose gel mRNA purification analysis
Analysis of mRNA purified from the CS-35 hybridoma cell line expressing the anti-LAM IgG3 antibody. A smear is visible in the lane containing the mRNA sample confirming that mRNA purification was successful. Due to the unstable nature of mRNA this was converted to cDNA for later variable domain amplification screening.

The CS-35 anti-LAM IgG3 hybridoma cell line was grown until confluent, where after the cells were harvested and lysed. The lysate was then passed over poly-dT coated magnetic agarose beads and the resulting eluate was analysed on an agarose gel and compared to an mRNA positive control. As can be seen in Figure 35, there is a visible, however faint, band in the first lane representing the positive control. The second lane represents the purified mRNA and a clear smear is visible indicating that the purification was successful.

5.4 Primer test

Based on the previously validated expression of antibodies the next step was commenced. This included the primer test screening for viable variable heavy and light chain domains for the scFv design. Following the conversion of the mRNA to cDNA, the next step was to isolate the variable heavy and light chain domains for later *in silico* assembly into the anti-LAM scFv.

For this murine primer sets from an antibody primer set kit were used. These primers were designed to anneal to the framework region in the variable domains of mouse antibodies (the anti-LAM IgG3 being derived from a murine hybridoma cell line), allowing the amplification of the antigen binding epitopes of the antibody. (Rademacher *et al*., 2007).

All the primer sets for the murine monoclonal antibody variable domains were tested. According to the Ig primer set kit (Novagen) used, the expected band size of variable chain amplifications is situated around 500 bp for both heavy and light chain variable domains. As can be seen in Figure 36 many primer pairs showed amplifications of cDNA fragments. Furthermore, some primer pairs showed unspecific binding and amplification.

The gene segments chosen to continue in the study were MuIgV$_H$5'-B, MuIgκV$_L$5'-B, MuIgκV$_L$5'-C, MuIgκV$_L$5'-D, MuIgκV$_L$5'-E, MuIgκV$_L$5'-F and MuIgκV$_L$5'-G.

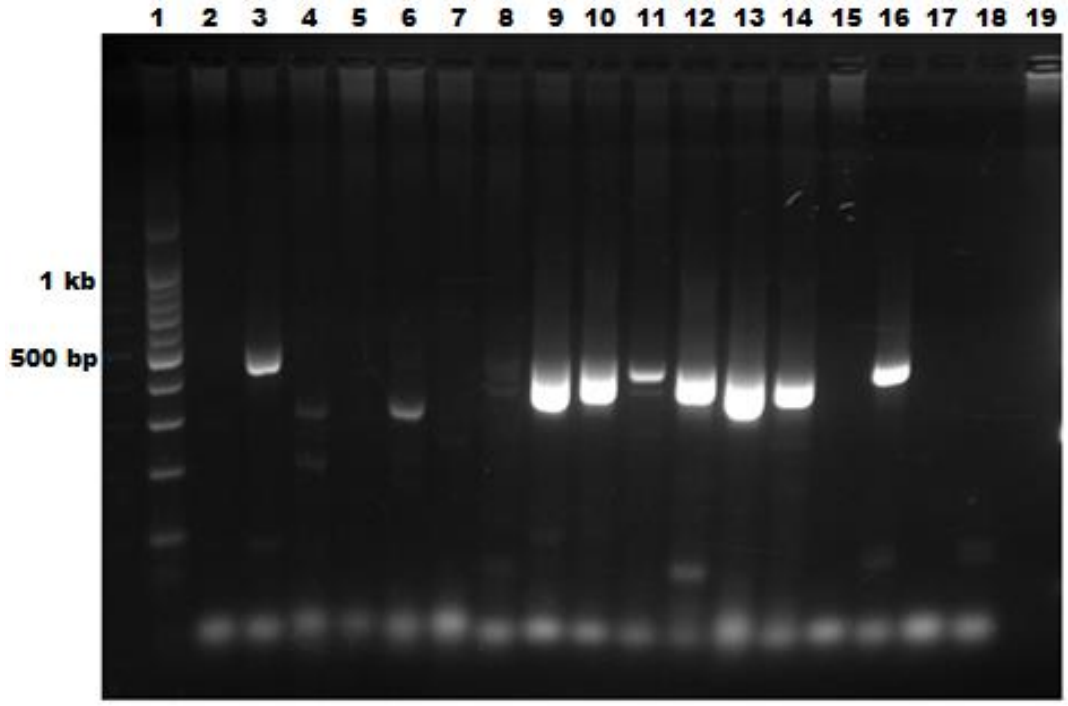

Figure 36 Heavy and light chain variable domain amplification.

The mouse Ig primer set kit for the amplification of the variable heavy and light chain domains was tested on the cDNA converted mRNA purified from the CS-35 anti-LAM IgG3 hybridoma cell line. A single heavy chain domain gave a clear 500 bp product **(lane 3)** and several of the light chain primer pairs resulted in a ~500 bp product. **(1)** 1 kb ladder **(2)** MuIgV$_H$5'-A **(3)** MuIgV$_H$5'-B **(4)** MuIgV$_H$5'-C **(5)** MuIgV$_H$5'-D **(6)** MuIgV$_H$5'-E **(7)** MuIgV$_H$5'-F **(8)** MuIgκV$_L$5'-A **(9)** MuIgκV$_L$5'-B **(10)** MuIgκV$_L$5'-C **(11)** MuIgκV$_L$5'-D **(12)** MuIgκV$_L$5'-E **(13)** MuIgκV$_L$5'-F **(14)** MuIgκV$_L$5'-G **(15)** MuIgMλV$_L$5'-A **(16)** positive control **(17)** Without Taq polymerase **(18)** Without cDNA **(19)** Without primers

Some primer pairs (MuIgV$_H$5'-C, MuIgV$_H$5'-E and MuIgκV$_L$5'-A) showed noticeable amplifications of up to multiple gene segments of a size <500 bp and were therefore not included in the further analysis. Some of these could also be due to primer dimerisation, given the high concentration of primers used.

The ~500 bp PCR products were gel purified and amplified using Taq polymerase. Due to the use of Taq polymerase the variable regions were amplified with 5'-overhangs, which removed the requirement for a preliminary digestion to be inserted

into the pGEM-T Easy vector. The orientation of the insert can be controlled when required via choice of appropriate restriction enzymes. However, as the only requirement from the clones was the sequence of the insert, the direction in which the gene segment was inserted was inconsequential. Following the insertion into the pGEM-T Easy vector, the product was sent for sequencing using M13 primers, both forward and reverse, for sequencing analysis.

5.5 ScFv *in silico* design process

5.5.1 Sequencing data analysis

The sequencing data quality was initially analysed using Chromas and the most reliable part of the sequencing data was isolated. This included the removal of the first 15-20 bp and removing any base pairs (bp) beyond 850-900 bp as the quality of the sequencing data beyond this point generally became unreliable. As the length of the inserted variable domain was only approximately 500 bp this segment would most likely contain the entire insert. Both forward and reverse primers were analysed, and a consensus sequence created to avoid single base mutations from ambiguities in the traces. This could potentially lead to incorrect amino acids, which could have detrimental effect on the binding affinity.

The forward and reverse sequences were annealed using BioEdit and the insert was identified by blasting the sequence against the vector sequence. This allowed the isolation of the variable domains for further *in silico* combination of the variable domains for the final steps of the basic scFv design.

5.5.2 Translation and identification of correct V_H and V_L domains

The vector sequence was translated in all reading frames using the expasy.org translational tool. Translation was required in all reading frames as insertion orientation was random as described previously. The reading frames that gave the longest translational product were considered to be correct, and the translated products were analysed for semi-conserved regions present in variable domains. One example hereof was the existence of two cysteines in the amino acid sequence. Following identification of the cysteines the sequences were analysed using a compilation of published variable domain sequences for reference (Kabat *et al*., 1991). This book gives an overview of all sequenced antibody variable regions and allowed this to be a point of reference for the identification of the framework regions of the variable domains. Since the framework regions are slightly more conserved than the variable domains, the correct variable heavy and light chain segments could be identified.

Following this process for all the above mentioned positive primer test amplifications, it was found that MuIgV_H5'-B indeed was the heavy chain variable fragment and that MuIgκV_L5'-F was the light chain variable fragment. The rest of the sequences showed only few resemblances with light chain variable domains and were therefore not carried on in the design process. As many hybridomas also express aberrant light chains it is not surprising to find them here as well (Carroll *et al*., 1988).

These results therefore indicate that only one heavy chain and one light chain are translated. This is in consensus with the hybridoma cell line expressing monoclonal

antibodies, in which there would be expected only one functional variable heavy and one light chain domain expressed.

5.5.3 *In silico* assembly of the anti-LAM scFv

Once identified, the nucleotide sequence was trimmed so that the sequence when translated would be in the first forward frame. This was required for insertion into the *P. pink* vector, which needs the inserted product to be in the correct frame.

The next step in the design process was the linking of the variable domains. Many linkers have been tested, however, the most utilised linker is the poly-glycine linker, (section 1.4.3.3) and this seemed a reasonable choice to use in the first instance. The shorter the linker, the greater the chance of the scFv forming unwanted dimers. Linkers shorter than 12 residues compromises proper folding of the scFv and force it to form multimers with other scFv molecules (Todorovska *et al*., 2001. Previous studies with 4 repeats of the poly-glycine motif, $(GGGGS)_4$, had still shown some degree of dimerisation (Emberson *et al*., 2005), so 5 repeats were included. The linker was created by alternating the codon sequences for glycine and serine to minimise loop-out deletions and the creation of secondary structures in the RNA and DNA (Trinh *et al*., 2004)

There are two possible conformations in which to design the scFv: V_H-linker-V_L or V_L-linker-V_H. Some studies indicate that there are some expression rate differences between the two; the former has shown higher expression rates, whereas the latter has shown higher binding affinity (Desplancq *et al*., 1994; Weisser and Hall, 2009). Furthermore, the V_L-linker-V_H conformation has shown to have a preference for

multimer formation compared to the V_H-linker-V_L conformation (Dolezal *et al*., 2000; Todorovska *et al*., 2001).

GAGGTTCAGCTCCAGCAGTCTGGGACTGTGCTGGCAAGGCCTGGGACT
TCCGTGAAGATGTCCTGCAAGGCTTCTGGCTACAGCTTTACCAACTACT
GGATGCACTGGGTAAAACAGAGGCCTGGACAGGGTCTAGAGTGGATTG
GTTCTATTTATCCTGGAAATAGTGATACTAACTACAAGCAGAAATTCAAG
GGCAAGGCCAAACTGACTGCAGTCACATCCGCCAGCACTGCCTACATG
GAGGTCAACAGCCTGACAAATGAGGACTCTGCGGTCTATTACTGTACAA
GATTTGGTAACTACGTTCCGTTTGCTTACTGGGGCCAAGGGACTCTGGT
CACTGGTGGCGGTGGCTCTGGTGGCGGTGGCTCTGGTGGCGGTGGCTC
TGGTGGCGGTGGCTCTGGTGGCGGTGGCTCTGATATCCAGATGACACA
GACTACATCCTCCCTGTCTGCCTCTCTGGGAGACAGAGTCACCATCGGT
TGCAGGGCAAGTCAGGACATTGGCAGTTATTTAAACTGGTATCAGCAGA
AACCAGATGGAGCTGTTAGACTCCTGATCTACTACACATCAAGATTACA
CTCAGGAGTCCCATCAAGGTTCAGTGGCAGTGGGTCTGGGACACATTTT
TCTCTCACTATTAGCAACCTGGAACAAGAAGATATTGGCACTTACTTTTG
CCACCAGGATACTAAGCCTCCGTATACGTTCGGATCGGGGACCAAGCT
GGAAATA

Figure 37 Initial nucleotide sequence of the assembled anti-LAM scFv

The nucleotide sequence for the anti-LAM scFv designed from the CS-35 anti-LAM IgG3 hybridoma cell line. The sequences for the heavy chain (red) and the light chain (blue) were obtained from purified PCR amplifications of the variable domains. The polyglycine linker (pink) was designed *in silico* with alternating codes for glycine.

The most commonly used conformation is therefore the V_H-linker-V_L conformation as high expression levels were of interest and it was decided that the V_H-linker-V_L was the conformation to be analysed first. The baseline nucleotide sequence of the scFv without modifications can be seen in Figure 37.

5.5.4 Modifications and optimisation of the anti-LAM scFv sequence

5.5.4.1 His-tag addition

With the baseline sequence of the anti-LAM scFv identified, it needed modifications for later purification. As the scFv was to be inserted into the pPinkα-HC vector, which would result in the secretion of the scFv into the supernatant of the culture, a means of purifying the scFv was required. For this reason a $(His)_6$-tag was added in the C-terminus. This would not only enable the scFv to be purified using a simple Ni^{2+}-column, but would also allow easy identification using anti-His antibodies for screening using dot-blots and western blot analysis systems.

Not only is the His-tag advantageous for the purification process it could potentially also be useful labelling anchor for site-specific ^{99m}Tc and ^{188}Re labelling (Tavaré *et al.*, 2009; Badar *et al*., 2014).

The final amino acid sequence of the expressed scFv can be seen in Figure 38. The top figure depicts the variable heavy and light chain domains in red and blue, respectively. The poly-glycine linker is depicted as pink and the His-tag is the yellow sequence at the C-terminus, a commonly used site. The bottom figure depicts the same scFv sequence, however here the framework regions are depicted as red and the CDR regions of the heavy and the light chains are shown in green.

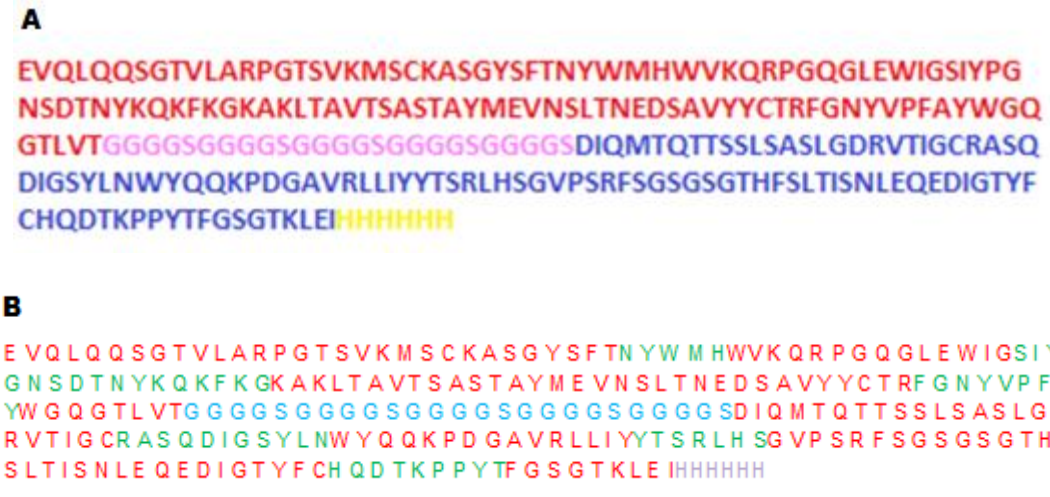

Figure 38 Overview of the final anti-LAM scFv amino acid sequence

The final sequence of the anti-LAM scFv generated *in silico* from the sequencing data from the amplified heavy and light chain domains of the CS 35 anti-LAM IgG3 hybridoma cell line.

(A) The red section refers to the heavy chain domain, the pink region is the poly-glycine linker, the dark blue refers to the light chain domain and the yellow domain is C-terminal the hexa-histidine tag. **(B)**Visualisation of the framework regions (red), the CDR regions (green), the linker region (blue) and the His-tag (purple).

5.5.4.2 Restriction site modifications

The internalisation process into the pPinkα-HC vector is the result of a fairly elaborate combination of restriction sites to optimise sequence alignment between the vector and the scFv (Figure 39).

One of the primary reasons for choosing the pPinkα-HC was to allow the expression of the scFv into the supernatant of the culture, significantly easing the process of purification. This is, as mentioned in section 1.5.4.1, allowed by the α-mating factor signal sequence which is situated just before the insertion site. To ensure functionality of this signal sequence a minimal distance between the gene of interest

and the signal sequence is required. For this reason, an MlyI site was inserted in the 5'end of the nucleotide sequence. MlyI is a blunt end restriction enzyme that recognises the following sequence:

5'- G A G T C $(N)_5$↓
3'- C T C A G $(N)_5$↑

The way it cuts the insert allows the removal of all traces of the restriction site and in combination with a StuI digest of the pPinkα-HC vector allows the generation of only 3 nucleotides between the signal sequence and the scFv sequence. More importantly, three nucleotides also prevent any frame shifting, which would prevent the expression of a functional product.

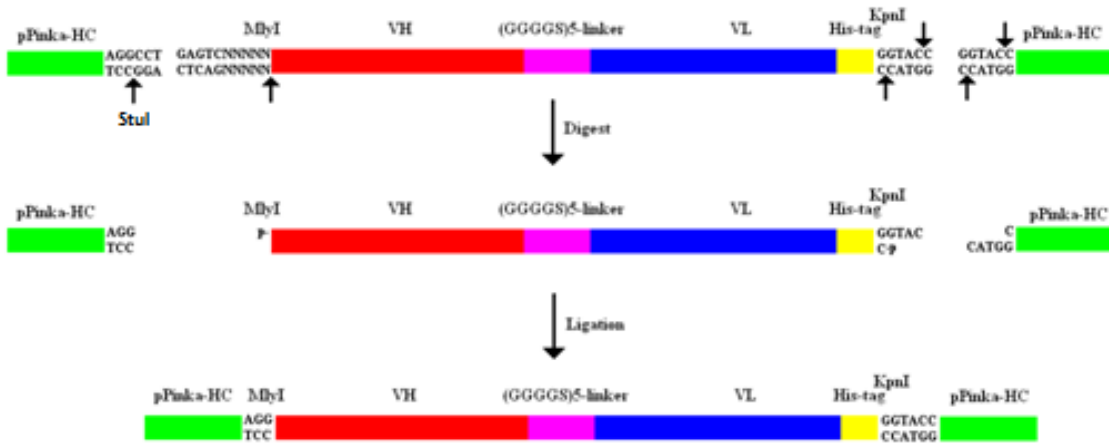

Figure 39 Insertion analysis and modification requirements of the scFv insert.
Due to the requirement of proximity of the α-mating factor signal sequence to the gene of interest and more importantly the in-frame insertion of the product a unique combination of restriction sites were required. An MlyI site in the 5' end of the scFv gene would allow the removal of the entire cleavage site. Combined with a StuI cleavage of the vector would result in only the inclusion of 3 bp between the α-mating factor signal sequence and the anti-LAM scFv. 3 bp furthermore ensure in-frame translation. Due to the nature of the blunt-end digest in the 5' end, a non-blunt end restriction site was required in the 3' end to ensure correct insertion of the gene. For this KpnI was chosen.

As MlyI is a blunt-end restriction enzyme a non-bunt end restriction enzyme had to be chosen for the 3'-end digest as to ensure the correct insertion orientation of the scFv sequence; a blunt-end insertion could result in an inverted insertion. For this reason a KpnI site was inserted into the 3' end of the nucleotide sequence, based on the recommendation of the manufacturer.

Following the insertion of the sites into the scFv sequence it was checked for restriction sites. It was found that two additional internal MlyI sites were present. As this would be detrimental to the insertion process the sequence was manually modified to remove the restriction site while retaining codon identity. The sequence was translated *in silico* to ensure that the translated product was unchanged.

The final modification to the nucleotide sequence was the addition of two stop codons. As the variable domains are only sections of a translated product they do not intrinsically contain stop codons, which had to be added manually. It was chosen to add two stop codons as this has previously been found to be more efficient in stopping translation than a single stop codon, which occasionally can be overlooked. The final modified nucleotide sequence can be seen in Figure 40.

As the host was to be *Pichia pastoris* the nucleotide sequence was generated from the peptide sequence based on the genetic code optimised for *Pichia pastoris*. The table used can be found in appendix 1. Finally, the *in silico* designed nucleotide sequence for the anti-LAM scFv was sent to Geneart for generation of the anti-LAM scFv pPinkα-HC plasmid.

gagtcgactggaggttcaattgcaacaatccggtactgttttggctagaccaggtacttccgttaagatg
tcctgtaaggcttccggttactccttcactaactactggatgcactgggttaagcaaagaccaggtcaag
gtttggagtggatcggttctatctacccaggtaactccgacacaaactacaagcagaagttcaagggta
aggctaagttgactgctgttacttccgcttccactgcttacatggaagttaattccttgactaacgaggatt
ccgctgtttactactgtactagattcggtaactacgttccattcgcttactggggtcagggtactttggtta
ctggtggtggtggatcaggtggtggtggttctggtggtggtggatccggtggtggtggatcaggtggtg
gtggatccgatattcaaatgacccagactacttcctccttgtccgcttctttgggtgacagagttactatcg
gttgtagagcttcccaggacatcggttcttacttgaactggtatcagcaaaagccagacggtgctgttag
attgttgatctactacacttccagattgcactccggtgttccatctagattttctggttccggttccggtact
cacttctctttgactatctccaacttggagcaagaggacattggaacttacttttgtcaccaggacactaa
gccaccatacactttcggttctggtactaagttggaaattcaccatcaccatcatcattaataaggtacc

Figure 40 Nucleotide sequence overview of the final modified product

Final modifications to the nucleotide sequence including the addition of the correct restriction sites for internalisation into the pPinkα- HC vector. Green= MlyI site, Red= stop codons, Blue= KpnI site

5.6 Discussion

The aim of this chapter was the development of a novel, more targeted agent for the delivery of either therapeutic or diagnostic radioactive isotopes to help in the fight against infectious diseases, in this case tuberculosis.

Due to the extremely versatile nature of antibodies, an antibody fragment, an scFv, was designed with an anti-LAM IgG3 as template. LAM, being one of the prominent survival and virulence factors of *M. tuberculosis*, was a natural first choice. As scFvs have a very short circulation time means that they are very well suited for imaging purposes. Furthermore, this also prevents the exposure of patients to prolonged exposure to radiation. However, the ~3.6 hours half-life would still allow the target microorganisms to be subjected to therapeutic radiation.

To ease the designing process a hybridoma cell line, CS-35, expressing an anti-LAM antibody, already existed.

Following mRNA purification and cDNA conversion, the library was analysed for the existence of variable heavy and light chain domains using primer sets specifically designed to anneal to the framework regions of the variable domains. The framework regions are less variable than the complementary determining regions of the variable domain, allowing the design of a limited, albeit numerous, primer sets.

The amplification was a success and multiple bands were amplified to the estimated size of ~500 bp (Figure 36). Despite the success, in some of lanes multiple bands were visible, all shorter than the expected 500 bp. The most likely reason for this can be found at the bottom of the gel. In all lanes, except the negative control without primers, a large concentrated smear is seen, indicating that the concentration of primers utilised higher than required and has likely resulted in primer dimerisation and/or non-specific binding and amplification.

There were technically 2 lanes containing amplified heavy chain variable regions, MuIgV$_H$5'-B and MuIgV$_H$5'-E, however the latter was not the expected 500 bp and was therefore not further investigated. Furthermore, sequencing of MuIgV$_H$5'-B revealed correct consensus sequences for variable heavy chain domains and was therefore concluded to be the heavy chain variable domain of the anti-LAM antibody.

With regards to the light chain variable domain several primer sets resulted in amplification: MuIgκV$_L$5'-B, MuIgκV$_L$5'-C, MuIgκV$_L$5'-D, MuIgκV$_L$5'-E, MuIgκV$_L$5'-F and MuIgκV$_L$5'-G. Some amplifications were more profound than others, but they were all sequenced and analysed, revealing that MuIgκV$_L$5'-F was the only fragment

containing identification segments for variable light chain. The rest of the light chain domains did not, following sequencing, show any elements that would identify them as variable light chain domains. It was therefore concluded that they were aberrant light chain domains, as mentioned in section 1.4.3.3, and were therefore not further included in the design process. This eventually led to having one light chain and one heavy chain domain, which would end up in the final scFv design.

The heavy and light chain variable domains were *in silico* joined in a V_H- linker- V_L conformation. There is no consensus when joining the variable domains whether it should be with the heavy chain domain first or last, however, there are some studies that have shown that the conformation decided for in this project tends to have a better expression rate over the V_L-linker-V_H conformation (Desplancq *et al*., 1994; Weisser and Hall, 2009).

The linker chosen was the classical poly glycine linker composed of repeats of four glycine residues followed by a single serine. An advantages of using this as a linker is that it introduces enough flexibility to allow proper folding of the scFv. The reason for choosing 5 repeats is that, as mentioned in section 1.4.3.3, the shorter the link, the higher degree of multimerisation of the scFv there is, and we were interested in single scFv molecules. The linker length has sometimes been used as a means to create multimers and multispecific scFv. We were however interested in analysing the properties of the monomeric peptide including binding affinity.

One of the disadvantages of the linker is its high hydrophilicity, which results in it being very solvent exposed. This furthermore increases the chance of encounters with proteases, which have better cleavage conditions due to the increased

exposure. Other linker designs have been evaluated, however these have mostly been involved in linker length (Alfthan *et al*., 1995; Albrecht *et al*., 2006). Furthermore, they are all, however, composed of hydrophilic and small amino acids in order to introduce the right degree of flexibility required. It is also important to choose the correct residues based on their tendencies to form secondary structures. The more likely they are to form α-helices or β-sheets the more likely they are to introduce rigidity to the linker and would have a negative impact on the correct folding of the scFv and possibly increase the chance of multimerisation. Again, monomeric scFvs were the area of interest in the first instance and for this reason the decision was made to go for the conventional polyglycine linker despite the potential degradation disadvantages.

Due to the non-structural nature of the linkers does make them potential interesting targets for the insertion of sites for site-specific radio nuclide labelling. This would not only easy labelling analysis but would also be beneficial in keeping the radio nuclides away from the binding site thereby potentially disrupting binding. However, the modifications have to be non-disruptive to the chemical properties of the linker including flexibility and hydrophilicity to ensure correct assembly of the variable domains.

The system for expression was chosen to be *P. pink* for several reasons. It has shown high protein expression levels, it is capable of post-translational modifications as disulphide bonds, of which two are present in the scFv, and glycosylations and this particular system allowed the secretion of the expressed protein into the supernatant for easy purification (Cereghino and Cregg, 2000). However, there are

some issues that could validate the expression in other systems. Preliminary analysis of the peptide sequence did not show any signs of glycosylation sites, and this could validate the expression in an *E. coli* system as *E. coli* has previously been shown to be able to mount a very high yield (Weisser and Hall, 2009). As a high yield is optimal for later identification and binding studies and the fact that no glycosylation sites were visible this could have been a valid choice. However, as the scFvs do contain disulphide bonds, scFvs expressed in *E. coli* would have to be artificially established. Although previous studies have indicated that the disulphide bonds in intrinsically stable scFvs are not necessarily essential for correct folding, it was not apparent what effect the loss of the disulphide bond would have on the designed scFv (Wörn and Plückthun, 1998). Using a eukaryotic system was therefore optimal. Furthermore, the *P. pink* system offered an easy way of manipulating expression initiation with the addition of methanol. This would ease the monitoring of expression and establishment of optimal supernatant harvest points. Furthermore, *P. pink* offered an easy selection method with the *ade2* knock-out allowing selection on adenine-free media.

Mammalian systems were not considered as an expression system as protein yield is generally very low (Braren *et al*., 2007; Leong and Chen, 2008). Furthermore, it is in theory not required given the relative simplicity of the scFv relative to the intact monoclonal antibody.

Now the anti-LAM scFv had been designed, the next step was to express the protein in the *P. pink* expression system and later analyse the protein for post-translational modifications and more importantly the binding affinity to LAM.

The above mentioned design of anti-LAM scFv was entirely based on the assumption that the antibody expressed from the CS-35 hybridoma cell line indeed would bind to LAM.

As this would later function as a positive control for the designed anti-LAM scFv binding affinity, it would be prudent to initially analyse the basic binding capacity of the antibody. This could be done by performing a sandwich western blot running solubilised LAM on a gel and utilising the anti-LAM antibody as primary antibody, followed by an anti-mouse HRP conjugated antibody for visualisation. This would validate whether the antibody does bind and would function as a base for comparison. However, this binding analysis would be of a qualitative form rather than quantitative.

Further analysis would include establishment of binding affinity, however, this would be in concert with the anti-LAM scFv in order to establish the effects on binding affinity by isolating the variable domains from the conserved regions of the antibody. However, it is not only the isolation of the variable domains from the rest of the monoclonal antibody that has an impact on the binding affinity of the scFv. Research has indicated that in some cases a C-terminal His-tag interferes with the antigen recognising site of the scFv, thereby having a negative impact on the binding affinity. By incorporating the His-tag in the N-terminal reduced this impact (Goel *et al*., 2000; Arnau *et al*., 2006). This is something that could be considered in the case that binding affinity of the purified molecule was found to be very low.

This, however, will be explored in the following chapter.

6 Analysis and optimisation of anti-LAM scFv expression

6.1 Introduction

In the previous chapter, an anti-LAM scFv was designed *in silico* based on the CS-35 anti-LAM IgG cDNA sequences produced from a hybridoma cell line. This design was sent to Geneart for cloning into the *P. pink* vector, and once the vector was received, the next step was to get it expressed and analyse the protein product.

The expression cell line chosen for its ease of use and generally high expression rates was *P. pink*, a genetically modified subtype of *P. pastoris* (Cereghino and Cregg, 2000). Furthermore, being a yeast expression system it has the capacity to add post-translational modifications and therefore better mimic mammalian expression compared to bacterial systems. As it was not known what the level of post-translational modifications of the scFv would be, choosing a bacterial system over a yeast system for higher expression might have had detrimental effect on the final product expressed. One of the further advantages of the *P. pastoris* system, including *P. pink,* is the versatility. Many parameters can be modified in order to attempt optimisation of expression.

The initial aim of expression was to get enough levels to both analyse via HPLC-MS to validate the expression of the correct protein. The second objective was to ensure high enough levels to be able to analyse the binding specificity and efficiency of the generated scFv. As most scFvs lose some of the binding affinity of the mother molecule, it was interesting to compare the binding to the original anti-LAM IgG3 from which it was isolated.

6.1.1 Specific aims

1) To amplify the plasmid in E. coli, and transform the amplified plasmid into the *Pichia pink* expression vector

2) To qualitatively assess the level of expression in transformed colonies to select clones for further analysis

3) To assess levels of degradation of the protein, and identify strategies for minimising its impact

4) To adjust the growth conditions and inhibition of proteolytic degradation to optimise the amount of retrieved product for downstream analysis

5) To use the products from (4) to validate that the expressed protein is anti-LAM scFv, ideally via HPLC-MS

6.2 Transformation of *Pichia pink* strains 1-4 with pPinkα-HC containing anti-LAM scFv

Following the return of the pPinkα-HC vector from Geneart, containing the anti-LAM scFv gene, the construct was internalised via electroporation, as elaborated in section 2.2.25, into the competent XL1-Blue *E. coli* cell line in order to amplify the plasmid for later transformation of *P. pink* and to obtain a stock of easily obtainable plasmid for potential downstream applications. *P. pink* was transformed using electroporation, which was the recommended mode of transformation by Invitrogen as described in section 2.2.25.

The transformed strains were plated onto three Pichia Adenine Dropout (PAD) plates and one YPD plate. As PAD plates are deficient in adenine, only transformed cells containing the vector will be able to grow. The negative control, consisting of non-transformed *P. pink*, was plated on one PAD plate. Furthermore, two positive controls of *P. pink* viability were included; one pre-transformation to ensure the viability of the cells before electroporation and one post-transformation to confirm that the cells have not lost viability during the electroporation process. Both were grown on traditional YPD agar. Transformed strains would show up as larger white colonies on the PAD plates compared to the small red untransformed colonies. The plates for grown for 4 days at 30°C enclosed in a lightly wound plastic bag to prevent loss of humidity.

As can be seen in Figure 41, the negative control on PAD shows no growth, indicating no *P. pink* growth without transformation with pPinkα-HC vector, and also that no contamination had taken place. Non-transformed *P. pink* was also analysed

on YPD plates prior to transformation to confirm the viability of the cells. As can be seen in Figure 41B and Figure 41C the plates are confluent which indicates fully viable cells both before (B) and after (C) electroporation. The last 3 plates show the growth of single white colonies on PAD plates representing successfully transformed clones amongst small pink colonies of non-transformed *P. pink*. Three plates were grown to increase the chance of finding successfully transformed clones.

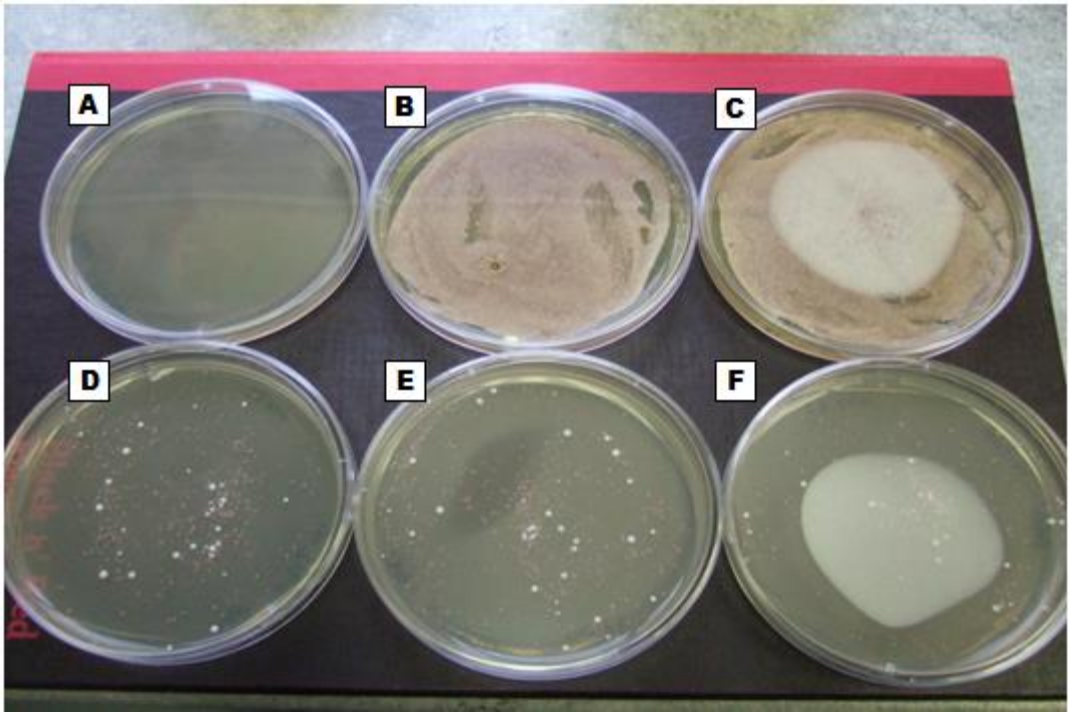

Figure 41 Transformation evaluation of *P. pink*.

Transformation analysis of *P. pink* with anti-LAM scFvpPink α-HC vector including controls. **(A)** PAD + Non-transformed *P. pink*. This was a negative control showing that the non-transformed *P. pink* was incapable of growing and furthermore confirmed that no contamination had taken place **(B)** YPD + Non-transformed *P. pink*. This worked as a positive control showing that the *P. pink* was viable prior to electroporation **(C)** YPD + transformed *P. pink*. This was a second positive control showing that the *P. pink* was still viable following electroporation **(D- F)** PAD + Transformed P. pink. White colonies (big) signify successful transformation, where small pink colonies are non-transformed *P. pink.*

Each white colony was hereafter isolated and analysed for anti-LAM scFv production in a small-scale screening.

6.3 Analysis of scFv expression from P. pink anti-LAM scFv clones

Following transformation of *P. pink* the white colonies were isolated on new PAD plates and catalogued for later ease of retrieval. In order to analyse the isolated clones for those expressing anti-LAM scFv, 5 mL of BMGY was inoculated with a sample picked from a clone and grown until an OD_{600} of 60 was reached. The culture was hereafter pelleted and resuspended in BMMY media to a final OD_{600} of 160-180 and grown for 48 hours. One sample of 400 µL was taken of the BMGY prior to switch to BMMY as a negative control, just after switch to BMMY, again as a negative control and finally after every 24 hours. Methanol was replenished once after 24 hours to a final concentration of 0.5%. This was done for all colonies evaluated.

The supernatant from the clones were then evaluated for scFv production via dot-blot analysis using an anti-hexa-His HRP-conjugated antibody for visualisation. This antibody would detect the His-tag designed into the scFv in the previous chapter. The positive control used was an anti-CD33scFv constructed by a former postdoctoral research associate, Louise Emberson (Emberson *et al*., 2002). The small volumes of the mini scale cultures made it logistically possible to analyse multiple colonies simultaneously and allowed a more efficient screening for an anti-LAM scFv producing transformant.

Dot blots use the same visualisation technology as western blots with the difference that the proteins are not transferred to a nitrocellulose membrane from a polyacrylamide gel, but rather transferred directly by loading the supernatant containing protein to a dot blot chamber and applying vacuum, which allows the supernatant to traverse the membrane leaving the peptide bound in the membrane in defined dots. Dot blots have the advantage over western blots that they can load up to several hundred µL compared to approximately 20 µL for western blots. Furthermore, they allow the screening of many clones simultaneously, where western blots are again fairly limited. This makes dot-blots especially suitable for the initial screening of colonies. In the dot blots in the present study 200 µL of samples were loaded in each well apart from positive controls, where 10 µL were loaded unless otherwise specified.

As can be seen in Figure 42, very weak dots are visible after 24 hours. The signal was faint, but demonstrated the first indications of protein expression. 45 clones were subsequently analysed for protein expression using this experimental procedure (data not included).

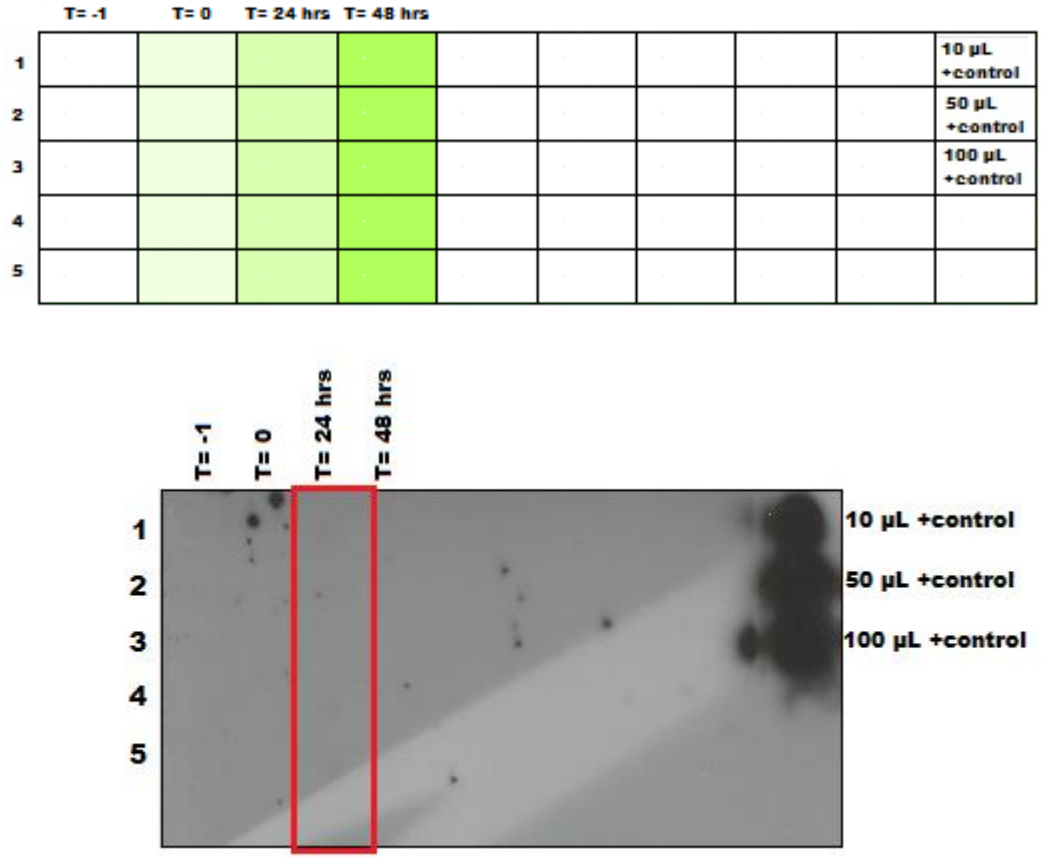

Figure 42 Initial screening of anti-LAM scFv expressing P. pink clones

Screening analysis of transformed P. pink clones for clones expressing His-tagged proteins. The top figure gives an overview of the loading profile of the dot-blot. The bottom figure shows the resulting dot-blot. Very faint dots are visible after 24 hours of expression in BMMY media (red square). Especially clones 4 and 5 showed protein expression. This was however gone after 48 hours, giving the first indications of protein degradation.

The 6 clones showing highest degree of expression after the first round of screening were analysed once more to verify their protein expression, and to compare the expression levels directly to enable selection of the clone with highest protein expression. The results of this screening are shown in Figure 43.

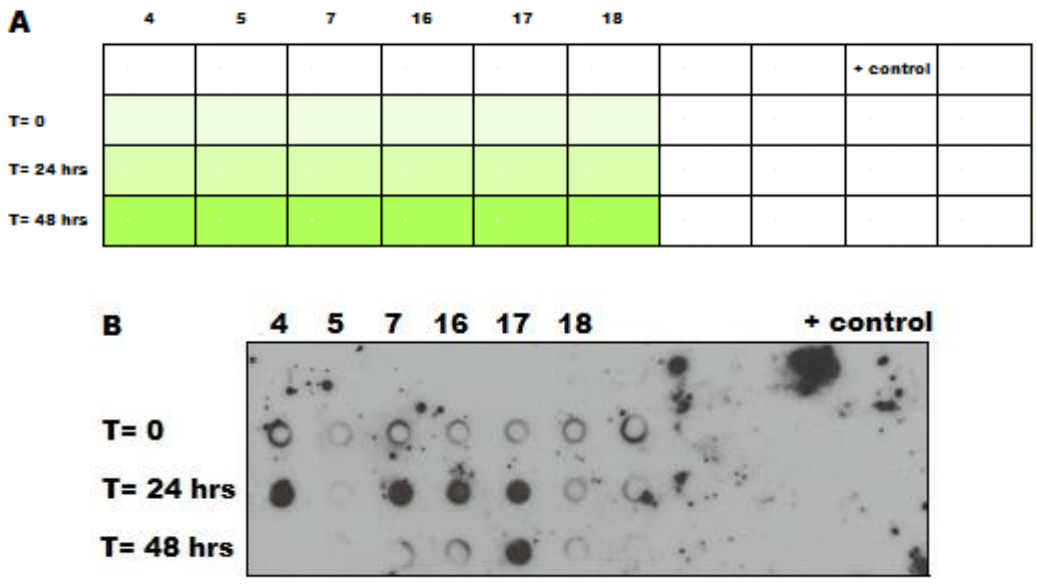

Figure 43 Second screening of high expressing clones.

6 clones that previously indicated expression were analysed again to identify the clone with highest and most stable protein expression. Clones 4, 5, 7, 16, 17 and 18 were re-analysed in mini scale cultures and visualised using dot-blot.

(A) Overview of the loading profile of the dot-blot. **(B)** Dot-blot showing samples from the 6 clones taken at T= 0 and hereafter every 24 hours for 48 hours in total. Four clones, 4, 7, 16 and 17 showed expression after 24 hours. Only clone 17 showed expression after 48 hours. The rings visible are likely background.

Clones 5 and 6 that previously showed protein expression did not show signs of any expression in the second round of analysis despite static parameters. Again, as in Figure 42, protein was undetectable after 48 hours suggesting degradation. Four clones were, however, positive for protein expression: 4, 7, 16 and 17. In particular clone 17 showed the highest degree of consistency in protein expression level when compared to the initial screening results. It furthermore seemed to show a higher degree of stability. For these reasons, this clone was carried forward for further analysis.

One problem encountered with the initial rounds of dot-blot and western blot analysis was the degree of background staining, an example of which can be seen in Figure 43. However, optimisation of washing conditions gradually decreased the background staining, which is demonstrated in later dot-blots.

Despite the promising results of protein expression from the screening analysis it has to be noted that 200 mL of supernatant was added to each well. For this reason purification was required in an attempt to maximise the concentration for later downstream analysis. In order to do this, the first step was to up-scale the cultures to increase the number of cells expressing protein, thereby hopefully increasing the end concentration of protein for later analysis.

6.4 Large-scale production and purification of anti-LAM scFv

The first step towards identifying the protein was the acquisition of a higher concentration of product on which analysis could be performed. This primarily required a large-scale production and then purification of the protein. This was accomplished using a Ni^{2+} column to capture the protein using the His-tag designed into the scFv in the previous chapter.

Cultures from P. pink anti-LAM scFv clone 17, selected for its apparent high expression levels, were grown as previously described with the following difference: the volume of the starter glycerol-containing BMGY culture was increased to 300 mL, resulting in a methanol-induced anti-LAM scFv expressing BMMY culture of approximately 100 mL. The culture was grown at 25°C for 24 hours and harvested by centrifugation at 5000 rpm. The anti-LAM scFv was immediately

purified from the supernatant using a His Trap Ni^{2+} column as described in section 2.2.29. The Ni^{2+} of the purification column is able to interact with the imidazole ring of histidine in the His-tag. As 6 histidines are present in direct succession the binding affinity is very efficient. The Ni^{2+} column however, interacts with all encountered imidazole rings resulting in low-affinity binding of non-specific proteins as well. By washing the column with a low concentration imidazole the non-specific proteins bound will be eluded quickly as the low imidazole concentration more easily outcompetes the single histidine binding facilitated compared to the stronger affinity of the His-tag. This therefore not only helps increase the concentration of the desired product but also increase the purity.

The anti-LAM scFv was grown accordingly onwards unless otherwise specified.

The first step in protein purification was the optimisation of the imidazole concentration required to optimally elute the scFv. Too high a concentration may not only elute scFv multimers but could also interfere with later HPLC-MS analysis. Too low a concentration might cause the protein to be not eluted at all. Furthermore, the analysis would also elucidate at what fraction the protein is eluted which would ease later purifications by skipping the need for a dot-blot analysis step prior to down-stream analysis.

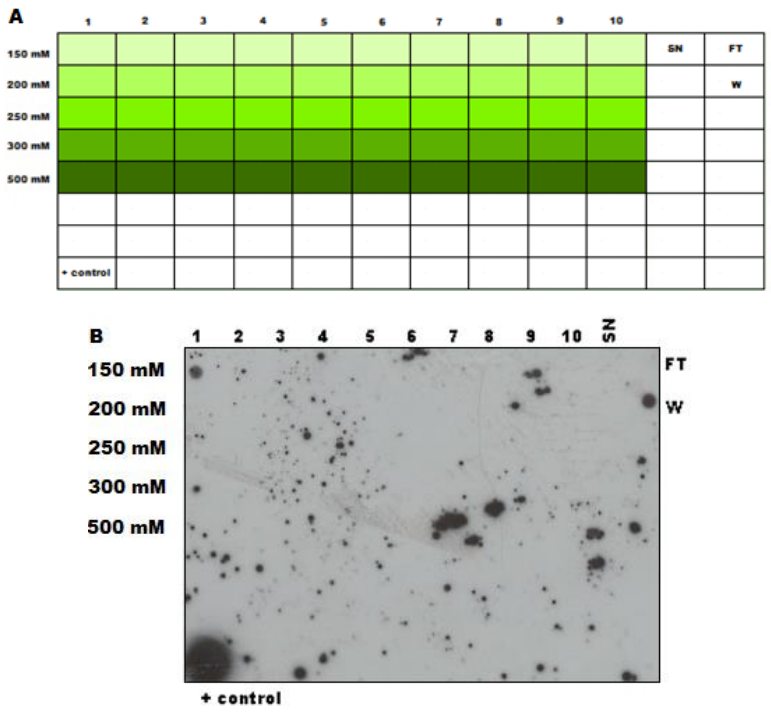

Figure 44 Initial protein purification optimisation on HisTrap^{TM} Ni^{2+} column

Initial analysis of protein purification at various imidazole concentrations using dot-blot analysis. Initial imidazole concentration of wash buffer was 100 mM. Supernatant (SN) prior to loading to column was analysed for protein content to analyse the degree of purification, the flow through (FT) was additionally included to analyse the degree of protein binding and wash (W) was also included to analyse any potential premature elution.2 dots are visible in the diagram: one in the wash elution and one in the initial elution sample at 150 mM imidazole.

At first a wash buffer with an imidazole concentration of 100 mM was implemented as a means to wash any low- affinity bound proteins out and only leave the scFv bound to the Ni^{2+} column. Following the 100 mM imidazole wash, a variety of elution buffers containing from 150 mM imidazole to 500 mM imidazole were washed through the column and collected at 10x1 mL elutions, which were then analysed using dot-blot analysis.

As can be seen in Figure 44, no dots were visible in the elution profile save the first dot in 150 mM imidazole concentration. Furthermore, a dot is visible in the wash,

indicating that a His-tagged protein is eluted in the wash buffer. This suggests that the His-tagged protein eluted in the first mL of 150 mM imidazole elution buffer is the left-over protein that had not quite been eluted in the wash buffer. To prevent premature elution, the concentration of imidazole was lowered to 25 mM. The purification was performed as previously with the exception that the 100 mM imidazole wash buffer now was utilised as an elution buffer. The protein samples were acquired as previously and the samples were again analysed using a dot-blot. As can be seen in Figure 45, the dot blot analysis of the elution profile changed. There was no longer any protein being eluted in the wash, which was further confirmed by the disappearance of protein in the first sample. The scFv was now being eluted in the 3rd and 4th sample (100 mM imidazole). This is consistent with the theory that the first couple of samples would contain primarily 25 mM imidazole wash buffer and thereby be too low an imidazole concentration to elute any scFv.

The optimised imidazole concentrations in both wash buffer and elution buffers were used henceforth in scFv purification.

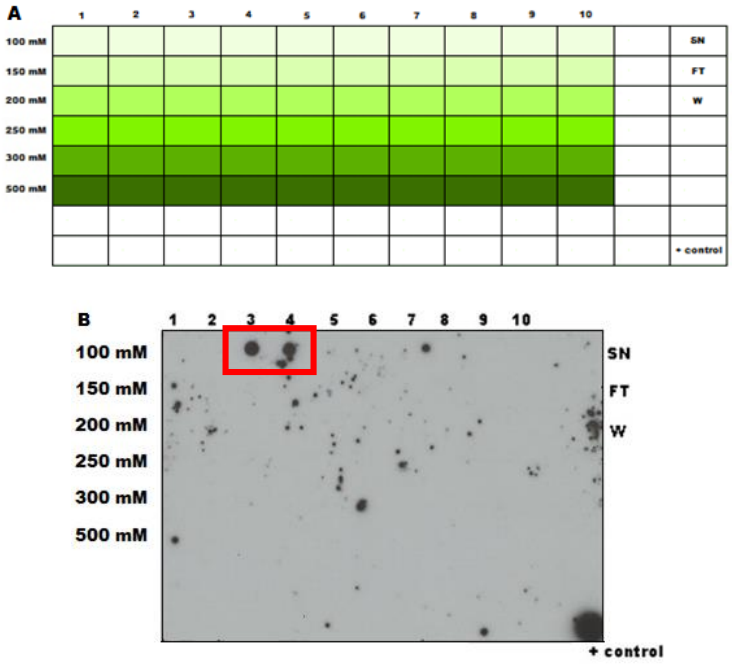

Figure 45 Optimised elution profile of anti-LAM scFv.

A) Schematic overview of the loading profile of the dot-blot analysing the second elution profile of anti-LAM scFv. **B)** Dot-blot analysis of optimised elution profile. Two dots were visible at 100 mM imidazole concentration at the third and fourth 1 mL sample (red box). 200 µL were loaded and 10 µL positive control.

6.5 Size analysis of eluted protein

A disadvantage of dot-blot analysis is the lack of size information. This demanded the analysis of the purified protein in a gel-separation based system. For this western blot analysis was chosen due to the sensitivity compared to Coomassie stained SDS-PAGE gels. This was important as SDS-PAGE gel wells have a more limited loading capacity than dot-blot wells (20 µL vs. 200 µL), and protein expression levels were already known to be low.

A new batch of scFv was purified according to the optimised conditions, with the exception that the only elution buffers used were 100 mM imidazole and 500 mM

imidazole. 500 mM imidazole was included to wash out any residual protein from the column.

The modified purification protocol showed an increased protein concentration (Figure 46B) compared to previous results and further size analysis could now be conducted. The elutions displaying the highest concentration of protein (100 mM imidazole elution samples 3-7were analysed on a western blot using an anti-his HRP conjugated antibody for visualisation (as described in section 2.2.32).

As can be seen in Figure 46C, there appears to be a band in the first lane, corresponding to the 3rd elution sample at 100 mM imidazole. More importantly, the positioning of the band shows a size of roughly 30 kDa. The theoretical molecular weight of the designed anti-LAM scFv without post-translational modifications was calculated to be approximately 27 kDa. Therefore, the band in the western blot most likely represents the scFv. No bands were apparent in the remaining lanes. This indicates that scFv concentration is below the limit of visualisation.

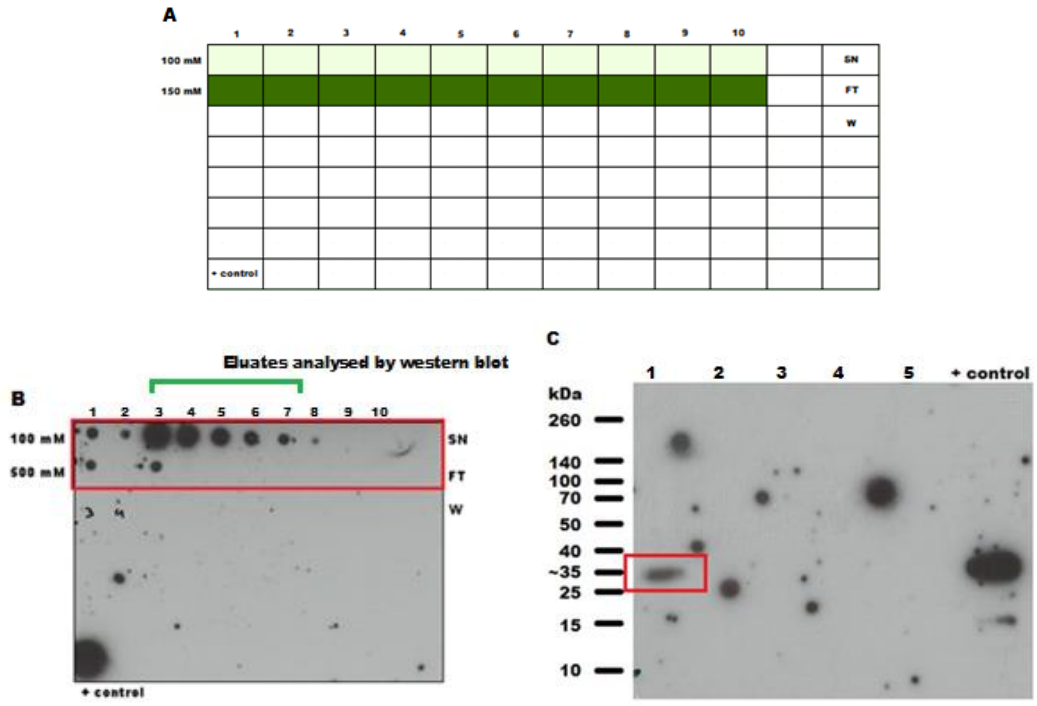

Figure 46 Dot blot and western blot size analysis of purified protein

A) Schematic overview of the loading profile of the dot blot over elution profile of purified expressed protein. **B)** Dot blot of elution profile of nickel purified cell culture supernatant. 200 µL was loaded from each sample and a 10 µL positive control was used.

C) Lane 1: 3rd elution sample at 100 mM imidazole from (B), lane 2: 4th elution sample at 100 mM imidazole from B 3: 5th elution sample at 100 mM imidazole from (B), 4: 6th elution sample at 100 mM imidazole from (B), 5: 7th elution sample at 100 mM imidazole from (B). 20 µL was loaded of each sample and 3 µL anti-CD33 scFv as positive control and size comparison.

Despite evidence of a protein of equivalent size detected by an anti-His antibody, additional HPLC-MS analysis was required for absolute confirmation that this was the anti-LAM scFv. This required a higher scFv concentration to be detectable by the HPLC-MS. Optimisation of the *P. pink* scFv expression was therefore required. However a major roadblock was the degradation that had been previously indicated and prior to optimisation of scFv expression, the levels of degradation had to be analysed.

6.6 Degradation analysis of the expressed anti-LAM scFv

It became apparent that the problem with obtaining high protein levels was largely down to protein degradation from the disappearance of dots after 24 hours.

As mentioned previously, this started becoming apparent in the small-scale screening process, however the exact level of degradation was still unknown. As dot-blot and western blots were reliant on the anti-His antibody for detection it was unknown whether the reduced detection levels were due to whole protein degradation, or whether it solely was due to the proteolytic cleavage of the His-tag from the scFv. A fast degradation of the His-tag could also have important implications for the purification of the protein as the lack of a His-tag would render the scFv uncapturable by the Ni^{2+} column.

To visualise the extent of the degradation of the purified protein a new batch was expressed and purified, as described previously, and can be seen in Figure 47A and Figure 47B. The samples 3-8 eluted at 100 mM imidazole and the 3rd and 4th sample eluted at 500 mM imidazole showed the highest levels of protein concentrations and were chosen for further degradation evaluation. They were run on an SDS-PAGE gels and Coomassie stained to give a preliminary indication of the extent of scFv degradation.

As can be seen in Figure 47C there were no bands visible in either of the loaded wells at the expected ~27 kDa. There were however thick smears at the bottom of all the wells suggesting degradation. One encouraging observations was that although there was no non-degraded protein seen in the Coomassie stained gel, it

revealed that if proteolytic degradation could be prevented there would be enough protein for further analysis.

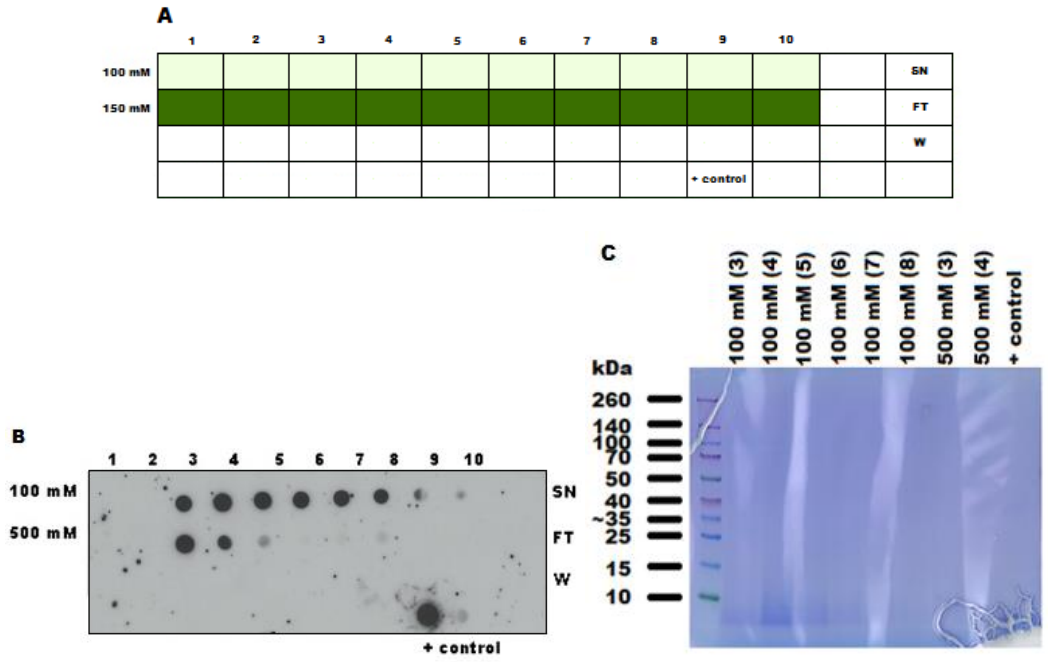

Figure 47 Degradation profile of the presumed anti-LAM scFv.

A) Schematic overview of the loading profile of the dot-blot for protein purification overview **B)** Dot-blot of HisTrap purified protein at 100 mM and 500 mM imidazole concentration. Supernatant, flow through and wash was included as previously. 200 µL of each sample was loaded as well as a 10 µL positive control **C)** Coomassie stained gels of the elutions from the dot-blot containing the highest levels of protein. 100 mM is the imidazole concentration and the number in brackets indicate elution sample from figure B.

As Coomassie staining has limited sensitivity the 4th sample from the 100 imidazole elution (containing the highest concentration of protein) was further analysed on a silver stained gel (Figure 48A) and a western blot (Figure 48B) as described in sections 2.2.32 and 2.2.34.

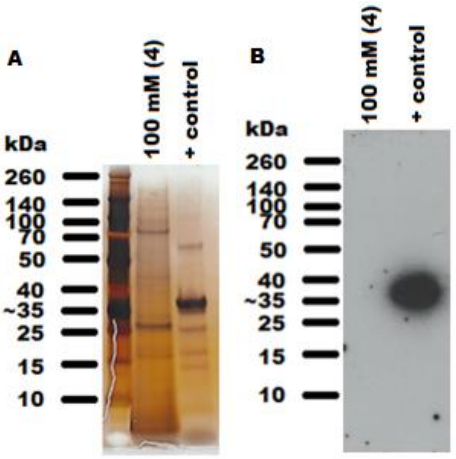

Figure 48 Simultaneous degradation analysis of the purified protein on both silver stain and western blot.

A) Silver stain analysis of the second lane of figure 41 C as this had the highest protein concentration of the elutions. A band just above 25 kDa is visible which is consistent with the theoretical value of ~27 kDa for the anti-LAM scFv. **B)** Western blot identical to the silver stain and run simultaneously. No band is visible in the first lane indicating proteolytic cleavage of the His-tag. Both gels were loaded with 20 µL of elution sample 4 at 100 mM from figure 41 and 3 µL of anti-CD33 scFv as positive control.

The silver stain analysis (Figure 48A) revealed that not all the protein was degraded and showed a band of ~27 kDa which correlated with the size of the band found in Figure 46C. It still showed a large smear at the bottom of the gel consistent with the Coomassie stained gel, again indicating degradation.

The western blot, which is anticipated to have roughly the same level of sensitivity as the silver stain, was run simultaneously to the silver stain. Interestingly, no band was visible at ~27 kDa as in the silver stained gel. This further indicates rapid degradation of the His-tag, allowing purification on the Ni^{2+} column but not visualisation on a western blot. Optimally this could be analysed by mass spectrometry however the concentration of the scFv was too low to be detectable by standard polyacrylamide gel.

Therefore, degradation appeared to be one of the major issues relating to expression of an intact scFv and for this reason this needed to be addressed if high protein concentration levels were to be achieved. For this two routes were proposed: either by the increase of initial protein concentration giving a larger batch to work with before degradation occurs, or by trying to inhibit the proteolytic degradation altogether.

As it was important to get a higher protein concentration at the same time, the initial focus was to attempt to increase the protein yield by optimising the growth and expression conditions.

6.7 Optimisation of growth conditions and oxygen levels for optimisation of anti-LAM scFv production

The first step for protein optimisation was growing the cultures in baffled flasks as opposed to regular conical flasks in order to increase aeration. Using the baffled flask the same culture volume (100 mL) was grown under the same conditions as previously described. In order to investigate the effects of increased aeration of the media, a sample (100 mL) from the same BMGY starter culture, which had been increased to 600 mL, was grown under the same conditions, but in a conventional non-baffled flask.

As can be seen in Figure 49, expressing protein in the baffled flasks seem to have a negative impact on the anti-LAM scFv expression levels. Furthermore, the difference in expression levels was apparent.

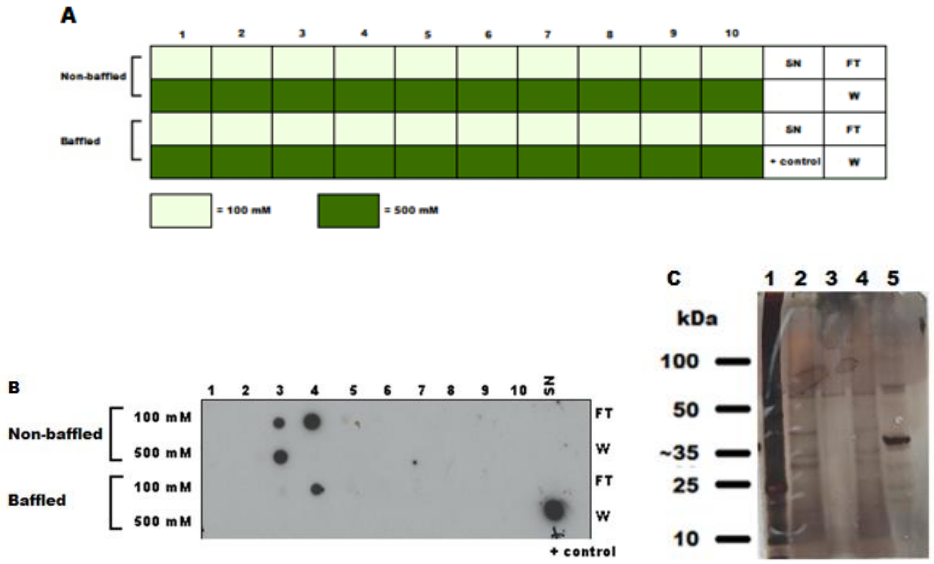

Figure 49 Analysis of the effect on protein expression between a baffled and regular conical flask

A) Schematic overview of the loading profile of the dot-blot in (B). **B)** Dot blot analysis of the purified protein from two cultures grown either in baffled flasks or conevntional flasks. Both elutions were done at both 100 mM imidazole and 500 mM imidazole concentration. 200 **C)** Silver stain analysis of the elutions with highest protein concentrations from the dot-blot analysis 1) Ladder 2) 4th elution sample from non-baffled flask100 mM imidazole 3) 3rd elution sample from non-baffled flask 500 mM imidazole 4) 4th elution sample from baffled flask100 mM imidazole.

To analyse whether flask morphology had any impact on the expression profile of the scFv, the elution samples that appeared to contain the highest levels of protein were analysed on a silver stained gel. These included the 4th elution sample collected at 100 mM imidazole from the non-baffled flask, the 3rd elution sample at 500 mM imidazole from the non-baffled flask and the 4th elution sample at 100 mM imidazole from the baffled flask.

There appeared to be no observable difference in either dimerisation or degradation of the protein. However, in the lane containing the 3rd elution sample at 500 mM

imidazole from the non-baffled flask, there appeared to be very little monomeric protein. This indicates that dimerised protein requires higher level of imidazole concentration for elution due to the presence of two His-tags.

.To further investigate the effects of oxygen levels in the scFv expression, the same culture volumes of 100 mL were grown in a small 100 mL flask and a big 500 mL flask, respectively. The size of the small flask was chosen to minimise the air pocket that would be available, intentionally reducing the aeration of the media. The cultures were otherwise grown as previously described. Optimally, this aeration would have been monitored had the equipment been available.

The media was harvested as normal and the scFv purified as described previously and analysed using dot-blot again after standard procedure. As can be seen in Figure 50B, there appears to be an overall much higher protein concentration in the larger flask when compared to the small flask.

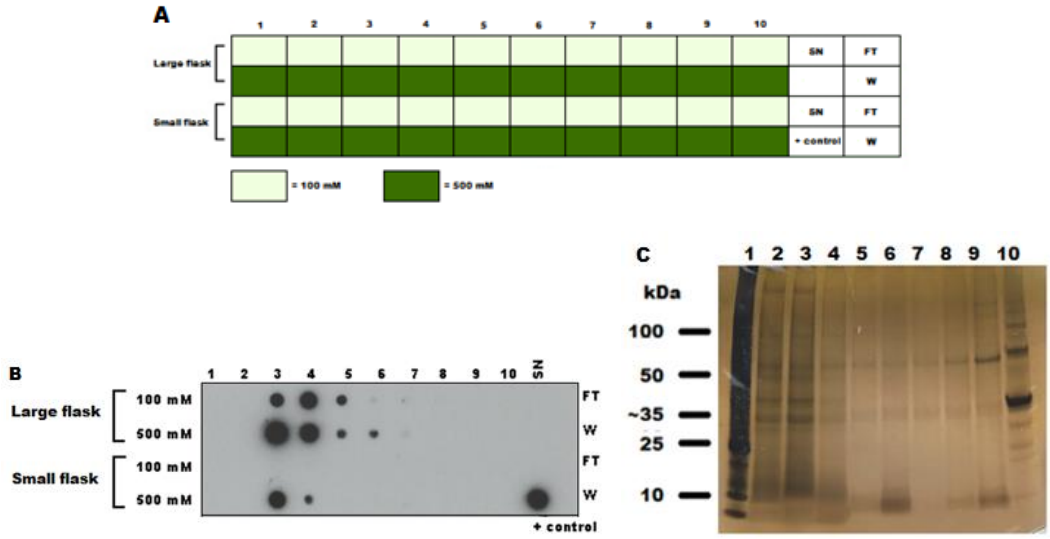

Figure 50 Expression and size analysis of constant volume (100 mL) cultures grown in large flasks (500 mL) and small flasks (100 mL)

A) Schematic overview of the loading profile of the dot-blot **B)** Dot-blot analysis of the elution profile of the Ni^{2+} column purified protein. 200 µL was loaded of each sample and 10 µL was used as a positive control. The expression rate appears much higher in the large flask compared to in the small flask **C)** A silver stain analysis of the following elutions from the dot blot 20 µL was loaded of each sample and 3 µL was used as a positive control: 1) Ladder 2) 3rd elution sample from large flask, 100 mM imidazole 3) 4th elution sample from large flask, 100 mM imidazole 4) 5th elution sample from large flask, 100 mM imidazole 5) 3rd elution sample from large flask, 500 mM imidazole 6) 4th elution sample from large flask, 500 mM imidazole 7) 5th elution sample from large flask, 500 mM imidazole 8) 3rd elution sample from small flask, 500 mM imidazole 9) 4th elution sample from small flask, 500 mM imidazole 10) Positive control.

In order to analyse whether the oxygen levels might have an impact on the stability or the dimerisation of the scFv, a silver stain analysis was conducted on the samples showing protein expression. These included samples 3-5 eluted at 100 mM imidazole from the large flask, samples 3-5 eluted at 500 mM imidazole from the large flask and 3rd and 4th sample eluted at 500 mM imidazole from the small flask. The silver stain was otherwise performed as previously described (section 2.2.34).

As can be seen in Figure 50C there are no differences seen between the lanes, apart from the expected fluctuations in intensity due to the difference in protein concentrations in the analysed elution samples.

As increasing the scFv expression appeared to be problematic and the Coomassie staining showed a decent, but degraded protein concentration, the efforts were changed to prevent scFv degradation rather than improve initial yield.

6.8 Inhibition of proteolytic degradation of anti-LAM scFv using casein in both complex and minimal media

One way of preventing the degradation of a desired protein is the addition of inconsequential bulk proteins such as casein to act as an alternative source on which the proteases can act. This would thereby in theory decrease the amount of proteases available to degrade the expressed protein. Casein was for this reason added to the expression media.

Furthermore, the complexity of the media has in some cases been found to have an impact on the degradation levels of the expressed protein. Minimal media (YNBM) can potentially prevent the expression of proteases and thereby inhibit the proteolytic degradation of the expressed protein. However, this normally also has a negative impact on the yield. Despite this, if the switch to minimal media could increase the stability of the protein it was considered worth investigating.

The starter cultures were set up as previously described in BMGY media and resuspended in either complex media (BMMY) or minimal media (YNBM). The cultures were then split into two flasks each of 50 mL final volume. Casein was added

to one BMMY culture and one YNBM culture and all the cultures were hereafter grown as previously described and scFv was purified from the supernatant as before. The samples were finally analysed by dot-blot and silver stain.

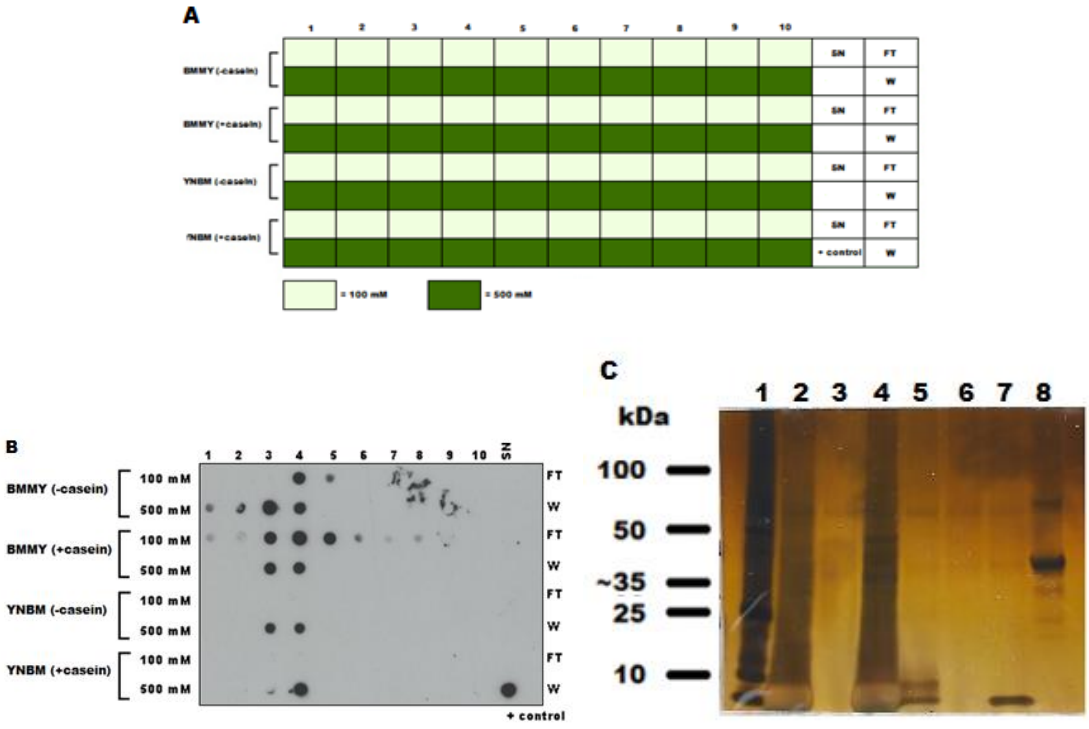

Figure 51 Degradation analysis of expression in complex (BMMY) and minimal (YNBM) media with or without casein

A) Schematic overview of the loading profile of the dot-blot. **B)** Dot blot analysis of the elution profile of the eluted purified protein. Protein expression generally appeared higher in complex media compared to minimal media as expected. Interestingly, the elution profile seemed to shift from high imidazole to low imidazole concentration elution when casein was added. **C)** Silver stain analysis of the elutions with highest protein concentration. 1) Ladder 2) BMMY (-cas) 100 mM (4) 3) BMMY (-cas) 500 mM (3) 4) BMMY (+ cas) 100 mM (4) 5) BMMY (+ cas) 500 mM (4) 6) YNBM (-cas) 500 mM (4) 7) YNBM (+ cas) 500 mM (4) 8) Positive control.

As can be seen in Figure 51B, growth in YNBM minimal media had a detrimental effect on the protein expression levels as anticipated. Casein had no effect on the protein levels in either YNBM or BMMY media. Interestingly however, in BMMY

media, the addition of casein shifted the elution (of the scFv towards the primarily 100 mM imidazole elution (BMMY + casein) as opposed to the primary elution at 500 mM imidazole (BMMY - casein).

The following samples, chosen from the dot blot, were hereafter analysed using silver staining (Figure 51C): 4th elution from BMMY (- casein) at 100 mM imidazole, 3rd elution from BMMY (- casein) at 500 mM imidazole, 4th elution from BMMY (+ casein) at 100 mM imidazole, 4th elution from BMMY (+ casein) at 500 mM imidazole, 4th elution from YNBM (- casein) at 500 mM imidazole and finally 4th elution from YNBM (+ casein) at 500 mM imidazole.

When analysed on a silver stained gel these elution samples did not show the same increased dimerisation profile as previously, which could have explained the increased imidazole concentration requirement.

Growth on the regular complex BMMY media appeared to have a more positive effect on the protein expression. The addition of casein seemed to have a shifting effect on the elution profile of the expressed protein. Without casein, a higher concentration of imidazole was required for full elution than with casein.

When the BMMY elutions were analysed on a silver stained gel there appeared to be a dark smear in the first elutions at 100 mM, both with and without casein. This had not occurred in either of the previously silver stained elutions. However, this could be due to leftover media in the Ni^{2+} column as a result of inadequate washing. Bands similar to the other lanes were still visible under the smear overall indicating that neither growth on minimal media nor the addition of casein had the desired effect on the protein concentration. Furthermore, casein did not seem to have any effect

on the protein degradation as the separation profile was identical to that without casein.

This indicated that growth on complex media without casein, which was the protocol up to this point, was the most successful so far. However, other parameters could still be changed in an attempt to decrease proteolytic degradation, such as variations in temperature and the addition of protease inhibitors.

6.9 Inhibition of proteolytic degradation by addition of protease inhibitors at various temperatures

As the addition of casein did not have any effect on the stability of the scFv, protease inhibitors were added to the media in a last attempt to decrease the proteolytic degradation of the expressed scFv. However, the addition of protease inhibitors generally has a negative impact on the growth of *P. pink* and for that reason it was hypothesised that the addition would decrease protein production due to reduced fitness of the cells, despite the potential increased stability of the product. Despite this drawback, it was worth investigating.

Furthermore, it was interesting to analyse the effects of reducing the incubation temperature as this might have an impact on the proteolytic activity of the proteases degrading the expressed protein. As *P. pink* is a relatively versatile organism, previous studies have shown that it is capable of growth at 20°C.

The anti-LAM producing *P. pink* strain clone 17 was therefore grown, in the presence and absence of protease inhibitors at both 20°C and 25°C in BMMY without casein in large non-baffled flasks in expression cultures of 50 mL. Two cultures were grown

at 20°C and two were grown at 25°C. Additionally, a protease table was added to one culture grown at each temperature. The cells were grown for 24 hours and the supernatant was harvested and purified as before.

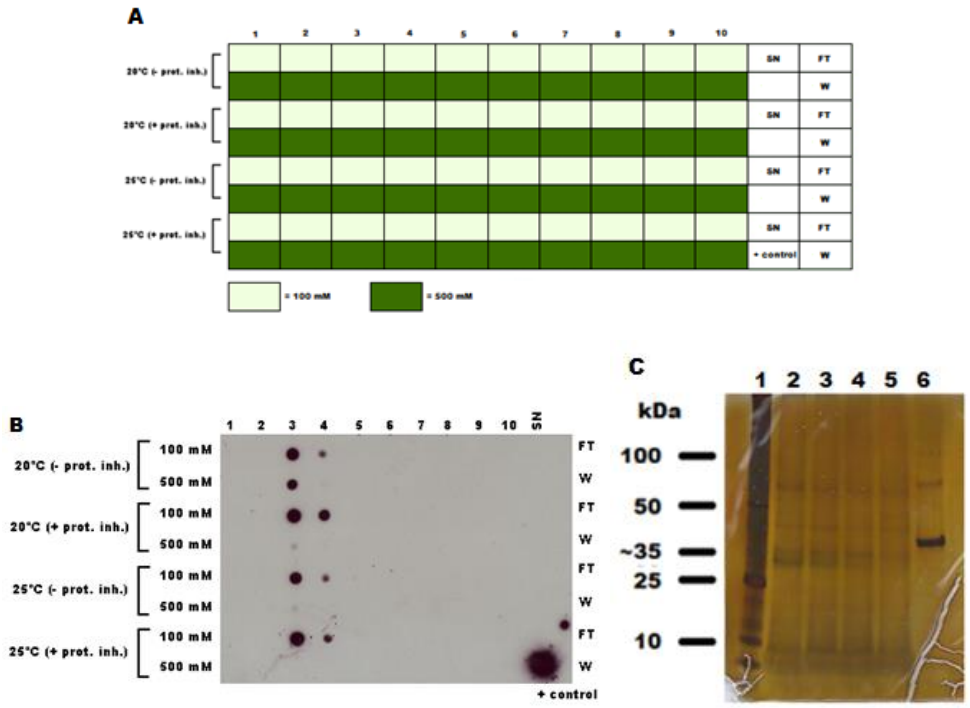

Figure 52 Analysis of effect of temperature and protease inhibitors on expression and degradation of expressed protein.

A) Schematic overview of the loading profile of the dot blot **B)** Dot blot analysis of the elution profile of the expressed protein under various conditions: 20°C or 25°C and with or without protease inhibitors (+/- prot.inh.). **C)** Silver stain analysis of the elutions containing the highest concentration of protein from (B). 20 µL was loaded of each sample and a 3 µL positive control 1) Ladder 2) 3rd elution sample from 20°C (- prot.inh.) 100 mM imidazole 3) 3rd elution sample from 20°C (+ prot.inh.) 100 mM imidazole 4) 3rd elution sample from 25°C (- prot.inh.) 100 mM imidazole 5) 3rd elution sample from 25°C (+ prot.inh.) 100 mM imidazole 6) Positive control.

As can be seen in Figure 52B there was a slight increase in protein expression at 20°C with protease inhibitors. When comparing the temperatures alone, 20°C seemed to have a very small increase in expression when compared to 25°C, however this could be due to variations in purification efficiencies.

The following elution samples were further analysed on silver stain to evaluate degradation and dimerisation patterns (Figure 52C): 3rd elution from culture grown at 20°C (- protease inhibitors) at 100 mM imidazole, 3rd elution from culture grown at 20°C (+ protease inhibitors) at 100 mM imidazole, 3rd elution from culture grown at 25°C (- protease inhibitors) at 100 mM imidazole, 3rd elution from culture grown at 25°C (+ protease inhibitors) at 100 mM imidazole. The silver stain was conducted as previously.

There was found to be no difference between the elutions indicating that the protease inhibitors had no effect on preventing proteolytic degradation of the protein. When analysing using silver stain to see if either of the parameters had any effect on the dimerisation of the product, there was again no noteworthy difference seen. The general consensus from the optimisation assays was that very little helped in reducing dimerisation or decreased degradation. Despite this, here were still many possibilities for optimisation of scFv expression and degradation prevention as will be discussed below, however time became the limiting factor.

6.10 Discussion

The aim of this chapter was the transformation of *Pichia pink* with the pPinkα-HC vector containing the designed anti-LAM scFv from chapter 5.

Following the transformation of the *P. pink* strain, the white transformed colonies were screened for both protein expression and optimal time point for harvesting of the media. As the vector in which the scFv was inserted contained the α mating

factor signal sequence from *S. cerevisiae*, the expressed scFv would be released into the supernatant, easing the acquisition of the protein.

As the screening of the clones progressed, it became readily apparent that most clones in fact did show some degree of expression, but the degree varied greatly. This can due to some extent be associated with the number of vectors were internalised during the transformation of the individual clones. However, there are some problems associated with the increased protein expression. First, if the vector content is too high this could result in an overproduction of protein and result in the formation of inclusion bodies and the result would be congested cells (Love *et al*., 2012). This would not only require lysis of the cells but most likely also denaturation and renaturation of the purified protein in order to retrieve the protein of interest. This would not only have an effect on the protein yield but would also complicate the harvesting process. Furthermore, the formation of inclusion bodies would be a rate-limiting step thereby inhibiting large-scale protein production and could furthermore lead to toxic levels to the cells reducing fitness and as a result reducing the expression levels (Love *et al*., 2012).

Several conditions were analysed, including variance in temperature and oxygen levels, in an attempt to not only increase scFv production but also reduce proteolytic degradation. Reducing cultivation temperature has in previous studies showed to have a substantial positive impact on the Fab expression in a *Pichia pastoris* system (Dragosits *et al*., 2009). The reduction of temperature in this study from 25°C to 20°C did not have any effect on either the expression levels or the degradation rate of the expressed protein (Figure 52B).

Another attempt included the reduction of oxygen levels as it was observed that during the initial screening in 50 mL falcon tubes, where there was expected low oxygenation compared to baffled flasks, protein expression was generally acceptable. However, when expression was moved to baffled flasks a reduction in protein expression was observed (data not included). A comparative study was set up to analyse the same culture in either baffled or non-baffled flasks. The results showed an increased expression in the non-baffled flasks indicating that high protein expression required lower oxygen contents, contradicting the fact that methanol metabolism requires oxygen (Jahic *et al*., 2002). However, other studies have shown the same effect of higher protein concentrations at lower oxygen levels (Charoenrat *et al*., 2005; Baumann *et al*., 2007; Baumann *et al*., 2010).

This effect could also potentially be the effect of increased stress on the cells in baffled flasks compared to regular conical flasks. This could increase lysis and could furthermore increase the proteolytic degradation, indirectly resulting in a lower yield. So perhaps the expression levels are comparable, but the product in the baffled flasks is degraded more rapidly.

Another possibility for the lack of scFv expression might simply be that it sometimes just isn't expressed or the expression rate goes down due to unmonitored changes in growth conditions. For this reason it could be interesting to analyse the scFv expression on mRNA level using qRT-PCR. This could not only elucidate whether the lack of scFv is due to degradation or lack of expression but could also validate the effects the various growth conditions has on the expression rate. *P. pink* is known for the very varied protein expression levels even under static conditions (Miller *et*

al., 2005). Transcriptional analysis could shed some light on the expressional pathway of the scFv.

A second problem became apparent as expression experiments progressed, which was degradation. This not only complicated basic identification but also made downstream analysis very elusive. Due to the nature of the His-tag, which was designed into the final scFv for ease of purification and identification, it was unfortunately also one of the most exposed epitopes of the scFv. This could potentially have made it very susceptible to protease cleavage, which would not only complicate purification, but would prevent detection by HRP-conjugated anti-His antibodies.

There are many potential reasons behind protein degradation and potential remedies. The most likely reason is due to protease activity. Proteases are vital components of any organism, from virus to mammalian cells. They are key players in protein maturation, degradation of outdated proteins for recycling and even for self defence against foreign bodies. As a consequence there is a great variety of proteases each with varying specificity, abundance and efficiency. As most of these activities are found within the cells, this is where the large majority of proteases are found. They can however be released into the extracellular space upon cell stress and cell lysis for which reason it is of great importance that the cells of the expression system are as much in optimal conditions as can be achieved. The problem with *P. pink* as an expression system is the activation of expression using methanol. Although *P. pink* is a methylotrophic organism it only tolerates methanol at low levels, not exceeding much more than 3% of the media (PichiaPink™ Expression System

manual, Invitrogen). This along with the experience that growth did not occur following the shift to methanol-containing media (data not shown) indicates that the cells were growing under sub-optimal conditions. This could lead to cell lysis and the release of proteases into the media leading to degradation of the anti-LAM scFv.

One of the options for the inhibition of degradation by proteases is the utilisation of either of three *P. pink* knock-out mutant strains. As mentioned above, these strains include knock-outs for the *prb1* gene encoding proteinase B, the *pep4* gene encoding proteinase A or both (Gleeson *et al*., 1998). As proteinase A is involved in the activation of proteinase B it could have been of particular interest to investigate this mutant as a potential substitute for the utilised "wt" *P. pink* strain. The problem with the mutant strains is however, that previous studies have shown that stability of the cells has been compromised by the mutations making them more fragile requiring extra care with not only storage but during fermentation as well (Gleeson *et al*., 1998) . The original *P. pink* strain was for this reason chosen for preliminary studies. However, it could be interesting to see if the mutants could have a positive effect on the stability of the protein in future experiments. General analysis of the peptide sequence and the susceptibility to proteases definitely indicates that proteolytic degradation might be the culprit of the low protein yield.

Another option, which was investigated was the use of protease inhibitors. In addition to them seemingly having little effect on the degradation levels of the expressed protein, protease inhibitors are furthermore generally fairly expensive and are not suitable for large-scale production of proteins in a small lab unless the advantages outweigh the disadvantages.

As briefly mentioned, a quick *in silico* proteolytic digest of the product indicated that it contains many proteolytic cleavage sites. As especially endoproteases have specific recognition sequences, an attempt could have been made to modify the sequence of the anti-LAM scFv to eradicate some of the cleavage sites. This however, would not be without potential consequences. Even modifications in the framework regions of the scFv could have an altering effect on the overall structure of the antigen recognising site. For this reason it could be argued that the most logical structural feature to attempt to modify is the His-tag. As this site is protruding from the protein it is more susceptible to proteolytic cleavage, but also easier to modify without affecting the structure of the scFv. Furthermore, without the His-tag it is, as mentioned, not only impossible to easily purify but also prevents the use of anti-His antibodies for western blot and dot-blot analysis. There is in fact some indication that some of the low detection levels of the expressed scFv when comparing western blots with their respective silver stains might be due to the loss of the His-tag. In a few instances there are very thin bands visible around the expected size in the silver stained gels without it being present in the western blot, ,despite being executed simultaneously. This problem could potentially be circumvented by using an anti-mouse variable domain antibody modified with HRP. The proteolytic cleavage of the His-tag could also have further implications for the purification itself. If the His-tag is cleaved off prematurely it does not allow purification using Ni^{2+} column. So even if high concentrations of protein are expressed, if the His-tag is not present acquiring the protein becomes a problem.

Another sensitive structural motif that is susceptible to proteolytic cleavage is the linker region. The linker chosen was the poly glycine linker $(GGGGS)_5$ due to the flexible and hydrophilic nature which would not only enable the correct folding of the scFv but the length would also prevent multimerisation (Alfthan *et al*., 1995). However, the protruding nature of the linker suffers the same disadvantages as the His-tag such as increased susceptibility to proteases due to the increased exposure (Alfthan *et al*., 1995). It could therefore be argued that other linker regions could be tested for improved stability. Furthermore, although linkers of shorter length have shown an increased degree of multimerisation, this effect does not appear to be significant before the length of the linker decreases to below 11 residues (Albrecht *et al*., 2006). As the length of the linker inserted in this project was 25 residues it could be argued that a decrease in length might have a positive impact on the stability by potentially decreasing the exposure to proteases.

Additional modifications of the structure could also involve analysing the effect utilising a V_L-linker-V_H conformation as opposed to the V_H-linker-V_L conformation evaluated in this study. Although it is unlikely to have an effect on the protease degradation of the peptide, it could have an impact on the expression levels of the scFv. Although the conformation utilised in this study is the one that has previously been shown to have the highest levels of expression (Desplancq *et al*., 1994; Weisser and Hall, 2009). Furthermore, studies have shown that the V_L-V_H conformation had a negative impact on antigen binding activity, whereas the V_H-V_L conformation retained 73% of parental antigen binding activity (Albrecht *et al*., 2006). With this in mind, it could still be a factor worth investigating.

One of the problems with the *P. pink* expression system was its instability in expression rates (Miller *et al*., 2005). For this reason, it could be interesting to transfer the expression of the anti-LAM scFv to *E. coli* to not only see if higher expression rates could be achieved, but also if this could have a positive effect on the stability of the product (Miller *et al*., 2005). As the expression rate in *E. coli* is higher than in *P. pink*, the protein would be able to be purified quicker and analysed before succumbing to proteolytic degradation (Miller *et al*., 2005).

Subsequent to the identification and production optimisation of the scFv, the most important factor was to establish the binding affinity of the scFv, which was not accomplished due to low protein concentrations. Although the IgG3, from which the scFv was *in silico* isolated, did show binding towards LAM, there is no guarantee that this binding affinity is directly transferred to the scFv. In fact, most scFvs show a decreased affinity towards the antigen compared to the parental molecule (Albrecht *et al*., 2006). This can to a large extent be attributed to the loss of the conserved regions, which despite having no direct impact on the complementary determining regions, do offer structural support, which when lacking could result in a slightly modified binding pocket. Furthermore, in the scFv the two variable domains are linked by a flexible linker that offers no more support for the molecule, than to keep the domains in such close proximity that aggregation would occur due to electrostatic interactions and hydrophobic patches.

The initial establishment of anti-LAM activity would be established by running a sandwich western of the LAM using the scFv as primary antibody. This would be visualised using the anti-His antibody previously utilised.

If binding was found positive, the next step would be to establish the affinity of the scFv. This would be established using BIAcore, which allows the establishment of the binding constant using Surface Plasmon Resonance technology (SPR). SPR uses flow technology to analyse the binding affinity of molecules in solution to immobilised antigens. A detector analyses the reflection angle of the immobilised antigen. Hereafter a flow of antibodies in solution is run over the antigens and upon binding the reflection angle changes and this is detected. By comparing the change in reflection associated with binding and following dissociation by running clear storage solution and analysing the reversion of reflection pattern, the binding constant of the analysed molecule can be detected. The binding constant of the designed anti-LAM scFv would be compared to the parental antibody that would function as a positive control. This way it would be possible to also quantitatively assess the effect on binding affinity by isolating the antigen binding part from the rest of the antibody.

There is the possibility of affinity maturation of the scFv, should the affinity have been compromised by being separated from the parental molecule. This can be done using phage display technologies (Renaut *et al*., 2012). This would not only allow the potential rescue of lost binding affinity but even an improvement of the K_D towards the antigen, LAM.

Following the establishment of the binding affinity, it would have been advantageous to repeat the experiments from chapter 3 and 4, but with UBI 29-41 exchanged for the anti-LAM scFv in order to establish the value of the anti-LAM scFv as a diagnostic or therapeutic targeting agent. Furthermore, as can be seen in Figure 53. There are

14 tyrosine residues in the anti-LAM scFv compared to the single tyrosine in UBI 29-41, making it potentially more useful as a therapeutic targeting agent as it can deliver a greater dose per targeting agent.

Figure 53 Number of tyrosine residues in the designed anti-LAM scFv

Overall, although the expressed protein could not be unequivocally demonstrated to be the anti-LAM scFv, there are several lines of evidence from the experiments in this chapter that suggest the correct protein was expressed. Namely, Figure 46 and the silver stains obtained from expression optimisation assays all showing a protein of the right size that also has a tendency to dimerise. Despite some work remaining to optimise the expression levels and reduce degradation, this chapter managed to meet most of its aims, and provides much of the groundwork for future efforts in producing an anti-LAM scFv.

7 General Discussion

The overall aim of this project was to develop novel diagnostic and/or therapeutic agents to help in the fight of troublesome pathogens.

7.1 ^{125}I as a therapeutic agent

The first half of the project revolved around the establishment of Auger electrons as new potential therapeutic agent. While there was no increase in mortality in any of the model organisms using either 1 MBq or 5 MBq ^{125}I there are several factors that could explain this:

1. The targeting compromised the delivery either by being too low a concentration or by having reduced binding
2. The LET of the isotope utilised was not high enough to cause substantial DNA damage.
3. The range of Auger electrons is too short to reach DNA to cause any DSB

In order to properly evaluate the potential future of Auger electrons as therapeutic agents these problems need to be addressed.

Firstly, the issue with lacking toxicity seen could be due to the targeting agent compromising the delivery of the Auger emitting isotope to the target microorganisms. This could be due to the concentration of UBI 29-41 being too low to mount a response by not delivering a high enough dose of ^{125}I, which would be seen as a decreased survival rate. By testing a variety of increasing concentrations

of UBI 29-41 to the activated ^{125}I it would be possible to evaluate whether the lack of mortality was due to inadequate peptide concentration.

Preliminary evaluations of peptide binding, using a simple binding experiment in which the microorganisms subjected to ^{125}I-UBI were washed in media and radiation associated with the cells, was subsequently established. Although only conducted on two organisms a single time each due to time and materials restraints, it showed negligible binding to cells following three round of washing. The Bq/cell were identical to the free iodine control, indicating that there was little to no specific binding beyond that of free activated iodine. Furthermore, the generation of positive iodine ions as a result of the Iodogen reagent could have caused the free iodine to bind to the negatively charged surface of *S. cerevisiae* which could have masked the binding of the peptide. Interestingly, the peptide did show ability to bind and cause cell death in previous experiments, indicating a fully functional peptide. Whether the Tris Iodination buffer had any effect on the binding ability is unknown. It is unlikely that the Iodogen reagent has had any effect on the chemical properties of the peptide as this was immobilised in the glass vial and the peptide was iodinated in a separate tube. A cold-labelled version of UBI 29-41 was prepared in order to see if the labelling process in itself could have had an effect on the binding capacity of the polypeptide. In initial studies, no difference in toxicity was observed when compared to the non-labelled peptide (data not shown), however this was not fully explored and is therefore not included as this is considered inconclusive.

Another aspect of the binding studies that could have been manipulated was the duration to which the organisms were exposed to the radiation prior to washing and

plating. This was only one hour which may have been too short to elicit toxic effects. Extending incubation time would allow UBI 29-41 enough time to bind properly to the cells, but also to increase the number of decays each organism would be subjected to. As the half-life of ^{125}I is 60 days, one hour or even two days (if including the growth on the plates in which some radiation was still present) is a very minor percentage of the half-life, meaning that most of the ^{125}I was not allowed time to decay. A larger study investigating various incubation times would have been worthwhile to execute to analyse if a greater effect could be attained. This could give some primary indications to the efficiency of targeting of UBI 29-41, which due to the short range of Auger electrons is vital for any genotoxicity to be seen.

Secondly, the Auger electron emitting isotope analysed in this project was ^{125}I. Despite being of shorter range compared to other isotopes, such as the more energetic^{123}I, it had other qualities like a long $T_{1/2}$ (~60 days) compared to the half-life of ^{123}I, 13.2 hours (O'Donoghue and Wheldon, 1996; Kassis, 2011). This made ^{125}I a good candidate to optimise toxicity experiments with. Furthermore, the labelling method would likely allow easy exchange with longer range isotopes such as ^{123}I. For this reason one of the next steps in evaluating the effects of Auger electrons would be the exchange of ^{125}I with ^{123}I although the labelling procedure would very likely have to be further optimised for ^{123}I.

Due to the higher energy of the Auger electrons and thereby longer range, it might be possible to reach the DNA and cause damage.

This leads to the final proposal: that the reason that no toxicity seen is because the distance to the microbial DNA from the membranes is still too great. To evaluate

this there are two immediate possibilities: The first is the analysis of genotoxicity using genetically modified organisms developed to visualise DNA damaging events. Many commercial microbial strains are available that are capable of visualising genotoxicity such as the Salmonella Ames test or the SOS Chromotest for bacterial strains and the GreenScreen genotoxicity assay for yeast based systems (Quillardet *et al*., 1982; Mortelmans and Zeiger, 2000; Cahill *et al*., 2004). As mentioned in section 4.7 these tests were able to visualise DSB, for example by reversion of histidine-dependence clones to histidine-independence, or by the detection of upregulation of SOS response genes by the incorporation of a *lacZ* under the control of *sfiA*, an SOS response gene. This could allow an insight into whether range is an issue, or dose being an issue.

Secondly, DNA damage in particular can also be assessed using qRT-PCR to measure SOS response genes in the model organisms subjected to Auger electrons. These could include RecA monitoring for bacterial strains and Rad51 for yeast strains (Clever *et al*., 1997; Walmsley *et al*., 1997; Cox, 2007). By evaluating the upregulation of the SOS-response it could give an indication if any DNA damage is occurring and that the lack of mortality seen could be due to a well-established SOS response. If no upregulation of the SOS-response genes alongside a binding analysis is seen this could indicate that the range is indeed too large for the Auger electrons to reach the DNA and cause any DSB.

One issue with antimicrobial peptides in general is the lack of specific binding (Walker *et al*., 2007). This can be useful for unspecific imaging purposes in cases where it is unknown if the cause of an inflammation or fever is caused by an infection,

however when it comes to therapy it is more beneficial to have a targeting agent with a higher specificity. One main issue with antimicrobial peptides is the non-target tissue accumulation (Akhtar *et al*., 2005; Meléndez-Alafort *et al*., 2005; Brouwer *et al*., 2006; Brouwer *et al*., 2008). If the peptides have been labelled with therapeutic isotopes, these isotopes are accumulated in non-target areas of the body, potentially damaging non-target tissue, commonly kidneys, liver intestines and bladder. Furthermore, diluting the targeting agent across non-target tissues would also require the administration of higher total dose of therapeutic agents, again leading to increased toxic dose accumulated in non-target tissues (Torchilin, 2000). This further strengthened the requirement for a stability analysis which did indeed show deconjugation of ^{125}I from UBI 29-41. This could have been very problematic in *in vivo* settings causing further systemic spreading of the radiation.

However, for this project, UBI 29-41 was a good targeting candidate due to the non-specific nature of antimicrobial peptides. This allowed the analysis of the toxic effects of Auger electrons on a variety of micro-organisms. This was primarily possible due to the controlled environment in which UBI 29-41 was utilised. Furthermore, the nature of the peptide (13 aa) with a single tyrosine residue made labelling optimisation straightforward. The use of the Iodogen labelling method made it easy for the exchange of ^{125}I with isotopes of higher LET such as ^{123}I. This would be interesting to, again, analyse in controlled *in vitro* settings, however, UBI 29-41 appears to have its greatest value as an imaging agent of infectious diseases due to the non-target bio distribution with accumulation in liver, intestines, kidneys and bladder (Akhtar *et al*., 2004; Akhtar *et al*., 2005). Nonetheless, UBI 29-41 still holds

value as a non-specific targeting agent for *in vitro* studies and would be useful for the later evaluation of higher energy isotopes.

7.2 ScFv construction and expression

Due to the unspecific targeting of UBI 29-41, the second part of the project revolved around the development and expression of an anti-LAM scFv. ScFvs hold an advantage over antimicrobial peptides in other aspects than specificity; scFvs are more adaptable to meet physiological requirements, such as the addition of parts of the Fc regions to increase circulation time (Milenic *et al*., 2004; Weisser and Hall, 2009) and it is possible, by modification of linker regions, to create multispecific targeting agents (Holliger *et al*., 1993; Illiades *et al*., 1997; Todorovska *et al*., 2001; Dolezal *et al*., 2003; Weisser and Hall, 2009).

The variable domains of the parental anti-LAM IgG3 molecule were successfully isolated and *in silico* linked by a flexible linker, inserted into a secretion vector and transformed into strain 1 of *Pichia pink* containing no protease knock outs.

Although expression was appeared to be successful, there was a great problem with degradation. Consequently, any future attempts to express the scFv would need to address this, perhaps firstly by investigating the level of degradation in any of the existing protease knock-out *P. pink* strains mentioned in section 1.5.4.1.1.

Although the concentrations of scFv never reached levels to perform glycosylation analysis it is likely that the scFv is not glycosylated; glycosylations primarily reside in the Fc region of the antibody (Youings *et al*., 1996; Ahmad *et al*., 2012). It may then be possible to increase the yield by expressing the anti-LAM scFv in a bacterial

system. However both post translational modification and folding would have to be interrogated prior to transfer as previously addressed.

The anti-LAM scFv developed in this project, could have significant diagnostic value. As LAM is released into urine it could greatly aid in the diagnosis of tuberculosis, especially in children and immune-compromised individuals, in which diagnosis is very difficult due to lack of immune response to the Mantoux tuberculin skin test and therefore often associated with false-negatives (Ducatti *et al*., 2006; Jassal and Bishai, 2009; Minion *et al*., 2011). As this further does not require *in vivo* administration to patients, the murine ancestry of the scFv is no longer of importance, only binding affinity.

Although *M. tuberculosis* is predominantly an intracellular bacterium, research has indicated that even during latent phase, there are some active extracellular bacilli present (Lewis, 2010; Gegenbacher and Kaufmann, 2012). This increases during the active phase which may open up for potential new ways of not only diagnosing for tuberculosis, but also to diagnose the extent of tuberculosis infection and localisation if the scFv could be modified to allow *in vivo* administration (Lewis,2010; Gegenbacher and Kaufmann, 2012).

With regards to therapeutics, one of the big disadvantages of *M. tuberculosis* is it being a primarily intracellular bacteria. Although research has indicated that even in latent phase, the bacteria are to some extent found in the extracellular space of the granulomas, there will be bacteria also found in the phagosomes of macrophages (Lewis, 2010; Gegenbacher and Kaufmann, 2012). Even when these phagocytic cells are overcome by the infection and initiate necrosis, the bacteria will most likely

be taken up by a newly recruited macrophage, going directly from one intracellular space to another. For this reason, the designed scFv would have to be internalised into the infected cells and into the phagosome they reside in if an Auger emitting isotope is to be used. This could be overcome by mimicking the work by Cornelissen *et al.* (2011). By modifying an immune conjugate directed towards phosphorylated histone 2A variant H2AX (γH2AX) with the HIV-derived cell penetrating peptide Tat, the immune conjugate was allowed nuclear localisation (Cornelissen *et al*., 2011). This opens up for the possibilities of internalising the therapeutic isotopes to the intracellular bacteria. One problem that remains is the lack of surface markers distinguishing infected from non-infected cells.

However, proteins with iodination of tyrosine residues have a tendency to be dehalogenised and metabolised when internalised, indicating that internalisation might not be optimal with the labelling techniques analysed in this project (Mattes *et al*., 1997; Milenic *et al*., 2004; Wu and Senter, 2005). A potential way to overcome this step is the utilisation of either an α- or β- emitter, such as ^{131}I (Wu and Senter, 2005). This way the scFv could be directed to the site of infection by the few extracellular bacteria present and the range of the radioactive particles would potentially allow the sterilisation of the bacteria from outside the phagocytic cells and/or induce apoptosis of the infected cells, allowing release of the bacteria from the intracellular pockets. However, this would potentially have damaging effects on the surrounding tissue due to crossfire-effects (Milenic *et al*., 2004). This could have fatal consequences in the late stages of infection for lung tissue already very damaged.

Another issue with tuberculosis is the generation of caseous granulomas, which raises the question as to the efficiency of transporting the therapeutic agent to the sites of infection. Although neo-vascularisation is observed in the latent stages, which would ease the access of the therapeutic agent to the site of infection, active cavitary tuberculosis has shown loss of vascularisation of the infected nodules, which could complicate the delivery of the nuclides if delivered at the wrong stages of disease development (Ulrichs *et al*., 2005).

M. tuberculosis is for this reason a generally problematic organism to eradicate and other targets could be deemed more favourable to initially treat such as extracellular pathogens. An example of which, could be *S. aureus* of which new types of multi resistant strains are continuously found (Enright *et al*., 2002; Alanis, 2005; Collingnon *et al*., 2009; Tübbicke *et al*., 2012). Due to the extracellular nature, *S. aureus* would be easily accessible to the targeted Auger emitting isotopes. One of the advantages of Auger electrons, if they could be found to be toxic to microorganisms if bound to the cells in an extracellular fashion, would be the reduced generated resistance. The problem with the existing antibiotics is that for each of them there is at least one mechanism of resistance that has been developed (Alanis, 2005). Furthermore, due to limited funding and time-limits, as a new therapeutic compound takes between 10-14 years to develop, most new antimicrobial compounds that have come out recently have been slight structural changes to already existing antibiotic chemicals and therefore rapidly generate new resistance (Alanis, 2005). Auger electrons and the generation of DSB in microbial DNA would be a new and potential useful technique to which microorganisms would have

problems generating resistance towards. The only way this would be accomplished would be the increased efficiency of the SOS response. However, obviously if an scFv is to be used as a targeting agent, the specificity has to be altered.

8 Conclusion

There were four aims to this thesis. UBI 29-41 was successfully labelled and it was concluded that the levels of Iodine recommended by the manufacturer was consistent with found data. The protocol for labelling was further optimised for the experimental setup needed for the evaluation of radiotoxic effects of Auger electrons. The evaluations of the toxic effect of Auger electrons were largely inconclusive. Under the conditions evaluated in this project no toxic effect was observed when compared with non-targeted ^{125}I in any of the four model organisms. However, the experimental setup allows easy manipulation for the evaluation of the radiological effects of other isotopes.

To introduce more specificity we wanted to design an scFv from an anti-LAM IgG3. The variable domains were successfully isolated, identified and the scFv was *in silico* assembled.

The pPinkα-HC vector containing the designed anti-LAM scFv was transformed into *P. pink* and a product of the expected size was successfully expressed.

The results presented in this thesis will therefore aid in the development of new antibiotics for infectious diseases.

9 References

Abubakar, I., Gautret, P., Brunette, G. W. *et al*., **"Global perspectives for prevention of infectious diseases associated with mass gatherings"**, *The Lancet Infectious Diseases vol. 12, pp. 66-74, 2012*

Adelstein, S. J., Kassis, A. I., Bodei, L. and Mariani, G., **"Radiotoxicity of Iodine-125 and other Auger electron-emitting radionuclides: background to therapy"**, *Cancer Biotherapy & Radiopharmaceuticals vol. 18, pp. 301-316, 2003*

Ahmad, Z. A., Yeap, S. K., Ali, A. M. *et al*., **"ScFv antibody: principles and clinical application"**, *Clinical and Developmental Immunology vol. 2012, Article ID 980250, 2012*

Akhtar, M. S., Iqbal, J., Khan, M. A. *et al*., **"^{99m}Tc-labeled antimicrobial peptide Ubiquicidine (29-41) accumulates less in *Escherichia coli* infection than *Staphylococcus aureus* infection"**, *Journal of Nuclear Medicine vol. 45, pp. 849- 856, 2004*

Akhtar, M. S., Qaisar, A., Irfanullah, J. *et al*., **"Antimicrobial peptide ^{99m}Tc-UBI 29-41 as human infection-imaging agent: clinical trial"**, *Journal of Nuclear Medicine vol. 46, pp. 567-573, 2005*

Alanis, A. J., **"Resistance to antibiotics: are we in the post-antibiotic era?",** *Archives of Medical Research vol. 36, pp. 697-705, 2005*

Albrecht, H., DeNardo, G. L. and DeNardo, S. J., **"Monospecific bivalent scFv-SH: Effects of linker length and location of an engineered cysteine on production, antigen binding activity and free SH accessibility"**, *Journal of Immunological Methods vol. 310, pp. 100-116, 2006*

Alfthan, K., Takkinen, K., Sizmann, D. *et al*., **"Properties of a single-chain antibody containing different linker peptides"**, *Protein Engineering, Design and Selection vol. 8, pp. 725-731, 1995*

Andersson, H., Elgqvist, J., Horvath, G. *et al*., **"Astatine-211-labeled antibodies for treatment of disseminated ovarian cancer: an overview of results in an ovarian tumor model"**, *Clinical Cancer Research vol. 9, pp. 3914S-3921S, 2003*

Arano, Y., Mukai, T., Akizawa, H. *et al*., **"Radiolabelled Metabolites of Proteins Play a Critical Role in Radioactivity Elimination from the Liver"**, *Nuclear Medicine and Biology vol. 22, pp. 555-564, 1995*

Arnau, J., Lauritzen, C., Petersen, G. E., Pedersen, J., **"Current strategies for the use of affinity tags and tag removal for the purification of recombinant proteins"**, *Protein Expression and Purification vol. 48, pp. 1-13, 2006*

Badar, A., Williams, J., de Rosales, R. T. *et al.*, **"Optimising the radiolabelling properties of technetium tricarbonyl and His-tagged proteins"**, *European Journal of Nuclear Medicine and Molecular Imaging Research vol. 4, article 14, 2014*

Balagurumoorthy, P., Xum X., Wang, K. *et al*., **"Effect of distance between decaying ^{125}I and DNA on Auger-electron induced double-strand break yield"**, *International Journal of Radiation Biology vol. 88, pp. 998-1008, 2012*

Battista, J. R., **"Against All Odds: The Survival Strategies of *Deinococcus radiodurans*"**, *Annual Reviews in Microbiology vol. 51, pp. 203-224, 1997*

Baumann, K., Maurer, M., Dragosits, M. *et al*., **"Hypoxic fed-batch cultivation of *Pichia pastoris* increases specific and volumetric productivity of recombinant proteins"**, *Biotechnology and Bioengineering vol. 100, pp. 177-183, 2007*

Baumann, K., Carnicer, M., Dragosits, M. *et al*., **"A multi-level study of recombinant *Pichia pastoris* in different oxygen conditions"**, *BMC Systems Biology vol. 4, pp. 141-460, 2010*

Becker, W. and Meller, J., **"The role of nuclear medicine in infection and inflammation"**, *The Lancet Infectious Diseases vol. 1, pp. 326- 333, 2001*

Beierwaltes, W. H., **"The treatment of thyroid carcinoma with radioactive iodine"**, *Seminars in Nuclear Medicine vol. 8, pp. 79-94, 1978*

Bello, J., Bello, H. R. and Granados, E., **"Conformation and aggregation of melittin: dependence on pH and concentration"**, *Biochemistry vol. 21, pp. 461-465, 1982*

Bennett, K. L., Matthiesen, T. and Roepstorff, P., **"Probing protein surface topology by chemical surface labeling, crosslinking, and mass spectrometry"**, *Methods in Molecular Biology vol. 146, pp. 113- 131, 2000*

Benua, R. S., Cicale, N. R., Sonenberg, M. and Rawson, R. W., **"The relation of radioiodine dosimetry to results and complications in the treatment of metastatic thyroid cancer"**, *The American Journal of Roentgenology, Radium Therapy, and Nuclear Medicine vol. 87, pp. 171-182, 1962*

Berthet, F.-C., Rasmussen, P. B., Rosenkrands, I. *et al*., **"A *Mycobacterium tuberculosis* operon encoding ESAT-6 and a novel low-molecular mass culture filtrate protein (CFP-10)"**, *Microbiology vol. 144, pp. 3195-3203, 1998*

Bierbaum, G. and Sahl, H.-G., **"Induction of autolysis of staphylococci by the basic peptide antibiotics Pep 5 and nisin and their influence on the activity of autolytic enzymes"**, *Archives of Microbiology vol. 141, pp. 249- 254, 1985*

Block, S. S., **"Disinfection, Sterilization, and Preservation"**, *Lippincott Williams & Wilkins, pp. 922, 2001*

Blok, D., Feitsma, R. I. J., Vermeij, P. and Pauwels, E. J. K., **"Peptide radiopharmaceuticals in nuclear medicine"**, *European Journal of Nuclear Medicine vol. 26, pp. 1511-1519, 1999*

Bold, T. D., Banaei, N., Wolf, A. J. and Ernst, J. D., **"Suboptimal activation of antigen-Specific CD4+ effector cells enables persistance of *M. tuberculosis In vivo*"**, *PLoS Pathogens vol. 7, e1002063, 2011*

Bora, N., **"Large-scale production of secreted proteins in *Pichia pastoris*"**, *Methods in Molecular Biology vol. 866, pp. 217-235, 2012*

Bradley, E. W., Chan, P. C. and Adelstein, S. J., **"The radiotoxicity of Iodine-125 in mammalian cells"**, *Radiation Research vol. 64, pp. 555-563, 1975*

Brady, D., O'Sullivan, J. M. and Prise, K. M., **"What is the role of the bystander response in radionuclide therapies?"**, *Frontiers in Oncology vol. 3, article 215, 2013*

Braren, I, Greunke, K., Umland, O. *et al*., **"Comparative expression of different antibody formats in mammalian cells and *Pichiapastoris*"**, *Biotechnology and Applied Biochemistry vol. 47, pp. 205-214, 2007*

Brennan, P. J., **"Structure, function, and biogenesis of the cell wall of *Mycobacterium tuberculosis*"**, *Tuberculosis vol. 83, pp. 91-97, 2003*

Brogden, K. A., **"Antimicrobial Peptides: Pore Formers or Metabolic Inhibitors in Bacteria"**, *Nature Reviews Microbiology vol. 3, pp. 238-250, 2005*

Brouwer, C. P. J. M., Bogaards, S., Wulferink, M. *et al*., **"Synthetic peptides derived from human antimicrobial peptide ubiquicidin accumulate at sites of infection and eradicate (multi-drug resistant) *Staphylococcus aureus* in mice"**, *Peptides vol. 27, pp. 2585-2591, 2006*

Brouwer, C. P. J. M., Wulferink, M. and Welling, M. M., **"The pharmacology of radiolabelled cationic antimicrobial peptides"**, *Journal of Pharmaceutical Sciences vol. 97, pp. 1633-1651, 2008*

Buchegger, F., Perillo-Adamer, F., Dupertuis, Y. M. and Delaloye, A. B., **"Auger radiation targeted into DNA: a therapy perspective"**, *European Journal of Nuclear Medicine and Molecular Imaging vol. 33, pp. 1352-1363, 2006*

Bryan, R. A., Huang, X., Morgenstern, A. *et al*., **"Radiofungicidal effects of external gamma radiation and antibody-targeted beta and alpha radiation on *Cryptococcus neoformans*"**, *Antimicrobial Agents Chemotherapy vol. 52, pp. 2232-2235, 2008*

Cao, P., Tang, X. M., Guan, Z. B. *et al*., **"Production and characterization of a bacterial single-chain antibody fragment specific to B-cell-activating factor of the TNF family"**, *Protein Expression and Purification vol. 43, pp. 157-164, 2005*

Cahill, P. A., Knight, A. W., Billinton, N. *et al*., **"The GreenScreen® genotoxicity assay: a screening validation programme"**, *Mutagenesis vol. 19, pp. 105-119, 2004*

Carroll, W. L., Mendel, E. and Levy, S., **"Hybridoma fusion cell lines contain an aberrant kappa transcript"**, *Molecular Immunology vol. 25, pp. 991-995, 1988*

Casadevall, A., Goldstein, H. and Dadachova, E., **“Targeting host cells harbouring viruses with radio-labelled antibodies”**, *Expert Opinion in Biological Therapy vol. 7, pp. 595-597, 2007*

Casali, N., **“*Escherichia coli* Host Strains”**, *Methods in Molecular Biology vol. 235, pp. 27-48, 2003*

Cereghino, J. L. and Cregg, J. M., **"Heterologous protein expression in the methylotrophic yeast *Pichia pastoris*"**, *FEMS Microbiology Reviews vol. 24, pp. 45-66, 2000*

Cereghino, G. P. L., Cereghino, J. L., Ilgen, C. and Cregg, J. M., **“Production of recombinant proteins in fermenter cultures of the yeast *Pichia pastoris*”**, *Current Opinion in Biotechnology vol. 13, pp. 329-332, 2002*

Chan, J., Fan, X. D., Hunter, S. W. *et al*., **"Lipoarabinomannan, a possible virulence factor involved in persistence of *Mycobacterium tuberculosis* within macrophages"**, *Infection and Immunity vol. 59, pp. 1755-1761, 1991*

Charoenrat, T., Ketudat-Cairns, M., Stendahl-Andersen, H. *et al*., **"Oxygen-limited fed-batch process: an alternative control for *Pichia pastoris* recombinant protein processes"**, *Bioprocess and Biosystems Engineering vol. 27, pp. 399-406, 2005*

Chatterjee, D. and Khoo, K.-H., **"Mycobacterial lipoarabinomannan: an extraordinary lipoheteroglycan with profound physiological effects"**, *Glycobiology vol. 8, pp. 113-120, 1998*

Chattopadhyay, S., Das, S. S., Chandra, S. *et al*., **"Synthesis and evaluation of ^{99m}Tc-moxifloxacin, a potential infection specific imaging agent"**, *Applied Radiation and Isotopes vol. 68, pp. 314-316, 2010*

Chen, C., Snedecor, B., Nishihara, J. *et al*., **“High-level accumulation of a recombinant antibody fragment in the periplasm of *Escherichia coli* requires a triple-mutant (degPprcspr) host strain”**, *Biotechnology and Bioengineering vol. 85, pp. 463-474, 2004*

Clever, B., Interthal, H., Schmuckli-Maurer, J. *et al*., **"Recombinational repair in yeast: functional interactions between Rad51 and Rad54 proteins"**, *The EMBO Journal vol. 16, pp. 2535-2544, 1997*

Cohen, R. and Engelberg, D., **"Commonly used Saccharomyces cerevisiae strains (e.g. BY4741, W303) are growth sensitive on synthetic complete medium due to poor leucine uptake"**, *FEMS Microbiology Letters vol. 273, pp. 239- 243, 2007*

Cole, W. C., DeNardo, S. J., Meares, C. F. et al., **"Comparative Serum Stability of Radiochelates for Antibody Radiopharmaceuticals"**, *The Journal of Nuclear Medicine vol. 28, pp. 83-90, 1987*

Cole, S. T., Eiglmeier, K., Parkhill, J. *et al*., **"Massive Gene Decay In the Leprosy Bacillus"**, *Nature vol. 409, pp. 1007-1011, 2001*

Collingnon, P., Powers, J. H., Chiller, T. M. *et al*., **"World Health Organization ranking of antimicrobials according to their importance in human medicine: a critical step for developing risk management strategies for the use of antimicrobials in food production animals"**, *Clinical Infectious Diseases vol. 49, pp. 132-141, 2009*

Cornelissen, B., Kersemans, V., Darbar, S. et al., **"Imaging DNA damage *in vivo* using γH2AX-targeted immunoconjugates"**, *Cancer Research vol. 71, pp. 4539-4549, 2011*

Cornish, J., Callon, K. E., Naot, D. *et al*., **"Lactoferrin is a potent regulator of bone cell activity and increases bone formation *in vivo*"**, *Endocrinology vol. 145, pp. 4366- 4374, 2004*

Cosma, C. L., Sherman, D. R. and Ramakrishnan, L., **"The Secret Lives of the Pathogenic Mycobacteria"**, *Annual Review of Microbiology vol. 57, pp. 641-676, 2003*

Cowan, S. T. and Shaw, C., **"Type Strain for *Staphylococcus aureus* Rosenbach"**, *Journal of Genetic Microbiology vol. 10, pp. 174-176, 1954*

Cox, M. M., **"Regulation of bacterial RecA protein function"**, *Critical Reviews in Biochemistry and Molecular Biology vol. 42, pp. 41-63, 2007*

Dadachova, E., Nakouzi, A., Bryan, R. A. and Casadevall, A., **"Ionizing radiation delivered by specific antibody is therapeutic against a fungal infection"**, *Proceedings in the National Academy of Science vol. 20, pp. 20, 2003*

Dadachova, E., Bryan, R, A., Frenkel, A. *et al*., **“Evaluation of acute haematological and long-term pulmonary toxicity of radioimmunotherapy of *Cryptococcus neoformans* infection in murine models”**, *Antimicrobial Agents Chemotherapy vol. 48, pp. 1004-1006, 2004*

Dadachova, E., Burns, T., Bryan, R. A. *et al*., **“Feasibility of radioimmunotherapy of experimental pneumococcal infection”**, *Antimicrobial Agents Chemotherapy vol. 48, pp. 1624-1629, 2004*

Dadachova, E., Bryan, R. A., Huang, X. *et al*., **"Comparative evaluation of capsular polysaccharide-specific IgM and IgG antibodies and F(ab')$_2$ and Fab fragments as delivery vehicles for radioimmunotherapy of fungal infection"**, *Clinical Cancer Research vol. 13, pp. 5629s-5635s, 2007*

Dadachova, E. and Casadevall, A., **“Radioimmunotherapy of Infectious Diseases”**, *Seminars in Nuclear Medicine vol. 39, pp- 146-153, 2009*

Davis, J. M. and Ramakrishnan, L., **“The role of the Granuloma in Expansion and Dissemination of Early Tuberculous Infection”**, *Cell vol. 136, pp. 37-49, 2009*

Dearling, J. L. J. and Pedley, R. B., **"Technological advances in radioimmunotherapy"**, *Clinical Oncology vol. 19, pp. 457-469, 2007*

Desjarlais, J. R., Lazar, G. A., Zhukovsky, E. A., and Chu, S. Y., **“Optimizing engagement of the immune system by anti-tumor antibodies: an engineer’s perspective”**, *Drug Discovery Today vol. 12, pp. 898-910, 2007*

Desplancq, D., King, D. J., Lawson, A. D. G. and Mountain, A., **"Multimerization behaviour of single chain Fv variants for the tumour-binding antibody B72.3"**, *Protein Engineering, Design & Selection vol. 7, pp. 1027-1033, 1994*

Dheda, K., Schwader, S. K., Zhu, B. *et al*., **"The Immunology of tuberculosis: From bench to bedside"**, *Respirology vol. 15, pp. 433-450, 2010*

Diez-Orejas, R., Molero, G., Navarro-Garcia, F. *et al*., **"Reduced virulence of *Candida albicans* MKC1 mutants: a role for mitogen-activated protein kinase in pathogenesis"**, *Infection and Immunity vol. 65, pp. 833-837, 1997*

Divangahi, M., Desjardins, D., Nunes-Alves, C. *et al*., **"Eicosanoid pathways regulate adaptive immunity to *Mycobacterium tuberculosis*"**, *Nature Immunology vol. 11, pp. 751-759, 2010*

Doherty, T. M., **"Immunotherapy for TB"**, *Immunotherapy vol. 4, pp. 629-647, 2012*

Dolezal, O., De Gori, R., Walter, M. *et al*., **"Single-chain Fv multimers of the anti-neuraminidase antibody NC10: the residue at position 15 in the VL domain of the scFv-0 (VL-VH) molecule is primarily responsible for formation of a tetramer-trimer equilibrium"**, *Protein Engineering vol. 16, pp. 47-56, 2003*

Dragosits, M., Stadlmann, J., Albiol, J. *et al*., **"The effect of temperature on the proteome of recombinant *Pichia pastoris***", *Journal of Proteome Research vol. 8, pp. 1380-1392, 2009*

Ducati, R. G., Ruffino-Netto, A., Basso, L. A. and Santos, D. S., **"The resumption of consumption - A review on tuberculosis"**, *Memórias do Instituto Oswaldo Cruz vol. 101, pp. 697-714, 2006*

Emberson, L. M., Trivett, A. J., Blower, P. J. and Nicholls, P. J., **"Expression of an anti-CD33 single-chain antibody by *Pichia pastoris***", *Journal of Immunological Methods vol. 305, pp. 135-151, 2005*

Enright, M. C., Robinson, D. A., Randle, G. *et al*., **"The evolutionary history of methicilin-resistant *Staphylococcus aureus* (MRSA)"**, *Proceedings of the National Academy of Sciences of the United Stated of America vol. 99, pp. 7687-7692, 2002*

Ernst, J. D., **"The immunological life cycle of tuberculosis"**, *Nature Reviews Immunology vol. 12, pp. 581-591, 2012*

Fauci, A. S. and Morens, D. M., **"The Perpetual Challenge of Infectious Diseases"**, *The New England Journal of Medicine vol. 366, pp. 454-461, 2012*

Falla, T. J., Karunaratne, D. N. and Hancock, R. E. W., **"Mode of action of the antimicrobial peptide indolicidin"**, *The Journal of Biological Chemistry vol. 271, pp. 19298-19303, 1996*

Feinendegen, L. E., **"Biological damage from the Auger effect, possible benefits"**, *Radiation and Environmental Biophysics vol. 12, pp. 85-99, 1975*

Fox, C., **"Resisting antibiotic resistance: legal strategies to maintain man's dominion over microbes"**, *Houston Journal of Health Law and Policy vol. 12, pp. 35-62, 2011*

Fraker, P. J. and Speck, J. C., **“Protein and cell membrane iodinations with a sparingly soluble chloramide, 1,3,4,6-tetrachloro-3a,6a-diphenylglycouril”**, *Biochemical and Biophysical Research Communications vol. 80, pp. 849-857*

Gasser, B. and Mattanovich, D., **"Antibody production with yeasts and filamentous fungi: on the road to large scale?"**, *Biotechnology Letters vol. 29, pp. 201-212, 2007*

Gegenbacher, M. And Kaufmann, S. H. E., **“*Mycobacterium tuberculosis*: Success through dormancy”**, *FEMS Microbiology Reviews vol. 36, pp. 514-532, 2012*

Gleeson, M. A. G., White, C. E., Meininger, D. P. and Komives, E. A., **“Generation of protease-deficient strains and their use in heterologous protein expression”**, *Methods in Molecular Biology vol. 103, pp. 81-94, 1998*

Glockshuber, R., Malia, M., Pfitzinger, I. *et al*., **“A comparison of strategies to stabilize immunoglobulin Fv-fragments”**, *Biochemistry vol. 29, pp. 1362-1367, 1990*

Goel, A., Colcher, D., Koo, J.-S. *et al*., **“Relative position of the hexahistidine tag effects binding properties of a tumor-associated single-chain scFv construct”**, *Biochimica et Biophysica Acta (BBA)- General Subjects vol. 1523, pp. 13-20, 2000*

Goldsmith, S. J. and Vallabhajosula, S., **"Clinically proven radiopharmaceuticals for infection imaging: mechanisms and applications"**, *Seminars in Nuclear Medicine vol. 39, pp. 2-10, 2009*

Grossman, N., Ron, E. Z. and Woldringh, C. L., **"Changes in cell dimensions during amino acid starvation of *Escherichia coli*"**, *Journal of Bacteriology vol. 152, pp. 35-41, 1982*

Guinn, K. M., Hickey, M. J., Mathur, S. K. *et al*., **"Individual RD1-region genes are required for export of ESAT-6/CFP-10 and for virulence of *Mycobacterium tuberculosis*"**, *Molecular Microbiology vol. 51, pp. 359-370, 2004*

Häfeli, U., Pauer, G., Failing, S. and Tapolsky, G., **"Radiolabeling of magnetic particles with rhenium-188 for cancer therapy"**, *Journal of Magnetism and Magnetic Materials vol. 225, pp. 73-78, 2001*

Hancock, R. E. and Chapple, D. S., **"Peptide Antibiotics"**, *Antimicrobial Agents and Chemotherapy vol. 43, pp. 1317-1323, 1999*

Haubner, F., Ohmann, E., Pohl, F. *et al*., **"Wound healing after radiation therapy: Review of the literature"**, *Radiation Oncology vol. 7, pp. 162-170, 2012*

Henle, E. S. and Linn, S., **"Formation, prevention, and repair of DNA damage by iron/hydrogen peroxide",** *The Journal of Biological Chemistry vol. 272, pp. 19095-19098, 1997*

Higgins, D. R. and Cregg, J. M., **"Introduction to *Pichiapastoris*"**, *Methods in Molecular Biology vol. 103, pp. 1-15, 1998*

Holliger, P., Prospero, T. and Winter, G., **"Diabodies: small bivalent and bispecific antibody fragments"**, *Proceedings of the National Academy of Science USA vol. 90, pp. 6444-6448, 1993*

Holliger, P. and Hudson, P. J., **"Engineering antibody fragments and the rise of single domains"**, *Nature Biotechnology vol. 23, pp. 1126-1136, 2005*

Huang, D. and Shusta, E. V., "**Secretion and surface display of green fluorescent protein using the yeast *Saccharomyces cerevisiae*",** *Biotechnology Progress vol. 21, pp. 349, 2005*

Hunter, S. W., Gaylord, H. and Brennan, P. J., **"Structure and antigenicity of the phosphorylated lipopolysaccharide antigens from the leprosy and tubercle bacilli"**, *The Journal of Biological Chemistry vol. 261, pp. 12345-12351, 1986*

ICRU Report 16, **"Linear Energy Transfer"**, *Issued June 15, 1970*

Illiades, P., Kortt, A. A. and Hudson, P. J., **"Triabodies: single chain Fv fragments without a linker form trivalent trimers"**, *FEBS Letters vol. 409, pp. 437-441, 1997*

Jahic, M., Rotticci-Mulder, J. C., Martinelle, M. *et al*., **"Modelling of growth and energy metabolism of *Pichia pastoris* producing a fusion protein"**, *Bioprocess and Biosystems Engineering vol. 24, pp. 385-393, 2002*

Jamieson, D. J., Stephen, D. W. S. and Terrière, E. C., **"Analysis of the adaptive oxidative stress response of *Candida albicans***", *FEMS Microbiology Letters vol. 138, pp. 83-88, 1996*

Janeway, C. A., Travers, P., Walport, M. and Schlomchik, M. J., **"Immunobiology: the immune system in health and disease"**, *Garland Science, 6th Edition, 2005*

Jassal, M. and Bishai, W. R., **"Extensively drug-resistant tuberculosis"**, *The Lancet Infectious Diseases vol. 9, pp. 19-30, 2009*

Jefferis, R., **"Glycosylation of recombinant antibody therapeutics"**, *Biotechnology Progress vol. 21, pp. 11- 16, 2005*

Jensen, K. F., **"The *Escherichia coli* K-12 "Wild Types" W3110 and MG1655 Have an *rph* Frameshift Mutation That Leads to Pyrimidine Starvation Due to Low *pyrE* Expression Levels"**, *Journal of Bacteriology vol. 175, pp. 3401-3407, 1993*

Jurcic, J. G., **"Targeted alpha-particle immunotherapy with Bismuth-213 and Actinium-225 for Acute Myeloid Leukemia"**, *Journal of Postgraduate Medicine, Education and Research vol. 47, pp. 14-17, 2013*

Kabat, E. A., Wu, T. T. Perry, H. M. *et al*., **"Sequences of proteins of immunological interest"**, *NIH publication, 5th edition, 1991*

Kaminski, M. S., Zasadny, K. R., Francis, I. R. et al., **"Radioimmunotherapy of B-Cell Lymphoma with [^{131}I]Anti-B1 (Anti-CD20) Antibody"**, *The New England Journal of Medicine vol. 329, pp. 459-465, 1993*

Kassis, A. I., Adelstein, S. J., Haydock, C. *et al*., **"Lethality of Auger electrons from the decay of Bromine-77 in the DNA of mammalian cells"**, *Radiation Research vol. 90, pp. 362-373, 1982*

Kassis, A. I., **"Cancer therapy with Auger electrons: are we almost there?"**, *Journal of Nuclear Medicine vol. 44, pp. 1479-1481, 2003*

Kassis, A. I., **"The amazing world of Auger electrons"**, *International Journal of Radiation Biology vol. 80, pp. 789-803, 2004*

Kassis, A. I. and Adelstein, J., **"Radiobiologic principles in radionuclide therapy"**, *The Journal of Nuclear Medicine vol. 46, pp. 4S-12S, 2005*

Kassis, A. I., **"Molecular and cellular radiobiological effects of Auger emitting radionuclides"**, *Radiation Protection Dosimetry vol. 143, pp. 241-247, 2011*

Kauffman, P. E. and Johnson, H. M., **"Stability of ^{125}I-labeled Staphylococcal Enterotoxins in Solid-Phase Radioimmunoassay"**, *Applied Microbiology vol. 29, pp. 776-779, 1975*

Keating, F. R., Wang, J. C., Luellen, T. J. *et al*., **"The measurement of the iodine-accumulating function of the human thyroid gland"**, The *Journal of Clinical Investigation vol. 28, pp. 217-227, 1949*

Khaw, B. AA., Fallon, F. T., Strauss, H. W. and Haber, E., **"Myocardial infarct imaging of antibodies to canine myosin with indium-111-diethylenetriamine pentaacetic acid"**, *Science vol. 209, pp. 295-297, 1980*

Khazaeli, M. B., Saleh, M. N., Liu, T. P. *et al*., **"Pharmacokinetics and immune response of ^{131}I-chimeric mouse/human B72.3 (human γ4) monoclonal antibody in humans"**, *Cancer Research vol. 51, pp. 5461-5466, 1991*

Kipriyanov, S. M., Moldenhauer, G., Martin, A. C. *et al*., **"Two amino acid mutations in an anti-human CD3 single chain Fv antibody fragment that affect the yield on bacterial secretion but not the affinity"**, *Protein Engineering vol. 10, pp. 445-453, 1997*

Knutson, K. L., Hmama, Z., Herrera-Velit, P. *et al*., **"Lipoarabinomannan of *Mycobacterium tuberculosis* promotes protein tyrosine dephosphorylation and inhibition of mitogen-activated protein kinase in human mononuclear phagocytes: the role of the Src homology containing tyrosine phosphatase 1"**, *The Journal of Biological Chemistry vol. 273, pp. 645-652, 1998*

Krause, R. M., **"Emerging infections: biomedical research reports"**, *1st Edition, Academic Press, 1998*

Krisch, R. E. and Ley, R. D., **"Induction of lethality and DNA breakage by the decay of iodine-125 in bacteriophage T4"**, *International Journal of Radiation Biology vol. 25, pp. 21-30, 1974*

Kurenuma, T., Kawamura, I., Hara, H. *et al*., **"The RD1 locus in the *Mycobacterium tuberculosis* genome contributes to activation of caspase-**

1 via induction of potassium ion efflux in infected macrophages", *Infection and Immunity vol. 77, pp. 3992-4001, 2009*

Lazarevic, V., Nolt, D. and Flynn, J L., **"Long-term control of *Mycobacterium tuberculosis* infection is mediated by dynamic immune responses"**, *The Journal of Immunology vol. 175, pp. 1107-1117, 2005*

Leong, S. S. J. and Chen, W. N., **"Preparing recombinant single chain antibodies"**, *Chemical Engineering Science vol. 63, pp. 1401-1414, 2008*

Leung, C. C., Tam, C. M., Chan, S. L. *et al*., **"Efficacy of the BCG revaccination programme in a cohort given BCG vaccination at birth in Hong Kong"**, *The International Journal of Tuberculosis and Lung Disease vol. 5, pp. 717-723, 2001*

Lewis, K. N., Liao, R., Guinn, K. M. *et al*., **"Deletion of RD1 from *Mycobacterium tuberculosis* mimics Bacille Calmette-Guérin attenuation"**, *Journal of Infectious Diseases vol. 187, pp. 117-123, 2003*

Lewis, K., **"Persister cells"**, *Annual Reviews of Microbiology vol. 64, pp. 357-372, 2010*

Loferer-Krößbacher, M., Klima, J. and Psenner, R., **"Determination of bacterial cell dry mass by transmission electron microscopy and densitometric image analysis"**, *Applied and Environmental Microbiology vol. 64, pp. 688-694, 1998*

Love, K. R., Politano, T. J., Panagiotou, V. *et al*., **"Systematic single-cell analysis of *Pichia pastoris* reveals secretory capacity limits productivity"**, *PLoS ONE vol. 7, e37915, 2012*

Lupetti, A., Welling, M. M.., Mazzi, U. *et al*., **"Technetium-99m labelled fluconazole and antimicrobial peptides for imaging of *Candida albicans* and *Aspergillus fumigatus* infections"**, *European Journal of Nuclear Medicine and Molecular Imaging vol. 29, pp. 674-679, 2002*

Lupetti, A., Welling, M. M., Pauwels, E. K. J. and Nibbering, P. H., **"Radiolabelled antimicrobial peptides for infection detection"**, *The Lancet Infectious Diseases vol. 3, pp. 223-229, 2003*

Madigan, M. T., Martinko, J. M. and Parker, J., **"Brock Biology of Microorganisms"**, *Pearson Education Inc., Tenth Edition, International Edition, 2003*

Mahairas, G. G., Sabo, P. J., Hickey, M. J. *et al*., **"Molecular analysis of genetic differences between *Mycobacterium bovis* BCG and virulent *M. bovis***", *Journal of Bacteriology vol. 178, pp. 1274-1282, 1996*

Maloy, W. L. and Kari, U. P., **"Structure-activity studies on magainins and other host defense peptides"**, *Biopolymers vol. 37, pp. 105-122, 1995*

Martineau, P., Jones, P. and Winter, G., **"Expression of an antibody fragment at high levels in the bacterial cytoplasm"**, *Journal of Molecular Biology vol. 280, pp. 117-127, 1998*

Martinez, L. R., Bryan, R. A., Apostolidis, C. *et al*., **"Antibody-guided alpha-radiation effectively damages fungal biofilms"**, *Antimicrobial Agents Chemotherapy vol. 50, pp. 2132-2136, 2006*

Mattes, M. J., Shih, L. B., Govindan, S. V. *et al*., **"The advantage of residualizing radiolabels for targeting B-cell lymphomas with radiolabeled anti-CD22 monoclonal antibody"**, *International Journal of Cancer vol. 71, pp. 429-435, 1997*

McVicker, G., Sun, L., Sohanpal, B. K. *et al*., **"SlyA Protein Activates *fibB* gene Expression and Type 1 Fimbriation in *Escherichia coli* K-12"**, *The Journal of Biological Chemistry vol. 286, pp. 32026-32035, 2011*

Melendez-Alafort, L., Rodriguez-Cortes, J., Ferro-Flores, G. *et al*., **"Biokinetics of ^{99m}Tc-UBI 29-41 in humans"**, *Nuclear Medicine and Biology vol. 31, pp. 373-379, 2005*

Michel, R. B., Brechbiel, M. W. and Mattes, M. J., **"A comparison of 4 radionuclides conjugated to antibodies for single-cell kill"**, *Journal of Nuclear Medicine vol. 44, pp. 632-640, 2003*

Milenic, D. E., Brady, E. D. and Brechbiel, M. W., **"Antibody-targeted radiation cancer therapy"**, *Nature Reviews Drug Discovery vol. 3, pp. 488-499, 2004*

Miller, K. D., Weaver-Feldhaus, J., Gray, S. A. *et al*., **"Production, purification, and characterization of human scFv antibodies expressed in *Saccharomyces***

cerevisiae*, *Pichia pastoris*, and *Escherichia coli", *Protein Expression and Purification vol. 42, pp. 255-267, 2005*

Minion, J., Leung, E., Talbot, E. *et al*., **"Diagnosing tuberculosis with urine lipoarabinomannan: Systematic review and meta-analysis"**, *European Respiratory Journal vol. 38, pp. 1398-1405, 2011*

Mortelmans, K. and Zeiger, E., **"The Ames *Salmonella*/microsome mutagenicity assay"**, *Mutation Research vol. 455, pp. 29-60, 2000*

Müller, C. and Schibli, R., **"Single Photon Emission Computed Tomography Tracer"**, *Recent Results in Cancer Research vol. 187, pp. 65-105, 2013*

Narra, V, R, Howell, R. W., Harapanhalli, R. S. *et al*., **"Radiotoxicity of some Iodine-123, Iodine-125 and Iodine-131-labeled compounds in mouse testes: implications for radiopharmaceutical design"**, *The Journal of Nuclear Medicine vol. 33, pp. 2196-2201, 1992*

Nosanchuk, J. D. and Dadachova, E., **"Radioimmunotherapy of fungal diseases: the therapeutic potential of cytocidal radiation delivered by antibody targeting fungal cell surface antigens"**, *Frontiers in Microbiology vol. 2, article 283, 2012*

Noss, E. H., Pai, R. K., Sellati, T. J. *et al*., **"Toll-like receptor 2-dependent inhibition of macrophage class II MHC expression and antigen processing by 19 kDa lipoprotein of *Mycobacterium tuberculosis*"**, *The Journal of Immunology vol. 167, pp. 910-918, 2001*

O'Donoghue, J. A. O. and Wheldon, T. E., **"Targeted radiotherapy using Auger electron emitters"**, *Physics in Medicine and Biology vol. 41, pp. 1973-1992, 1996*

Otvos, L., **"Antibacterial peptides and proteins with multiple cellular targets"**, *Journal of Peptide Science vol. 11, pp. 697-706, 2005*

Paillas, S., Boudousq, V., Piron, B. *et al*., **"Apoptosis and p53 are not involved in the anti-tumor efficacy of (125)I-labeled monoclonal antibodies targeting the cell membrane"**, *Nuclear Medicine and Biology vol. 40, pp. 471-480, 2013*

Pearl, J. E., Saunders, B., Ehlersm S. *et al*., **"Inflammation and lymphocyte activation during Mycobacterial Infection in the interferon-γ-deficient mouse"**, *Cellular Immunology vol. 211, pp. 43-50, 2001*

Pechère, J. C., **"Patients' Interviews and Misuse of Antibiotics"**, *Clinical Infectious Diseases vol. 33, pp. S170-S173, 2001*

Pedraza-Lopéz, M., Ferro-Flores, G., Mendiola-Cruz, M. T. and Morales-Ramírez, P., **"Assessment of radiation-induced DNA damage caused by the incorporation of ^{99m}Tc-radiopharmaceuticals in murine lymphocytes using single cell gel electrophoresis"**, *Mutation Research vol. 465, pp. 139-144, 2000*

Phaeton, R., Wang, X. G., Einstein, M. H. *et al*., **"Radioimmunotherapy with an Antibody to the HPV16 E6 Oncoprotein is Effective in an Experimental Cervical Tumor Expressing Low Levels of E6"**, *Cancer Biology & Therapy vol. 10, pp. 1041-1047, 2010*

Poirier, V. and Av-Gay, Y., **"Mycobacterium tuberculosis modulators of the macrophages' cellular events"**, *Microbes and Infection vol. 14, pp. 1211-1219, 2012*

Porro, D. and Mattanovich, D., **"Recombinant protein production in yeasts"**, *Methods in Molecular Biology vol. 267, pp. 241-258, 2004*

Powers, D. B., Amersdorfer, P., Poul, M.-A. *et al*., **"Expression of single-chain Fv-Fc fusions in *Pichia pastoris*"**, *Journal of Immunology Methods vol. 251, pp. 123-135, 2001*

Pym, A. S., Brodin, P., Brosch, R. *et al*., **"Loss of RD1 contributed to the attenuation of the live tuberculosis vaccines *Mycobacterium bovis* BCG and *Mycobacterium microti*"**, *Molecular Microbiology vol. 46, pp. 709-717, 2002*

Quillardet, P., Huisman, O., D'Ari, R. and Hofnung, M., **"SOS chromotest, a direct assay of induction of an SOS function in *Escherichia coli* K-12 to measure genotoxicity"**, *Proceedings of the National Academy of Sciences of the United States of America vol. 79, pp. 5971-5975, 1982*

Rademacher, C., Shoemaker, G. K., Kim, H.-S. *et al*., **"Ligand Specificity of CS-35, a monoclonal antibody that recognises Mycobacterial Lipoarabinomannan: a model system for oligofuranoside-protein interaction"**, *Journal of American Chemical Society vol. 129, pp. 10489-10502, 2007*

Rai, R. C., Dwivedi, V. P., Chatterjee, S. *et al*., **"Early secretory antigenic target-6 of *Mycobacterium tuberculosis*: enigmatic factor in pathogen-host interactions"**, *Microbes and Infection vol. 14, pp. 1220-1226, 2012*

Reilly, R. M. and Kassis, A., **"Targeted Auger electron radiotherapy of malignancies", From:, Monoclonal Antibody and Peptide-Targeted Radiotherapy of Cancer"**, 1st edition, John Wiley & Sons, 2010

Renaut, L., Monnet, C., Dubreuil, O. *et al*., **"Affinity maturation of antibodies: optimized methods to generate high-quality scFv libraries and isolate IgG candidates by high-throughput screening"**, *Methods in Molecular Biology vol. 907, pp. 451-461, 2012*

Rivera, J., Nakouzi, A. S., Morgenstern, A. *et al.*, **"Radiolabeled Antibodies to *Bacillus anthracis* Toxins Are Bactericidal; and Partially Therapeutic in Experimental Murine Anthrax"**, *Antimicrobial Agents and Chemotherapy vol. 53, pp. 4860-4868, 2009*

Roca, A. I. and Cox, M. M., **"The RecA protein: structure and function"**, *Critical Reviews in Biochemistry and Molecular Biology vol. 25, pp. 415–45, 1990*

Rodrigues, L. C., Pereira, S. M., Cunha, S. S. *et al*., **"Effect of BCG revaccination on incidence of tuberculosis in school-aged children in Brazil: the BCG-REVAC cluster randomised trial"**, *The Lancet vol. 366, pp. 1290-1295, 2005*

Sadeghi, M., Enferadi, M. and Shirazi, A., **"External and internal radiation therapy: Past and future directions"**, *Journal of Cancer Research and Therapeutics vol. 3, pp. 239-248, 2010*

Schoffelen, R., Franssen, G., McBride, W. J. *et al*., **"Pretargeted immunoPET for imaging human colonic cancer in a mouse model"**, *Journal of Nuclear Medicine vol. 51 (suppl. 2), Abstract 61, 2010*

Scott-Browne, J. P., Shafiani, S., Tucker-Heard, G. *et al*., **"Expansion and function of Foxp3-expressing T regulatory cells during tuberculosis"**, *The Journal of Experimental Medicine vol. 204, pp. 2159-2169, 2007*

Sharkey, R. M. and Goldenberg, D. M., **"Cancer radioimmunotherapy"**, *Immunotherapy vol. 3, pp. 349-370, 2011*

Silva, C. R., Valsa, J. O., Caniné, M. S., **"Evaluation of Technetiium-99m decay on *Escherichia coli* inactivation: effects of physical or chemical agents"**, *Yale Journal of Biology and Medicine vol. 71, pp. 7-14, 1998*

Simmaco, M., Mignogna, G. and Barra, D., **"Antimicrobial peptides from amphibian skin: what do they tell us?"**, *Biopolymers vol. 47, pp. 435-450, 1998*

Skeiky, Y. A. W. and Sadoff, J. C., **"Advances in tuberculosis vaccine strategies"**, *Nature Reviews vol. 4, pp. 469-476, 2006*

Staud, F., Nishikawa, M., Morimoto, K. et al., **"Disposition of Radioactivity after Injection of Liver-Targeted Proteins Labelled with ^{111}In or ^{125}I. Effect of Labelling on Distribution and Excretion of Radioactivity in Rats"**, *Journal of Pharmaceutical Sciences vol. 88, pp. 577-585, 1999*

Steinstraesser, L., Ring, A., Bals, R. *et al*., **"The human host defense peptide LL37/hCAP accelerates angiogenesis in PEGT/PBT biopolymers"**, *Annals of Plastic Surgery vol. 56, pp. 93- 98, 2006*

Streatfield, S. J., Howard, J, A., **"Plant production systems for vaccines"**, *Expert Reviews in Vaccines vol. 2, pp. 763-775, 2003*

Streatfield, S. J., **"Approaches to achieve high-level heterologous protein production in plants"**, *Plant Biotechnology vol. 5, pp. 2-15, 2007*

Tai, M. S., Mudgett-Hunter, M., Levinson, D. *et al*., **"A bifunctional fusion protein containing Fc-binding fragment B of staphylococcal protein A amino terminal to antidigoxin single-chain Fv"**, *Biochemistry vol. 29, pp. 8024-8030, 1990*

Tavaré, R., Torres, R., De Rosales, M. et al., **"Efficient Site-Specific Radiolabeling of a Modified C2A Domain of Synaptotagmin I with $[^{99m}Tc(CO)_3]^+$: A New Radiopharmaceutical for Imaging Cell Death"**, *Bioconjugate Chemistry vol. 20, pp. 2071-2081, 2009*

Thomas, G. S. and Maddahi, J., **"The Technetium shortage"**, *Journal of Nuclear Cardiology vol. 17, pp. 993-998, 2010*

Todorovska, A., Roovers, R. C., Dolezal, O. *et al*., **“Design and application of diabodies, triabodies and tetrabodies for cancer targeting”**, *Journal of Immunological Methods vol. 248, pp. 47-66, 2001*

Torchilin, V. P., **"Drug targeting"**, *European Journal of Pharmaceutical Sciences vol. 11, pp. S81-S91, 2000*

Trakulsomboon, S., Danchaivijitr, S., Rongrungruang, Y. *et al*., **"First Report of Methicillin-Resistant Staphylococcus aureus with Reduced Susceptibility to Vancomycin in Thailand"**, *Journal of Clinical Microbiology vol. 39, pp. 591-595, 2001*

Trinh, R., Gurbaxani, B., Morrison, S. L. and Seyfzadeh, M., **"Optimization of codon pair use within the $(GGGGS)_3$ linker sequences results in enhanced protein expression"**, *Molecular Immunology vol. 40, pp. 717-722, 2004*

Trott, K.-R., **"Can we reduce the incidence of second primary malignancies occurring after radiotherapy"**, *Radiotherapy and Oncology vol. 91, pp. 1-3, 2009*

Tubiana, M., **"Can we reduce the incidence of second primary malignancies occurring after radiotherapy? A critical review",** *Radiotherapy and Oncology vol. 91, pp. 4-15, 2009*

Tübbicke, A., Hübner, C., Kramer, A. *et al*., **"Transmission rates, screening methods and costs of MRSA- a systematic literature review related to the prevalence in Germany"**, *European Journal of Clinical Microbiology Infectious Diseases vol. 31, pp. 2497- 2511, 2012*

Tyson, C. B., Lord, P. G. and Wheals, A. E., **"Dependency of size of *Saccharomyces cerevisiae* cells on growth rate"**, *Journal of Bacteriology vol. 138, pp. 92-98, 1979*

Udwadia, Z. F., Amale, R. A., Ajbani, K. K. and Rodrigues, C., **"Totally drug-resistant tuberculosis in India"**, *Clinical Infectious Diseases vol. 54, pp. 579-581, 2012*

Uenak, P. and Uenak, T., **"Self-radiolysis of Iodobenzene labelled with ^{125}I"**, *Journal of Radioanalytical and Nuclear Chemistry vol. 96, pp. 281-291, 1985*

Ulrichs, T., Kosmiadi, G. A., Jörg, S. *et al*., **"Differential organisation of the local immune response in patients with active cavitary tuberculosis or with nonprogressive tuberculoma"**, *Journal of Infectious Diseases vol. 192, pp. 89-97, 2005*

Urch, D. S. and Welch, M. J., **"Radiochemistry and radiopharmaceuticals"**, *Annual Reports section "A" (Inorganic Chemistry) vol. 102, pp. 542- 563, 2006*

Van der Wel, N., Hava, D., Houben, D. *et al*., **"*M. tuberculosis* and *M. leprae* translocate from the phagolysosome to the cytosol in myeloid cells"**, *Cell vol. 129, pp. 1287-1298, 2007*

Velajati, A. A., Masjedi, M. R., Farnia, P. *et al*., **"Emergence of new forms of totally drug-resistant tuberculosis bacilli"**, *Chest vol. 136, pp. 420-425, 2009*

Waibel, R., Alberto, R., Willuda, J. *et al*., **"Stable one-step technetium-99m labelling of His-tagged recombinant proteins with a novel Tc(I)–carbonyl complex"**, *Nature Biotechnology vol. 17, pp. 897-901, 1999*

Walker, R. C., Jones-Jackson, L. B., Martin, W. *et al*., **"New imaging too old for the diagnosis of infection"**, *Future Microbiology vol. 2, pp. 527-554, 2007*

Walmsley, R. M., Billinton, N. and Heyer, W. -D., **"Green Fluorescent Protein as a reporter for the DNA damage-induced gene *RAD54* in *Saccharomyces cerevisiae*"**, *Yeast vol. 13, pp. 1535-1545, 1997*

Wang, X. G., Revskaya, E., Bryan, R. A. *et al*., **"Treating Cancer as an Infectious Disease- Viral Antigens as Novel Targets for Treatment and Potential Prevention of Tumors of Viral Etiology"**, *PLoS ONE 2, e1114, 2007*

Weisser, N. E. and Hall, J. C., **"Applications of single-chain variable fragment antibodies in therapeutics and diagnostics"**, *Biotechnology Advances vol. 27, pp. 502-520, 2009*

Welling, M. M., Paulusma-Annema, A., Balter, H. S. *et al*., **"Technetium-99m labeled antimicrobial peptides discriminate between bacterial infections and sterile inflammation"**, European Journal of Nuclear Medicine vol. 27, pp. 292-301, 2000

Welling, M. M., Lupetti, A., Balter, H. S. *et al*., **"^{99m}Tc-Labeled antimicrobial peptide for detection of bacterial and *Candida albicans* infections"**, *The Journal of Nuclear Medicine vol. 42, pp. 788-794, 2001*

Welling, M. M., Mongera, S., Lupetti, A. *et al*., **"Radiochemical and biological characteristics of ^{99m}Tc-UBI 29-41 for imaging of bacterial infections"**, *Nuclear Medicine and Biology vol. 29, pp. 413-422, 2002*

Wilson, I. and Stanfield, R., **"Antibody-antigen interactions: new structures and new conformational changes"**, *Current Opinions in Structural Biology vol. 4, pp. 857-867, 1994*

Wu, A. M. and Senter, P. D., **"Arming antibodies: prospects and challenges for immunoconjugates"**, *Nature Biotechnology vol. 23, pp. 1137- 1146, 2005*

Wörn, A. and Plückthun, A., **"An intrinsically stable antibody scFv fragment can tolerate the loss of both disulphide bonds and fold correctly"**, *FEBS Letters vol. 427, pp. 357-361, 1998*

Wörn, A. and Plückthun, A., **"Stability engineering of antibody single-chain Fv fragments"**, *Journal of Molecular Biology vol. 305, pp. 989-1010, 2001*

WHO Global Tuberculosis Report 2012

Xu, L. Y., Butler, N. J., Makrigirogos, G. M. *et al*., **"Bystander effect produced by radiolabeled tumor cells *in vivo*"**, *Proceedings of the National Academy of Sciences USA vol. 99, pp. 13765-13770, 2002*

Yang, L., Weiss, T. M., Lehrer, R. I. and Huang, H. W., **"Crystallization of antimicrobial pores in membranes: magainin and protegrin"**, *Biophysical Journal vol. 79, pp. 2002- 2009, 2000*

Youings, A., Chang, S.-C., Dwek, R. A. and Scragg, I. G., **"Site-specific glycosylation of human immunoglobulin G is altered in four rheumatoid arthritis patients"**, *The Biochemical Journal vol. 314, pp. 621- 630, 1996*

Zanetti, M., Gennaro, R., Scocchi, M. and Skerlavaj, B., **"Structure and biology of cathelicins"**, *Advances in Experimental Medical Biology vol. 479, pp. 203-218, 2000*

Zasloff, M., **"Antimicrobial peptides of multicellular organisms"**, *Nature vol. 415, pp. 389-395, 2002*

Zhang, Y., Liu, R. and Wu, X., **"The proteolytic systems and heterologous protein degradation in the methylotrophic yeast *Pichiapastoris*"**, *Annual Microbiology vol. 57, pp. 553-560, 2007*

Web 1: http://2009.igem.org/Team:SupBiotech-Paris/Concept1

Web 2: http://www.cancerresearchuk.org

Web 3: http://www.sigmaaldrich.com/catalog/product/sigma/t0656?lang=en&region=GB

Web 4: www.BioNumbers.org

10 Appendix

Pichia pastoris: (Genetic code: Standard)

Fields: Triplet | Amino acid | Fraction | Frequency/Thousand | (Number)

TTT	F	0.56	23.9	1013	TCT	S	0.29	23.5	996
TAT	Y	0.45	14.7	622	TGT	C	0.65	8.3	353
TTC	F	0.44	19.1	810	TCC	S	0.20	16.3	693
TAC	Y	0.55	18.3	777	TGC	C	0.35	4.5	191
TTA	L	0.15	14.9	634	TCA	S	0.19	15.6	663
TAA	*	0.53	0.9	38	TGA	*	0.18	0.3	13
TTG	L	0.33	31.4	1332	TCG	S	0.09	7.2	305
TAG	*	0.29	0.5	21	TGG	W	1.00	9.9	418
CTT	L	0.17	16.0	677	CCT	P	0.35	15.3	648
CAT	H	0.54	10.5	447	CGT	R	0.16	6.9	291
CTC	L	0.08	7.6	321	CCC	P	0.16	6.7	285
CAC	H	0.46	8.9	378	CGC	R	0.05	2.3	99
CTA	L	0.12	11.2	475	CCA	P	0.40	17.1	725
CAA	Q	0.62	23.9	1015	CGA	R	0.11	4.6	195
CTG	L	0.16	15.3	648	CCG	P	0.10	4.1	172
CAG	Q	0.38	14.5	616	CGG	R	0.05	2.2	93
ATT	I	0.51	31.7	1347	ACT	T	0.40	23.3	989
AAT	N	0.48	23.5	998	AGT	S	0.15	12.1	514
ATC	I	0.31	19.3	819	ACC	T	0.24	13.7	580
AAC	N	0.52	25.7	1090	AGC	S	0.09	7.4	315
ATA	I	0.18	11.5	486	ACA	T	0.25	14.3	605
AAA	K	0.47	30.2	1280	AGA	R	0.47	19.9	846
ATG	M	1.00	19.2	813	ACG	T	0.11	6.3	267
AAG	K	0.53	34.4	1460	AGG	R	0.16	6.6	281
GTT	V	0.42	26.7	1131	GCT	A	0.45	29.6	1256
GAT	D	0.59	37.2	1578	GGT	G	0.43	26.6	1130
GTC	V	0.23	14.5	615	GCC	A	0.25	16.7	707
GAC	D	0.41	26.2	1110	GGC	G	0.14	8.6	365
GTA	V	0.16	10.1	430	GCA	A	0.24	15.9	675
GAA	E	0.58	40.2	1706	GGA	G	0.32	20.0	849
GTG	V	0.20	12.8	543	GCG	A	0.06	3.7	158
GAG	E	0.42	29.6	1255	GGG	G	0.10	6.4	271